

ESTUDIO DE SISTEMAS LÍQUIDO
IÓNICO/CARBÓN ACTIVO Y SU APLICACIÓN
EN LA RETENCIÓN DE CONTAMINANTES

ESSAYS ON IONIC LIQUID/ACTIVATED
CARBON SYSTEMS AND THEIR APPLICATION
TO POLLUTANTS REMOVAL

Doctoral dissertation, Madrid 2012
JESÚS LEMUSTORRES

UNIVERSIDAD AUTÓNOMA DE MADRID
FACULTAD DE CIENCIAS
Sección Ingeniería Química



**“Estudio de sistemas líquido iónico/carbón activo y su
aplicación en la retención de contaminantes”**

**“Essays on ionic liquid/activated carbon systems and
their application to pollutants removal”**

Tesis Doctoral

Jesús Lemus Torres

Madrid, 2012

UNIVERSIDAD AUTÓNOMA DE MADRID
FACULTAD DE CIENCIAS
Sección de Ingeniería Química



**“Estudio de sistemas líquido iónico/carbón activo y su
aplicación en la retención de contaminantes”**

**“Essays on ionic liquid/activated carbon systems and
their application to pollutants removal”**

MEMORIA

que para optar al grado de
Doctor con Mención Europea

presenta

Jesús Lemus Torres

Directores: Dr. Juan José Rodríguez Jiménez
Dr. José Francisco Palomar Herrero

Madrid, 2012

D. José Palomar Herrero, Profesor Titular de Universidad, y **D. Juan José Rodríguez Jiménez**, Catedrático de Universidad, ambos profesores del Área de Ingeniería Química y pertenecientes al Departamento de Química-Física Aplicada de la Universidad Autónoma de Madrid.

HACEN CONSTAR: que el presente trabajo, titulado: “Estudio de sistemas líquido iónico/carbón activo y su aplicación en la retención de contaminantes”, presentado por D. Jesús Lemus Torres, ha sido realizado bajo su dirección, en los laboratorios del Área de Ingeniería Química, en la Universidad Autónoma de Madrid y que, a su juicio, reúne los requisitos de originalidad y rigor científico necesarios para ser presentado como Tesis Doctoral.

Y para que conste a efectos oportunos, firmamos el presente informe en Madrid a dieciséis de junio de dos mil doce.

José Francisco Palomar Herrero

Juan José Rodríguez Jiménez

A mi madre y a mi hermana

Contents

ACKNOWLEDGEMENTS

RESUMEN/SUMMARY

INTRODUCTION

CHAPTER 1. SIGNIFICANCE OF THE PROPOSED RESEARCH	1
1.1. General assessment of ionic liquids	1
1.1.1. A short history of ionic liquids	4
1.1.2. Selected applications of ionic liquids.	6
1.1.3. Environmental impact of ionic liquids. Outline of toxicity	8
CHAPTER 2. TREATMENTS OF IONIC LIQUIDS FROM AQUEOUS EFFLUENTS	11
2.1. Overview of ionic liquids removal from aqueous phase.	11
2.2. Adsorption as separation treatment	14
2.3. Characterization of adsorbents	15
2.4. Adsorption of ionic liquids from aqueous phase on activated carbon	22
2.2.1. Thermodynamic study	23
2.2.2. Kinetic study	26
2.2.3. Recovery of ionic liquid and activated carbon regeneration	28

CHAPTER 3. ADVANCED MATERIALS BASED ON IONIC LIQUIDS ON SOLID SUPPORTS	29
3.1. Introduction to advanced materials	29
3.1.1. Supported ionic liquid phase (SILP)	29
3.1.2. Encapsulated ionic liquid (ENIL)	30
3.2. Characterization of advanced materials	31
3.3. Applications of advanced materials: uptake of gaseous pollutants	36
3.3.1. Chlorinated volatile organic compounds (Cl-VOCs)	37
3.3.2. Ammonia (NH ₃)	38
3.3.3. Experimental uptake/desorption tests	38
CHAPTER 4. IONIC LIQUIDS SIMULATIONS BY USING COSMO-RS METHOD	43
4.1. Introduction to COSMO-RS method	43
4.2. Sigma-profile: the key of COSMO-RS	51
4.3. Prediction of thermophysical properties of ionic liquids	53
References	59

RESULTS AND DISCUSSION

Adsorption of ionic liquids from aqueous phase

Paper I. ADSORPTION OF IONIC LIQUIDS FROM AQUEOUS EFFLUENTS BY ACTIVATED CARBON

Carbon. 2009 (47) 1846-1856.

1. Introduction

2. Procedure

- 2.1. Materials and method
- 2.2. Adsorption/desorption experiments
- 2.3. Characterization of AC adsorbent
- 2.4. Computational details

3. Results and discussion

- 3.1. Experimental
- 3.2. Computational

4. Conclusions

References

Supplementary material

Paper II. DEVELOPING CRITERIA FOR THE RECOVERY OF IONIC LIQUIDS FROM AQUEOUS PHASE BY ADSORPTION WITH ACTIVATED CARBON

Separation and Purification Technology. 2012 (97), 11-19.

1. Introduction

2. Procedure

- 2.1. Experimental
- 2.2. Computational

3. Results and discussion

- 3.1. Adsorption of ILs from aqueous solutions
- 3.2. Adsorbent regeneration and ILs recovery

4. Conclusions

References

Supplementary material

Paper III. ON THE KINETICS OF IONIC LIQUIDS ADSORPTION ONTO ACTIVATED CARBONS FROM AQUEOUS SOLUTION

(Manuscript) *Industrial and Engineering Chemistry Research*. 2012.

- 1. Introduction**
- 2. Procedure**
 - 2.1. Materials and method
 - 2.2. Batch mode adsorption tests
 - 2.3. Adsorption kinetic models
- 3. Results and discussion**
 - 3.1. Comparison of the adsorption kinetics of OmimPF₆ and phenol
 - 3.2. Adsorption of OmimPF₆ onto modified activated carbons
- 4. Conclusions**

References

Supplementary material

Preparation, characterization and applications of advanced materials based on ionic liquids

Paper IV. CHARACTERIZATION OF SUPPORTED IONIC LIQUID PHASE (SILP) MATERIALS PREPARED FROM DIFFERENT SUPPORTS

Adsorption. 2011 (17) 561-571.

- 1. Introduction**
- 2. Procedure**
 - 2.1. Materials and methods
 - 2.2. Characterization and instruments
- 3. Results and discussion**
 - 3.1. Quantification of the IL amount on SILP materials
 - 3.2. Textural properties of SILP materials
 - 3.3. Thermal stability of SILP materials, TGA and DSC study
 - 3.4. SEM and EDX studies
- 4. Conclusions**

References

Paper V. REMOVAL OF CHLORINATED ORGANIC
VOLATILE COMPOUNDS BY GAS PHASE ADSORPTION
WITH ACTIVATED CARBON

Chemical Engineering Journal. 2012

(<http://dx.doi.org/10.1016/j.cej.2012.09.021>)

1. Introduction

2. Procedure

- 2.1. Materials and methods
- 2.2. Experimental
- 2.3. Computational details

3. Results and discussion

- 3.1. Analysis of the influence of operating conditions
- 3.2. Adsorption onto modified activated carbons

4. Conclusions

References

Supplementary material

Paper VI. ENCAPSULATED IONIC LIQUIDS (ENILs): FROM
CONTINUE TO DISCRETE LIQUID PHASE

Chemical Communications. 2012, (48), 10046-10048

1. Main text

2. Procedure

- 2.1. Submicrocapsule C_{Cap} synthesis
- 2.2. ENIL preparation
- 2.3. Characterization
- 2.4. NH_3 capture tests in TGA
- 2.5. NH_3 capture tests in fixed-bed column

References

CONCLUSIONES/CONCLUSIONS	223
APPENDIX 1. Nomenclature	231
APPENDIX 2. Diffusion of results	235
APPENDIX 3. Physical and chemical properties of gaseous solutes	239
APPENDIX 4. Adsorption of Cl-VOCs on SILP materials in fix bed reactor	243

ACKNOWLEDGEMENTS

Me gustaría agradecer al Dr. José Palomar el haberme dado la oportunidad de caminar juntos en este mundo fascinante de los líquidos iónicos. Gracias por creer en mí, por ser jefe, compañero y referencia durante estos cinco años. No podría haber tenido un director mejor.

Al Dr. Juan José Rodríguez sus consejos, su ánimo, su tiempo, su excelente labor como director y, por supuesto, el ser como es, su sentido del humor y cercanía, es un ejemplo para todos.

Al Dr. Miguel Ángel Gilarranz su rigor científico, su disponibilidad, su apoyo y su confianza en mi trabajo. Ha sido un placer haber trabajado durante este tiempo contigo.

A la Dra. María José Martín el haberme dado la oportunidad de colaborar en su grupo de investigación de la Universitat de Girona. Gracias por tu hospitalidad y por tu tiempo. Gracias a Esther, Carla, Alba A. y Alba C. por su acogida y amistad durante mi estancia en Girona.

I would also like to thank Professor João Coutinho for giving me the opportunity to work with him and his research group at the University of Aveiro, where I spent three unforgettable months. I would also like to thank to the entire research group to give me the warmest of welcomes that I could imagine. I thank Catarina, Jorge, Sonia, Pedro, Mara, Luis, Marta, Carlos, Filipa, Ana Rita and a big etcetera for all the great moments.

A los servicios comunes de investigación, SIdI, SEGAINVEX, centro de computación científica y préstamo de biblioteca. En especial a los técnicos de laboratorio del SIdI su colaboración. A Quique de microscopía, su amistad, a Ana, Lola y Antonio de resonancia, su ayuda en el aprendizaje de la técnica y a Luis y Pascual de análisis elemental, la atención y dedicación en los resultados.

A mis compañeros de la sección departamental. Durante estos cinco años he tenido la fortuna de conocer a compañeros que nunca olvidaré. En particular, me gustaría agradecer a Sonia todo lo que hemos pasado y conseguido juntos, a Cristina su acogida en el laboratorio al comienzo de esta tesis, a Israel, Irene y Diana todos los grandes momentos que hemos compartido en la planta piloto, a Luis el ser el mejor de los técnicos de laboratorio y por último, a Marisa el cuidar de nosotros.

A los compañeros del laboratorio del C6: Gema, Macarena, Carmen, María y José Alberto, gracias por ser unos compañeros excelentes y por los buenos ratos que hemos pasado juntos. Me he sentido muy querido por todos vosotros.

A los compañeros del pequeño pero emergente grupo de los líquidos iónicos: Elia, María, Juan y Salama. Podemos estar orgullosos del trabajo que hemos realizado juntos.

Otros compañeros de la sección como son los doctores Víctor Monsalvo, Elena Díaz, Ariadna Álvarez, Zahara Martínez, Jorge Bedia, Noelia Alonso, Francisco Heras, Juan Zazo, Montse Tobajas, Carmen Belén Molina, Asunción Quintanilla y un largo etcétera que han permitido que el lugar de trabajo sea como mi segunda casa.

A los directores de la sección, José Antonio Casas y Ángel Fernández, su trabajo y dedicación al grupo.

También me gustaría agradecer a todos los compañeros con los que he trabajado y tenido la suerte de publicar. A Luisa Gómez, Mounia Al Bahri, Víctor Ferro, Santiago Torrecilla y Francisco Rodríguez.

También me gustaría agradecer a los estudiantes de proyecto fin de carrera que han confiado en nuestro grupo para desarrollar sus trabajos. Guardo un gran recuerdo de Álvaro, Ismael, Víctor, David y Asmae.

Al Dr. Ruben Martínez el ser amigo y apoyo durante la realización de esta tesis y al grupo de Ciencia de Materiales del CSIC.

Fuera del ámbito académico, hay dos personas que lo son todo para mí. Mi madre y mi hermana. Mi madre es mi motor, un estímulo diario. Todo el amor que me da cada día hace que sea prácticamente imposible quitarme la sonrisa de la cara. Mi hermana es mi referente. No hay paso ni decisión que tome sin su apoyo. El resultado de esta tesis es tan mío como suyo. No se puede querer más a una persona. Tenerla tan cerca es verdaderamente una suerte. Este trabajo está dedicado a ellas dos, porque lo representan todo en mi vida. Gracias por estar ahí en cada momento que os he necesitado. Os quiero.

Por supuesto, agradezco a mi padre y mis hermanos su apoyo y cariño. Por estar siempre que os he necesitado.

A mis sobrinos, cuñado, cuñadas, tí@s y prim@s. También a mis compañer@s de carrera y a mis amig@s. A tod@s os agradezco que me hayáis ayudado a conseguir este resultado.

La realización del este trabajo ha sido posible gracias al apoyo económico prestado a través de los proyectos CTQ2009-09983, LIQUORGPAS-S2009/PPQ-1545 y CTQ2011-26758 del Ministerio de Ciencia e Innovación y CTQ2008-01591 y CTQ2008-05641 de la Comunidad de Madrid y a la concesión del contrato de personal investigador de apoyo en el marco del IV plan regional de investigación científica e innovación tecnológica de la Comunidad de Madrid (Orden N° 6032/2008/02 CPI/0585/2008).

**ESSAYS ON IONIC LIQUID/ACTIVATED CARBON SYSTEMS AND THEIR
APPLICATION TO POLLUTANT REMOVAL**

Doctoral dissertation, [Madrid 2012](#), Jesús Lemus Torres



Resumen/Summary

XI-XXV

RESUMEN

Los líquidos iónicos (LIs) constituyen un nuevo tipo de disolventes que están siendo investigados intensamente como posible alternativa de menor impacto ambiental a los disolventes orgánicos volátiles convencionales en procesos de reacción y separación. El interés originado por los LIs, tanto académica como industrialmente, radica en sus excelentes propiedades: volatilidad muy baja, estabilidad térmica y química alta y un amplio espectro de capacidad disolvente. Además, el par iónico catión/anión que compone el LI puede seleccionarse para conseguir propiedades específicas, por lo que resultan disolventes de diseño con un gran potencial para aplicaciones prácticas. A pesar de ser considerados como una alternativa de bajo impacto ambiental (disolventes de *química verde*), debido fundamentalmente a su baja volatilidad que previene su emisión a la atmósfera, presentan un amplio rango de toxicidades, baja biodegradabilidad y una potencial acumulación en suelos. Además, los LIs pueden ser parcial o totalmente miscibles en agua, por lo que es previsible que su aplicación a gran escala genere corrientes de proceso contaminadas por estos compuestos, que requerirán soluciones adecuadas.

Dado que el objetivo central de la Tesis Doctoral es el estudio de sistemas LI-carbón activo (CA), se ha analizado, en primer término, la interacción entre estos dos componentes. Para ello se realiza un estudio termodinámico de la adsorción de un conjunto de LIs sobre una amplia variedad de CAs de distinta naturaleza química y textura porosa, lo que, además servirá para obtener información de utilidad para una posible aplicación en el tratamiento de efluentes acuosos contaminados por LIs. La combinación anión/catión permite conseguir un amplio espectro de características en los LIs estudiados. Por su parte, los materiales adsorbentes se han caracterizado mediante un conjunto de técnicas con el objeto de establecer relaciones entre su naturaleza física y química y su capacidad de adsorción. Además, el método químico-cuántico COSMO-RS se ha utilizado para estimar propiedades termodinámicas y moleculares de sistemas trifásicos (soluto-disolvente-adsorbente), lo que ha permitido el análisis de la adsorción desde un punto de vista molecular. Como resultados relevantes de la presente Tesis Doctoral se concluye que CAs con una microporosidad alta y una concentración de grupos oxigenados superficiales baja se comportan como materiales óptimos para la retención de LIs hidrofóbicos, mientras que la adsorción de LIs hidrofílicos puede mejorarse aumentando la cantidad de grupos oxigenados superficiales del carbón, particularmente mediante la inclusión de grupos hidroxilo, que favorecen las interacciones de enlace de hidrógeno con los grupos

básicos de los **LI**s hidrofílicos. Asimismo, se estudia la cinética de adsorción de un **LI** de referencia en un **CA** comercial bajo diferentes condiciones de operación (agitación, tamaño de partícula, temperatura y concentración inicial del **LI**). Se han empleado varios modelos cinéticos para describir los datos experimentales de adsorción con el fin de desarrollar criterios para mejorar la velocidad del proceso. Los resultados muestran que la cinética de adsorción del **LI** es sensiblemente más lenta que la de fenol, que ha sido usado como soluto de referencia. El análisis cinético indica que el mecanismo de adsorción está controlado por la transferencia de materia en el interior de los poros, como se ha demostrado para una amplia variedad de **CAs**, por lo que una selección adecuada del tamaño de partícula del adsorbente cobra especial importancia de cara a su aplicación práctica en la retención de **LI**s por adsorción en **CA**. En resumen, los resultados de esta primera parte de la Tesis Doctoral se presentan como guía para la adsorción de **LI**s de diferente naturaleza sobre **CA** en corrientes acuosas, tanto desde el punto de vista de las condiciones de operación como de las propiedades del adsorbente. Por último, se aborda la regeneración del **CA** saturado y la recuperación del **LI**, proponiendo la acetona como disolvente adecuado para este proceso.

A continuación se estudia la preparación, caracterización y aplicación de materiales avanzados basados en **LI** y **CA**. El diseño de estos materiales pretende aprovechar las propiedades termodinámicas de los **LI**s como disolventes y mejorar la cinética de transferencia de materia en operaciones L-G o S-G (absorción, adsorción o catálisis heterogénea). Los materiales **SILP** (Supported Ionic Liquid Phase) consisten en una fina capa de **LI** soportada sobre un sólido poroso. Estos materiales minimizan las limitaciones de los **LI**s al disminuir el consumo de disolvente y mejorar la velocidad de transferencia de materia. Inicialmente, se estudió la adsorción de compuestos orgánicos volátiles clorados (**Cl-VOCs**) con **CAs** comerciales para disponer de una base de referencia, valorando la posible aplicación de los materiales antes indicados, basados en **LI** y sólidos porosos, para la separación de estos compuestos, reconocidos como contaminantes peligrosos. El estudio de la aplicación de sistemas **SILP** para la retención de **Cl-VOCs**, reveló, sin embargo, que la funcionalización de **CAs** mediante la incorporación de **LI**s disminuye su capacidad para retener compuestos clorados desde un punto de vista termodinámico. Este resultado preliminar motivó un replanteamiento de la investigación sobre el tratamiento de corrientes gaseosas mediante sistemas **LI-CA**. Por una parte se planteó el estudio de solutos gaseosos que presenten más altas afinidades por el **LI**, como es el caso del amoníaco, elegido como químicamente favorable para su absorción con **LI**s, de acuerdo con publicaciones previas del grupo. Por otra

parte, se abordó el diseño de nuevos materiales basados en **LIs** alternativos a los sistemas **SILP**, que contengan una mayor cantidad de **LI** y mejoren el comportamiento de las fases absorbentes (**LI**) o adsorbentes (**AC**) de referencia. En este contexto surge el concepto de líquido iónico encapsulado (**ENIL**), material propuesto por primera vez en esta Tesis Doctoral y que consiste en microesferas huecas de carbón poroso rellenas de **LI** en su interior. Los materiales **ENIL** pueden alcanzar un 85% en peso de **LI**, pero confinado en una esfera de tamaño submicrométrico (~ 450 nm). Estos materiales se ensayan en el presente trabajo con resultados interesantes para la separación de amoníaco (**NH₃**) de corrientes gaseosas mediante experimentos llevados a cabo tanto en equipo de microbalanza, como en columna de lecho fijo. Se concluye que los materiales **ENIL** presentan capacidades de retención tan altas como los **LIs** puros, pero con velocidades de transferencia de materia mejoradas con respecto tanto al **LI** como a las esferas huecas de carbón. Por tanto, los sistemas **ENIL** abren nuevos campos de aplicación, entre los que se pueden incluir procesos de separación, catalíticos o electroquímicos.

Como contribución adicional de la presente Tesis Doctoral se ha propuesto una caracterización sistemática de estos nuevos materiales mixtos **LI/CA** (tanto **SILP** como **ENIL**). En este sentido se consiguió establecer que el análisis elemental (**AE**) permite la cuantificación de forma precisa e inmediata del **LI** imidazolio incorporado en el soporte, técnica que se ha demostrado útil en una amplia variedad de sólidos. Por su parte, la adsorción/desorción de nitrógeno y la porosimetría de mercurio permiten evaluar la distribución del **LI** en la estructura porosa del soporte utilizado, habiéndose observado una incorporación jerárquica del **LI** sobre el sólido. La microscopía electrónica de barrido (**SEM**) y de transmisión (**TEM**) posibilitan observar la disposición del **LI** en la matriz sólida, así como apreciar la morfología de estos materiales, evidenciando que la superficie externa de los mismos está cubierta por cantidades altas de **LI**. Mediante la espectroscopía de rayos X de energía dispersiva (**EDX**) se detectan determinados elementos presentes en los sistemas mixtos, como P, F o B. El análisis termogravimétrico (**TGA**) y la calorimetría diferencial de barrido (**DSC**) permiten evaluar la estabilidad térmica de estos materiales mixtos, concluyendo que su estabilidad y el mecanismo de descomposición del **LI** están influenciados por la superficie química del soporte sólido.

Otro de los objetivos del presente trabajo ha sido la utilización de herramientas de simulación molecular como soporte a las líneas de investigación experimentales, que adquieren especial interés a la hora de trabajar con **LI**s, debido al gran número de combinaciones iónicas posibles. La simulación molecular se refiere a un conjunto de métodos computacionales útiles para describir el comportamiento de la materia a partir de información de sus moléculas. Entre los modelos disponibles, la metodología **COSMO-RS** presenta un gran potencial para su aplicación al desarrollo de nuevos procesos basados en **LI**s. **COSMO-RS** predice propiedades termodinámicas a partir de cálculos químico-cuánticos de modelos moleculares simples, sin necesidad de datos experimentales previos. Su aplicación ha permitido obtener información valiosa en relación con diferentes partes de este trabajo, como la predicción de propiedades de **LI**s (densidad, viscosidad, volumen molecular) y de sus mezclas (datos de equilibrio G-L, L-L, L-S y G-S) para validaciones y justificaciones de su comportamiento experimental. Por otro lado, permite el diseño de **LI** o **CA** con propiedades adecuadas para la retención de contaminantes gaseosos, mediante el cálculo de constantes de equilibrio, información clave para las operaciones de separación G-L o G-S (constante de Henry y coeficientes de reparto). Esta simulación ofrece un procedimiento eficaz para la selección del par iónico catión-anión para unas propiedades óptimas del **LI**, evitando de este modo largos y costosos estudios experimentales, así como para valorar el efecto de los grupos superficiales en **CAs** para una funcionalización idónea de cara a su posterior aplicación como materiales adsorbentes. Además, la interpretación de las interacciones intermoleculares en base a entalpías de exceso en mezclas binarias que incluyen **LI** se ha mostrado de gran utilidad para el diseño de sistemas para la separación de amoníaco gaseoso basados en **LI**s o la adsorción de **LI**s de distinta naturaleza química con **CA** en fase acuosa.

Estructura de la Tesis Doctoral:

La **Introducción** pretende situar en un contexto teórico los resultados experimentales, así como articular los diferentes conceptos incluidos en la tesis y justificar el interés y la importancia de la investigación desarrollada.

El **Capítulo 1** de la Tesis presenta una valoración de los **LIs**, a través de su definición, características y evolución histórica. Se describen las principales aplicaciones de los **LIs** en diversos ámbitos de la ingeniería química y por último se recogen recientes estudios de toxicidad y biodegradabilidad de **LIs** en sistemas acuosos.

El **Capítulo 2** reúne las distintas propuestas bibliográficas para el tratamiento de los **LIs** en fase acuosa y presenta la adsorción como la solución propuesta en la Tesis Doctoral. A continuación, se detallan las diferentes técnicas de caracterización utilizadas para el análisis de los **CAs** empleados como adsorbentes. Se describe la experimentación para el análisis tanto termodinámico como cinético de la adsorción de **LIs** sobre **CA**, concluyendo con una propuesta para la regeneración del **CA** y la recuperación del **LI**.

El **Capítulo 3** presenta diferentes materiales avanzados basados en **LIs** soportados sobre distintos sólidos. En primer lugar, los **LIs** soportados (**SILP**), recientemente descritos en bibliografía y aplicados de forma eficiente en distintos tratamientos catalíticos y operaciones de separación, así como los **LIs** encapsulados (**ENIL**) que se han preparado, caracterizado y aplicado por primera vez como sistemas para la retención de gases en la presente Tesis Doctoral. A continuación, se detalla el uso de distintas técnicas de caracterización aplicadas al estudio de las propiedades de estos materiales avanzados. Asimismo, en este capítulo se recoge una justificación de los contaminantes gaseosos estudiados en el trabajo, como son los compuestos orgánicos volátiles clorados y el amoníaco (**Cl-VOCs** y **NH₃**). Por último, se presenta una detallada descripción de la experimentación desarrollada para la retención de estos compuestos gaseosos, mediante materiales **ENIL**, llevándose a cabo ensayos en sistema de microbalanza y en columna de adsorción de lecho fijo. Se detallan, asimismo, los modelos matemáticos empleados para describir los resultados experimentales y evaluar el efecto de los variables de operación sobre los procesos de separación estudiados.

El **Capítulo 4** se centra en la descripción del método químico-cuántico **COSMO-RS**, para la predicción de datos termodinámicos de los distintos sistemas estudiados en el presente trabajo. Se justifica su uso y se muestran sus posibilidades. Se exponen las distintas propiedades de interés en las operaciones de separación estudiadas, como coeficientes de reparto, entalpías de exceso, constantes de Henry o propiedades fisicoquímicas de los compuestos puros, como densidad, viscosidad o volumen molecular.

El apartado de **resultados y discusión** se ha organizado en forma de un compendio de contribuciones científicas publicadas en revistas internacionales como resultado del trabajo de investigación realizado durante el desarrollo de la presente Tesis Doctoral. Estos resultados se pueden clasificar en dos grandes bloques: el primero de ellos se centra en el tratamiento de **LI**s en fase acuosa y el segundo en la preparación, caracterización y aplicación de materiales avanzados basados en **LI**s sobre una matriz sólida, principalmente **CA**s.

De este modo, el primer bloque de resultados consta de 3 publicaciones, en las que se propone una guía para la retención de **LI**s de corrientes acuosas, basada en la adsorción sobre **CA**s comerciales. El **Artículo I** presenta las isothermas de adsorción de 17 **LI**s sobre un **CA** comercial en fase acuosa. Se ha utilizado el método químico-cuántico **COSMO-RS** para describir las interacciones intermoleculares existentes en estos sistemas trifásicos (**LI**-agua-**CA**). También se muestra la caracterización de los sistemas mixtos (**LI/CA**). Por último, se propone la regeneración del **CA**, junto con la recuperación del **LI**, utilizando acetona como disolvente.

El **Artículo II** extiende el espectro de **LI**s estudiados a un total de 27, así como el número de materiales adsorbentes, que incluye 12, con propiedades estructurales y químicas diversas. Esta variedad de **LI**s permite evaluar la influencia tanto del anión como del catión, así como del efecto de la porosidad y la naturaleza química del adsorbente en el proceso de adsorción. Además, gracias al estudio de las interacciones intermoleculares mediante **COSMO-RS**, se proponen funcionalizaciones optimizadas del **CA** que favorecen la adsorción de los **LI**s hidrofílicos, *a priori* refractarios a la adsorción sobre los **CA**s comerciales ensayados.

El **Artículo III** describe un estudio cinético de la adsorción de un **LI** de referencia bajo diferentes condiciones de operación, como temperatura, tamaño de partícula, agitación y concentración inicial de **LI**, así como el tipo de **CA** utilizado. El estudio cinético permite establecer los mecanismos que determinan el proceso de adsorción y evaluar cómo afectan las condiciones de operación a las etapas controlantes.

La evaluación conjunta de las 3 contribuciones sirve de guía para definir las características del material adsorbente y las condiciones de operación que favorecen la adsorción tanto en términos termodinámicos como cinéticos.

- [Artículo I](#): Ionic liquids removal from aqueous effluents by adsorption onto activated carbon. *Carbon*. 2009 (47) 1846-1856.
- [Artículo II](#): Developing criteria for the recovery of ionic liquids from aqueous phase by adsorption with activated carbon. *Separation and Purification Technology*. 2012 (97) 11-19.
- [Artículo III](#): On the kinetics of ionic liquids adsorption onto activated carbons from aqueous solution. *Industrial and Engineering Chemistry Research*. 2012 (submitted)

El siguiente bloque de resultados se recoge en 3 contribuciones. El [Artículo IV](#) se centra en la preparación y caracterización de nuevos materiales basados en [LIs](#) y soportes sólidos de diferente naturaleza. Se utilizan una amplia gama de técnicas de caracterización que permiten evaluar la cantidad y disposición de los [LIs](#) en la superficie del soporte, su estabilidad térmica y la morfología del material resultante. También se estudia el efecto de la naturaleza del soporte en la incorporación del [LI](#), la máxima cantidad del mismo que se puede incorporar, así como una valoración de sus propiedades en futuras aplicaciones en el ámbito de la Ingeniería Química.

Este bloque prosigue con la aplicación de materiales adsorbentes para el tratamiento de efluentes gaseosos, como procesos de referencia con el que evaluar la eficiencia de los materiales avanzados con [LIs](#). El [Artículo V](#) estudia la retención de compuestos orgánicos volátiles clorados ([Cl-VOCs](#)) utilizando [CAs](#) en un sistema de lecho fijo. La propuesta de funcionalizaciones eficientes se realizó mediante el estudio de las interacciones intermoleculares adsorbente-adsorbato con [COSMO-RS](#). Se presenta una caracterización sistemática del [CA](#) virgen y modificado química y térmicamente, para una justificación concluyente de los resultados obtenidos. Una vez finalizado el estudio de la adsorción como proceso de referencia, el [Anexo IV](#) recoge los resultados obtenidos con materiales avanzados ([SILP](#)) para el tratamiento de estos solutos, observándose una mejora de la velocidad de retención de los materiales [SILP](#) respecto a los [CAs](#), pero una menor capacidad de retención, debido a la relativamente baja solubilidad de los [Cl-VOCs](#) en los [LIs](#).

Estos resultados llevaron a la selección del amoníaco para los estudios subsiguientes, en relación con el tratamiento de corrientes gaseosas, así como al diseño de nuevos materiales que aumentarán las capacidades de retención, incorporando una gran cantidad de [LI](#), mejorando simultáneamente las propiedades de transporte respecto al [LI](#) o al [CA](#) por separado.

El [Artículo VI](#) describe la preparación, caracterización y aplicación de [LIs](#) encapsulados ([ENIL](#)) como materiales optimizados para el tratamiento de contaminantes gaseosos. Estos materiales novedosos están basados en la idea de pasar de una fase continua ([LI](#)) a un fluido discretizado ([ENIL](#)), que ofrece un área de contacto más favorable. Este material mantiene las ventajas del [LI](#) como disolvente y mejora las cinéticas de transferencia de materia respecto al mismo, como demuestra la aplicación exitosa de [ENIL](#) en la retención de amoníaco (NH_3). El artículo recoge la experimentación desarrollada para la absorción/desorción en sistemas de microbalanza y en columna de lecho fijo.

- [Artículo IV](#): Characterization of Supported Ionic Liquid Phase ([SILP](#)) materials prepared from different supports. *Adsorption*. 2011 (17) 561-571.
- [Artículo V](#): Effective adsorption of chlorinated organic volatile compounds on commercial activated carbon. *Chemical Engineering Journal*. 2012 (CEJ-D-12-02603R1).
- [Artículo VI](#): Encapsulated Ionic Liquids ([ENILs](#)): From continue to discrete liquid phase. *Chemical communications*. 2012 (48) 10046-10048.

Finalmente, se presenta una sección con las [Conclusiones](#), que recogen las contribuciones originales de la Tesis Doctoral, así como una serie de propuestas de trabajo futuro que se encuentran actualmente en desarrollo.

Completan la Tesis Doctoral cuatro [Apéndices](#). El [Apéndice I](#) recoge las publicaciones (artículos científicos y contribuciones a congresos) derivados de la Tesis Doctoral. El [Apéndice II](#) muestra una nomenclatura detallada de las abreviaturas utilizadas a lo largo de la Tesis. El [Apéndice III](#) detalla las propiedades químicas y físicas de los contaminantes gaseosos utilizados, amoníaco, monoclorometano, diclorometano y cloroformo, y el [Apéndice IV](#) muestra los resultados de la experimentación llevada a cabo con materiales [SILP](#) en el tratamiento de [Cl-VOCs](#) en columna, para la justificación de la elección de un nuevo soluto y la preparación de materiales avanzados más efectivos para su aplicación como fases separadoras.

SUMMARY

Ionic liquids (ILs) are a new class of solvents that are being intensively investigated as a possible alternative with less environmental impact to conventional volatile organic solvents in reaction and separation processes. The interest awakens by ILs, both academically and industrially, lies in their excellent properties: low volatility, high chemical and thermal stability and a wide range of solvent capacity. Furthermore, the ionic combination makes the IL can be selected to achieve specific properties, so they result design solvents with a great potential for practical applications. Despite being considered as alternative with low environmental impact (*green chemistry* solvents) due to their low volatility, which prevents its release into the atmosphere, they present a wide range of toxicities, low biodegradability and potential accumulation in soils. Furthermore, ILs may be partial or completely miscible in water, so their application at large scale is expected to generate wastewater containing ILs which will demand suitable solutions.

Since the main objective of this Thesis is the research on IL-activated carbon (AC) systems, it has been analyzed the interaction between these two components. A thermodynamic study of the adsorption of a set of ILs on a wide variety of ACs with different chemical nature and porous texture may provide useful information for possible application in the treatment of aqueous effluents containing ILs. The anion/cation combinations keep achieving a broad spectrum of IL features. The adsorbent materials have been characterized by a variety of techniques to establish relationships between the physical and chemical nature and its adsorption capacity. Furthermore, the quantum-chemical program COSMO-RS allows to estimate thermodynamic and molecular properties of triphasic systems (solute-solvent-adsorbent), to analyze the adsorption from a molecular point of view. As most relevant results depicted in this Thesis can be concluded that ACs with high microporosity and low concentration in surface oxygenated groups (SOGs) perform as optimal materials for retention of hydrophobic ILs, while the adsorption of hydrophilic ILs can be improved by increasing the amount of SOGs, particularly by the inclusion of hydroxyl groups that favor the hydrogen bonding interactions with the basic groups of the hydrophilic ILs. It is also examined the adsorption rate of a reference IL in a commercial AC under diverse operating conditions (batch shaking, particle size, temperature and initial IL concentration). Several kinetic models have been used to describe adsorption experimental data in order to develop approaches which improve processing rate. The results show that adsorption kinetic of IL is

substantially slower than phenol, used as reference solute. Kinetic analysis indicates that the adsorption mechanism is controlled by mass transfer inside the pores, so that a proper selection of the adsorbent particle size is of particular importance for the practical application of an adsorption treatment **ILs**. In summary, this first part of the study is presented as a guide for the adsorption of different nature **ILs** on **AC** in aqueous phases, both from the point of view of the operating conditions and the adsorbent properties. Finally, it was dealt the **AC** regeneration and the recovery of saturated **IL**, proposing acetone as solvent for this process.

Subsequently, it is studied the preparation, characterization and application of advanced materials based on **IL** and **AC**. The purpose of these materials is to preserve the thermodynamic properties of **ILs** as solvents and improve the mass transfer in the treatment L-G or S-G (absorption, adsorption, heterogeneous catalysis). **SILP** (Supported Ionic Liquid Phase) consists on an **IL** thin layer supported on a solid porous. Such materials minimize the **ILs** limitations to reduce the operating cost and improve the mass transfer rate. It was studied the adsorption of chlorinated volatile organic compounds (**Cl-VOCs**) on commercial **ACs**, in order to provide a benchmark, assessing the possible application of the aforementioned materials, based on **IL** and porous solids, for the separation of these pollutants. However, the application of **SILP** systems on the **Cl-VOCs** retention revealed that **ACs** functionalization by incorporating **ILs** decreases its ability to retain chlorinated compounds from a thermodynamic standpoint. This preliminary result led to reconsider the research about gaseous treatment using **IL-AC** systems. On one side, it was considered the study of new gaseous solutes which show higher affinities toward **IL**, such as ammonia, chosen as chemically favorable solute for its absorption on **ILs**, according to previous publications in our group. Moreover, it was dealt the design of novel materials based on system **ILs** as alternative to **SILP**, containing a larger amount of **IL** and improving the absorbent (**IL**) or adsorbent (**AC**) behavior of the reference phases. In this context it was arisen the encapsulating ionic liquid (**ENIL**) concept, material proposed for first time in this Thesis consisting on hollow microspheres of porous carbon filled by **IL** inside them. **ENIL** materials may reach 85% of **IL** weight, but confined into a sphere of submicron size (~ 450 nm). These materials have been tested in the present study with interesting results for the ammonia (NH_3) separation presenting in gas streams by experiments conducted both in equipment microbalance and fixed bed column. It was concluded that the **ENIL** materials exhibit retention capacities similar to neat **ILs**, but the transfer rates were improved with respect to both **IL** and carbon hollow spheres. Therefore,

ENIL systems open up new application fields which may include separation processes, catalytic or electrochemical.

As a further contribution of this Doctoral Thesis a systematic characterization of these novel materials based on IL and AC was proposed (both SILP as ENIL). In this sense, it was established that elemental analysis (EA) allows to immediately and accurately quantify the incorporation of imidazolium-based IL on the support, a technique that has been usefully proved in a wide variety of solids. Meanwhile, the nitrogen adsorption/desorption and mercury porosimetry to assess the distribution of IL in the porous structure on the support, having observed a hierarchical IL incorporation on the solid. Scanning electron microscopy (SEM) and transmission (TEM) enable to observe the placing of IL on the solid matrix, and also to assess the morphology of these materials, showing that the outer surface is covered by high amounts of IL. Energy-dispersive X-ray spectroscopy (EDX) detects certain elements present in advanced material, such as P, F or B. Thermogravimetric analysis (TGA) and differential scanning calorimetry (DSC) assess the thermal stability of these materials mixed, concluding that its stability and the IL decomposition mechanism are influenced by the chemistry surface of the solid support.

Another objective of this work is the use of molecular simulation tools to support the experimental research lines, which are of particular interest in the field of ILs, due to the large number of possible ion combinations. Molecular simulation refers to a set of useful computational methods which describe the matter behavior from information from its molecules. Among the available models, the COSMO-RS method has great potential for application to the development of new processes based on ILs. COSMO-RS predict thermodynamic properties from quantum-chemical calculations based on simple molecular models without previous experimental data. Its implementation has yielded valuable information regarding different parts of this Doctoral Thesis, as predicting properties of ILs (density, viscosity, molecular volume) and their mixtures (G-L equilibrium data, L-L, L-S and G-S) for validation and experimental justifications for their behavior. On the other hand, allows the design of IL or AC with suitable properties for the retention of gaseous pollutants, by calculating the equilibrium constants, key information for G-L separation operations or G-S (Henry's constant and partition coefficients). This simulation provides an efficient procedure for selecting the anion-cation ion pair for optimal properties of IL, thus avoiding lengthy and expensive experimental studies and to evaluate the effect of the surface oxygen groups in ACs

for a suitable functionalization of face for further application as adsorbent materials. Moreover, the intermolecular interactions understanding based on excess enthalpies of binary mixtures including IL is show as useful for the design of systems in order to gaseous ammonia separation based on ILs or adsorption of ILs from aqueous phase using AC with different chemical nature.

Structure of the Doctoral Thesis:

Introduction aims to place in a theoretical context the experimental results, articulate the different items included in this Thesis and justify the interest and importance of the conducted research.

Chapter 1 does an assessment on IL, by means of its definition, characteristics and historical development. It describes their main applications in various fields of Chemical Engineering and finally it is collected recent studies about the toxicity and biodegradability of ILs in aqueous systems.

Chapter 2 gathers various literature IL treatments in aqueous phase and presents the adsorption as the solution proposes in this Doctoral Thesis. Below it is detailed various characterization techniques used for analysis of the tested adsorbents. It is described the experimentation both thermodynamic and kinetic analysis of the adsorption of IL on AC, concluding with a proposal for the AC regeneration and the IL recovery.

Chapter 3 presents different advanced materials based on IL supported on different porous solids. Initially, the supported ionic liquid phase (SILP) recently described in literature and efficiently applied to various catalytic treatments and separation processes and also, the encapsulated ionic liquids (ENILs) which have been prepared, characterized and applied for first time in separation systems in this Doctoral Thesis. Following, it is detailed the use of different characterization techniques applied to these advanced materials, and finally it is shown a justification of the solutes studied, such as chlorinated volatile organic compounds (Cl-VOCs) and ammonia (NH₃). Finally a detailed description of experiments carried out for the separation of these gaseous compounds, such assays on microbalance system and column. Likewise, it is detailed mathematical analysis used to evaluate operating conditions in the experimental data.

Chapter 4 focuses on the use of simulation tools and the description of quantum-chemical method COSMO-RS for the prediction of thermodynamic data of the different systems studied in this work. It is justified its use and it is showed the advantages of simulation tools and also the key parameters for its management (σ -profile). It describes the different properties of interest in separation operations studied as partition coefficients, excess enthalpies, Henry constant or physical properties of the tested compounds, such as density, viscosity and molecular volume.

Results and Discussion section is organized as a compendium of scientific contributions published in international journals as a result of research conducted during the development of this Doctoral Thesis. These results can be classified into two main sections. The first is focused on the treatment of ILs in aqueous phase while the second is centered on the preparation, characterization and application of advanced materials based on IL on a solid matrix, mostly AC.

Thus, the first section of results consists of 3 publications which propound a guideline for the treatment of IL from aqueous phases based on the adsorption on commercial ACs. Paper I presents the adsorption isotherms of 17 ILs on a commercial AC in aqueous phase. It has been used the quantum-chemical program COSMO-RS to describe these intermolecular interactions existing in these triphasic systems (IL-water-AC). It has been also shown the characterization of mixed systems (IL/AC). Finally, it is proposed the AC regeneration and the IL recovery, using acetone as solvent.

Paper II extends to 27 the spectrum of studied ILs, and the number of adsorbent materials, which includes 12 with different structural and chemical properties. This variety of ILs keeps to evaluate the influence both the cation and anion as well as the effect of the porosity and chemical nature of the adsorbent in the adsorption process. Moreover, thanks to the study of intermolecular interactions by means of COSMO-RS are proposed suitable functionalizations of AC which may favor the adsorption of hydrophilic ILs, *a priori* refractory to adsorption on the commercial ACs tested.

Paper III describes a kinetic study of the adsorption of a reference IL under different operating conditions such as temperature, particle size, initial IL concentration and batch

shaking and also the type of **AC**. The kinetic study let us to establish the mechanisms controlling the adsorption process and evaluate how affect the operating conditions to the determining steps.

The combined evaluation of these 3 contributions is a guide to define the characteristics of the adsorbent material and operating conditions that may favor the adsorption both thermodynamic and kinetic terms.

- **Paper I**: Aqueous Ionic liquids removal from effluents by adsorption onto activated carbon. *Carbon*. 2009 (47) 1846-1856.
- **Paper II**: Developing criteria for the recovery of ionic liquids from Aqueous phase by adsorption with activated carbon. *Separation and Purification Technology*. 2012 (97) 11-19.
- **Paper III**: On the kinetics of ionic liquids adsorption onto activated carbons from Aqueous Solution. *Industrial and Engineering Chemistry Research*. 2012 (submitted)

The next block of results consists on 3 contributions. **Paper IV** is focused on the preparation and characterization of new materials based on **IL** and solid supports of different nature. It is used a wide range of characterization techniques to assess the quantity and disposition of the **IL** on the surface support, their thermal stability and morphology. It has been also studied the effect on the nature of the support after the incorporation of the **IL**, the maximum amount of it that can be incorporated, and an evaluation of their properties in further applications in the field of Chemical Engineering.

This section continues with the application of adsorbent materials for gaseous solutes treatment as reference processes to evaluate the efficiency of advanced materials containing **ILs**. **Paper V** studies the adsorption of chlorinated volatile organic compounds (**Cl-VOCs**) using **ACs** in a fixed bed system. The proposal of efficient functionalizations on the **AC** was made by studying the adsorbent-adsorbate intermolecular interactions using **COSMO-RS**. It is presented a systematic characterization of fresh and chemically and thermally modified **AC** in order to justify the results. Once the study of adsorption as reference process is concluded, **Appendix IV** depicts the results obtained with advanced materials (**SILP**) for the treatment of these solutes, showing an improvement in the adsorption rates for materials **SILP** respect to **ACs**, but a lower adsorption capacity because of the relatively low solubility of **IL** in **Cl-VOCs**.

These results led to the selection of ammonia for subsequent studies related to the treatment of gaseous pollutants, as well as the design of new materials which ability to incorporate a large amount of IL, with the challenge of simultaneously improving the transport properties respect to the neat IL or the AC.

Paper VI describes the preparation, characterization and application of encapsulated ionic liquids (ENILs) as optimized materials for the treatment of gaseous pollutants. These novel materials based on the idea of moving from continue (IL) to discrete fluid phase (ENIL), which provides a more favorable contact area. This material maintains the advantages of IL and improves the mass transfer properties respect the neat IL, as it is demonstrated by the successful application of ENIL material in ammonia (NH₃) uptake. This paper describes the sorption/desorption experiments developed on a microbalance system and fixed bed column.

- Paper IV: Characterization of Supported Ionic Liquid Phase (SILP) materials prepared from different supports. *Adsorption*. 2011 (17) 561-571.
- Paper V: Effective adsorption of chlorinated volatile organic compounds on commercial activated carbon. *Chemical Engineering Journal*. 2012 (CEJ-D-12-02603R1).
- Paper VI: Encapsulated Ionic Liquids (ENILs): From discrete liquid phase to continue. *Chemical Communications*. 2012 (48) 10046-10048.

Finally, there is a section with the main Conclusions, which reflect the novel contributions of this Doctoral Thesis and also a set of proposals for future work which is currently in development.

This Doctoral Thesis is rounded out by four Appendices. Appendix I includes the publications (scientific papers and conference contributions) derived from the doctoral thesis. Appendix II shows a detailed classification of the abbreviations used throughout the Thesis. Appendix III lists the physical and chemical properties of the gaseous pollutants tested, ammonia, monochloromentane, dichloromethane and chloroform and Appendix IV shows the experimentation results carried out in column experiments using SILP materials in the treatment of Cl-VOCs, in order to justify the selection of a new solute and to prepare more effective advanced materials for use as separation media.

ESSAYS ON IONIC LIQUID/ACTIVATED CARBON SYSTEMS AND THEIR APPLICATION TO POLLUTANT REMOVAL

Doctoral dissertation, [Madrid 2012](#), Jesús Lemus Torres



Chapter 1

SIGNIFICANCE OF THE PROPOSED RESEARCH

1-9

CHAPTER 1. SIGNIFICANCE OF THE PROPOSED RESEARCH

1.1. General assessment of ionic liquids

Much attention has recently focused on the subject of the ionic liquids (ILs) since the mid of nineties [1,2]. ILs became one of the most interesting and rapidly developing areas of modern physical chemistry, technologies and engineering [3,4]. The number of papers and patents published on this topic has grown almost exponentially, as can be seen in Figure 1.1, which demonstrated the cooperation between academia and industry [5]. Due to their unique physicochemical characteristics [6,7], ILs are being designed as greener solvents to replace conventional volatile solvents which could lead to photochemical smog, ozone depletion, and global climate change [8]. ILs are showing increasingly promising perspectives in the diverse fields of synthesis [9], catalysis/biocatalysis [10-12], materials science [13,14], electrochemistry [15,16], biochemistry [17], pharmacology [18] and separation technology [19,20] at both the laboratory level and the industrial scale. All these contributions represent a motivation in the field of the ILs.

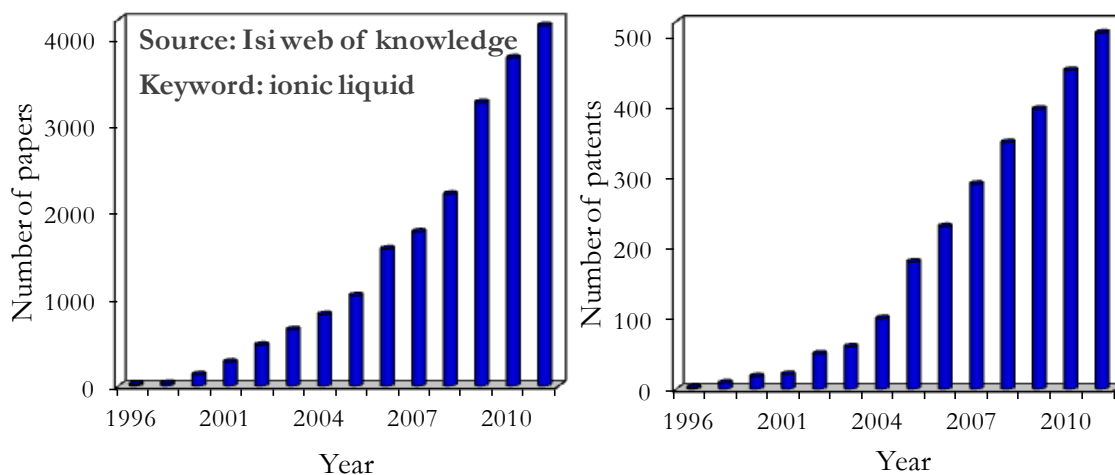
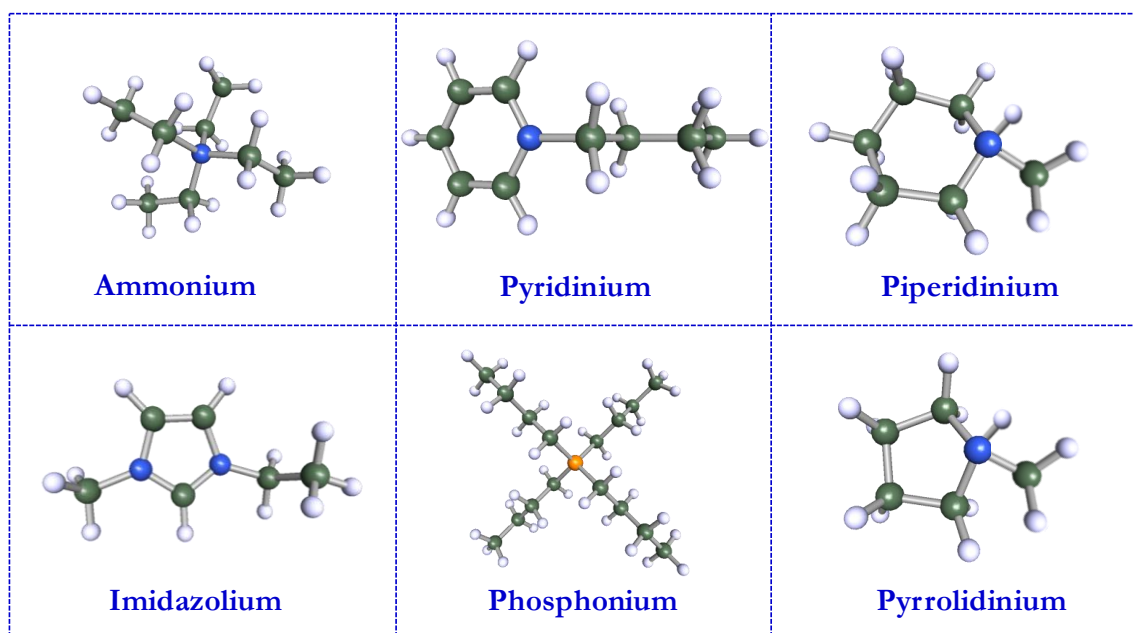


Figure 1.1. Annual growth of IL patents and publications, 1996–2011.

ILs are defined as ionic species with a melting point below 100 °C and usually composed of an organic cation (e.g., imidazolium, pyridinium, pyrrolidinium, phosphonium or ammonium) [21] and inorganic anions, including Cl^- , PF_6^- , BF_4^- , and more currently organic anions, such as trifluoromethylsulfonate $[\text{CF}_3\text{SO}_3]^-$, trifluoroacetate $[\text{CF}_3\text{CO}_2]^-$, bis[(trifluoromethyl)sulfonyl]imide $[(\text{CF}_3\text{SO}_2)_2\text{N}]^-$ (i. e., NTf_2^-), etc. The structures of some common cations and anions of ILs are shown in Figure 1.2. The substituents can vary independently and include linear alkyl chains as well as highly functionalized, branched, aromatic, or cyclic moieties; the structural variability of ILs is enormous. The relatively large size of one or both ions in ILs and their low symmetry cause the relatively low melting points of these materials.

The growing interest about the ILs has been derived from their unique valuable properties, such as non-volatility and non-flammability at ambient conditions, high solvent capacity, chemical and thermal stabilities, high ionic conductivity and wide electrochemical potential window [22-25]. Moreover, the tunable properties of ILs through and endless combination of cations and anions (more than 10^6 of potential ion combination), allow the design of solvents for the development of more efficient processes and products. The general properties of ILs result from the merged properties of the cations and anions and include those that are acidic, basic, hydrophilic and hydrophobic. The anion is currently used to control the water miscibility, although the cation can also influence the hydrophobicity. Physical properties such as melting point, boiling point, density, and viscosity, can be also found in a wide range of values, depending on the ion combination.

Common cations of ILs:



Common anions of ILs:

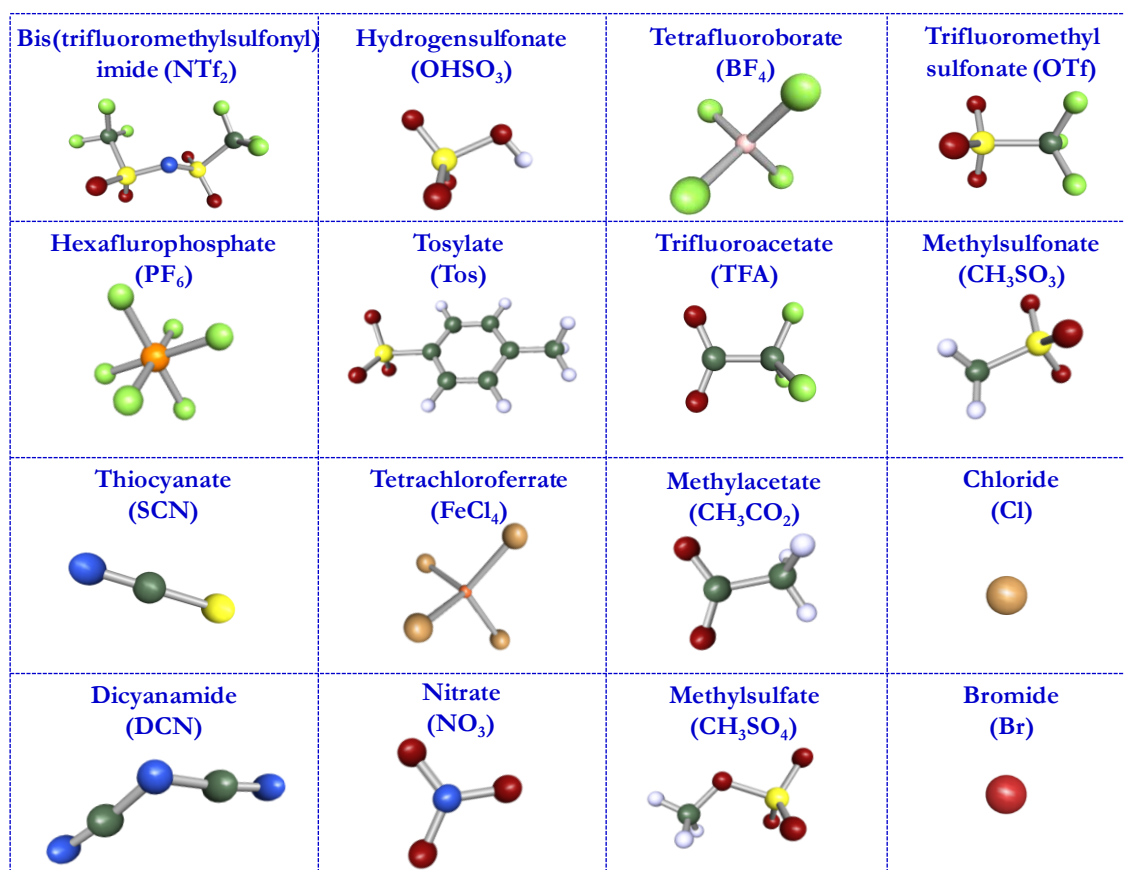


Figure 1.2. Typical ionic components of ILs

1.1.1. History of ionic liquids

The synthesis of the first IL dates from 1914, when Paul Walden was the first who reported the physical properties of ethylammonium nitrate (EtNH_3NO_3) [26]. The discovery of this new class of liquids did not awaken any significant interest at the time. Nowadays, however, this is widely acknowledged as the start of the field of ILs, and it has left an important legacy. The current definition for ILs is resulted from here: ILs are most commonly defined as materials that are composed of cations and anions which melt at or below 100 °C. It was two decades later, in 1934 when it was published the first patent related to ILs [27] (Figure 1.3). In this patent it was demanded that certain organic salts have the ability to solve cellulose and alter its reactivity. However, this publication did not generate any noteworthy interest in the scientific community.

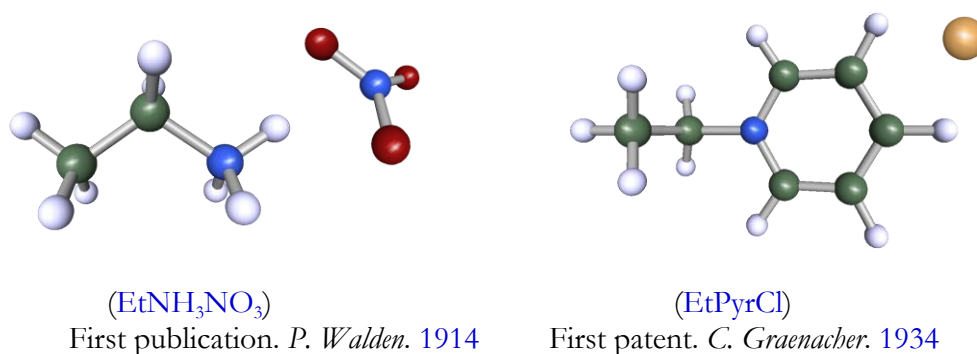


Figure 1.3. Two first ILs synthesized.

Later on, in 1948 this IL was followed by chloroaluminate based ILs, by Hurley and Wier, and it wake up more interesting to electrochemist rather than to organic or catalytic chemist [28]. In 1982 the imidazolium based-ILs were synthesized by J.S. Wilkes et al. obtaining itself as the most stable cation [29]. It was the beginning of the imidazolim-based ILs, which lately are being the most used kind of ILs because of its low viscosity and price, compared to other cations.

The first industrial application was known in 2003 introduced by BASF, sited in Ludwigshafen, Germany [30]. Of all the cooperation between industry and academy, BASF has done the most publicly to implement IL technology. They possess the principal patent, have the widest range of applications, and work openly with leading academics. Probably, **Biphasic Acid Scavenging utilizing ILs (BASIL)** process is the most successful example of an industrial process using IL technology. The BASIL process economically avoids the problems

resulting from solids generation by making use of ILs to scavenge acids. Instead of using a tertiary amine, a 1-alkylimidazole is used to scavenge acids produced. As the imidazole reacts with the acid, an alkylimidazolium salt is formed which is an IL at the reaction temperature. As a liquid, the alkylimidazolium salt can be easily removed by a liquid-liquid phase separation. In addition, economic reclamation of the 1-alkylimidazole through deprotonation is possible [31,32].

Table 1.1. Main discoveries in the IL history

Year	Discovery
1914	Synthesis of the first IL[26]
1934	First IL patent[27]
1948	Discovery of the chloroaluminated IL[28]
1982	Imidazolium is recognised as a IL cation[29]
2003	First industrial application (BASF)[30]

Nowadays, the diversity of industrial and commercial applications is quite astounding; not just in the number, but also in their wide variety, arising from close cooperation between academia and industry, as can be appreciated in Figure 1.4.

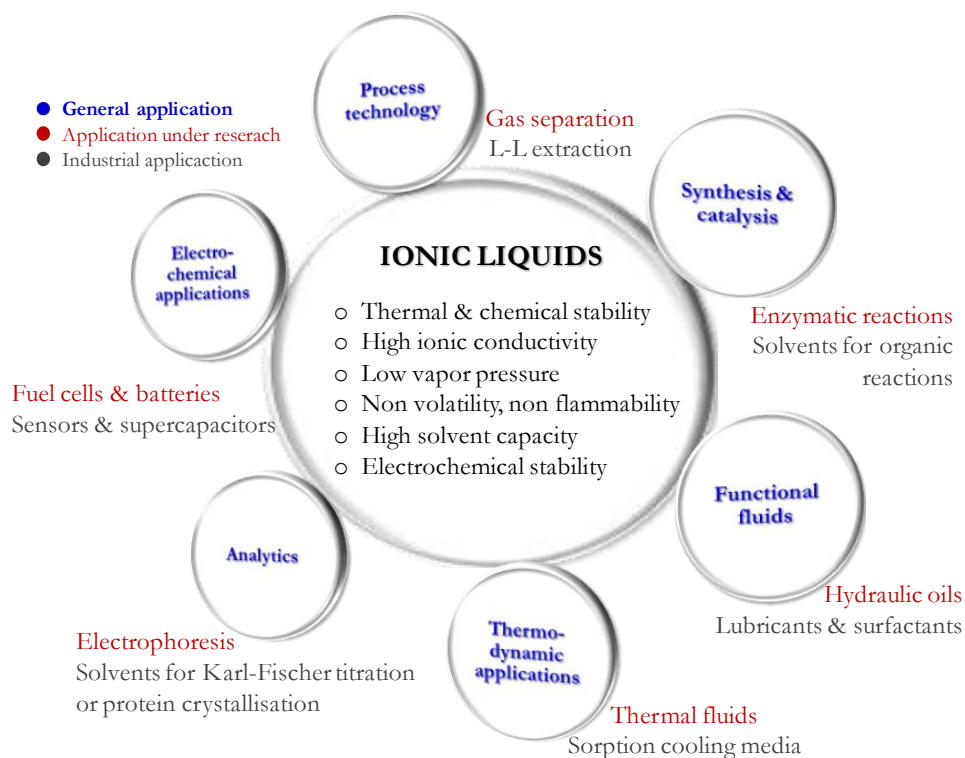


Figure 1.4. Schematic representation of ILs advantages and applications

1.1.2. Selected applications of ionic liquids

The early history of ILs research was dominated by their electrochemical applications as electrolytes. They have excellent electrochemical properties such as high ion content, high ionic conductivity, wide electrochemical windows, non-volatility and non-flammability, and thus, attracted the attention as electrolyte solutions for lithium ion batteries, fuel cells, solar cells, and capacitors [1]. Although ILs show excellent ionic conductivities at room temperature, this derives from the component ions themselves, which are mostly useless as target ions such as lithium cations, protons, or iodide anions. For example, they have been extensively studied as secondary battery electrolytes. These electrolytes require properties such as high ionic conductivity, non-flammability and non-corrosiveness [33]. Traditional magnetic fluids have had problems of volatility and phase separation. The new magnetic IL overcomes these problems, and is expected to be applied to many fields, including the use as a sealing agent for the motor axis [34].

ILs are intrinsically excellent candidates for industrial applications as alternative to volatile organic solvents. Organic solvents have been known for several centuries, and obviously occupy most of the solvent market in industry. However, if the properties of ILs and organic solvents are to be compared (see Table 1.2), it could be anticipated that industry may be a natural environment for ILs. Since a lot of properties of ILs have yet to be discovered, at the current level of development, ILs can nicely complement, and even sometimes work better than organic solvents in a number of industrial processes. This statement should not however diminish the fact that ILs have plenty of academic applications, and their unique properties due to their structure, make them exciting compounds for theoretical and computational studies.

Table 1.2. Comparison of molecular organic solvents and ILs

Organic solvent	Property	Ionic liquid
> 10 ³	Number of compounds	> 10 ⁶
Significant	Vapour pressure	Negligible
Usually flammable	Flammability	Usually inflammable
Conventional polarity	Polarity	Polarity differs
Limited range	Tuneability	Virtually unlimited range
Normally cheap	Cost	All price classes
Green imperative	Recyclability	Cost and green imperative
0.2-100	Viscosity (cP)	22-40000
0.6-1.7	Density (g·cm³)	0.8-3.3

The development of engineering applications with ILs extends to the mid of nineties when the first examples of continuous catalytic processes using ILs and the first studies of IL-based extractions were published [35]. Ever since, the use of ILs has seen tremendous progress in many fields of chemistry and engineering, and the first commercial applications have been previously mentioned. Remarkably, many IL properties can be tuned by structural modifications at their cation and anion, which give them a wide window of physical and chemical properties. Due to their unique properties, ILs have also generated significant interest in a wide variety of engineering applications.

ILs are being used as solvents in organic synthesis that are currently replacing many of the volatile organic compounds (VOCs) [36]. ILs are being also examined in catalytic reactions [37,38]. The first report of an IL used as a catalyst was in Friedel-Crafts acylation in 1986 [39]. Nevertheless, it is only in the last two decades that there has been an explosion in their use in a wide range of catalytic reactions, as hydroformylation, alkylation, oxidation or condensation between other [40].

A summary of the principle applications of ILs in separation technology is present in this chapter. One of the main research fields is their exploitation as solvents for liquid-liquid extractions, because of their immiscibility with water, as well as the high solubility of the organic species in them [41-45]. Extraction of aromatics from aromatic/aliphatic mixture with ILs is expected to require less process steps and less energy consumption than extraction with conventional solvents due to negligible vapour pressure [46-49]. Moreover, ILs were further extended to the extraction of heavy metal ions, such as Hg^{2+} and Ca^{2+} [50]. Since ILs exhibits a very high selectivity and large solubility make them very suitable as entrainers for separation processes, but also due to their extremely low volatilities and their good or even very good thermal stabilities [51].

It has been also described their use as absorbents in gas separation processes [52], mainly in CO_2 capture [53-55] and absorption of SO_2 [56,57], because their gas emissions from various combustion processes have become the major source for air pollution and greenhouse effect. Many other gaseous solutes have been also reported in separation processes using IL-based absorbent material, as NH_3 [58,59], volatile organic compounds [60] and hydrofluorocarbons [61,62] and reactive absorption of propylene [63,64]. Absorption on ILs can provide an effective solution for removal of pollutants from gas streams with further recovery. However, the key factor is the selection of an appropriate IL, used as absorbent [65], aspect successfully solves by means of molecular simulation, where the solubility of gaseous

solutes in ILs, in terms of the contributions of the different solute–solvent intermolecular interactions, was successfully applied [58,59,66,67].

Moreover, much effort and many resources have been expended on developing ILs to enhance the already advantageous combination of permeability and selectivity of supported ILs membranes [68-70]. So, membrane processes are also expected to have the potential to be less energy intensive and less voluminous [71,72]. A hybrid membrane gas absorption process, combining the advantages of absorption (high selectivity) and membranes (small size) could be a worthwhile alternative in separation processes.

Attending to the variation in the IL structure, it was observed that ILs containing costly functionalized [73], deuterated [74], fluorinated [75], or chiral ions [76] have been designed to be used in small amounts in other applications with very high added value, as analytical applications, electrolytes, sensors, and coatings.

1.1.3. Ionic liquids in the environment. Outline of toxicity

Chemical engineers have been developing ILs to replace conventional volatile organic solvents that contribute to serious air pollution. However, it has been reported that ILs can exhibit environmental toxicity, biodegradability and persistency into the environment [77-85]. While ILs cannot vaporize at common operating conditions leading to air pollution, mainly based on their negligible vapor pressure, they present miscibility with water that may be the cause of environmental aquatic hazard. So, their use at large scale may cause to transfer to the aquatic environment and the generation of wastewaters from IL industrial processing may represent an important problem which demands adequate solutions.

While ILs cause little threat to atmospheric toxicity, a growing number of evidences suggest that they can be toxic to aquatic organisms, including bacteria, plants, invertebrates, and fish. The boom of designer solvent synthesis has sparked a corresponding increase in rapid IL toxicity testing, so it has been recently evaluated in different microorganisms involving, *Vibrio fischeri* [86,87], *Daphnia magna* [88], animal cells [89], algae [90], *Escherichia coli* [91], lactic acid producing bacteria [92] and acetyl-cholinesterase [93]. As can be inferred from these large number of studies, ILs present high toxicity, being highly influenced by their chemical structure. So, a recent study of our group [77] demonstrated that the ILs ecotoxicity can be directly related with their polarity [94]. In fact, hydrophobic ILs are more toxic than hydrophilic ones, because of their higher capacity to accumulate in biological membranes. So, details of their solubility in aqueous effluents may be able to provide relevant information on

the toxicity of specific ILs in the environment [88,95,96]. Generally, IL toxicity decreases with the increase of localized negative (or positive) charge in the anion (or cation), which means that anions with a single negative atom are likely less toxic or do not affect significantly toxicity. Thus, those ILs with longer alkyl chains on the cations were more toxic [86]. Moreover, taking into account the cation of IL, some publications have shown that the aromatic cations (imidazolium and pyridinium) are, in general, more toxic than the non-aromatic ILs, such as pyrrolidinium, piperidinium, phosphonium or ammonium [97,98].

Biodegradability could be a drawback in designing safer and sustainable ILs, because the tendency of most ILs to be thermally and chemically stable, as can be reflected by their great stability in relation to biological degradation processes [99,100]. Moreover, because of ILs present elevated stability in water these compounds could become as persistent pollutants in wastewaters. For this reason, it is fundamental to solve the further consequences and the environmental risk of the presence of ILs in aqueous streams. Taking into account the chemical structure, the biodegradability of ILs appears to be a cumulative contribution from the ion combination. Biodegradable anions are usually organic species, such as octyl sulfates, acetate and naphthenic acids like 3-cyclohexylpropionate [101]. For inorganic anions, the biodegradation efficiency decreased in the hydrophilic order $\text{PF}_6^- > \text{BF}_4^- > \text{Cl}^-$ [102]. Summarizing, as the ILs could become persistent pollutants and break through classical treatment systems into natural waters may require effective treatments aqueous effluents.



Chapter 2

TREATMENTS OF IONIC LIQUIDS FROM AQUEOUS EFFLUENTS

CHAPTER 2. TREATMENTS OF IONIC LIQUIDS FROM AQUEOUS EFFLUENTS

2.1. Overview of ionic liquids treatment from aqueous phase

ILs are classified as green solvents in comparison to conventional organic solvents, but their chemical and thermal stability and the high solubility of some of them in water is of significant relevance and they may cause a serious risk to the environment since their wide range of toxicity and biodegradability. Their synthesis and industrial applications could produce waste streams containing considerable amount of ILs in water effluents [103,104] and it might represent an important problem demanding adequate solutions. Therefore, the potential of ILs to become persistent pollutants requires the development of effective technical strategies for removing ILs from aqueous streams. This chapter assesses the techniques related to the purification of the water containing ILs.

Several publications have focused their attention on oxidative and thermal degradation of ILs in aqueous phase [105-107]. The oxidative degradation showed that the greatest degradation efficiency for imidazolium ILs was achieved with a combination of UV light and a catalytic oxidant such as hydrogen peroxide or titanium dioxide. Imidazolium cations of hydrophilic ILs are easily degraded by chemical oxidation, although the toxicity of the remaining anions and oxidation products has to be considered. The usefulness of advanced oxidation systems for the degradation of largely hydrophobic ILs in water has barely been examined [108-110]. Oxidative degradation in the presence of reactive peroxides generated by Fenton reagent has been also applied for the removal of ILs from water [110-113]. The level of degradation was dependent on the alkyl chain length [106], where it was showed that increasing the alkyl chain lowered the rate of IL degradation. On the other hand, the influence of the anion has been also analyzed, demonstrating that anions, originating from ILs or found

in the background, highly influence IL degradation efficiency. Additionally, the negatively charged anions can interact with the positively charged catalyst used in Fenton reactions, and may influence the oxidation process [113].

Biological treatments seem to be more environmentally friendly compared to chemical decomposition process [102,114-119]. However, they have been limited by the low biodegradability of ILs and even high toxicity to some microorganism of the long cations containing long alkyl chain [120]. Biodegradability of ILs is a complicate treatment due to their chemical and physical properties. Firstly, ILs consist of large organic cations, such as imidazolium, pyridinium and phosphonium, among others, with alkyl chain substituents that alter the hydrophobicity of the compounds, and combined with a variety of anions of different chemical nature, giving an enormous range of cation/anion combinations. In addition, many different functional groups have already been incorporated into IL cations and anions, e.g., alkenes, ethers, esters, alcohols, etc. Consequently, understanding the biodegradability mechanism of these functionalized ILs becomes more complicated. In general, ILs have been demonstrated difficult to be biodegradable using standard tests of biodegradability [81,121]. Certain level of biodegradability has been founded with the addition of short functional group (ether, hydroxyl and others) to cations of IL [101,116,122,123], or including in the IL anions with organic character as acetate, glycolate, alkylsulfate, etc. However, it has been recently reported a study that shows an efficient biodegradation of common ILs by using a microorganism (*Sphingomonas paucimobilis* bacterium) specifically selected for this purpose [119].

In any case, the alternative of recovering ILs by non-destructive separation methods should be promoted in terms of viability and sustainability. Due to the high costs of ILs and the environmental and financial policy of the waste framework legislation, recovery and regeneration are fundamental issues in process development based on IL systems [124].

Therefore, the research on non-destructive treatments for removing ILs from wastewater present the additional interest of the opportunity of later recovery of IL compound [125]. Generally, the techniques employed for regeneration and recovery of ILs, such as vacuum distillation [126], crystallization [127], liquid–liquid extraction [128,129], nanofiltration [130] or pervaporation [131], cannot be easily applied the treatment of ILs in water at low concentrations.

Adsorption is an important technology that is widely used to remove several kinds of pollutants from water [132,133]. The effectiveness of sorption depends fundamentally on the characteristics of the substance to be adsorbed and on the type of adsorbent. In addition, operating conditions could lead to short contact times to ensure equilibration. Adsorbents such as AC [134,135], ion-exchange resin [136], activated sludge [137] and fermentation waste [136] have all been used to remove hydrophilic ILs from aqueous solutions. In terms of uptake, the ion-exchange resin exhibits the best adsorption efficiency, but the process is relatively slow. AC gives a faster rate of sorption, but the affinity of hydrophilic ILs for this sorbent is much poorer compared to ion exchange resin, while the adsorption on activated sludge and fermentation waste is insignificant. Taking into account the kinetic of the adsorption, the higher average pore diameter in AC facilitates the comparatively easy diffusion of ILs into the pore structure, enhancing the rate of the sorption [134,135]. The affinity of ILs for AC was noted resulting of diverse intermolecular interactions (polar, π - π , van der Waals and hydrogen bonding) [138]. Ion exchange is minimal at acidic and neutral pH, but is significantly enhanced at basic pH values, where deprotonation and the generation of negatively charged functional groups takes place on the carbon surface [136]. The role of van der Waals interactions between the non-polar groups of the cation and the organic matter has also been investigated using soil and sediments [137,139-143].

These previous reported works showed the adsorption as a non very successful technique for ILs treatment from aqueous phase, however preliminary essays in our laboratory indicated that the AC as a proper adsorbent material for the optimization of this treatment, because of its excellent and versatile properties to this end.

2.2. Adsorption on activated carbon as separation treatment

Between all the possible adsorbent candidates, AC is one of the most interesting materials. Their adsorptive properties are due to their high surface area, microporous structure and high degree of surface reactivity. Moreover, their chemical properties are easily adaptable, which make them attractive to modulate their surface groups in order to uptake different kinds of adsorbates, depending on our needs [144]. ACs are used to purify, decolorize, separate, and concentrate, permitting recovery, remove, or modify the harmful constituents from liquid solutions [145-147]. Consequently, AC adsorption is of interest to many economic sectors and concern areas as diverse as food, pharmaceutical, chemical, petroleum, nuclear and vacuum industries as well as for the treatment of industrial waste water [148,149]. The surface physical and chemical structure of ACs takes importance in the interaction between solid-liquid interfaces and the AC adsorption of different solutes from solutions. So, the study of the aspects concerns to remove/recover ILs from aqueous solutions using ACs as outstanding material for the treatment of IL may be one of the objectives of the present dissertation.

2.3. Characterization of adsorbents

The characterization of the solid adsorbents by different techniques allows us correlating the porous structure and surface chemistry of the adsorbents with their capacity for retaining different solutes from gas or aqueous streams. Table 2.1 lists the characterization techniques used to evaluate the physical and chemical properties of the adsorbents used in the research.

Table 2.1. Characterization techniques of adsorbents.

Characterization technique	Equipment used
Elemental analysis, EA	Perkin–Elmer analyzer (210 CHN model)
Nitrogen adsorption isotherms	Quantachrome apparatus (Autosorb-1 model)
Nitrogen adsorption isotherms	Micromeritics apparatus (Tristar II 3020 model)
Mercury porosimetry	Quantachrome apparatus (PM-3310 model)
Temperature programmed desorption, TPD	IR absorption analyzer (Siemens, model Ultramat 22)
Thermogravimetric analysis, TGA	Mettler Toledo Instrument (TGA/SDTA851e model)
Differential scanning calorimetry, DSC	Mettler Toledo instrument (DSC/821e model)
pH _{slurry} measurements	Crison pH-meter (basic 20 model)
Transmission electron microscopy, TEM	Philips 420 and JEM-4000 EX devices
Scanning electron microscopy, SEM	SEM (Hitachi S-3000N model)
Energy dispersive X-ray, EDX	EDX analyzer (INCAx-sight model)

Following it is detailed the information that can be extracted from the different techniques for the solid sorbents used in the work:

Elemental analysis:

Elemental analyses of solid adsorbent materials were carried out in order to obtain carbon, hydrogen and nitrogen elemental percentages. This technique is based on the total oxidation of the samples by means of a complete and instantly combustion, where it is quantified the CO₂ and H₂O concentration by infrared spectroscopy analyzers. The N₂ underwent during the analysis is determined by a thermal conductivity detector.

Nitrogen adsorption isotherms:

The adsorption isotherm can be defined as the amount of adsorbate (N_2) uptakes on a porous solid at different relative pressure of gas, keeping constant the temperature (77 K). Each isotherm point was obtained at an equilibrium point between the adsorbed gas volume and the relative pressure of the gas (P/P_0). When the relative pressure is next to the unity, it is possible to determine the amount of adsorbate uptake for decreasing values of relative pressure, knowing the resulted curve as desorption isotherm. From the adsorption desorption of N_2 at 77 K analyses it can be calculated the total surface area (A_{BET}), external area (A_s), pore width, pore distribution size and the pore volume as micro and mesopore.

In order to determine the total surface area from this technique, IUPAC recommends the methodology developed by Brunauer, Emmett y Teller [150], who develop the well known equation of BET. This equation relates the volume of adsorbed gas (N_2) in a monolayer of adsorbate on a solid (AC) at a determinate relative pressure (P/P_0). The BET equation was used to obtain the apparent A_{BET} at relative pressure between 0.02 and 0.2 and the Dubinin–Radushkevich equation for micropore volume estimation. The difference between the volume of N_2 adsorbed (as liquid) at 0.95 relative pressure and the micropore volume was taken as mesopore volume [151].

The micropore volume was calculated from the adsorption branch of the isotherm by means of t -method, applying the Hasley equation [152]. Lately, the mesopore volume was calculated from the amount of nitrogen adsorbed at relative pressure of 0.96 in the desorption branch of the isotherm. This zone is equivalent to pores with 50 nm of pore diameter, subtracting the micropore volume calculated by t -method to the total pore volume.

Experimentally, the samples were, previously to the analysis, outgassed by two different ways, depending on the equipment used. In Tristar apparatus the samples were outgassed during 8 hours at 150 °C to an atmospheric pressure. On the other hand, in Quantachrome apparatus the samples were outgassed at 150 °C for 5 h to a residual pressure of 10^{-3} Pa.

Mercury porosimetry:

Mercury intrusion porosimetry was used to determine the mesopore and macropore volumes and pore size distribution of the samples, where the adsorption of gases cannot be applied, so the mesopore volume in the range not covered ($2 < d_{pore} < 6$ nm) by mercury porosimetry is obtained from the N₂ isotherm. It can be based on the non wettability of mercury, i.e. the constant angle with the solid surface is higher than 90° and so the pressure has to be higher in order to come into the pores. In the mercury porosimetry measurements the estimation of pore diameter from the applied pressure was based on the Washburn equation.

$$\Delta P_r = -2\gamma \cos\theta \quad \text{eq. 2.1}$$

where ΔP_r is the need pressure to force the mercury put into a pore of radius r , γ is the surface tension of mercury and it was taken as 4.8×10^{-3} N·cm⁻¹ and θ is the mercury contact angle, estimated as 141° [153-155].

The textural analysis carried out by means of adsorption-desorption N₂ isotherms and mercury porosimetry cover the whole porosity of the surface of the solid samples. This analysis reflects the distributions of the hollows and pores and their quantification based on different characteristics parameter, such us:

- *Specific surface* (A_{BET}) is the total surface per unit of solid weigh. In this sense, the inner surface corresponds to the micro and narrow mesopores of the solid, while the *external surface* (A_s) is mainly the surface is held to wide mesopore and macropore.
- *Pore volume* is the totally volume of the pores per unit of solid mass. IUPAC (International Union of Pure and Applied Chemistry) admits three kinds of pores, depending on its size: micropore ($d_{\text{pore}} < 2 \text{ nm}$), mesopore ($2 < d_{\text{pore}} < 50 \text{ nm}$) and macropore ($d_{\text{pore}} > 50 \text{ nm}$).
- *Pore diameter* is the transversal section of each pore. The shape of most of the material is considered as cylindrical; however, AC based material present slit-shaped (parallel plates) or ink-bottle pores (narrow neck and wide body).
- *Pore size distribution* represents the pore volume corresponding to the diameter of considered pore. From the distribution study it can be inferred what kinds of pore diameter are more often and their quantification, giving a better description of the porous structure.

Temperature programmed desorption (TPD):

The nature, distribution and amount of surface oxygen groups were analyzed by temperature programmed desorption under N_2 flow. For the TPD analyzes samples of 100 mg was placed in a vertical quartz tube in nitrogen flow of $1 \text{ NL}\cdot\text{min}^{-1}$ at a heating rate of $10 \text{ }^\circ\text{C}\cdot\text{min}^{-1}$ from 50 to $1100 \text{ }^\circ\text{C}$. The evolved amounts of CO and CO_2 were continuously analyzed. The CO and CO_2 TPD profiles were deconvoluted using PeakFit 4.12, selecting a multiple Gaussian function to fit each deconvolution peak [156]. The desorbed amount of CO and CO_2 is a measure to quantify the surface oxygen groups contained in the AC, however there are differences in the literature to assign the intervals for the specific functional groups, because of the temperature peak of the curve can be affect by the textural properties of the tested material, the temperature rate or other characteristics of the experimental systems used.

Table 2.2 collects the temperature desorption intervals for the assignation of different surface oxygen groups taking into account data reported in the literature [157-161].

Table 2.2. Assessment of oxygen surface groups from deconvolution of TPD profiles for the activated carbons.

Functional groups	Evolved groups	Desorption temperature (°C)
Carboxylic acids	CO ₂	100 - 400
Carboxylic anhydride	CO, CO ₂	400 - 600
Lactones	CO ₂	500 - 700
Phenols	CO	600 - 700
Carbonyl	CO	700 - 900
Chromenes	CO	750 - 850
Pirones	CO ₂	800 - 1100

Thermogravimetric analysis (TGA):

TGA analysis keeps us to determine the humidity loss, decomposition and transformation related with the studied material. The analyses were conducted under nitrogen atmosphere with a heating rate of 10 °C·min⁻¹. The accuracy of temperature and mass measurements was 0.1 °C and 10⁻³ mg, respectively. A dynamic method was used with a temperature range from 50 to 600 °C at a heating rate of 10 °C·min⁻¹ while purging with 50 ml·min⁻¹ of dry nitrogen. The mass of the sample placed in TGA analyses were between 4 and 12 mg. Aluminum pans with a capacity of 70 ml were used. The temperature measurements were carried out with accuracy better than 0.1 °C. Methodology, based on accurate thermogravimetric measurements and developed for the analysis of decomposition of samples, that undergo an $\alpha_{(s)} \rightarrow \beta_{(s)} + \gamma_{(g)}$.

Differential scanning calorimetry (DSC):

DSC curves of samples were determined at a $10\text{ }^{\circ}\text{C}\cdot\text{min}^{-1}$ heating rate between 50 and 600 $^{\circ}\text{C}$. In all experiments, stainless steel pans with a volume of 120 μl and a purge flow of 50 $\text{ml}\cdot\text{min}^{-1}$ of dry nitrogen were used. The sample mass range used in DSC experiments was between 10 and 20 mg and the temperature measurements were carried out with accuracy better than 0.1 $^{\circ}\text{C}$. The nature of the decomposition process (exothermic or endothermic) can be deduced depending on the orientation of the obtained peaks.

Both analyses (TGA and DSC) let us establish the proper conditions in order to carry out the thermal treatment of the samples and also check the thermal stability of the ACs.

Transmission electron microscopy:

The transmission electron microscopy (TEM) keeps us to gain structural and morphological information at nanometric level. In this technique an electrons beam is focused on a thin sample by two condensed lenses. After crossing the sample, the electrons are collected and focused on an objective lens and moreover the image is increased with two projector lenses. Finally, the image is projected over a fluorescence screen.

Experimentally, the powder samples were dispersed using an organic solvent (ethanol for carbonaceous samples and hexane for samples contained IL, in order to not take out the IL from the solid matrix) and were place on copper grids. Once evaporate the solvent the samples were analyzed using the transmission electron microscopy.

Scanning electron microscopy and energy dispersive X-ray

The Scanning electron microscopy (SEM) is a technique which keeps us to know structural and morphological information at micrometric level about the shape and size of the solid material and the particles incorporate to. In SEM microscopy, electrons beams are incised over the sample, with accelerating voltage of 20 kV. The beam is carried by the surface of the sample thank a collection of deflective coils. When the primary beam is on contact with the sample surface, some of the electrons are reflected and others are entered into some atomic layers, following a path before come back to the surface. The intensity of the emissions is varied depending on the angle between the incident beams with the surface material, i.e. depends on the morphology of the sample. The samples were placed in the microscope chamber after gold metallization treatment and the emitted signs were collected by a detector and were amplified (25000× increases). In this study was used a scanning electron microscopy coupled to an analyzer by energy dispersive X-ray.

SEM and TEM techniques keep us to obtain structural and morphological information at micrometric (SEM) and nanometric (TEM) level and make possible to detect different phases or porosities in the studied samples.

$\text{pH}_{\text{slurry}}$ measurements:

The acid or basic character of the material is relatively complex by the classical characterization techniques based on the adsorption of gaseous molecules with acid or basic character. Nevertheless, aqueous phase reactions, pH measurements give interesting information about the surface polar character, denoted as $\text{pH}_{\text{slurry}}$, which indicates about the electronic surface of the material [162]. The $\text{pH}_{\text{slurry}}$ were determined measuring, until constant value, the pH of an aqueous suspension of catalyst in distilled water ($1 \text{ g} \cdot 10 \text{ mL}^{-1}$) [163].

2.4. Adsorption of ionic liquids from aqueous phase on activated carbon

This dissertation introduces the first research on a effective treatment of imidazolium-based ILs from aqueous streams by adsorption using ACs as an affordable environmental application [164,165], thanks to the favourable IL-AC interactions. The results are collected in [Paper I](#) and [Paper II](#). As the combination of anion and cation making the ILs are numerous, it was found a great diversity of available ILs, opening a wide range of physical and chemical properties. So, current studies include the adsorptions of 27 ILs in aqueous solution using ACs as adsorbents in a batch system using ACs as adsorbents. Adsorption isotherms data for all ILs are successfully fitted to the Freundlich and Langmuir equations. Factors strongly influencing the adsorption capacities were the hydrophobic nature of both cation and anion of IL and its size. Considering the chemical nature of the IL, there is a rise in the adsorption capacity of AC as imidazolium-based ILs are composed of hydrophobic cations (Omim⁺ or Hxmim⁺) and anions (NTf₂⁻ or PF₆⁻), yielding the significant retention of ~1000 mg of IL per gram of adsorbent (for OmimPF₆). These results strongly support the potential of adsorption with ACs for recovering hydrophobic ILs from water solutions.

The physical and chemical properties of AC are also highly influencing the adsorption of ILs. Current results have evidenced that some steric effects restricting the adsorption of ILs with large molecular volume. Taking into account the porous structure of the adsorbents, it was proved that microporous/narrow mesoporous ACs ($d_{pore} < 8$ nm) present highest adsorption capacities. The dependence of the adsorption uptake considering the chemical structure of the ILs can be explained by means of the quantum-chemical COSMO-RS model, which provides information of the intermolecular interactions between the IL and the AC. Some insight into the adsorbent modifications needed for improving of the adsorption of specific ILs were achieved and successfully applied to the adsorption of hydrophilic ILs by oxidized ACs. Consequently, hydrophilic ILs could be more efficiently removed from aqueous streams by using ACs with high content of polar groups in their surface, which promote

hydrogen bonding adsorbate–adsorbent interactions. Based on this, commercial ACs were subjected to chemical treatments for increasing their polarity with the aim of improving the adsorption of hydrophilic ILs (short alkyl chains, Emim⁺, and hydrophilic anions, Cl⁻ or MeSO₃⁻), whereas the retention of hydrophobic ILs was improved by thermal treatment of commercial ACs, which removes polar groups from their surface.

We have also developed a thermodynamic study from the equilibrium data. The values of ΔH , ΔG , and ΔS were calculated, indicating the nature of the process. The enthalpy of the process is negative, implying an exothermic adsorption process and the estimated values for free energy changes were negative, indicating the spontaneous character of the adsorption. These results are indicative of a physical adsorption phenomenon. The kinetic aspects involved in the adsorption process are also discussed. So, a detailed kinetic analysis of the adsorption of a hydrophobic IL (OmimPF₆) by commercial ACs was performed including the effect of main operating conditions as stirring velocity, AC particle size, temperature and IL initial concentration.

2.4.1. Thermodynamic study

It has been developed the thermodynamic study from the equilibrium data. The amount adsorbed q_e (mmol·g⁻¹) at each equilibrium concentration C_e (mmol·L⁻¹) was calculated by using the expression:

$$q_e = \frac{C_0 - C_e}{w} \quad \text{eq. 2.2}$$

where C_0 represents the initial adsorbate concentration and w is the adsorbent dose. Two well-known isotherms equations were used to fit the equilibrium data: Langmuir (eq. 2.3) and Freundlich (eq. 2.4) models, which are written as:

$$q_e = \frac{q_{\max} BC_e}{1 + BC_e} \quad \text{eq. 2.3}$$

where C_e is equilibrium concentration of solute in solution, q_e is amount of solute on the solid sorbent at equilibrium, B is the equilibrium constant related to the affinity of the binding sites for the solute or the Langmuir constant, and q_{\max} is the sorbent capacity (maximum possible amount of solute adsorbed per unit mass of adsorbent).

$$q_e = K_F C_e^n \quad \text{eq. 2.4}$$

where K_F is a constant that is taken as an indicator of the adsorption capacity, since, as K_F increases, the adsorption capacity increases. Parameter n gives an idea of the grade of heterogeneity in the energetic centers distribution and is related to the magnitude of the adsorption driving force.

The adsorption involves the accumulation of molecules from a liquid phase onto the external and internal surface area of the adsorbent. This surface fact is a group of interactions among the aqueous phase, the adsorbate, and the adsorbent. The thermodynamic analysis provides information about the process ability to take place and the stability of the adsorbed phase as well. If it is assumed the adsorption process as a dynamic process of adsorption/desorption, it can be formulated as a chemical reaction: $A + B \leftrightarrow AB$, where the equilibrium constant K can be expressed as follows:

$$K = \frac{[AB]}{[A][B]} \quad \text{eq. 2.5}$$

A is the free IL in the aqueous phase at the equilibrium, C_e ($\text{mmol}\cdot\text{L}^{-1}$); AB is the IL onto the solid phase at the equilibrium, q_e ($\text{mmol}\cdot\text{L}^{-1}$), referred to the aqueous phase, and B is the IL free, $(M - q_e)$ ($\text{mmol}\cdot\text{L}^{-1}$), referred to the IL in the aqueous phase in relation to the maximum capacity, M ($\text{mmol}\cdot\text{g}^{-1}$). Then, eq. 2.5 can be rewritten as:

$$K = \frac{q_e}{C_e(M-q_e)} \quad \text{eq. 2.6}$$

where q_e and C_e resolve the isotherms.

Applying the Van't Hoff equation to the adsorption equilibrium it can be calculated the enthalpy of the process [166]. If ΔH does not depend on the temperature or does a little, and the $\ln(1/C_e)$ versus $(1/T)$ plots corresponding to a given value of q_e are reasonable linear, then the slopes of these plots yield the enthalpies divided by the ideal gas constant. This method permits the calculation of ΔH at various levels of surface coverage.

$$\ln \frac{1}{C_e} = \ln K_0 - \frac{\Delta H}{RT} \quad \text{eq. 2.7}$$

where ΔH is the isosteric heat of adsorption, R is the ideal gas constant, T is the absolute temperature, and K_0 is a pre-exponential factor.

The free energy of adsorption has been calculated from the equation derived from the Gibbs adsorption equation [167]:

$$\Delta G = \frac{-RT}{n} \quad \text{eq. 2.8}$$

where ΔG is in $\text{kJ}\cdot\text{mol}^{-1}$ of IL consider as solute. Therefore, ΔG depends on the temperature and the parameter n of the Freundlich equation.

Lately, the entropy change values can be estimated using previously calculated ΔH and ΔG values and the Gibbs-Helmholtz equation:

$$\Delta S = \frac{\Delta H - \Delta G}{T} \quad \text{eq. 2.9}$$

So, the values of thermodynamic parameters of adsorption such as free energy, enthalpy, and entropy are calculated, and can illustrate the nature of the process [168].

2.4.2. Kinetic study

A detailed kinetics study of the adsorption is essential to supply the fundamental information required for the design and operation of adsorption equipment, detailed in [Paper III](#). Many attempts have been made to formulate a general expression describing the kinetics of adsorption on solid surfaces for liquid-solid phase sorption systems. This dissertation presents 5 different kinetic models in order to describe the experimental kinetic curves of IL adsorption of commercial ACs. The experimental and theoretical evidences indicated that intra-particle diffusion is the prevailing rate-controlling step in the adsorption mechanism of the OmimPF₆, used as reference IL, onto AC. So, the adsorption rate of the IL can be efficiently enhanced by decreasing the adsorbent particle size.

The hyperbolic model [169] is a simple mathematical equation widely used to fit kinetic experimental data in terms of the empirical coefficients q_e and k_f . The parameter q_e is the asymptotic value of q_t and is commonly used as a reference of maximum uptake of solute on the adsorbent and it can be fitted to the expression:

$$q_t = \frac{q_e \cdot t}{k_f + t} \quad \text{eq. 2.10}$$

The pseudo first-order (eq. 2.11) for the liquid-solid adsorption is an empirical kinetic model proposed in the Lagergren's original paper [170], which provides a pseudo-first order rate constant k_1 by defining the driving force for the process as $(q_e - q_t)$:

$$\log(q_e - q_t) = \log q_e - \frac{k_1}{2.303} t \quad \text{eq. 2.11}$$

Pseudo-second-order (eq. 2.12) and Lagergren (eq. 2.13) models [171,172] are modifications of the pseudo-first order equation by defining the driving adsorption forces as $(q_e - q_t)^2$ and $(q_e - q_t)^n$, respectively, providing the apparent rate constants k_2 and k_3 for the adsorption process.

$$\frac{t}{q_t} = \frac{1}{k_2 q_e^2} + \frac{t}{q_e} \quad \text{eq. 2.12}$$

$$\frac{t}{q_t} = \frac{1}{k_s q_e^n} + \frac{t}{q_e} \quad \text{eq. 2.13}$$

In these last three simple models, all the steps of adsorption such as external diffusion, internal diffusion, and adsorption are gathered together in the rate constant and it is assumed that the difference between the average and the equilibrium solid phase concentrations is the driving force for adsorption.

Alternatively, the intraparticle diffusion model in [eq. 2.14 \[162\]](#) is a phenomenological kinetic model assuming that adsorbate transport through the adsorbent particle is the prevailing rate-controlling step in the adsorption process, which is often the case, especially in a well stirred batch systems [\[173-176\]](#). The parameter k_{id} is defined as the pore diffusion rate constant, whereas the intercept I is a constant related with the thickness of boundary layer.

$$q_t = k_{id} t^{1/2} + I \quad \text{eq. 2.14}$$

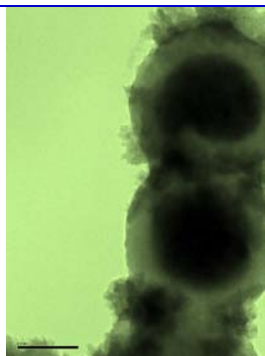
There are many different reasons influencing the adsorption rate for a solved solute on a porous adsorbent. Parameters such as particle size or porosity of the adsorbent are included in kinetics mathematical models. On the other hand, the operating conditions such as batch shaking, initial solute concentration or temperature could determine the equilibrium time.

All the units of the different constants and variables are reported in the [Appendix I](#).

2.4.3. Recovery of ionic liquid and activated carbon regeneration

It is important to remember that ILs are still quite expensive media and their regeneration makes such a technology economically all the more justified. With independence of the different efficiency reported destructive treatments, such as thermal degradation [107], chemical oxidation [112,113] or biological treatments [116-119], they do not permit the IL recovery.

It is proposed a successful regeneration process for the exhausted adsorbent, based on acetone solvent, validated for two commercial ACs. Acetone was chosen as regenerant agent because of its preferential chemical properties. Acetone is an excellent solvent for several ILs (tested for OmimPF₆) and moreover acetone can be easily removed from regenerating solution by means of a simply atmospheric distillation, obtaining the recovery of the IL compound, whose chemical structure was analyzed by ¹H-NMR spectroscopy.



Chapter 3

ADVANCED MATERIALS BASED ON IONIC LIQUIDS ON SOLID SUPPORTS

CHAPTER 3. ADVANCED MATERIALS BASED ON IONIC LIQUID AND ACTIVATED CARBON

3.1. Introduction to IL-based materials

This chapter introduces two kind of novel advanced materials based on IL and activated carbons (AC), called supported ionic liquid phase (SILP) and encapsulated ionic liquid (ENIL). There are often restrictions due to the physical properties of neat ILs, such as high density and viscosity, which greatly impede fluid flow and limit the mass transfer rate from the viewpoint of practice. These negative effects have motivated the development of new advanced materials based on the idea to combine IL (high solvent capacity) with solid supports, approaching the advantages of the separately neat compounds to only one material. This combination makes them highly attractive for potential applications, such as catalysis [177-179], electrochemistry [180] and separation processes [181-183].

The use of novel IL-based materials in this dissertation is focused on the application as sorbents in gas treatments. The development of efficient systems for the gas application does not only concern the optimization of their thermodynamic properties to retain gaseous solutes by sorption process, where the IL based materials play an outstanding role, but also the optimization of the transport properties to enhance the mass transfer rate.

3.1.1. Supported ionic liquids phase (SILP)

Supported ionic liquid phase (SILP) consists on a small amount of IL dispersed on the internal surface of a porous material, creating a physisorbed thin film in a nanometric range, schematized in Figure 3.1. The concept of SILP materials have recently been introduced to overcome the mass transfer limitation of ILs and reduce their required amount due to enhanced solute-SILP interactions, resulting a lower cost and improved efficiency [182,183]. Making use of the high exchange surface and short diffusion distances presented by these materials, greatly efficient catalytic [184], electrochemistry [185] or separation processes [182] could be achieved. Moreover, the combination of ILs and organic or inorganic supports allows the synthesis of tailor made SILP systems for a variety of applications [182,186-188]. Precisely, the used of SILP materials have been demonstrated to be efficient in a continuous gas cleaning process, such as CO₂ [189], SO₂ [183] and alkenes [190] and they are going to be asses as sorbent material in the present dissertation. It is important to remark that their use as

solid sorbents is macroscopically an adsorption but microscopically adsorption and absorption processes may be involved.

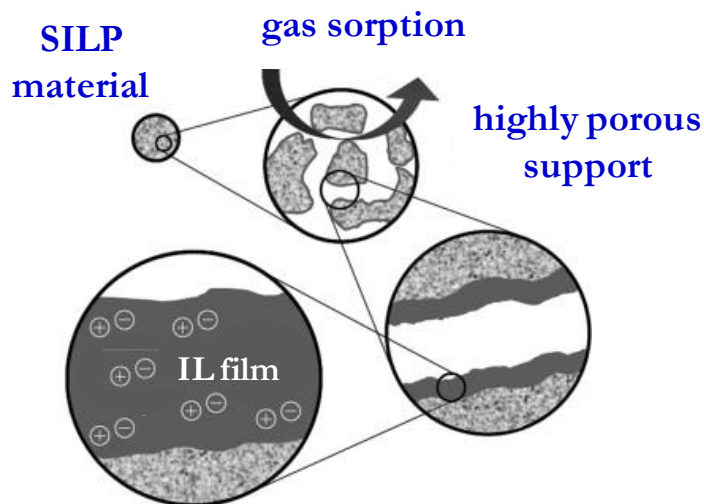


Figure 3.1. Schematic representation of a Supported Ionic Liquid Phase (SILP).

3.1.2. Encapsulated ionic liquid (ENIL)

It is presented a novel material called encapsulated ionic liquid (ENIL) consisting on IL confined into hollow submicrocapsules and depicted in Figure 3.2. The low amount of IL contained in SILP material may limit its benefit as solvent in reactions or separation processes. In this sense, ENIL material discretizes the IL in small drops to increase the surface contact area and to improve mass transfer rate, but keeping the thermodynamic properties of the IL; therefore, moving from continue to discrete fluid. The small size and huge total interfacial area of microcapsules can contribute to overcome the difficulties in potential applications caused by high viscosity of the IL [191,192].

The starting point for ENIL design was the high affinity found between ILs and AC, demonstrated by adsorption experiments with a wide number of IL compounds [165]. In recent years, studies have been performed on the immobilization of ILs onto porous frameworks [191,193-195], however herein is presented the original version on ENIL material which allows to achieve apparently solid materials with a 85% content in mass of IL but in submicrometric particle size. ENIL systems present the tuning properties of IL solvents but enhancing the mass transfer rate which controls the further applications thank to the increment of the surface contact area upon the discretization of the IL fluid encapsulated in

submicroparticles. ENIL is a new class of advanced materials with remarkable versatility and favorable characteristics, which can be used to well-established technologies based on solid systems, but also can contribute to many IL research fields, including catalysis, electrochemistry or separation processes.

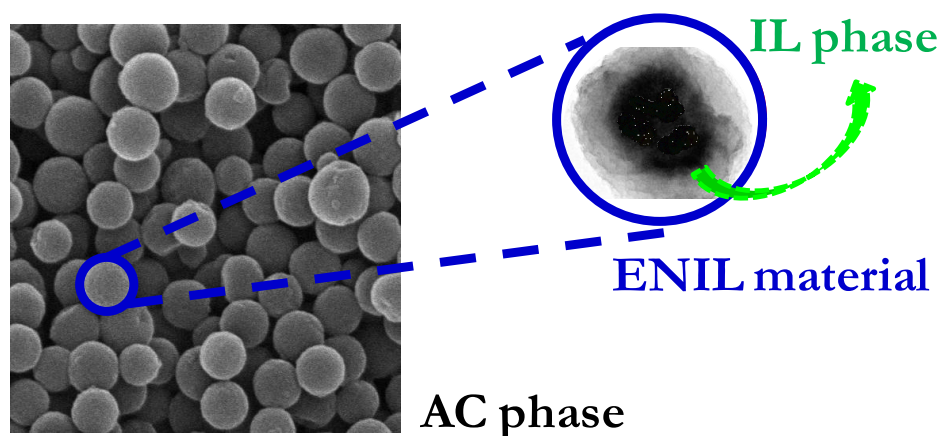


Figure 3.2. Schematic representation of an Encapsulated Ionic Liquid (ENIL).

3.2. Characterization of advanced materials

Because of the great advantages of advanced IL based materials and the need of a deeper understanding of their properties as reaction and separation media, the objective is to gather methods to conveniently characterize aspects of these materials as chemical composition, porous structure, thermal stability and morphology. Table 3.1 shows the different used techniques and the information that they provide. There are some previous publication separately assessed these characterization techniques, such thermal stability [183], surface porosity [196] or microscopy [195]. Other publication used infrared spectroscopy for verifying the presence of certain IL on solid support by [197] or the presence of some metallic atoms by X-ray photoelectron spectroscopy [191]. Table 3.1 collects the information that can be extracted from the different techniques proposed and applied in our laboratory to characterize IL-based advanced materials:

Table 3.1. Characterization techniques of IL-based advanced materials

Characterization technique	Information
Elemental analysis	IL quantify on solid support
Energy dispersive X-ray	presence of certain atoms
Nitrogen adsorption isotherms	microp. and mesopore volume quantification
Mercury porosimetry	mesop. and macropore volume quantification
Themogravimetric analysis	thermal stability (quantitative)
Differential scanning calorimetry	thermal stability (qualitative)
Transmission electron microscopy	morphology
Scanning electron microscopy	morphology

Elemental analysis and energy dispersive X-ray:

The development of quantitative procedures for determining the amount of IL incorporate to the supports is of interest not only to check the advanced material preparation, but also to evaluate the IL stability in determinate applications. In the case of solids containing imidazolium-based IL, elemental analysis was proposed as procedure to reliably quantify the IL content on the solid matrix, since it can be followed the presence of certain atoms as nitrogen. On the other hand, scanning electron microscopy is equipped with an energy dispersive X-ray (EDX) analyzer. This technique keeps us to know the distribution of the different chemical elements of interest in solid material, that take importance in the IL field because it is significant to check if the ions of the IL are presented in the synthesized material.

Nitrogen adsorption/desorption isotherms and mercury porosimetry:

Nitrogen adsorption isotherms and mercury porosimetry are complementary characterization techniques which inform us about how the IL is placed on the porous structure of solid matrix. Nitrogen adsorption desorption shows the distribution on micro and mesopores of solid material. On the other hand, mercury porosimetry is focused on wide mesopore ($d_{pore} > 6$ nm) and macropore, which took importance depending on the porous material studied. This merged information is important to check how the IL is distributed on the porous surface, to know the characteristic may gather the supporting material in order to incorporate high amounts of IL and the steric limitation of solid support could present. To our knowledge, it is the first time that is presented both techniques, but there are previous works collected the separately information [198-200].

Thermogravimetric analysis and differential scanning calorimetry:

Thermal properties of IL-based advanced materials were studied by using both thermogravimetric analysis (TGA) and differential scanning calorimetry (DSC) methods. TGA of tested materials under nitrogen atmosphere registers the mass losses and systematic TGA studies of the solid supports showed low losses, since the carbonaceous and inorganic materials tested are thermally very stable materials. However, the samples containing IL collected a weight loss during the analysis attributed to the IL loss. These measurements allow to quantify the amount of IL decomposed and the temperature when it occurs as it was collected in the literature [201,202], but for first time it has been systematically analyzed depending of the support used.

DSC method registers the energetic changes in the tested samples. Previous publications used the DSC analysis for the estimation of the heat capacity, glass-transition, freezing and melting temperatures [23,202]. For first time, it has been reported the DSC analysis at high temperature (25-600 °C). Exothermic and endothermic peaks can be obtained depending on the kind of decomposition happened, generally attributed to the anion and cation decomposed, in the case of IL. Moreover, depending on the material used as support these thermal changes can be highly influenced, so depending of its further applications and thank to these analysis, it can be chosen the proper material to ensure thermal stability at the operating conditions. Figure 3.3 shows an example of thermal study for a neat imidazolium based IL. The TGA curve describes when 1-hexyl-3-methylimidazolium hexafluorophosphate (HxmimPF₆) is decomposed and DSC curve reports two exothermic peaks (over zero line), which are assigned to PF₆⁻ anion at 370 °C and subsequently imidazolium cation at 400 °C.

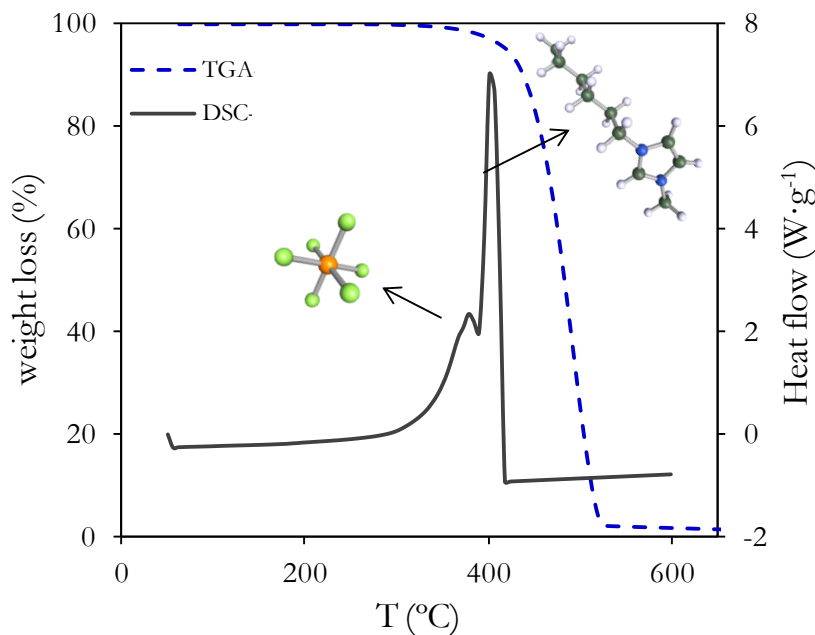


Figure 3.3. TGA (blue line) and DSC (black line) curves of HxmimPF₆ under nitrogen atmosphere with a heating rate of 10 °C·min⁻¹.

Transmission electron microscopy and scanning electron microscopy:

The microstructure and morphology of carbonaceous materials as support and IL-based system as SILP and ENIL were analyzed by transmission electron microscopy (TEM) and scanning electron microscopy (SEM). The pertinent microscopic analyses at the time to validate the experimental results are required. For example, Figure 3.4A-C shows some images in synthesis route of encapsulated ionic liquid material (ENIL), starting by the precursor carbon capsules which are formed by a siliceous solid shell and a solid core (A), the final carbonaceous capsules, consisting on porous shell and hollow core structure (C_{Cap}, B) and the encapsulated IL material (ENIL-R₁, C), containing the same proportion in weigh of IL and carbonaceous material. This analysis informs about the different step happening in the synthesis route of ENIL material in order to valid a right preparation.

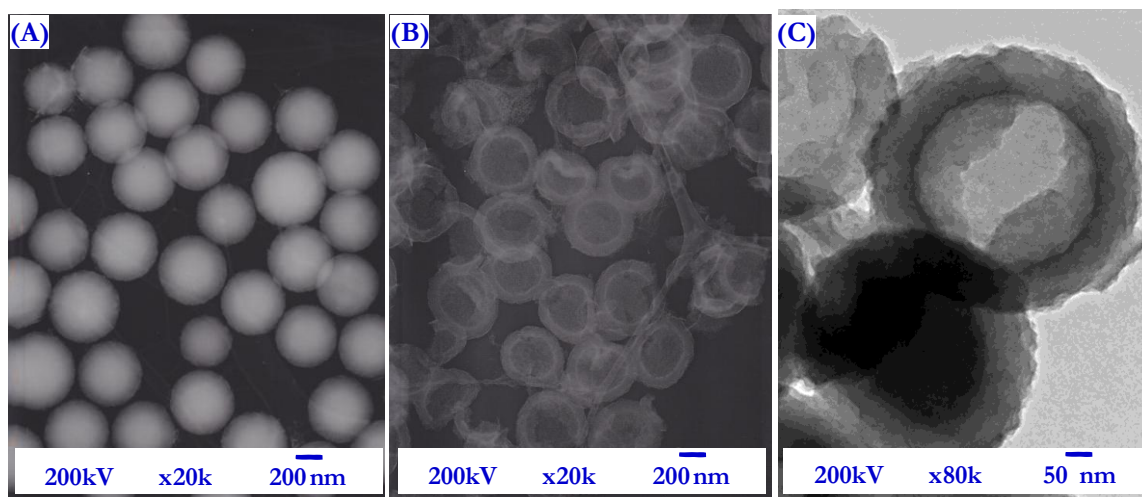


Figure 3.4. TEM images of precursor carbon capsules (A) the final carbonaceous carbon capsules C_{Cap} (B) and the final ENIL-R₁ material (C).

The morphology of solid samples was also analyzed by scanning electron microscopy (SEM). An example of the use of this technique in the correct synthesis of carbon capsules filled by IL (ENIL) is showed in the next images, resulting a well-defined vision of the analyzed sample, as can be seen in the Figure 3.5. The synthesis of carbon capsules (C_{Cap}) initially presented a deflected shape (A) which prevented the correct incorporation of IL, while Figure 3.5B showed the desired spherical shape in the carbon capsules. Figure 3.5C-D show the morphology by adding growing amounts of IL and it can be appreciated that ENIL material filled by a moderate amount of IL keeps the spherical morphology (C), while saturated ENIL material losses this morphology (D).

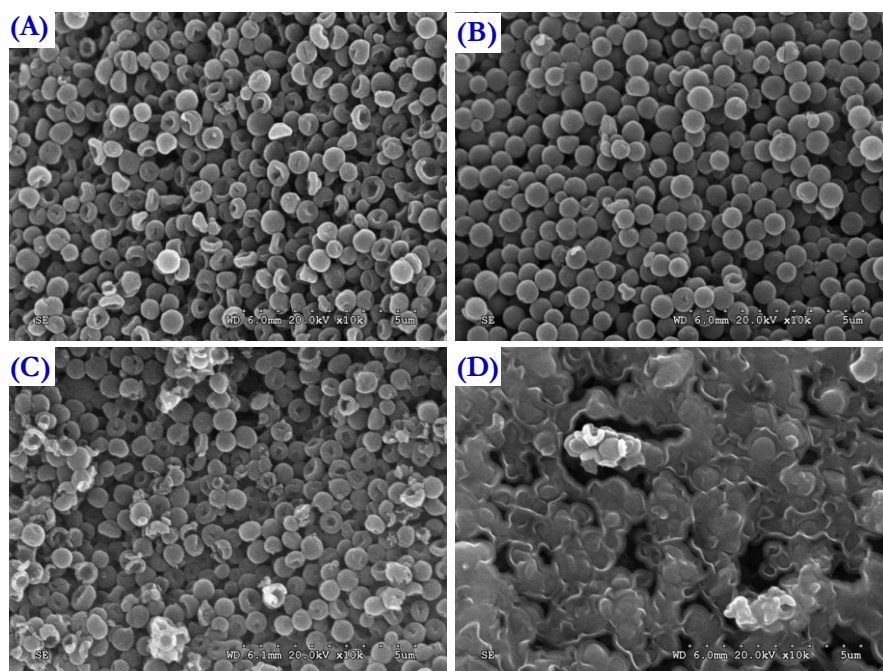


Figure 3.5. SEM images of carbon capsules with deflected (A) and spherical shape (B), mid filled of IL (ENIL-R₂, C) and saturated of IL (ENIL-R₅, D).

3.3. Applications of advanced materials: uptake of gaseous pollutants

In this dissertation, we introduce the application of advanced materials based on ILs in a continuous gas cleaning process. As preliminary study, it was investigated the adsorption of chlorinated volatile organic compounds on commercial ACs by means of experimentation in fixed bed reactor columns, obtaining a reference process in order to further applications using advanced materials based on IL. The next step involved the application of SILP materials prepared with ACs to uptake Cl-VOCs in fixed bed experiments; however, the incorporation of ILs to the carbonaceous matrix decreased the adsorption capacity of the system respect to the AC. So, it was set out the study of other pernicious gaseous pollutant with higher affinity toward ILs, such as ammonia [203]. On the other hand, the application of ENIL material as alternative to SILP was dealt, because the properties of ENIL could improve the absorption capacities of neat IL, commercial AC or SILP materials. So, this chapter assesses and justifies the treatment of different pollutants from gaseous streams using different experimental tests, describing the different models used to analyze the experimental data obtained.

3.3.1. Chlorinated volatile organic compounds (Cl-VOCs)

Chlorinated volatile organic compounds (Cl-VOCs) of formula $C_xH_yCl_z$ stand out for their high toxicities. Currently, the emission of organic chlorinated compounds into the atmosphere is a significant concern. Chloroform (TCM), dichloromethane (DCM) and monochloromethane (MCM) are some of the most common chlorinated compounds in residual gas streams. A brief summary of each chloromethane with their properties and industrial applications are collected in [Appendix 3](#). Because of their high toxicity [\[204\]](#), carcinogenic character [\[205\]](#), the potential contribution to the destruction of the ozone layer and to the global warming [\[206\]](#), their emission is progressively restricted by strong legal regulations. So, this leads to the necessity of developing effective and economic treatment easily compatible with the environment.

Nowadays, the main treatments for the removal of these pollutants are their incineration, but it may lead to more hazardous byproducts than the original contaminants, such as phosgene, dioxins and furans [\[207,208\]](#). On the other hand, at low Cl-VOCs concentration the use of catalysts is required for reducing the thermal needs [\[209,210\]](#). Thus, some other solutions are being investigated [\[211-213\]](#). Hydrodechlorination using different active catalyst, like Pt, Rh or Pd, is one of the most promising [\[214-216\]](#), although catalyst deactivation is so far a main disadvantage [\[217-219\]](#). Biological treatments using biofilters and biotrickling filters have been also studied [\[220-222\]](#). Adsorption, absorption and condensation are the most common non-destructive techniques for the removal/recovery of Cl-VOCs from gas streams [\[223-227\]](#). Adsorption on solid surfaces is an efficient, effective and economic process for removing hazardous and environmentally undesirable chemical compounds [\[144\]](#). Although adsorption can occur on a variety of surfaces, only a few porous materials are known to possess sufficiently high efficiencies for adsorbing chlorinated volatile organic compounds [\[228\]](#). Among porous substrates, the following have been successfully employed for performing separation tasks: activated carbon fibers, zeolites, and microporous silicas [\[229\]](#). The adsorption property of molecules inside pores depends not only on the character of the adsorbent surface but also on the shape, size, and chemical nature of the adsorptive species [\[230\]](#), so adsorbate properties may have to take into account for further treatments.

3.3.2. Ammonia (NH₃)

Ammonia is the most abundant base in the atmosphere and it is thus important in neutralizing acidifying pollutants such as sulphur dioxide (SO₂) and nitrogen oxides (NO_x), leading to particulate ammonium (NH₄⁺) in the atmosphere [231]. So, NH₃ emissions are important contributors to atmospheric pollution, leading to a wide range of different environmental problems which include the formation of fine particulate matter, eutrophication of ecosystems, acidification of soils and alteration of the global greenhouse balance [232-234]. Therefore, the development of techniques capable of capturing nitrogen reactive pollutants or reducing the volatility of ammonia-containing systems is of great interest. Between the most attractive treatments, separation by novel absorbents [235] and adsorbents [236] or elimination by dielectric barrier discharge reactors [237] are found. Recently task specific ILs used as potential ammonia absorbents at near-ambient temperatures and atmospheric pressure were proposed by our group [58,59], choosing 1-2-(hydroxyethyl)-3-methylimidazolium tetrafluoroborate (EtOHmimBF₄) as a proper IL due to the presence of the hydrogen bond donor, OH group, by means of simulation COSMO-RS tool. The absorption of NH₃ on neat ILs may serve of based in the comparison of ENIL efficiency to uptake NH₃ from gas streams.

3.3.3. Experimental uptake/desorption tests

This section depicts the two kinds of experimental set up used in the present dissertation for testing the uptake of the gaseous pollutants -chlorinated volatile organic compounds and ammonia- by different sorbents, such as AC, IL, SILP and ENIL materials.

Column experiments:

A realistic uptake model based on packed bed column was considered in order to the treatment of Cl-VOCs and NH₃ (used as solutes) using AC, SILP or ENIL as sorbent materials. The experimental setup consist on a continuous flow system (Microactivity-Reference unit, PID End&Tech), making up basically of a quartz fixed-bed column (1/4 inch diameter) coupled to a gas chromatograph with a flame ionization detector (Varian 450-GC) for Cl-VOCs or coupled to a quadrupole mass analyzer (OmniStar/ ThermoStar) in the case of NH₃, as can be seen in Figure 3.6. Experimental breakthrough curves were conducted under different operating conditions (temperature, pressure, total gas flow, inlet gas

concentration and bed length). Next, desorption experiments were performed after exhaustion of the sorbents using the same experimental set-up, passing a N_2 flow rate of $100 \text{ mL}\cdot\text{min}^{-1}$ through the column.

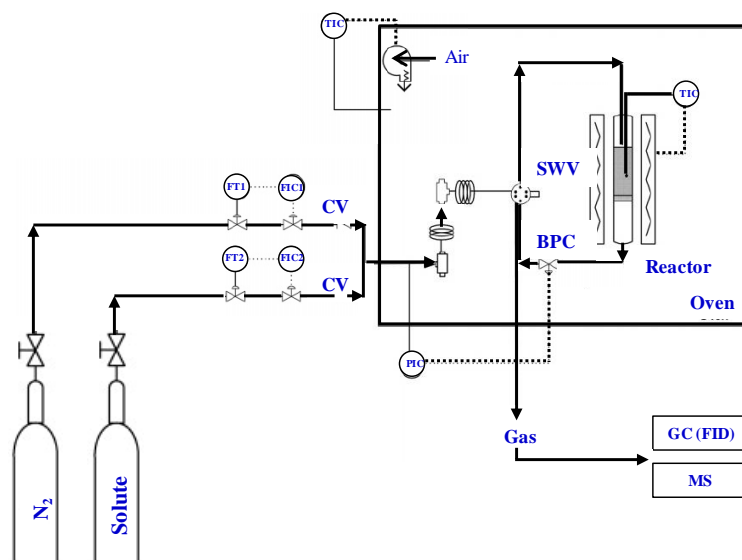


Figure 3.6. Schematic diagram of fix bed reactor for the gaseous solutes (NH_3 and Cl-VOCs) sorption treatment.

Gravimetric experiments:

The absorption and desorption curves were carried out in a TGA system at atmospheric pressure and $35 \text{ }^\circ\text{C}$ using around 20 mg of IL. The uptake kinetic and equilibrium data of the gaseous solute on neat ILs or ENIL materials were obtained by setting the inlet concentration of solute mixing with pure nitrogen and monitoring the weight increase of the sample, which allowed us comparing the absorption capacity of the neat IL with the advanced material based on IL and solid support at atmospheric pressure. The equilibrium was assumed when no further weight change was observed upon time (weight change rate $< 0.001 \text{ mg}\cdot\text{h}^{-1}$). The equilibration time depended on the sorbent material. The sorption and desorption curves were obtained in the same thermogravimetric system at $35 \text{ }^\circ\text{C}$. The balance has a weight range of $0 - 1000 \text{ mg}$ with a resolution of 0.1 mg . The temperature of the sample was maintained constant with a regulated external thermostat bath. Desorption was carried out at the sorption temperature with continuous dry nitrogen flow ($100 \text{ N}\cdot\text{cm}^3\cdot\text{min}^{-1}$), registering the loss of weight attributed to the desorption of the solute previously uptake. Figure 3.7 shows the experimental installation for this sorption technique.

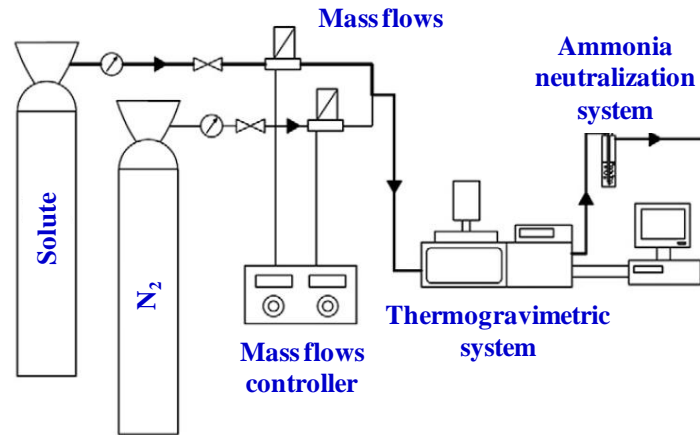


Figure 3.7. Schematic diagram of thermogravimetric analyzer for ammonia treatment.

Mathematic models:

This chapter presents the mathematical modeling used to describe the experimental data of different solutes (Cl-VOCs and NH_3) retention process carried out in thermogravimetric measurements or fixed bed columns using the different sorbent materials. Two theoretical models have been suggested to systematically fit the experimental data. Pseudo second order model for thermogravimetric analysis [238] and Yoon and Nelson model for fixed bed column experiments [239,240]. Figure 3.8 shows the examples of experimental data (dots) and predicted fits (lines) for the experimental measurements.

In gravimetric analysis, the mass of gas retained per mass of sorbent material versus time is registered. The saturation capacity (q_s) coincides when the capacity q_t is constant upon time at a given temperature and pressure, as can be seen in Figure 3.8A. On the other hand, the entire breakthrough curves were obtained in a fix bed reactor for different gaseous pollutants on sorbent materials, as can be seen in the example of Figure 3.8B. It was obtained the values of solute adsorption capacity at saturation (q_s) of different sorbent materials from the breakthrough curves for each experiment, calculated by:

$$q_s = \frac{Q}{m} \int_0^{t_s} C_0 - C dt \quad \text{eq. 3.1}$$

where Q is the gas flow rate ($\text{N}\cdot\text{L}\cdot\text{min}^{-1}$); m is the mass of adsorbent in the column (mg); t the time flow at which $C=C_0$ and C_0 and C the inlet and outlet DCM concentrations ($\text{mg}\cdot\text{L}^{-1}$).

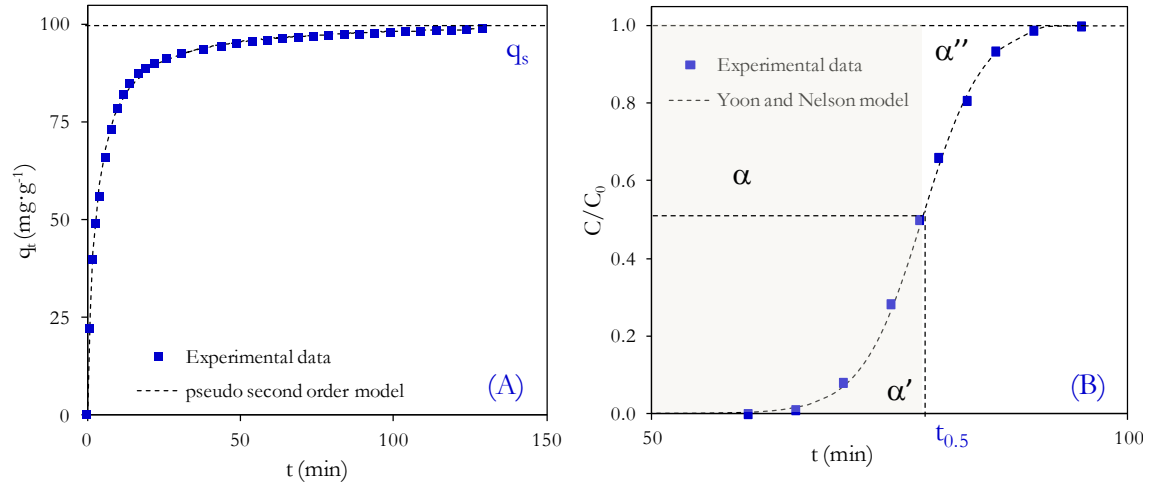


Figure 3.8. Graphical illustration of thermogravimetric analysis data (A) and the breakthrough curve (B).

Pseudo second order model:

The experiments related with sorption of ammonia on different solid supports carried out in the thermogravimetric analyzer were fitted by means of pseudo second order model. This expression is based on the kinetics in the retention capacity of different solutes onto sorbent material [238,241]:

$$q_t = \frac{q_s k_2 t}{1 + q_s k_2 t} \quad \text{eq. 3.2}$$

where k_2 is the pseudo-second-order rate constant, q_s is the amount of solute uptaken at equilibrium, and q_t is amount of solute on the surface of the adsorbent at any time, t . It can be rearranged and linearized, resulting:

$$\frac{t}{q_t} = \frac{1}{k_2 q_s^2} + \frac{t}{q_s} \quad \text{eq. 3.3}$$

This model has been successfully applied to describe the breakthrough curves of contaminant gases onto solid sorbents [228,242].

Yoon and Nelson model:

It is presented a theoretical approach based on gas adsorption kinetics. This theory is based on the assumption that the rate of decrease in the probability of adsorption for each molecule is proportional to the probability for adsorption (Q) and the probability for breakthrough (P):

$$-\frac{dQ}{dt} = \alpha Q P \quad \text{eq. 3.4}$$

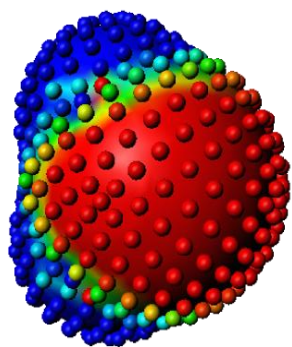
The theoretical model developed by Yoon and Nelson [239,240,243,244] was applied to describe the entire breakthrough curves and can be fitted to the expression:

$$t = t_{0.5} + \frac{1}{k} \ln \frac{C}{C_0 - C} \quad \text{eq. 3.5}$$

where C_0 and C are inlet and outlet concentration of adsorbate ($\text{mg}\cdot\text{L}^{-1}$), t is the adsorption time (min), k is the rate constant (time^{-1}), and $t_{0.5}$ is the time required for 50% adsorbate breakthrough (min). We may assume that the quantity of gas which breaks through the AC during the time interval $t = 0$ to $t = t_{0.5}$ is the same as the quantity of contaminant adsorbed during the time interval from $t = t_{0.5}$ until the AC is saturated with the gas, obtaining a symmetric breakthrough curve. The kinetic constant of Yoon and Nelson model (k) is directly depended on a dimensionless constant of proportionality (k'), the inlet concentration of chloromethane (C_0), the flow rate (Q) and inversely proportional to the mass of adsorbent:

$$k = \frac{k' C_0 Q}{m} \quad \text{eq. 3.6}$$

The Yoon and Nelson model is illustrated graphically in an example of a breakthrough curve of dichloromethane onto commercial AC of Figure 3.8B where the grey area α' is equal to the white area α'' , giving a symmetric breakthrough curve. This model has been successfully applied to describe the breakthrough curves of contaminant gases onto solid sorbents [239,240,243,244].



Chapter 4

IONIC LIQUIDS SIMULATIONS BY USING COSMO-RS

CHAPTER 4. IONIC LIQUIDS SIMULATIONS BY USING COSMO-RS

4.1. Introduction to COSMO-RS method

Estimation of ILs properties by means of computational tools is a field in development, motivating by the low but growing number of available experimental data and the lack of knowledge of the nature and behavior of this kind of solvents [245,246]. COSMO-RS is presented as a predictive method for the thermodynamic properties of fluids and liquid mixtures that uses a statistical thermodynamics approach based on the results of quantum chemical calculations on individual molecules [247,248]. The quantum chemical model, the so called “COnductor-like Screening MOdel” (COSMO), is an efficient variant of dielectric continuum solvation methods. In COSMO calculations the solute molecules are calculated in a virtual conductor environment. In such an environment the solute molecule induces a polarization charge density (σ) on the interface between the molecule and the conductor, i.e. on the molecular surface. These charges act back on the solute and generate a more polarized electron density than in vacuum. During the quantum chemical self-consistency algorithm, the solute is thus converged to its energetically optimal state in a conductor with respect to electron density. The polarization charge density of the COSMO calculation (also called screening charge density), which is a good local descriptor of the molecular surface polarity, is used to extend the model towards “Real Solvents” (COSMO-RS) [248,249]. The polarization density distribution on the surface of each molecule i is converted into a distribution-function, the so called σ -profile $p^i(\sigma)$, which gives the relative amount of surface with polarity σ on the surface of the molecule. The σ -profile for the entire solvent of interest S , which might be a mixture of several compounds, $p_S(\sigma)$ can be built by adding the $p_i(\sigma)$ of the components weighted by their mole fraction x_i in the mixture.

$$p_S(\sigma) = \sum_{i \in S} x_i p^i(\sigma) \quad \text{eq. 4.1}$$

Figure 4.1 shows the molecular structure and the polarization charge density (σ), as a color surface map of two ILs, showing different colors depending on the reactivity of the molecule segment. The chloride anion confers on IL more polar character and it is represented as red color (BmimCl, Figure 4.1A), while a greenish color is characteristic of non polar substances, such as BmimNTf₂ shows in Figure 4.1B.

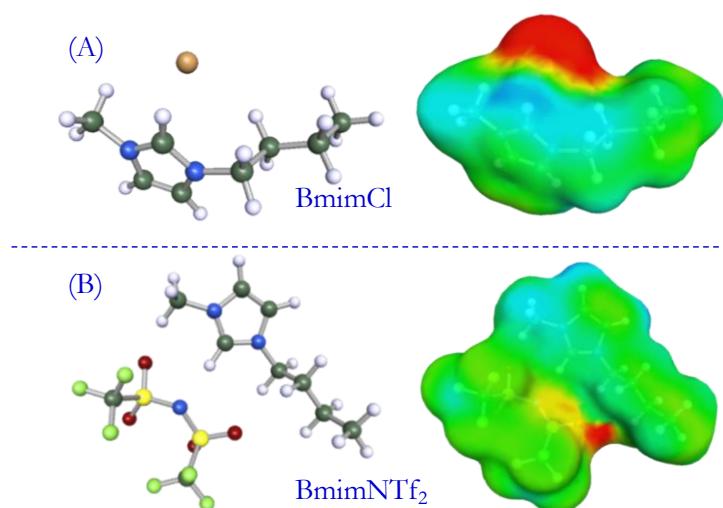


Figure 4.1. COSMO surface polarity and molecular geometry of two ILs, BmimCl (A) and BmimNTf₂ (B).

COSMO-RS method develops a thermodynamic and statistic treatment based on σ -Profile in order to determine the thermo-physical properties of a fluid from the electronic information of the molecules, i.e. moving from microscopic to macroscopic information. COSMO-RS essentially calculate the interaction energy involving solute and solvent molecules, $E(\sigma, \sigma')$, assessing the interaction between an effective molecular surface, a_{eff} , taking into account the segment of the molecule surface and the gap with polarizable charge σ y σ' , respectively. The interaction energy of the solute and solvent molecules is calculated integrating, in the whole contact surface, the energy need to separate the segment with density charge, σ y σ' , until a distance where the electronic potential between both segments of opposite charge will be zero. COSMO-RS method set up interaction of molecules in a fluid might be: i) hydrogen bonding, ii) Van der Waals and iii) Electrostatic (Polar or Misfit), that include five parameters, as to know, effective contact area (a_{eff}), hydrogen bonding strength coefficient (c_{HB}), threshold for hydrogen bonding (σ_{donor} , $\sigma_{acceptor}$) y van der Waals coefficient ($\tau(e)$), see more detailed in the next sections, being fixed by measuring up to experimental data. Once being calculated the interaction energy between solute/solvent, it can be assessed in thermodynamic terms the state of the compounds in a mixture. Because of that, a statistic-thermodynamic treatment has been developed, where the initial expression defines the chemical potential of a charge density segment, σ , in the system S (σ -Potencial):

$$\mu_s(\sigma) = -R \cdot T \cdot \ln \left\{ \int p_s(\sigma') \cdot \exp \left(\frac{\mu_s(\sigma') - a_{\text{eff}} \cdot E(\sigma, \sigma')}{R \cdot T} \right) \cdot d\sigma' \right\} \quad \text{eq. 4.2}$$

where $\mu_s(\sigma)$ is the affinity measure of the system, S , by a polarity surface segment, σ . So, it can be defined that $\mu_s(\sigma)$ is the chemical potential of an average contact surface, a_{eff} , and surface polarization charge density, σ , in a system, S , at a temperature T . From this expression of σ -potential it can be calculated the chemical potential of a molecule X in the liquid S :

$$\mu_s^{X_i} = \mu_{C,S}^{X_i} + \mu_{R,S}^{X_i} \implies \int p^{X_i}(\sigma) \cdot \mu_s(\sigma) \cdot d\sigma - \lambda_c \cdot R \cdot T \cdot \ln A_s \quad \text{eq. 4.3}$$

where the parameters $\mu_{C,S}^{X_i}$ y $\mu_{R,S}^{X_i}$ are the combinational and residual contributions to the chemical potential, λ_c is the fixed parameter and A_s is the average value of the solvent surface. Lately, the activity coefficient, γ , of a solute X in a solvent S can be calculated from the chemical potential, by means of the equation:

$$\gamma_s^X = \exp \left(\frac{\mu_s^X - \mu_X^X}{R \cdot T} \right) \quad \text{eq. 4.4}$$

It results that the entirely description of the thermodynamic state of solute X in a solvent S . The calculus obtained from COSMO-RS were carried out by means of COSMOtherm program and the company COSMOlogic, which rely with wide data bases with more than 5000 compounds and more than 200 ILs.

In this situation, COSMO-RS uses the self-consistent state of molecules embedded in a virtual conductor ($\epsilon = \infty$), as it is readily achievable by COSMO calculations, as a new reference state for molecules in solution, without assuming that this state is of any real meaning. There can be no doubt that this state of ideal screening is much closer to the real situation of molecules in solution, at least in polar solvents, than the usually chosen reference state of molecules in vacuum, because it takes account of the electrostatic screening of molecules by their surrounding, and even of the resulting backpolarisation of the solutes. It is important that we are able to calculate the state of the molecules in vacuum using the same quantum chemistry method because this will enable us to calculate the energy difference between the gas phase and the condensed phase, which is needed for vaporization data.

A liquid is considered to be a group of almost closely packed ideally screened molecules, as schematically shown in [Figure 4.2](#). Each part of surface has a direct contact partner. But in reality, there is no conducting medium between them as has been assumed in the reference state. Therefore, the energy difference between the real situation of such contact and the ideally screened situation has to be defined as a local electrostatic interaction energy, which results from the contact of the molecules. Considering a contact on a region of molecular surface of area a_{eff} (effective contact area), and considering that the two contacting pieces of molecular surface had average ideal screening charge densities σ and σ' in the conductor, it is possible to calculate this interaction energy as the energy which is necessary to remove the residual screening charge density $\sigma + \sigma'$ from the contact. Apparently, in the special situation of $\sigma = -\sigma'$, there is nothing to remove and hence, the interaction energy is zero. Such a contact here is called “ideal electrostatic contact”, in which each molecule just screens its partner just like a conductor would do. In the general case, there is some misfit of the partners, i.e. where $\sigma + \sigma'$ does not vanish, the energy of removal is given by elementary electrostatic theory as:

$$E_{\text{misfit}} = a_{\text{eff}} e_{\text{misfit}}(\sigma, \sigma') = a_{\text{eff}} \frac{\alpha'}{2} (\sigma, \sigma')^2 \quad \text{eq. 4.5}$$

where $e_{\text{misfit}}(\sigma, \sigma')$ means the misfit energy density on that contact surface and α' is a general misfit constant which can be calculated approximately, but in the end will be fitted to experimental data as fine-tuning. As it is reported in the literature [\[248,250\]](#), this misfit term to a great deal subsumes quite well the polarisation response of the molecules to the misfit situation. If there is no correlation between the different misfit charges, as we may hope to be the case for neutral compounds, the total electrostatic energy difference between the ideally screened ensemble and the real ensemble is given by the integral of misfit energy functional $e_{\text{misfit}}(\sigma, \sigma')$ over the entire intramolecular contact area. In the misfit case of ions, misfit interactions have to be taken into account.

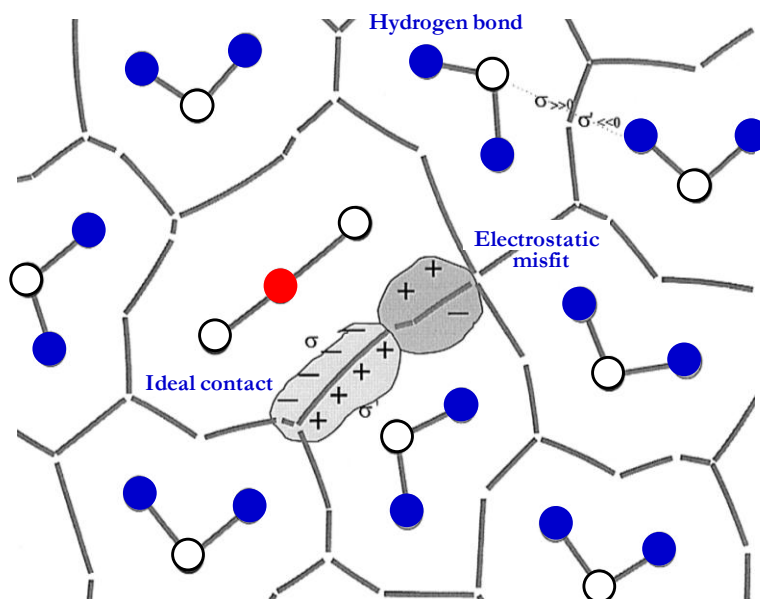


Figure 4.2. Schematic illustration of polar density charge (σ) between solute and solvent.

As discussed above, hydrogen bonding is greatly covered by the electrostatics, but it has to be parameterised the extra hydrogen bonding energy resulting from interpenetration of the atomic electron densities in some reasonable way. This energy should only come into play if two sufficiently polar pieces of surface of opposite polarity are in contact, and it should be the more important, the more polar both surface pieces are. Taking the screening charge density (σ) as a local measure of polarity, the next function realizes such behavior:

$$E_{HB}(\sigma, \sigma') = a_{eff} e_{HB}(\sigma, \sigma') = a_{eff} c_{HB} \min[(0, \min(\sigma_{donnor} + \sigma'_{HB}) \max(0, \sigma_{acceptor} - \sigma'_{HB})] \quad \text{eq. 4.6}$$

with $\sigma_{donnor} = \min(\sigma, \sigma')$ and $\sigma_{acceptor} = \max(\sigma, \sigma')$. σ_{HB} is some threshold for hydrogen bonding and c_{HB} is the strength coefficient. Both parameters are general and have to be adjusted to experimental data.

Eq. 4.6 might look rather complicated, but it does the following: it is zero, unless the more negative of the two screening charge densities is less than the threshold $-\sigma_{HB}$, and unless the more positive exceeds σ_{HB} . Because positive molecular regions get negative screening charge, the negative σ now is the donor part of the H-bond, and the positive is the acceptor. In this case, the hydrogen bonding energy is proportional to the product of the excess screening

charge densities, i.e., to $(\sigma_{\text{donnor}} + \sigma_{\text{HB}}) (\sigma_{\text{accetor}} - \sigma_{\text{HB}})$ which is a negative, i.e. an attractive, energy by the opposite sign of σ_{donnor} and σ_{accetor} .

It is assumed that the vdW energy contributions can be expressed by element-specific parameters $\tau(e)$, which have to be fitted to experimental data. Then, the vdW energy gain of a molecule X during the transfer from the gas phase to any solvent is given by the integral of $\gamma(e)$ over the molecular surface, respectively:

$$E_{vdW}^X = \sum_{\alpha \in X} a_{\alpha}^X \tau(E(\alpha)) \quad \text{eq. 4.7}$$

with a_{α}^X being the molecular surface on atom α , and $e(\alpha)$ indicating the element of atom α . Because this vdW contribution is independent of any neighborhood relations, it is not really interaction energy, but it may be considered as an energy contribution to the reference state in solution. Thus, the state of a molecule embedded in a vdW interacting conductor is considered as reference state. Within this approximation, vdW interactions do not contribute to the free energies of transfer between different liquid states, i.e. they do not contribute to activities, but only to the liquid–gas transfer, i.e. to vaporisation data.

Summarizing, the interactions of molecular surfaces in COSMO-RS are given by an interaction energy functional $e(\sigma, \sigma') = e_{\text{misfit}}(\sigma, \sigma') + e_{\text{HB}}(\sigma, \sigma')$, which does only depend on the polarities, misfit and hydrogen bonding i.e. on the screening charge densities, of the interacting surfaces, plus a vdW contribution which is included in the reference state energy. The generic interaction functional $e(\sigma, \sigma')$ has three adjustable parameters α' , σ_{HB} , and c_{HB} , while the vdW term has one adjustable parameter per element. In addition to these explicit parameters, it should be noted that the screening charge densities and hence, the entire parameterisation, depend on the detailed values of the element-specific radii which are used in the cavity construction.

There are two molecular models commonly applied to simulate the IL compounds and quantify their σ -profile values:

- i. **C⁺+A⁻** model considers independent counterions of IL
- ii. **CA** model considers the ion-paired structure to simulate the IL compound.

Depending on the request of the simulation, it can be used either model, i.e. screening of ILs was done using C^+A^- model, which requires lower computational cost and it was demonstrated previously for the selection of an IL in carbon dioxide, ammonia or toluene treatments [58,59,66,67,251], while a different computational approach consists of considering the ion-paired (**CA** model) structure to simulate the IL compound was also consider which is significantly more computationally demanding but includes the effects of counterion interactions in the calculations. In this case, G-S or G-L partition coefficients, density or molecular volume were obtained for the molecule as a whole. This alternative molecular model has successfully been successfully applied to properties estimations of IL systems [252-254].

The most important advantages from COSMO-RS method are bellow listed:

- Prediction of thermodynamic properties without previous experimental data.
- Quantitative and qualitative description of physico-chemical interactions between the molecules of the neat components or mixtures.
- Reasonably description to the temperature dependence on the estimations of properties.
- Solve the difference between isomers and so estimate their contribution to the mixture properties.
- Intramolecular interactions and effects linked to hydrogen bonding are included in the estimation of properties.

Lately, it is listed some of the different and varied COSMO-RS applications:

- i. Developing and optimization of the own method, by means of the validation of the estimation by comparing with experimental data [252,255,256].
- ii. Determining thermodynamic and equilibrium data [257-259].
- iii. Interpretation of the macroscopic behavior of a system from a molecular point of view [260-262].
- iv. Choice of solvent or proper system for certain applications [263-265].
- v. Designing of novel product or process [266-268].

To sum, COSMO-RS is a novel approach to the calculation of activity coefficients of compounds in pure compound and liquid mixtures, where the screening charge density σ supplied by a virtual conductor on the molecular surface and provided by COSMO is the key

parameter for molecular interactions in COSMO-RS, which is the best exchange between computational cost and accuracy. The entire framework of a COSMO-RS calculation is summarized as a flow chart in, Figure. 4.3.

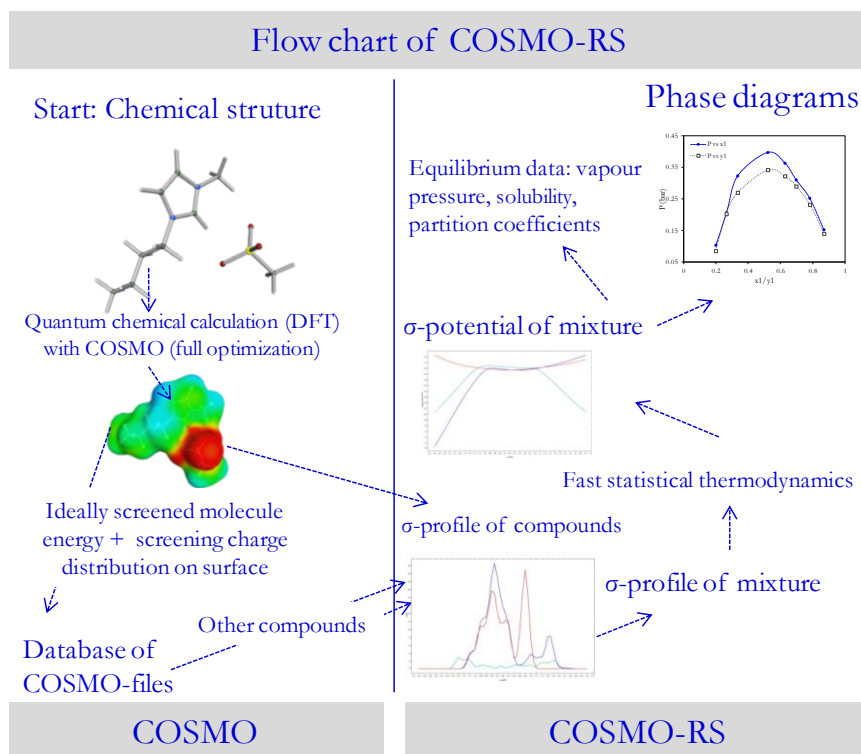


Figure. 4.3. Flow chart of COSMO-RS.

So, COSMO-RS method is presented as a potential tool in order to be used as simulator for a variety of general solvent properties, and ILs in particular, such can be seen in Figure 4.4.

COSMO-RS method

Properties estimation

<u>Pure compounds</u>	<u>Binary systems</u>	<u>Triphasic systems</u>
<ul style="list-style-type: none"> • Density • Viscosity • Molecular volume • Vapour pressure • Boiling point 	<ul style="list-style-type: none"> • Excess enthalpy • Activity coefficient • Salt solubility • pK_a • G-L equilibrium <ul style="list-style-type: none"> ✓ <i>K_{Henry}</i> ✓ <i>Solubility</i> 	<ul style="list-style-type: none"> • L-L equilibrium <ul style="list-style-type: none"> ✓ <i>Partition coefficient</i> ✓ <i>K_{ow}</i>

Figure. 4.4. Properties estimation by means of COSMO-RS in different systems.

4.2. Sigma-profile: the key of COSMO-RS

σ -profile gives the relative amount of surface with polarity σ on the surface of the molecule. It is a graphic, simple and intuitive guide to understand the physical-chemical behavior of the compounds. Following, in order to clarify the concept of σ -profile it can be found an explanation for two typical and polarity different solvents, such as water and hexane. The histogram supplied by COSMO-RS can be qualitatively divided in three main regions upon next cut-off values: hydrogen bond donor ($\sigma_{\text{HB}} < -0.0082 \text{ e}\cdot\text{\AA}^{-2}$) and acceptor ($\sigma_{\text{HB}} > 0.0082 \text{ e}\cdot\text{\AA}^{-2}$) regions and non-polar region ($-0.0082 < \sigma < 0.0082 \text{ e}\cdot\text{\AA}^{-2}$)

The σ -profile of water, represented in Figure 4.5, is very broad and almost symmetric (respect 0, 0). On the negative side, water shows a broad peak at about -0.015 resulting from the two polar hydrogen atoms, while on the positive side, the same broad peak at +0.015 is present, resulting from the lone pairs of the oxygen atom while in between, there is only very little surface resulting from the intermediate regions on the molecule. The symmetry of the σ -profile is of high importance for the properties of water, because symmetry implies, at least, the principal availability of the ideal partner surface for each piece of surface in the system. Hence, water shows a lot of very favorable and almost ideal interaction, regarding electrostatics as well as H-bonding. This is the reason why water “likes itself” very much and why it has a high boiling point and surface tension.

Hexane is used as a representative alkane compound. Since alkanes do not have significant electrostatic moments, the σ -profiles of alkanes are rather narrow. Nevertheless, two peaks can be detected, in the non polar region, resulting from the hydrogens on the negative side and from the carbons on the positive side. A more detailed explanation can be found in literature [269].

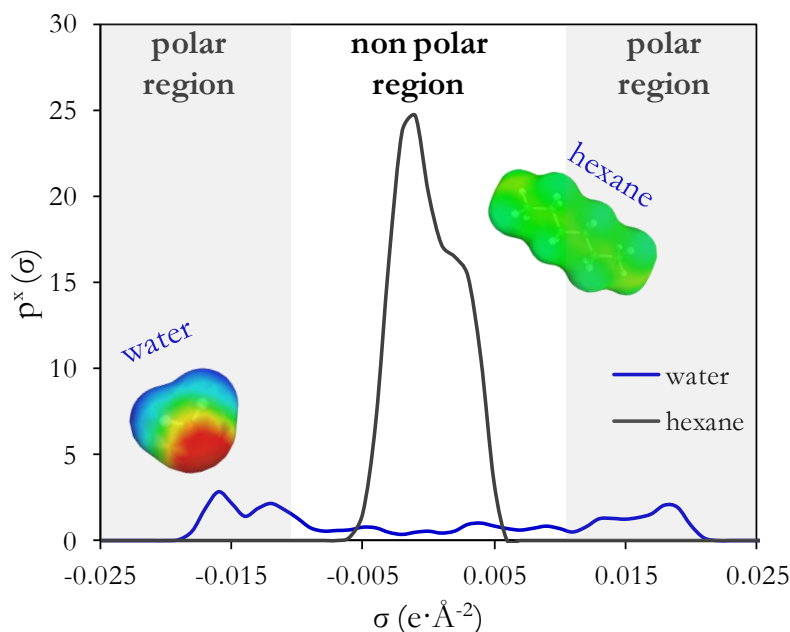


Figure 4.5. σ -profiles of two representative solvents, water and hexane, at room temperature.

As an example, let us consider the surface polarization charge densities of some cations and anions of common ILs (Figure 4.6). The 3D charge distribution (σ) of the negatively charged Cl^- anion is represented in its polar surface by a deep red color. Therefore, the chloride anion can be considered a hydrogen bond acceptor segment. Similarly, PF_6^- is visualized in the polar surface by a light orange color. It indicates a lower polar character in PF_6^- with respect to Cl^- . NTf_2^- also shows a weak hydrogen bond acceptor fragment (corresponding to $-\text{SO}_2$ groups). In addition, NTf_2^- presents an electronic charge mainly due to the $-\text{CF}_3$ groups of the anion. The surface of these non-polar fragments is represented in green. The polarisable surface of the imidazolium, ammonium and pyridinium cations with a common butyl side chain are also shown. As can be seen, the surface of the cations is mainly non-polar, i.e., green, with a tendency to blue-green on the more polarized fragments.

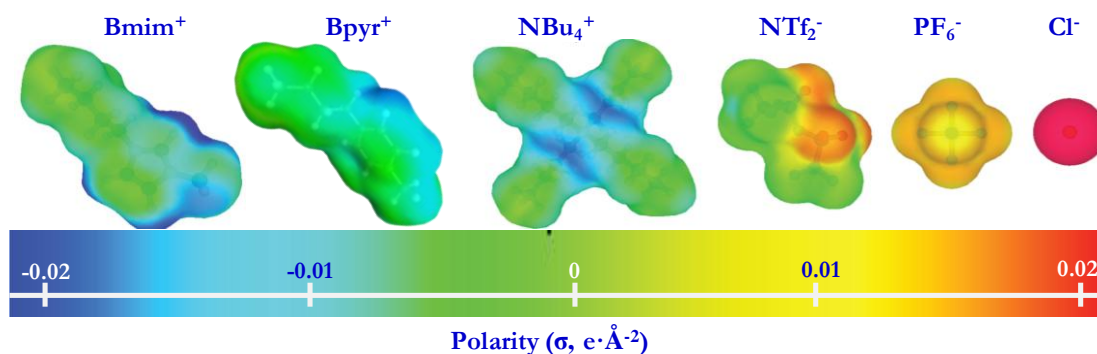


Figure. 4.6. Surface polarization charge density of some representative cations and anions of ILs.

4.3. Prediction of thermophysical properties of ionic liquids

It would be of great value to count with predictive models that could reliably calculate the thermodynamic properties of solvents in general, ILs in particular, and their interaction with other compounds. In this context, COSMO-RS model is regarded as a valuable method for predicting the thermodynamic properties of ILs mixtures on the basis of quantum chemical calculations for the individual molecules [270], providing an unique *a priori* computational tool for designing IL with specific properties [254,271]. In fact, several publications have demonstrated the general suitability of COSMO-RS method to predict properties of IL systems, which can divide into three kinds of systems:

- i. Pure compounds estimate physical properties of individual molecules [272], such as the prediction of densities [253], vapor pressures and vaporization enthalpies [273].
- ii. Biphasic systems consider the activity coefficients at infinite dilutions [274,275], gas solubilities and Henry's law constants [58,59,276] and the G-L equilibria of conventional organic solvents and ILs [252,270,277,278].
- iii. Triphasic systems evolve the L-L equilibria of ternary mixtures of organic compounds and ILs [279-281].

This would help us to scan a set of ILs in order to find appropriate candidates for a certain task or to design new ILs for special applications. Moreover, recent results showed that

COSMO-RS successfully simulate the interactions between AC surface groups and different solutes. This information can be useful for tailoring the ACs with the objective of improving their adsorption capacities by further functionalization.

Pure compounds:

Physical properties (δ , μ , M_{volume} , Parachor):

Depending on the further application of the IL, it has to be into account the physical properties, but some of them are not reported in the literature, so it is necessary to predict them. However, ILThermo [282] is a website where is being up to date several experimental parameters related with ILs field.

Physical properties, such as *density* (ρ), *viscosity* (μ) and *molecular volume* (M_{volume}), have been calculated in order to predict or justify the behavior of IL in determinate applications, as explanation of the steric factor of AC in the adsorption of ILs with different *molecular volume* (Paper II) or the slow kinetic behavior in the adsorption of OmimPF₆ on AC because of their high *viscosity* (Paper III).

Parachor is defined in eq. 4.8, where M_{weight} is the molecular weight γ the surface tension and ρ denotes the *density* [26,283,284]. As an additive quantity the *Parachor* has been used in solving various structural problems, as in Paper I, where *Parachor* introduces intermolecular interactions between IL molecules to some extent.

$$Parachor = \frac{M_{\text{weight}} \gamma^{\frac{1}{4}}}{\rho} \quad \text{eq. 4.8}$$

Biphasic systems:

Henry constant (K_H):

The solubility of a gas in a liquid is sometimes described in terms of Henry's law constant [285,286]. The numerical value of K_H is reversely proportional to the predicted concentration of solute retained in the sorbent phase at constant temperature in the equilibrium, following the expression:

$$K_H = \frac{P_{\text{eqGas}}^{\text{solute}}}{x_{\text{sorbent}}^{\text{solute}}} \quad \text{eq. 4.9}$$

where $x_{\text{sorbent}}^{\text{solute}}$ is the mole fraction of the solute in the condensed phase and $P_{\text{eqGas}}^{\text{solute}}$ is the partial pressure of compound in the gas phase in the equilibrium. Therefore, lower value of K_H mean higher affinity of the sorbent material for solute compound.

K_H has been calculated in order to evaluate the affinity between a wide variety of gaseous solutes and different sorbent materials. Previous works has successfully demonstrated the predictability of K_H simulation by COSMO-RS [58,59,66]. The present dissertation shows the interaction in term of Henry constant between ACs and chlorinated volatile organic compounds in [Paper V](#) and between ILs and ammonia in [Paper VI](#).

Excess enthalpy (H^E):

Excess enthalpy, H^E , is a thermodynamic parameter which has been calculated for different systems in the present work. The H^E is the change in enthalpy from the two pure compounds (organic and IL, for example) to the mixture. Thus, it involves the disruption of interactions in the pure compounds and the establishment of new interactions in the mixture [287,288]. COSMO-RS estimations for H^E of solute-IL mixtures was successfully applied to analyze the G-L or G-S equilibrium data in terms of the hydrogen bonding, misfit (polar) and van der Waals intermolecular interactions:

$$H^E = H^E(H - Bond) + H^E(misfit) + H^E(Vdw) \quad \text{eq. 4.10}$$

[Paper I](#) and [Paper II](#) show the contributions due to biphasic systems in order to know the interaction of IL with the AC. While [Paper V](#) shows the interaction between different model of ACs and three chlorinated volatile organic compounds (monochloromethane, dichloromethane and chloroform), which is valuable tool for designing ACs with desired characteristics for the different kinds of solutes. Moreover, excess enthalpies have been also calculated in order to establish the preferential interaction between ammonia as pollutant using ILs as sorbent, reported in [Paper VI](#).

Triphasic systems:

Octanol-water partition coefficient (K_{ow}):

The octanol–water partition coefficient (K_{ow}) is a widely used parameter for predicting the hydrophobicity of solvents compare with octanol [289,290]. Mathematically can be expressed as the ratio between the solute (IL) concentration solved in octanol and that IL concentration solved in water:

$$K_{ow} = \frac{C_{IL}^{octanol}}{C_{IL}^{water}} \quad \text{eq. 4.11}$$

Since experimental K_{ow} values are only available for a few ILs in the literature, they were calculated by COSMO-RS method. The behavior of ILs in water can illustrate about the adsorption capacity on AC. The experimental results indicated that ILs with high hydrophobicity (higher K_{ow}) present elevated affinity toward the AC surface (apolar character), as was demonstrated in Paper I.

Partition coefficient ($\text{Log } P$):

The partition coefficient ($\text{Log } P$) is the ratio of concentrations of a compound in a mixture of two immiscible phases at infinite dilution [291].

$$\text{Log } (P) = \text{Log} \left(\frac{C_{IL}^{AC}}{C_{IL}^{water}} \right) \quad \text{eq. 4.12}$$

Hence this distribution coefficient can be used to evaluate the difference in solubility of the IL in AC and water phases, calculated by COSMO-RS for the AC molecular models in Paper I and Paper II. Two AC molecular models were used for $\text{Log } (P)$ estimation, as can be seen in Figure 4.7. AC phase is modeled by mixing AC structures in a molar proportion of AC (90): AC-OH (10). This molar proportion is an approach based on the proportion of the oxygen surface groups containing hydroxyl groups obtained by experimental measurements in the AC used.

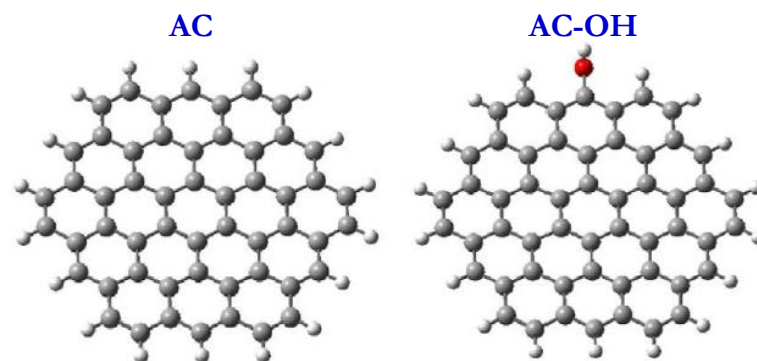


Figure. 4.7. Molecular model for AC used in COSMO-RS calculations.

References:

- [1] Wasserscheid P, Welton T. Ionic liquids in synthesis. Weinheim: Wiley-VCH; 2008.
- [2] Robin D. Rogers, Kenneth R. Seddon. Ionic Liquids IIIA: fundamentals, progress, challenges and opportunities transformations and processes. Washington (DC): American 674 Chemical Society; 2005.
- [3] Huddleston JG, Willauer HD, Swatloski RP, Visser AE, Rogers RD. Room temperature ionic liquids as novel media for 'clean' liquid-liquid extraction. *Chemical Communications* 1998;16:1765-6.
- [4] Dupont J, de Souza RF, Suarez PAZ. Ionic liquid (molten salt) phase organometallic catalysis. *Chem.Rev.* 2002;102(10):3667-91.
- [5] Plechkova NV, Seddon KR. Applications of ionic liquids in the chemical industry. *Chem.Soc.Rev.* 2008;37(1):123-50.
- [6] Padua A, Gomes M, Lopes J. Molecular solutes in ionic liquids: A structural, perspective. *Acc.Chem.Res.* 2007;40(11):1087-96.
- [7] Sowmiah S, Srinivasadesikan V, Tseng MC, Chu YH. On the Chemical Stabilities of Ionic Liquids. *Molecules* 2009;14(9):3780-813.
- [8] Zhu S, Chen R, Wu Y, Chen Q, Zhang X, Yu Z. A Mini-Review on Greenness of Ionic Liquids. *Chemical and Biochemical Engineering Quarterly* 2009;23(2):207-11.
- [9] Hallett JP, Welton T. Room-Temperature Ionic Liquids: Solvents for Synthesis and Catalysis. 2. *Chem.Rev.* 2011;111(5):3508-76.
- [10] Parvulescu V, Hardacre C. Catalysis in ionic liquids. *Chem.Rev.* 2007;107(6):2615-65.
- [11] van Rantwijk F, Sheldon R. Biocatalysis in ionic liquids. *Chem.Rev.* 2007;107(6):2757-85.
- [12] Olivier-Bourbigou H, Magna L, Morvan D. Ionic liquids and catalysis: Recent progress from knowledge to applications. *Applied Catalysis A-General* 2010;373(1-2):1-56.
- [13] Itoh H, Naka K, Chujo Y. Synthesis of gold nanoparticles modified with ionic liquid based on the imidazolium cation. *J.Am.Chem.Soc.* 2004;126(10):3026-7.
- [14] Nakashima T, Kimizuka N. Interfacial synthesis of hollow TiO₂ microspheres in ionic liquids. *J.Am.Chem.Soc.* 2003;125(21):6386-7.
- [15] Hapiot P, Lagrost C. Electrochemical reactivity in room-temperature ionic liquids. *Chem.Rev.* 2008;108(7):2238-64.
- [16] Armand M, Endres F, MacFarlane D, Ohno H, Scrosati B. Ionic-liquid materials for the electrochemical challenges of the future. *Nature Materials* 2009;8(8):621-9.

- [17] Jain N, Kumar A, Chauhan S, Chauhan SMS. Chemical and biochemical transformations in ionic liquids. *Tetrahedron* 2005;61(5):1015-60.
- [18] Hough W, Smiglak M, Rodriguez H, Swatloski R, Spear S, Daly D. The third evolution of ionic liquids: active pharmaceutical ingredients. *New journal of chemistry* 2007;31(8):1429-36.
- [19] Han X, Armstrong DW. Ionic liquids in separations. *Acc.Chem.Res.* 2007;40:1079-86.
- [20] Bates ED, Mayton RD, Ntai I, Davis JH. CO₂ capture by a task-specific ionic liquid. *J.Am.Chem.Soc.* 2002;124(6):926-7.
- [21] Weingaertner H. Understanding ionic liquids at the molecular level: Facts, problems, and controversies. *Angewandte Chemie-International Edition* 2008;47(4):654-70.
- [22] Earle MJ, Esperanca JMSS, Gilea MA, Lopes JNC, Rebelo LPN, Magee JW, et al. The distillation and volatility of ionic liquids. *Nature* 2006;439(7078):831-4.
- [23] Domanska U. Thermophysical properties and thermodynamic phase behavior of ionic liquids. *Thermochimica Acta.* 2006;448(1):19-30.
- [24] Seddon KR. Room-temperature ionic liquids: Neoteric solvents for clean catalysis. *Kinetics and Catalysis.* 1996;37(5):693-7.
- [25] Fredlake CP, Crosthwaite JM, Hert DG, Aki SNVK, Brennecke JF. Thermophysical properties of imidazolium-based ionic liquids. *J.Chem.Eng.Data.* 2004;49(4):954-64.
- [26] Sugden S, Wilkins H. The parachor and chemical constitution. Part XII. Fused metals and salts. *Journal of the Chemical Society* 1929.
- [27] Graenacher C, Cellulose solution. Patent number 1943176. 9 Jan 1934.
- [28] Hurley FH, Wier TP. Electrodeposition of Metals from Fused Quaternary Ammonium Salts. *J.Electrochem.Soc.* 1951;98(5):203-6.
- [29] Wilkes JS, Levisky JA, Wilson RA, Hussey CL. Dialkylimidazolium Chloroaluminate Melts a New Class of Room-Temperature Ionic Liquids for Electrochemistry, Spectroscopy, and Synthesis. *Inorg.Chem.* 1982;21(3):1263-4.
- [30] Wasserscheid P. Chemistry Volatile times for ionic liquids. *Nature.* 2006;439(7078):497.
- [31] Freemantle M. BASF'S smart ionic liquid. *Chemical & Engineering News.* 2003;81(13):9.
- [32] Rogers RD, Seddon KR. Ionic liquids Solvents of the future? *Science.* 2003;302(5646):792-3.
- [33] Bonhote P, Dias AP, Papageorgiou N, Kalyanasundaram K, Gratzel M. Hydrophobic, highly conductive ambient-temperature molten salts. *Inorg.Chem.* 1996;35(5):1168-78.
- [34] Hayashi S, Hamaguchi H. Discovery of a Magnetic Ionic Liquid BmimFeCl₄ (vol 33, pg 1590, 2004). *Chem.Lett.* 2005;34(5):740.

- [35] Hano T, Ohtake T, Matsumoto M, Kitayama D, Hori F, Nakashio F. Extraction Equilibria of Amino-Acids with Quaternary Ammonium Salt. *J.Chem.Eng.Japan* 1991;24(1):20-24.
- [36] Fry SE, Pienta NJ. Effects of Molten-Salts on Reactions Nucleophilic Aromatic-Substitution by Halide-Ions in Molten Dodecyltributyl-Ph Salts. *J.Am.Chem.Soc.* 1985;107(22):6399-400.
- [37] Zhao H. Innovative applications of ionic liquids as "green" engineering liquids. *Chem.Eng.Commun.* 2006;193(12):1660-77.
- [38] Sheldon R. Catalytic reactions in ionic liquids. *Chemical Communications.* 2001;23:2399-407.
- [39] Boon JA, Levisky JA, Pflug JL, Wilkes JS. Friedel Crafts Reactions in Ambient-Temperature Molten-Salts. *J.Org.Chem.* 1986;51(4): 480-3.
- [40] Welton T. Ionic liquids in catalysis. *Coord.Chem.Rev.* 2004;248(21-24):2459:77.
- [41] Visser AE, Holbrey JD, Rogers RD. Hydrophobic ionic liquids incorporating N-alkylisoquinolinium cations and their utilization in liquid-liquid separations. *Chemical Communications* 2001;23:2484-5.
- [42] Visser AE, Swatloski RP, Griffin ST, Hartman DH, Rogers RD. Liquid/liquid extraction of metal ions in room temperature ionic liquids. *Sep.Sci.Technol.* 2001;36(5-6):785-804.
- [43] Freire MG, Santos LMNBF, Fernandes AM, Coutinho JAP, Marrucho IM. An overview of the mutual solubilities of water-imidazolium-based ionic liquids systems. *Fluid Phase Equilib.* 2007;261(1-2):449-454.
- [44] Freire MG, Neves CMSS, Carvalho PJ, Gardas RL, Fernandes AM, Marrucho IM, et al. Mutual Solubilities of water and hydrophobic ILs. *J Phys Chem B.* 2007;111(45):13082-9.
- [45] Pereira JFB, Lima AS, Freire MG, Coutinho JAP. Ionic liquids as adjuvants for the tailored extraction of biomolecules in aqueous biphasic systems. *Green Chem.* 2010;12(9):1661-9.
- [46] Garcia J, Garcia S, Torrecilla JS, Rodriguez F. Synergistic liquid-liquid extraction of toluene from heptane with mixtures of BmimBF₄ and OmimBF₄ ionic liquids. Icheap-9: 9th International Conference on Chemical and Process Engineering. 2009;17:1579-84.
- [47] Garcia J, Garcia S, Torrecilla JS, Rodriguez F. N-butylpyridinium bis-(trifluoromethylsulfonyl)imide ionic liquids as solvents for the liquid-liquid extraction of aromatics from their mixtures with alkanes: Isomeric effect of the cation. *Fluid Phase Equilib.* 2011;301(1):62-6.
- [48] Garcia S, Larriba M, Garcia J, Torrecilla JS, Rodriguez F. Separation of toluene from n-heptane by liquid-liquid extraction using binary mixtures of BpyBF₄ and 4bmpyTf₂N ionic liquids as solvent. *Journal of Chemical Thermodynamics.* 2012;53:119-24.
- [49] Garcia S, Larriba M, Garcia J, Torrecilla JS, Rodriguez F. Liquid-liquid extraction of toluene from n-heptane using binary mixtures of N-butylpyridinium tetrafluoroborate and N-butylpyridinium bis(trifluoromethylsulfonyl)imide ionic liquids. *Chem.Eng.J.* 2012;180:210-5.

- [50] Wei GT, Yang ZS, Chen CJ. Room temperature ionic liquid as a novel medium for liquid/liquid extraction of metal ions. *Anal.Chim.Acta* 2003;488(2):183-92.
- [51] Mokrushin V, Assenbaum D, Paape N, Gerhard D, Mokrushina L, Wasserscheid P, et al. Ionic Liquids for Propene-Propane Separation. *Chem.Eng.Technol.* 2010;33(1):63-73.
- [52] Han D, Row K. Recent Applications of Ionic Liquids in Separation Technology. *Molecules.* 2010;15(4):2405-26.
- [53] Bara JE, Carlisle TK, Gabriel CJ, Camper D, Finotello A, Gin DL, et al. Guide to CO₂ Separations in Imidazolium-Based Room-Temperature Ionic Liquids. *Ind Eng Chem Res* 2009;48(6):2739-51.
- [54] Carvalho PJ, Alvarez VH, Machado JJB, Pauly J, Daridon J, Marrucho IM, et al. High pressure phase behavior of CO₂ in 1-alkyl-3-methylimidazolium bis(trifluoromethylsulfonyl) imide ionic liquids. *Journal of Supercritical Fluids.* 2009;48(2):99-107.
- [55] Karadas F, Atilhan M, Aparicio S. Review on the Use of Ionic Liquids (ILs) as Alternative Fluids for CO₂ Capture and Natural Gas Sweetening. *Energy Fuels.* 2010;24:5817-28.
- [56] Hart R, Pollet P, Hahne DJ, John E, Llopis-Mestre V, Blasucci V, et al. Benign coupling of reactions and separations with reversible ionic liquids. *Tetrahedron.* 2010;66(5):1082-90.
- [57] Shiflett MB, Yokozeki A. Chemical Absorption of Sulfur Dioxide in Room-Temperature Ionic Liquids. *Ind Eng Chem Res* 2010;49(3):1370-7.
- [58] Palomar J, Gonzalez-Miquel M, Bedia J, Rodriguez F, Rodriguez JJ. Task-specific ionic liquids for efficient ammonia absorption. *Separation and Purification Technology.* 2011;82(0):43-52.
- [59] Bedia J, Palomar J, Gonzalez-Miquel M, Bedia J, Rodriguez F, Rodriguez JJ. Screening ionic liquids as suitable ammonia absorbents on the basis of thermodynamic and kinetic analysis. *Separation and Purification Technology.* 2012;95:188-95.
- [60] Quijano G, Couvert A, Amrane A, Darracq G, Couriol C, Le Cloirec P, et al. Potential of ionic liquids for VOC absorption and biodegradation in multiphase systems. *Chemical Engineering Science* 2011;66(12):2707-12.
- [61] Shiflett MB, Yokozeki A. Solubility and diffusivity of hydrofluorocarbons in room-temperature ionic liquids. *AIChE J.* 2006;52(3):1205-19.
- [62] Shiflett MB, Yokozeki A. Liquid-liquid equilibria of hydrofluoroethers and ionic liquid EmimNTf₂. *J.Chem.Eng.Data* 2007;52(6):2413-8.
- [63] Ortiz A, Ruiz A, Gorri D, Ortiz I. Room temperature ionic liquid with silver salt as efficient reaction media for propylene/propane separation: Absorption equilibrium. *Separation and Purification Technology* 2008;63(2):311-8.
- [64] Ortiz A, Galan LM, Gorri D, de Haan AB, Ortiz I. Kinetics of reactive absorption of propylene in RTIL-Ag⁺ media. *Separation and Purification Technology* 2010;73(2):106-13.

- [65] Blach P, Fourmentin S, Landy D, Cazier F, Surpateanu G. Cyclodextrins: A new efficient absorbent to treat waste gas streams. *Chemosphere* 2008;70(3):374-80.
- [66] Palomar J, Gonzalez Miquel M, Polo A, Rodriguez F. Understanding the Physical Absorption of CO₂ in Ionic Liquids Using the COSMO-RS Method. *Industrial engineering chemistry research* 2011;50(6):3452-63.
- [67] Gonzalez-Miquel M, Palomar J, Omar S, Rodriguez F. CO₂/N₂ Selectivity Prediction in Supported Ionic Liquid Membranes (SILMs) by COSMO-RS. *Ind Eng Chem Res* 2011;50(9):5739-48.
- [68] Ortiz A, Gorri D, Irabien A, Ortiz I. Separation of propylene/propane mixtures using Ag⁺-RTIL solutions. Evaluation and comparison of the performance of gas-liquid contactors. *J.Membr.Sci.* 2010;360(1-2):130-41.
- [69] Ortiz A, Maria Galan L, Gorri D, de Haan AB, Ortiz I. Reactive Ionic Liquid Media for the Separation of Propylene/Propane Gaseous Mixtures. *Ind EngChem Res.* 2010;49(16):7227-22.
- [70] Ortiz A, Ruiz A, Gorri D, Ortiz I. Room temperature ionic liquid with silver salt as efficient reaction media for propylene/propane separation: Absorption equilibrium. *Separation and Purification Technology* 2008;63(2):311-8.
- [71] Myers C, Pennline H, Luebke D, Ilconich J, Dixon JK, Maginn EJ, et al. High temperature separation of carbon dioxide/hydrogen mixtures using facilitated supported ionic liquid membranes. *J.Membr.Sci.* 2008;322(1):28-31.
- [72] Scovazzo P. Determination of the upper limits, benchmarks, and critical properties for gas separations using stabilized room temperature ionic liquid membranes (SILMs) for the purpose of guiding future research. *J.Membr.Sci.* 2009;343(1-2):199-211.
- [73] Visser AE, Swatoski RP, Reichert WM, Mayton R, Sheff S, Wierzbicki A, et al. Task-specific ionic liquids for the extraction of metal ions from aqueous solutions. *Chemical Communications* 2001;01:135-6.
- [74] Hardacre C, Holbrey JD, McMath SEJ. A highly efficient synthetic procedure for deuterating imidazoles and imidazolium salts. *Chemical Communications* 2001;4:367-8.
- [75] Merrigan TL, Bates ED, Dorman SC, Davis JH. New fluorous ionic liquids function as surfactants in conventional room-temperature ionic liquids. *Chemical Communications* 2000;20:2051-2.
- [76] Wasserscheid P, Bosmann A, Bolm C. Synthesis and properties of ionic liquids derived from the 'chiral pool'. *Chemical Communications* 2002;3:200-1.
- [77] Torrecilla JS, Palomar J, Lemus J, Rodriguez F. A quantum-chemical-based guide to analyze/quantify the cytotoxicity of ionic liquids. *Green Chem.* 2010;12(1):123-34.
- [78] Ranke J, Stolte S, Stormann R, Arning J, Jastorff B. Design of sustainable chemical products The example of ionic liquids. *Chem.Rev.* 2007;107(6):2183-206.

- [79] Garcia-Lorenzo A, Tojo E, Tojo J, Teijeira M, Rodriguez-Berrocal FJ, Gonzalez MP, et al. Cytotoxicity of selected imidazolium-derived ionic liquids in the human Caco-2 cell line. Sub-structural toxicological interpretation through a QSAR study. *Green Chem.* 2008;10(5):508-16.
- [80] Kulacki KJ, Lamberti GA. Toxicity of imidazolium ionic liquids to freshwater algae. *Green Chem.* 2008;10(1):104-10.
- [81] Romero A, Santos A, Tojo J, Rodriguez A. Toxicity and biodegradability of imidazolium ionic liquids. *J.Hazard.Mater.* 2008;151(1):268-73.
- [82] Latala A, Nedzi M, Stepnowski P. Toxicity of imidazolium and pyridinium based ionic liquids towards algae. *Chlorella vulgaris*, *Oocystis submarina* (green algae) and *Cyclotella meneghiniana*, *Skeletonema marinoi* (diatoms). *Green Chem.* 2009;11(4):580-8.
- [83] Latala A, Nedzi M, Stepnowski P. Toxicity of imidazolium and pyridinium based ionic liquids towards algae. *Bacillaria paxillifer* (a microphytobenthic diatom) and *Geitlerinema amphibium* (a microphytobenthic blue green alga). *Green Chem.* 2009;11(9):1371-6.
- [84] Ventura SPM, Goncalves AMM, Goncalves F, Coutinho JAP. Assessing the toxicity on C3mimTf₂N to aquatic organisms of different trophic levels. *Aquatic Toxicology* 2010;96(4):290-7.
- [85] Ventura SPM, Gardas RL, Goncalves F, Coutinho JAP. Ecotoxicological risk profile of ionic liquids: octanol-water distribution coefficients and toxicological data. *Journal of Chemical Technology and Biotechnology* 2011;86(7):957-63.
- [86] Docherty KM, Kulpa CF. Toxicity and antimicrobial activity of imidazolium and pyridinium ionic liquids. *Green Chem.* 2005;7(4):185-9.
- [87] Ventura SPM, Marques CS, Rosatella AA, Afonso CAM, Goncalves F, Coutinho JAP. Toxicity assessment of various ionic liquid families towards *Vibrio fischeri* marine bacteria. *Ecotoxicol.EnvIRON.Saf.* 2012;76:162-8.
- [88] Couling DJ, Bernot RJ, Docherty KM, Dixon JK, Maginn EJ. Assessing the factors responsible for ionic liquid toxicity to aquatic organisms via quantitative structure-property relationship modeling. *Green Chem.* 2006;8(1):82-90.
- [89] Jastorff B, Molter K, Behrend P, Bottin-Weber U, Filser J, Heimers A, et al. Progress in evaluation of risk potential of ionic liquids-basis for an eco-design of sustainable products. *Green Chem.* 2005;7(5):362-72.
- [90] Latala A, Stepnowski P, Nedzi M, Mroziak W. Marine toxicity assessment of imidazolium ionic liquids: Acute effects on the Baltic algae *Oocystis submarina* and *Cyclotella meneghiniana*. *Aquatic Toxicology* 2005;73(1):91-8.
- [91] Lee SM, Chang WJ, Choi AR, Koo YM. Influence of ionic liquids on the growth of *Esherichia coli*. *Korean Journal of Chemical Engineering* 2005;22(5): 687-90.
- [92] Matsumoto M, Mochiduki K, Kondo K. Toxicity of ionic liquids and organic solvents to lactic acid-producing bacteria. *Journal of Bioscience and Bioengineering* 2004;98(5):344-7.

- [93] Stock F, Hoffmann J, Ranke J, Stormann R, Ondruschka B, Jastorff B. Effects of ionic liquids on the acetylcholinesterase a structure-activity relationship consideration. *Green Chem.* 2004;6(6):286-90.
- [94] Cho CW, Jeon YC, Pham TPT, Vijayaraghavan K, Yun YS. The ecotoxicity of ionic liquids and traditional organic solvents on microalga *Selenastrum capricornutum*. *Ecotoxicol. Environ. Saf.* 2008;71(1):166-71.
- [95] Zhao DB, Liao YC, Zhang ZD. Toxicity of ionic liquids. *Clean-Soil Air Water* 2007;35(1):42-8.
- [96] Ranke J, Muller A, Bottin Weber U, Stock F, Stolte S, Arning J. Lipophilicity parameters for ionic liquid cations and their correlation to in vitro cytotoxicity. *Ecotoxicol. Environ. Saf.* 2007;67(3):430-8.
- [97] Stolte S, Arning J, Bottin-Weber U, Mueller A, Pitner W, Welz-Biermann U, et al. Effects of different head groups and functionalised side chains on the cytotoxicity of ionic liquids. *Green Chem.* 2007;9(7):760-7.
- [98] Stolte S, Matzke M, Arning J, Boeschen A, Pitner W, Welz-Biermann U, et al. Effects of different head groups and functionalised side chains on the aquatic toxicity of ionic liquids. *Green Chem.* 2007;9(11):1170-9.
- [99] Coleman D, Gathergood N. Biodegradation studies of ionic liquids. *Chem. Soc. Rev.* 2010;39(2):600-7.
- [100] Stolte S, Arning J, Thoeming J. Biodegradability of Ionic Liquids Test Procedures and Structural Design. *Chemie Ingenieur Technik.* 2011;83(9):1454-67.
- [101] Stolte S, Abdulkarim S, Arning J, Blomeyer-Nienstedt A, Bottin-Weber U, Matzke M, et al. Primary biodegradation of ionic liquid cations, identification of degradation products of 1-methyl-3-octylimidazolium chloride and electrochemical wastewater treatment of poorly biodegradable compounds. *Green Chem.* 2008;10(2):214-24.
- [102] Gathergood N, Scammells PJ, Garcia MT. Biodegradable ionic liquids Part III. The first readily biodegradable ionic liquids. *Green Chem.* 2006;8(2):156-60.
- [103] Petkovic M, Seddon K, Rebelo L, Pereira C. Ionic liquids: a pathway to environmental acceptability. *Chem. Soc. Rev.* 2011;40(3):1383-403.
- [104] Thi P, Cho C, Yun Y. Environmental fate and toxicity of ionic liquids: A review. *Water Res.* 2010;44(2):352-72.
- [105] Itakura T, Hirata K, Aoki M, Sasai R, Yoshida H, Itoh H. Decomposition and removal of ionic liquid in aqueous solution by hydrothermal and photocatalytic treatment. *Environmental Chemistry Letters* 2009;7(4):343-5.
- [106] Stepnowski P, Zaleska A. Comparison of different advanced oxidation processes for the degradation of room temperature ionic liquids. *Journal of Photochemistry and Photobiology A-Chemistry* 2005;170(1):45-50.

- [107] Awad W, Gilman J, Nyden M, Harris R, Sutto T, Callahan J. Thermal degradation studies of alkyl-imidazolium salts and their application in nanocomposites. *Thermochimica acta*. 2004;409(1):3-11.
- [108] Li X, Zhao J, Li Q, Wang L, Tsang SC. Ultrasonic chemical oxidative degradations of 1,3-dialkylimidazolium ionic liquids and their mechanistic elucidations. *Dalton transactions* 2007;19:1875-80.
- [109] Siedlecka EM, Czerwicka M, Stolte S, Stepnowski P. Stability of Ionic Liquids in Application Conditions. *Current Organic Chemistry* 2011;15(12):1974-91.
- [110] Siedlecka EM, Mroziak W, Kaczynski Z, Stepnowski P. Degradation of 1-butyl-3-methylimidazolium chloride ionic liquid in a Fenton-like system. *J.Hazard.Mater.* 2008;154(1-3):893-900.
- [111] Siedlecka E, Stepnowski P. The effect of alkyl chain length on the degradation of alkylimidazolium- and pyridinium-type ionic liquids in a Fenton-like system. *Environ.Sci.Pollut.Res.Int.* 2009;16(4):453-8.
- [112] Czerwicka M, Stolte S, Muller A, Siedlecka E, Golebiowski M, Kumirska J. Identification of ionic liquid breakdown products in an advanced oxidation system. *J.Hazard.Mater.* 2009;171(1-3):478-83.
- [113] Siedlecka E, Golebiowski M, Kaczynski Z, Czupryniak J, Ossowski T, Stepnowski P. Degradation of ionic liquids by Fenton reaction the effect of anions as counter and background ions. *Applied catalysis.B, Environmental* 2009;91(1-2):573-9.
- [114] Gathergood N, Garcia MT, Scammells PJ. Biodegradable ionic liquids: Part I. Concept, preliminary targets and evaluation. *Green Chem.* 2004;6(3):166-75.
- [115] Garcia MT, Gathergood N, Scammells PJ. Biodegradable ionic liquids Part II. Effect of the anion and toxicology. *Green Chem.* 2005;7(1):9-14.
- [116] Markiewicz M, Jungnickel C, Markowska A, Szczepaniak U, Paszkiewicz M, Hupka J. 1-Methyl-3-octylimidazolium Chloride-Sorption and Primary Biodegradation Analysis in Activated Sewage Sludge. *Molecules* 2009;14(11):4396-405.
- [117] Neumann J, Grundmann O, Thoeming J, Schulte M, Stolte S. Anaerobic biodegradability of ionic liquid cations under denitrifying conditions. *Green Chem.* 2010;12(4):620-7.
- [118] Deive F, Rodriguez A, Varela A, Rodrigues C, Leitao M, Houbraeken J. Impact of ionic liquids on extreme microbial biotypes from soil. *Green Chem.* 2011;13(3):687-96.
- [119] Abrusci C, Palomar J, Pablos J, Rodriguez F, Catalina F. Efficient biodegradation of common ionic liquids by *Sphingomonas paucimobilis* bacterium. *Green Chem.* 2011;13(3):709-17.
- [120] Coleman D, Gathergood N. Biodegradation studies of ionic liquids. *Chem.Soc.Rev.* 2010;39(2):600-37.

- [121] Docherty KM, Dixon JK, Kulpa CF, Jr. Biodegradability of imidazolium and pyridinium ionic liquids by an activated sludge microbial community. *Biodegradation* 2007;18(4):481-93.
- [122] Deng Y, Morrissey S, Gathergood N, Delort A, Husson P, Gomes MFC. The Presence of Functional Groups Key for Biodegradation in Ionic Liquids: Effect on Gas Solubility. *Chemosuschem* 2010;3(3):377-85.
- [123] Wang H, Malhotra SV, Francis AJ. Toxicity of various anions associated with methoxyethyl methyl imidazolium-based ionic liquids on *Clostridium*. *Chemosphere* 2011;82(11):1597-603.
- [124] Fernandez JF, Neumann J, Thoeming J. Regeneration, Recovery and Removal of Ionic Liquids. *Current Organic Chemistry* 2011;15(12):1992-2014.
- [125] Clare B, Sirwardana A, MacFarlane D. Synthesis, Purification and Characterization of Ionic Liquids. *Top.Curr.Chem.* 2009;290:1-40.
- [126] Blahusiak M, Schlosser S, Cvengros J, Martak J. New approach to regeneration of an ionic liquid containing solvent by molecular distillation. *Chemical Papers* 2011;65(5):603-7.
- [127] Cervera JLS, Koenig A. Recycling Concept for Aluminum Electrodeposition from the Ionic Liquid System EmimTf₂N-AlCl₃. *Chem.Eng.Technol.* 2010;33(12):1979-88.
- [128] Ventura SPM, Neves CMSS, Freire MG, Marrucho IM, Oliveira J, Coutinho JAP. Evaluation of Anion Influence on the Formation and Extraction Capacity of Ionic-Liquid-Based Aqueous Biphasic Systems. *J Phys Chem B* 2009;113(27):9304-10.
- [129] Neves CMSS, Ventura SPM, Freire MG, Marrucho IM, Coutinho JAP. Evaluation of Cation Influence on the Formation and Extraction Capability of Ionic-Liquid-Based Aqueous Biphasic Systems. *J Phys Chem B* 2009;113(15):5194-9.
- [130] Krockel J, Kragl U. Nanofiltration for the separation of nonvolatile products from solutions containing ionic liquids. *Chem.Eng.Technol.* 2003;26(11):1166-8.
- [131] Schafer T, Rodrigues CM, Afonso CAM, Crespo JG. Selective recovery of solutes from ionic liquids by pervaporation a novel approach for purification and green processing. *Chemical Communications* 2001;17:1622-3.
- [132] Martin MJ, Artola A, Balaguer MD, Rigola M. Activated carbons developed from surplus sewage sludge for the removal of dyes from aqueous solutions. *Chem.Eng.J.* 2003;94(3):231-9.
- [133] Martin MJ, Serra E, Ros A, Balaguer MD, Rigola M. Carbonaceous adsorbents from sewage sludge and their application in a combined activated sludge-powdered activated carbon (AS-PAC) treatment. *Carbon* 2004;42(7):1389-94.
- [134] Farooq A, Reinert L, Levêque J, Papaiconomou N, Irfan N, Duclaux L. Adsorption of ionic liquids onto activated carbons: Effect of pH and temperature. *Microporous and Mesoporous Materials* 2012;158(0):55-63.
- [135] Anthony JL, Maginn EJ, Brennecke JF. Solution thermodynamics of imidazolium-based ionic liquids and water. *J Phys Chem B* 2001;105(44):10942-9.

- [136] Vijayaraghavan K, Pham TPT, Cho CW, Won SW, Choi SB, Juan M, et al. An Assessment on the Interaction of a Hydrophilic Ionic Liquid with Different Sorbents. *Ind Eng Chem Res.* 2009;48(15):7283-8.
- [137] Beaulieu JJ, Tank JL, Kopacz M. Sorption of imidazolium-based ionic liquids to aquatic sediments. *Chemosphere* 2008;70:1320-8.
- [138] Ghatee M, Moosavi F. Physisorption of Hydrophobic and Hydrophilic 1-Alkyl-3-methylimidazolium Ionic Liquids on the Graphenes. *The journal of physical chemistry.C* 2011;115(13):5626-36.
- [139] Matzke M, Thiele K, Müller A, Filser J. Sorption and desorption of imidazolium based ionic liquids in different soil types. *Chemosphere* 2009;74(4):568-74.
- [140] Mroziak W, Jungnickel C, Skup M, Urbaszek P, Stepnowski P. Determination of the adsorption mechanism of imidazolium-type ionic liquids onto kaolinite: implications for their fate and transport in the soil environment. *Environmental chemistry* 2008;5(4):299-306.
- [141] Stepnowski P. Preliminary assessment of the sorption of some alkyl imidazolium cations as used in ionic liquids to soils and Sediments. *Aust.J.Chem.* 2005;58(3):170-3.
- [142] Stepnowski P, Mroziak W, Nischhauser J. Adsorption of alkylimidazolium and alkylpyridinium ionic liquids onto natural soils. *Environ.Sci.Technol.* 2007;41(2):511-6.
- [143] Studzinska S, Kowalkowski T, Buszewski B. Study of ionic liquid cations transport in soil. *J.Hazard.Mater.* 2009;168(2-3):1542-7.
- [144] Bansal R, Goyal M. Activated carbon adsorption. Florida: Taylor and Francis; 2005.
- [145] Li L, Liu S, Zhu T. Application of activated carbon derived from scrap tires for adsorption of Rhodamine B. *Journal of Environmental Sciences-China* 2010;22(8):1273-80.
- [146] Demirbas E, Dizge N, Sulak MT, Kobya M. Adsorption kinetics and equilibrium of copper from aqueous solutions using hazelnut shell activated carbon. *Chem.Eng.J.* 2009;148(2-3):480-7.
- [147] Yin CY, Aroua MK, Daud WMAW. Review of modifications of activated carbon for enhancing contaminant uptakes from aqueous solutions. *Separation and Purification Technology* 2007;52(3):403-15.
- [148] Ahmaruzzaman M. Adsorption of phenolic compounds on low-cost adsorbents: A review. *Adv.Colloid Interface Sci.* 2008;143(1-2):48-67.
- [149] Yang J, Baek K, Kwon T, Yang J. Adsorption of chlorinated solvents in nonionic surfactant solutions with activated carbon in a fixed bed. *Journal of Industrial and Engineering Chemistry* 2009;15(6):777-9.
- [150] Brunauer S, Emmett PH, Teller E. Adsorption of gases in multimolecular layers. *J.Am.Chem.Soc.* 1938;60:309-19.

- [151] Sing K. Adsorption methods for the characterization of porous materials. *Advances in colloid and interface science* 1998;76:3-11.
- [152] Halsey G. Physical Adsorption on Non-Uniform Surfaces. *J.Chem.Phys.* 1948;16(10):931-7.
- [153] Lowell S, Shields JE. Hysteresis, Entrapment, and Wetting Angle in Mercury Porosimetry. *J.Colloid Interface Sci.* 1981;83(1):273-8.
- [154] Lowell S, Shields JE. Influence of Contact-Angle on Hysteresis in Mercury Porosimetry. *J.Colloid Interface Sci.* 1981;80(1):192-6.
- [155] Lowell S, Shields JE. Influence of Pore Potential on Hysteresis and Entrapment in Mercury Porosimetry Pore Potential Hysteresis Porosimetry. *J.Colloid Interface Sci.* 1982;90(1):203-11.
- [156] Rey A, Faraldos M, Casas JA, Zazo JA, Bahamonde A, Rodriguez JJ. Catalytic wet peroxide oxidation of phenol over Fe/AC catalysts: Influence of iron precursor and activated carbon surface. *Applied Catalysis B-Environmental* 2009;86(1-2):69-77.
- [157] Figueiredo JL, Pereira MFR, Freitas MMA, Orfao JJM. Modification of the surface chemistry of activated carbons. *Carbon* 1999;37(9):1379-89.
- [158] Figueiredo JL, Pereira MFR. The role of surface chemistry in catalysis with carbons. *Catalysis Today* 2010;150(1-2):2-7.
- [159] Moreno-Castilla C, Carrasco-Marin F, Maldonado-Hodar FJ, Rivera-Utrilla J. Effects of non-oxidant and oxidant acid treatments on the surface properties of an activated carbon with very low ash content. *Carbon* 1998;36(1-2):145:51.
- [160] Moreno-Castilla C, Lopez-Ramon MV, Carrasco-Marin F. Changes in surface chemistry of activated carbons by wet oxidation. *Carbon* 2000;38(14):1995-2001.
- [161] Szymanski GS, Karpinski Z, Biniak S, Swiatkowski A. The effect of the gradual thermal decomposition of surface oxygen species on the chemical and catalytic properties of oxidized activated carbon. *Carbon* 2002;40(14):PII S0008-6223(02)00188-4: 2627-39.
- [162] Srivastava S, Tyagi R, Pant N. Adsorption of Heavy-Metal Ions on Carbonaceous Material Developed from the Waste Slurry Generated in Local Fertilizer Plants. *Water Res.* 1989;23(9):1161-5.
- [163] Zazo JA, Fraile AF, Rey A, Bahamonde A, Casas JA, Rodriguez JJ. Optimizing calcination temperature of Fe/activated carbon catalysts for CWPO. *Catalysis Today* 2009;143(3-4):341-6.
- [164] Lemus J, Palomar J, Heras F, Gilarranz MA, Rodriguez JJ. Developing criteria for the recovery of ionic liquids from aqueous phase by adsorption with activated carbon. *Separation and Purification Technology* 2012;97:11-9.
- [165] Palomar J, Lemus J, Gilarranz MA, Rodriguez JJ. Adsorption of ionic liquids from aqueous effluents by activated carbon. *Carbon* 2009;47(7):1846-56.

- [166] Gustafso, RL, Albright RL, Heisler J, Lirio JA, Reid OT. Adsorption of Organic Species by High Surface Area Styrene-Divinylbenzene Copolymers. *Industrial & Engineering Chemistry Product Research and Development* 1968;7(2):107.
- [167] Bell JP, Tsezos M. Removal of Hazardous Organic Pollutants by Biomass Adsorption. *Journal Water Pollution Control Federation* 1987;59(4):191-8.
- [168] Cotoruelo LM, Marques MD, Rodriguez-Mirasol J, Cordero T, Rodriguez JJ. Adsorption of aromatic compounds on activated carbons from lignin: Equilibrium and thermodynamic study. *Ind Eng Chem Res.* 2007;46(14):4982-90.
- [169] Cotoruelo LM, Marques MD, Rodriguez-Mirasol J, Rodriguez JJ, Cordero T. Cationic dyes removal by multilayer adsorption on activated carbons from lignin. *Journal of Porous Materials* 2011;18(6):693-702.
- [170] Ho Y. Citation review of Lagergren kinetic rate equation on adsorption reactions. *Scientometrics* 2004;59(1):171-7.
- [171] Ho YS, McKay G. Pseudo-second order model for sorption processes. *Process Biochemistry* 1999;34(5):451-65.
- [172] Cotoruelo LM, Marques MD, Rodriguez-Mirasol J, Rodriguez JJ, Cordero T. Lignin-based activated carbons for adsorption of sodium dodecylbenzene sulfonate: Equilibrium and kinetic studies. *J. Colloid Interface Sci.* 2009;332(1):39-45.
- [173] Kannan N, Sundaram M. Kinetics and mechanism of removal of methylene blue by adsorption on various carbons a comparative study. *Dyes and Pigments* 2001;51(1):25-40.
- [174] Mezenner NY, Bensmaili A. Kinetics and thermodynamic study of phosphate adsorption on iron hydroxide-eggshell waste. *Chem. Eng. J.* 2009;147(2-3):87-96.
- [175] Qadeer R. Kinetic study of erbium ion adsorption on activated charcoal from aqueous solutions. *Adsorption-Journal of the International Adsorption Society* 2005;11(1):51-5.
- [176] Qiu H, Lv L, Pan B, Zhang Q, Zhang W, Zhang Q. Critical review in adsorption kinetic models. *Journal of Zhejiang University-Science a* 2009;10(5):716-24.
- [177] Mehnert CP, Cook RA, Dispenziere NC, Afeworki M. Supported ionic liquid catalysis A new concept for homogeneous hydroformylation catalysis. *J. Am. Chem. Soc.* 2002; 124(44):12932-3.
- [178] Riisager A, Fehrmann R, Flicker S, van Hal R, Haumann M, Wasserscheid P. Very stable and highly regioselective supported ionic-liquid-phase (SILP) catalysis: Continuous flow fixed-bed hydroformylation of propene. *Angewandte Chemie-International Ed.* 2005;44(5):815-9.
- [179] Mikkola JT, Virtanen PP, Kordás K, Karhu H, Salmi TO. SILCA—Supported ionic liquid catalysts for fine chemicals. *Applied Catalysis A: General* 2007;328(1):68-76.
- [180] Shangguan X, Zhang H, Zheng J. Direct electrochemistry of glucose oxidase based on its direct immobilization on carbon ionic liquid electrode and glucose sensing. *Electrochem. Commun.* 2008;10(8):1140-3.

- [181] Vangeli OC, Romanos GE, Beltsios KG, Fokas D, Kouvelos EP, Stefanopoulos KL, et al. Grafting of Imidazolium Based IL on the Pore Surface of Nanoporous Materials-Study of Physicochemical and Thermodynamic Properties. *J Phys Chem B* 2010;114(19):6480-91.
- [182] Riisager A, Fehrmann R, Haumann M, Wasserscheid P. Supported ionic liquids: versatile reaction and separation media. *Topics in Catalysis* 2006;40(1-4):91-102.
- [183] Kohler F, Roth D, Kuhlmann E, Wasserscheid P, Haumann M. Continuous gas-phase desulfurisation using supported ionic liquid phase (SILP) materials. *Green Chem.* 2010;12(6):979-84.
- [184] Steinrueck H-, Libuda J, Wasserscheid P, Cremer T, Kolbeck C, Laurin M, et al. Surface Science and Model Catalysis with Ionic Liquid-Modified Materials. *Adv Mater.* 2011;23(22-23):2571-87.
- [185] Liu H, Liu Y, Li J. Ionic liquids in surface electrochemistry. *PCCP. Physical chemistry chemical physics* 2010;12(8):1685-97.
- [186] Riisager A, Fehrmann R, Haumann M, Wasserscheid P. Supported Ionic Liquid Phase (SILP) catalysis: An innovative concept for homogeneous catalysis in continuous fixed-bed reactors. *European Journal of Inorganic Chemistry.* 2006;4:695-706.
- [187] Werner S, Szesni N, Bittermann A, Schneider MJ, Harter P, Haumann M, et al. Screening of Supported Ionic Liquid Phase (SILP) catalysts for the very low temperature water-gas-shift reaction. *Applied Catalysis A-General* 2010;377(1-2):70-5.
- [188] Joni J, Haumann M, Wasserscheid P. Continuous gas-phase isopropylation of toluene and cumene using highly acidic Supported Ionic Liquid Phase (SILP) catalysts. *Applied Catalysis A: General* 2010;372(1):8-15.
- [189] Wasserscheid P. Continuous reactions using ionic liquids as catalytic phase. *Journal of Industrial and Engineering Chemistry* 2007;13(3):325-38.
- [190] Hintermair U, Gong Z, Serbanovic A, Muldoon MJ, Santini CC, Cole-Hamilton DJ. Continuous flow hydroformylation using supported ionic liquid phase catalysts with carbon dioxide as a carrier. *Dalton Transactions* 2010;39(36):8501:10.
- [191] Li S, Wang J, Kou Y, Zhang S. Ionic-Liquid-Grafted Rigid Poly (p-Phenylene) Microspheres: Efficient Heterogeneous Media for Metal Scavenging and Catalysis. *Chem.-Eur.J.* 2010;16(6):1812-8.
- [192] Shi F, Zhang QH, Li DM, Deng YQ. Silica-gel-confined ionic liquids: A new attempt for the development of supported nanoliquid catalysis. *Chemistry-a European Journal* 2005;11(18):5279-88.
- [193] Rodriguez-Perez L, Teuma E, Falqui A, Gomez M, Serp P. Supported ionic liquid phase catalysis on functionalized carbon nanotubes. *Chemical Communications.* 2008(35): 4201-3.
- [194] Gelesky MA, Chiaro SSX, Pavan FA, dos Santos JHZ, Dupont J. Supported ionic liquid phase rhodium nanoparticle hydrogenation catalysts. *Dalton Transactions.* 2007;47: 5549-53.

- [195] Yang WW, Lu YC, Xiang ZY, Luo GS. Monodispersed microcapsules enclosing ionic liquid of 1-butyl-3-methylimidazolium hexafluorophosphate. *React Funct Polym.* 2007;67(1):81-6.
- [196] Lazzari M, Mastragostino M, Pandolfo AG, Ruiz V, Soavi F. Role of Carbon Porosity and Ion Size in the Development of Ionic Liquid Based Supercapacitors. *J.Electrochem.Soc.* 2011;158(1):22-5.
- [197] Xiang ZY, Lu YC, Zou Y, Gong XC, Luo GS. Preparation of microcapsules containing ionic liquids with a new solvent extraction system. *Reactive & Functional Polymers* 2008;68(8):1260-5.
- [198] Ruta M, Yuranov I, Dyson PJ, Laurency G, Kiwi-Minsker L. Structured fiber supports for ionic liquid-phase catalysis used in gas-phase continuous hydrogenation. *Journal of Catalysis* 2007;247(2):269-76.
- [199] Zhang ZM, Wu LB, Dong J, Li BG, Zhu SP. Preparation and SO₂ Sorption/Desorption Behavior of an Ionic Liquid Supported on Porous Silica Particles. *Ind Eng Chem Res.* 2009;48(4):2142-8.
- [200] Tatárová I, Fáber R, Denoyel R, Polakovič M. Characterization of pore structure of a strong anion-exchange membrane adsorbent under different buffer and salt concentration conditions. *Journal of Chromatography A* 2009;1216(6):941-7.
- [201] Hao Y, Peng J, Hu S, Li J, Zhai M. Thermal decomposition of allyl-imidazolium-based ionic liquid studied by TGA-MS analysis and DFT calculations. *Thermochimica Acta.* 2010;501(1-2):78-83.
- [202] Fernandez A, Torrecilla JS, Garcia J, Rodriguez F. Thermophysical properties of 1-ethyl-3-methylimidazolium ethylsulfate and 1-butyl-3-methylimidazolium methylsulfate ionic liquids. *J.Chem.Eng.Data* 2007;52:1979-83.
- [203] Carvalho PJ, Coutinho JAP. Non-ideality of Solutions of NH₃, SO₂, and H₂S in Ionic Liquids and the Prediction of Their Solubilities Using the Flory-Huggins Model. *Energy Fuels* 2010;24:6662-6.
- [204] W.J. Hayes ERL. *Handbook of Pesticide Toxicology*. San Diego: Academic Press; 1991.
- [205] Tancrede M, Wilson R, Zeise L, Crouch EAC. The Carcinogenic Risk of some Organic Vapors Indoors a Theoretical Survey. *Atmos.Environ.* 1987;21(10).
- [206] Goldberg ED. Halogenated Hydrocarbons Past, Present and Near-Future Problems. *Sci.Total Environ.* 1991;100:17:28.
- [207] Verhulst D, Buekens A, Spencer P, Eriksson G. Thermodynamic behavior of metal chlorides and sulfates under the conditions of incineration furnaces. *Environ.Sci.Technol.* 1996;30(1):50-6.
- [208] Buekens A, Huang H. Comparative evaluation of techniques for controlling the formation and emission of chlorinated dioxins/furans in municipal waste incineration. *J.Hazard.Mater.* 1998;62(1):1-33.

- [209] Ballikaya M, Atalay S, Alpay H, Atalay F. Catalytic combustion of methylenechloride. *Combustion Sci.Technol.* 1996;120(1-6):169-84.
- [210] Atalay S, Alpay H, Atalay F. Catalyst preparation and testing for catalytic combustion of chloromethanes. 2002;69: 355-64.
- [211] Li C, Lee W, Chen C, Wang Y. CH₂Cl₂ decomposition by using a radio-frequency plasma system. *Journal of Chemical Technology and Biotechnology* 1996;66(4):382-8.
- [212] Everaert K, Baeyens J. Catalytic combustion of volatile organic compounds. *J.Hazard.Mater.* 2004;109(1-3):113-39.
- [213] Wang J, Chen J. Removal of dichloromethane from waste gases with a bio-contact oxidation reactor. *Chem.Eng.J.* 2006;123(3):103-7.
- [214] Gomez-Sainero L, Seoane X, Arcoya A. Hydrodechlorination of carbon tetrachloride in the liquid phase on a Pd/carbon catalyst: kinetic and mechanistic studies. *Applied Catalysis B-Environmental* 2004;53(2):101-10.
- [215] Gomez-Sainero L, Seoane X, Fierro J, Arcoya A. Liquid-phase hydrodechlorination of CCl₄ to CHCl₃ on Pd/carbon catalysts: Nature and role of Pd active species. *Journal of Catalysis* 2002;209(2):279-88.
- [216] Gomez-Sainero L, Seoane X, Tijero E, Arcoya A. Hydrodechlorination of carbon tetrachloride to chloroform in the liquid phase with a Pd/carbon catalyst. Study of the mass transfer steps. *Chemical Engineering Science* 2002;57(17):3565-74.
- [217] Alvarez-Montero MA, Gomez-Sainero LM, Juan-Juan J, Linares-Solano A, Rodriguez JJ. Gas-phase hydrodechlorination of dichloromethane with activated carbon-supported metallic catalysts. *Chem.Eng.J.* 2010;162(2):599-608.
- [218] Alvarez-Montero MA, Gomez-Sainero LM, Martin-Martinez M, Heras F, Rodriguez JJ. Hydrodechlorination of chloromethanes with Pd on activated carbon catalysts for the treatment of residual gas streams. *Applied Catalysis B-Environmental* 2010;96(1-2):148-56.
- [219] Alvarez-Montero MA, Gomez-Sainero LM, Mayoral A, Diaz I, Baker RT, Rodriguez JJ. Hydrodechlorination of chloromethanes with a highly stable Pt on activated carbon catalyst. *Journal of Catalysis* 2011;279(2):389-96.
- [220] Zuber L, Dunn I, Deshusses M. Comparative scale-up and cost estimation of a biological trickling filter and a three-phase airlift bioreactor for the removal of methylene chloride from polluted air. *J.Air Waste Manage.Assoc.* 1997;47(9):969-75.
- [221] Cox H, Deshusses M, Converse B, Schroeder E, Iranpour R. Odor and volatile organic compound treatment by biotrickling filters: Pilot-scale studies at hyperion treatment plant. *Water Environ.Res.* 2002;74(6):557-63.
- [222] Yu Jian-ming, Chen Jian-meng, Wang Jia-de. Removal of dichloromethane from waste gases by a biotrickling filter. *Journal of Environmental Sciences-China* 2006;18(6):1073-6.

- [223] Ghoshal A, Manjare S. Selection of appropriate adsorption technique for recovery of VOCs: an analysis. *J Loss Prev Process Ind* 2002;15(6):413-21.
- [224] Gallego E, Roca FJ, Perales JF, Guardino X. Comparative study of the adsorption performance of a multi-sorbent bed (Carbotrap, Carbopack X, Carboxen 569) and a Tenax TA adsorbent tube for the analysis of volatile organic compounds (VOCs). *Talanta*. 2010;81(3):916-24.
- [225] Anfruns A, Canals-Batlle C, Ros A, Lillo-Rodenas MA, Linares-Solano A, Fuente E, et al. Removal of odour-causing compounds using carbonaceous adsorbents/catalysts prepared from sewage sludge. *Water Science and Technology* 2009;59(7):1371-6.
- [226] Anfruns A, Martin MJ, Montes-Moran MA. Removal of odorous VOCs using sludge-based adsorbents. *Chem.Eng.J.* 2011;166(3):1022-31.
- [227] Ren X, Chen C, Nagatsu M, Wang X. Carbon nanotubes as adsorbents in environmental pollution management: A review. *Chem.Eng.J.* 2011;170(2-3):395-410.
- [228] Cochrane EL, Lu S, Gibb SW, Villaescusa I. A comparison of low-cost biosorbents and commercial sorbents for the removal of copper from aqueous media. *J.Hazard.Mater.* 2006;137(1): 198-206.
- [229] Matsumoto A, Zhao JX, Tsutsumi K. Adsorption behavior of hydrocarbons on slit-shaped micropores. *Langmuir* 1997;13(3):496-501.
- [230] Hernandez MA, Gonzalez AI, Rojas F, Asomoza M, Solis S, Portillo R. Adsorption of chlorinated compounds (chlorobenzene, chloroform, and carbon tetrachloride) on microporous SiO₂, Ag-doped SiO₂ and natural and dealuminated clinoptilolites. *Ind Eng Chem Res* 2007;46(10):3373-81.
- [231] Koornneef J, Ramirez A, van Harmelen T, van Horssen A, Turkenburg W, Faaij A. The impact of CO₂ capture in the power and heat sector on the emission of SO₂, NO_x, particulate matter, volatile organic compounds and NH₃ in the European Union. *Atmos. Environ.* 2010;44(11):1369-85.
- [232] Sutton MA, Fowler D. Introduction: fluxes and impacts of atmospheric ammonia on national, landscape and farm scales. *Environmental Pollution* 2002;119(1):PII S0269-7491(01)00145-2:7-8.
- [233] Erisman JW, Sutton MA. Reduced nitrogen in ecology and the environment: Special issue of the ESF-FWF Conference in partnership with LFUI, October 2006. *Environmental Pollution* 2008;154(3):140-9.
- [234] Sutton MA, Erisman JW, Dentener F, Moeller D. Ammonia in the environment: From ancient times to the present. *Environmental Pollution* 2008;156(3):583:604.
- [235] Brettschneider O, Thiele R, Faber R, Thielert H, Wozny G. Experimental investigation and simulation of the chemical absorption in a packed column for the system NH₃-CO₂-H₂S-NaOH-H₂O. *Separation and Purification Technology* 2004;39(3):139-59.

- [236] Jung SY, Lee SJ, Park JJ, Lee SC, Jun HK, Lee TJ, et al. The simultaneous removal of hydrogen sulfide and ammonia over zinc-based dry sorbent supported on alumina. *Separation and Purification Technology* 2008;63(2):297-302.
- [237] Park CW, Byeon JH, Yoon KY, Park JH, Hwang J. Simultaneous removal of odors, airborne particles, and bioaerosols in a municipal composting facility by dielectric barrier discharge. *Separation and Purification Technology*. 2011;77(1):87-93.
- [238] Ho YS, McKay G. Pseudo-second order model for sorption processes. *Process Biochemistry* 1999;34(5):451-65.
- [239] Yoon YH, Nelson JH. Application of Gas-Adsorption Kinetics .1. a Theoretical-Model for Respirator Cartridge Service Life. *Am.Ind.Hyg.Assoc.J.* 1984;45(8):509-16.
- [240] Yoon YH, Nelson JH. Application of Gas-Adsorption Kinetics .2. a Theoretical-Model for Respirator Cartridge Service Life and its Practical Applications. *Am.Ind.Hyg.Assoc.J.* 1984;45(8):517-24.
- [241] Ho YS, McKay G. Kinetic models for the sorption of dye from aqueous solution by wood. *Process Saf. Environ. Prot.* 1998;76(B2):183-91.
- [242] Vijayaraghavan K, Palanivelu K, Velan M. Biosorption of copper (II) and cobalt (II) from aqueous solutions by crab shell particles. *Bioresour. Technol.* 2006;97(12):1411-9.
- [243] Lodewyckx P, Wood G, Ryu S. The Wheeler-Jonas equation: a versatile tool for the prediction of carbon bed breakthrough times. *Carbon* 2004;42(7):1351-5.
- [244] Burkert CAV, Barbosa GNO, Mazutti MA, Maugeri F. Mathematical modeling and experimental breakthrough curves of cephalosporin C adsorption in a fixed-bed column. *Process Biochemistry* 2011;46(6):1270-7.
- [245] Buggert M, Cadena C, Mokrushina L, Smirnova I, Maginn EJ, Arlt W. COSMO-RS Calculations of Partition Coefficients: Different Tools for Conformational Search. *Chem. Eng. Technol.* 2009;32(6):977-86.
- [246] Navas A, Ortega J, Vreekamp R, Marrero E, Palomar J. Experimental Thermodynamic Properties of 1-Butyl-2-methylpyridinium Tetrafluoroborate $b2mpyBF_4$ with Water and with Alkan-1-ol and Their Interpretation with the COSMO-RS Methodology. *Ind Eng Chem Res.* 2009;48(5):2678-90.
- [247] Klamt A, Eckert F. COSMO-RS: a novel and efficient method for the *a priori* prediction of thermophysical data of liquids. *Fluid Phase Equilib.* 2000;172(1):43-72.
- [248] Klamt A, Jonas V, Burger T, Lohrenz JCW. Refinement and parametrization of COSMO-RS. *Journal of Physical Chemistry a.* 1998;102(26): 5074-85.
- [249] Eckert F, Klamt A. Fast solvent screening via quantum chemistry: COSMO-RS approach. *AIChE J.* 2002;48(2):369-85.
- [250] Gmehling J. Present status of group-contribution methods for the synthesis and design of chemical processes. *Fluid Phase Equilib.* 1998;144(1-2):37-47.

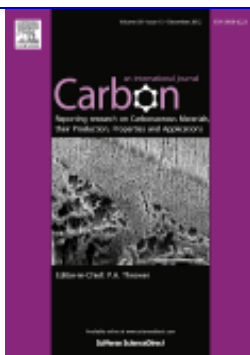
- [251] Bedia J, Ruiz E, de Riva J, Ferro VR, Palomar J, Rodriguez JJ. Optimized ionic liquids for toluene absorption. *AIChE J.* 2012. DOI 10.1002/aic.13926
- [252] Banerjee T, Singh MK, Khanna A. Prediction of binary VLE for imidazolium based ionic liquid systems using COSMO-RS. *Ind Eng Chem Res* 2006;45(9): 3207-19.
- [253] Palomar J, Ferro VR, Torrecilla JS, Rodriguez F. Density and molar volume predictions using COSMO-RS for ionic liquids. An approach to solvent design. *Ind Eng Chem Res.* 2007;46(18):6041-8.
- [254] Palomar J, Torrecilla S, Ferro VR, Rodriguez F. Development of an *a priori* Ionic Liquid Design Tool. 1. Integration of a novel COSMO-RS Molecular Descriptor on Neural Networks. *Industrial engineering chemistry research* 2008;47:4523-32.
- [255] Mu T, Rarey J, Gmehling J. Performance of COSMO-RS with sigma profiles from different model chemistries. *Ind Eng Chem Res* 2007;46(20): 6612-29.
- [256] Klamt A, Eckert F. Prediction, fine tuning, and temperature extrapolation of a vapor liquid equilibrium using COSMOtherm. *Fluid Phase Equilib.* 2007;260(2):12256-9.
- [257] Goss K. Predicting Adsorption of Organic Chemicals at the Air-Water Interface. *Journal of Physical Chemistry a.* 2009;113(44).
- [258] Wittekindt C, Goss K. Screening the partition behavior of a large number of chemicals with a quantum-chemical software. *Chemosphere* 2009;76(4):460-4.
- [259] Puzyn T, Mostrag A, Falandysz J, Kholod Y, Leszczynski J. Predicting water solubility of congeners: Chloronaphthalenes-A case study. *J.Hazard.Mater.* 2009;170(2-3): 1014-22.
- [260] Marrero E, Ortega J, Palomar J. Thermodynamic study of (alkyl esters + α,ω -alkyl dihalides) VII: H_m^E and V_m^E for 20 binary mixtures $\{x\text{C}_{\mu-1}\text{H}_{2\mu-1}\text{CO}_2\text{C}_3\text{H}_7 + (1-x)\text{alpha,omega-ClCH}_2(\text{CH}_2)_{\nu-2}\text{CH}_2\text{Cl}\}$, where $\mu=1$ to 4, $\alpha=1$ and $\nu=\omega= 2$ to 6. An analysis of behavior using the COSMO-RS methodology. *Journal of Chemical Thermodynamics* 2009;41(3):367-82.
- [261] Eckert F, Leito I, Kaljurand I, Kuett A, Klamt A, Diedenhofen M. Prediction of Acidity in Acetonitrile Solution with COSMO-RS. *Journal of Computational Chem.* 2009;30(5):799-810.
- [262] Toghiani RK, Toghiani H, Maloney SW, Boddu VM. Prediction of physicochemical properties of energetic materials. *Fluid Phase Equilib.* 2008;264(1-2):86-92.
- [263] Burghoff B, Schiferli J, Marques JS, de Haan AB. Extractant screening and selection for methyl tert-butyl ether removal from aqueous streams. *Chemical Engineering Science* 2009;64(12):2887-92.
- [264] Kumar AAP, Banerjee T. Thiophene separation with ionic liquids for desulphurization: A quantum chemical approach. *Fluid Phase Equilib.* 2009;278(1-2):1-8.
- [265] Spiess AC, Eberhard W, Peters M, Eckstein MF, Greiner L, Buechs J. Prediction of partition coefficients using COSMO-RS: Solvent screening for maximum conversion in biocatalytic two-phase reaction systems. *Chem.Eng.Process* 2008;47(6):1034-41.

- [266] Palomar J, Torrecilla JS, Lemus J, Ferro VR, Rodriguez F. A COSMO-RS based guide to analyze/quantify the polarity of ionic liquids and their mixtures with organic cosolvents. *Physical Chemistry Chemical Physics* 2010;12(8):1991-2000.
- [267] Fermeglia M, Longo G, Toma L. Computer Aided Design for Sustainable Industrial Processes: Specific Tools and Applications. *AIChE J.* 2009;55(4):1065-78.
- [268] Cadoret L, Yu C, Huang H, Lee M. Effects of physical properties estimation on process design: a case study using AspenPlus. *Asia-Pacific Journal of Chem. Eng.* 2009;4(5):729-34.
- [269] Klamt A. *COMSO-RS: from quantum chemistry to fluid phase thermodynamics and drug design*. Amsterdam: Elsevier, 1st ed. 2005.
- [270] Diedenhofen M, Klamt A. COSMO-RS as a tool for property prediction of IL mixtures-A review. *Fluid Phase Equilib.* 2010;294(1-2):31-8.
- [271] Palomar J, Torrecilla JS, Ferro VR, Rodriguez F. Development of an a Priori Ionic Liquid Design Tool. 2. Ionic Liquid Selection through the Prediction of COSMO-RS Molecular Descriptor by Inverse Neural Network. *Ind Eng Chem Res* 2009;48(4):2257-65.
- [272] Coutinho JAP, Carvalho PJ, Oliveira NMC. Predictive methods for the estimation of thermophysical properties of ionic liquids. *Rsc Advances* 2012;2(19):7322-46.
- [273] Diedenhofen M, Klamt A, Marsh K, Schaefer A. Prediction of the vapor pressure and vaporization enthalpy of 1-n-alkyl-3-methylimidazolium-bis-(trifluoromethanesulfonyl) amide ionic liquids. *Physical Chemistry Chemical Physics* 2007;9(33):4653-6.
- [274] Diedenhofen M, Eckert F, Klamt A. Prediction of infinite dilution activity coefficients of organic compounds in ionic liquids using COSMO-RS. *J.Chem.Eng.Data* 2003;48(3):475-79.
- [275] Banerjee T, Khanna A. Infinite dilution activity coefficients for trihexyltetradecyl phosphonium ionic liquids: Measurements and COSMO-RS prediction. *J.Chem.Eng.Data* 2006;51(6):2170-7.
- [276] Ab Manan N, Hardacre C, Jacquemin J, Rooney DW, Youngs TGA. Evaluation of Gas Solubility Prediction in ILs using COSMOthermX. *J.Chem.Eng.Data* 2009;54(7):2005-22.
- [277] Freire MG, Santos LMNBF, Marrucho IM, Coutinho JAP. Evaluation of COSMO-RS for the prediction of LLE and VLE of alcohols plus ionic liquids. *Fluid Phase Equilib.* 2007;255(2):167-78.
- [278] Kato R, Gmehling J. Systems with ionic liquids: Measurement of VLE and $\gamma(\infty)$ data and prediction of their thermodynamic behavior using original UNIFAC, mod. UNIFAC(DO) and COSMO-RS(O1). *Journal of Chemical Thermodynamics* 2005;37(6):603-19.
- [279] Domanska U, Pobudkowska A, Eckert F. Liquid-liquid equilibria in the binary systems (1,3-dimethylimidazolium, or 1-butyl-3-methylimidazolium methylsulfate plus hydrocarbons). *Green Chem.* 2006;8(3):268-76.

- [280] Freire MG, Ventura SPM, Santos LMNBF, Marrucho IM, Coutinho JAP. Evaluation of COSMO-RS for the prediction of LLE and VLE of water and ionic liquids binary systems. *Fluid Phase Equilib.* 2008;268(1-2):74-84.
- [281] Ferreira AR, Freire MG, Ribeiro JC, Lopes FM, Crespo JG, Coutinho JAP. Overview of the L-L Equilibria of Ternary Systems Composed of Ionic Liquid and Aromatic and Aliphatic Hydrocarbons, and Their Modeling by COSMO-RS. *Ind Eng Chem Res.* 2012;51(8):3483-507.
- [282] Ionic Liquids Database- (ILThermo). 2010; Available at: <http://ilthermo.boulder.nist.gov/ILThermo/mainmenu.uix>. Accessed 7/23, 2006.
- [283] McGowan JC. Analysis of polyimide dielectric coatings using attenuated total reflectance. *Anal Chem* 1969;41:2074-85.
- [284] Freire MG, Carvalho PJ, Fernandes AM, Marrucho IM, Queimada AJ, Coutinho JAP. Surface tensions of imidazolium based ionic liquids: Anion, cation, temperature and water effect. *J. Colloid Interface Sci.* 2007;314(2):621-30.
- [285] Zhang X, Liu Z, Wang W. Screening of ionic liquids to capture CO₂ by COSMO-RS and experiments. *AIChE J.* 2008;54(10):2717-28.
- [286] Ramalingam A, Banerjee T. Prediction and Validation of Carbon Dioxide Gas Solubility in Ionic Liquids at T = 298 K and Atmospheric Pressure using Quantum Chemical Approach. *Chemical Product and Process Modeling.* 2011;6(1):20-7.
- [287] Ortega J, Vreekamp R, Marrero E, Penco E. Thermodynamic properties of 1-butyl-3-methylpyridinium tetrafluoroborate and its mixtures with water and alkanols. *J. Chem. Eng. Data* 2007;52(6):2269-76.
- [288] Ortega J, Vreekamp R, Penco E, Marrero E. Mixing thermodynamic properties of 1-butyl-4-methylpyridinium tetrafluoroborate b4mpyBF₄ with water and with an alkan-1ol (methanol to pentanol). *Journal of Chemical Thermodynamics* 2008;40(7):1087-94.
- [289] Schroeder B, Santos LMNBF, Rocha MAA, Oliveira MB, Marrucho IM, Coutinho JAP. Prediction of environmental parameters of polycyclic aromatic hydrocarbons with COSMO-RS. *Chemosphere* 2010;79(8):821-9.
- [290] Wille S, Buggert M, Mokrushina L, Arlt W, Smirnova I. Effect of Electrolytes on Octanol-Water Partition Coefficients: Calculations with COSMO-RS. *Chem. Eng. Technol.* 2010;33(7):1072-82.
- [291] Ingram T, Richter U, Mehling T, Smirnova I. Modelling of pH dependent n-octanol/water partition coefficients of ionizable pharmaceuticals. *Fluid Phase Equilib.* 2011;305(2):197-203.

**ESSAYS ON IONIC LIQUID/ACTIVATED CARBON SYSTEMS AND THEIR
APPLICATION TO POLLUTANT REMOVAL**

Doctoral dissertation, [Madrid 2012](#), Jesús Lemus Torres



Paper I

*ADSORPTION OF IONIC LIQUIDS FROM AQUEOUS
EFFLUENTS BY ACTIVATED CARBON*

79-106

J. Palomar, J. Lemus, M.A. Gilarranz, J.J. Rodríguez
IONIC LIQUIDS REMOVAL FROM AQUEOUS EFFLUENTS BY
ADSORPTION ONTO ACTIVATED CARBON

Carbon. 2009 (47) 1846-1856

Resumen

Este primer capítulo presenta un estudio detallado de la separación de líquidos iónicos imidazolios de corrientes acuosas por adsorción en carbones activos comerciales. Se han realizado experimentos de equilibrio para obtener isothermas de adsorción de líquidos iónicos en carbón activo a diferentes temperaturas. La influencia tanto del anión como del catión fue analizada gracias al estudio de 17 líquidos iónicos. El papel de la superficie química del adsorbente también fue analizado, utilizando carbones activos modificados química y físicamente. La incorporación de líquido iónico a la superficie del carbón activo fue analizada por medio de isothermas de adsorción-desorción de nitrógeno a 77 K y por análisis elemental. Además, el programa químico-cuántico COSMO-RS ha permitido estimar propiedades termodinámicas y moleculares de sistemas trifásicos soluto-adsorbente-adsorbato, lo que permite el análisis del mecanismo de adsorción desde un punto de vista molecular. Los resultados de este trabajo han permitido concluir que la adsorción con carbón activo es una aplicación abordable desde el punto de vista medioambiental para eliminar líquidos iónicos hidrofóbicos de corrientes acuosas, proponiendo el uso de acetona para la regeneración del adsorbente. También se ha demostrado que la adsorción de líquidos iónicos hidrofílicos se puede mejorar mediante la modificación de la cantidad y naturaleza de los grupos oxigenados superficiales del carbón, particularmente mediante la inclusión de grupos hidroxilos que favorecen las interacciones de enlace de hidrógeno con los grupos básicos de los líquidos iónicos hidrofílicos.

Abstract

The separation of imidazolium based ionic liquids (ILs) from aqueous solution by adsorption has been investigated using a commercial activated carbon (AC) as adsorbent. Equilibrium experiments were carried out for obtaining the adsorption isotherms of ILs on AC at different temperatures. The influence of both cation and anion was analyzed by studying 17 different ILs. The role of the surface chemistry of the adsorbent was also examined using ACs modified by oxidative and thermal treatments. The incorporation of IL on the AC surface was studied by N₂ adsorption-desorption measurements and elemental analysis. In addition to this, a COSMO-RS computational approach was developed to estimate molecular and thermodynamic properties of the solvent-adsorbate-adsorbent system, which allowed us to analyze the adsorption mechanism from a molecular point of view. The results of this work indicate that the adsorption with AC is an affordable environmental application to remove hydrophobic ILs from water streams, proposing the use of acetone for adsorbent regeneration. It has also been demonstrated that the adsorption of refractory hydrophilic ILs can be improved modifying the amount and nature of oxygen groups on the AC surface, particularly by including hydroxyl groups to promote hydrogen-bonding interactions with the basic groups of hydrophilic ILs.

1. Introduction

The room temperature ionic liquids (ILs) possess an array of properties that make them attractive for academy and industry: extremely low vapour pressure, high thermal and chemical stabilities, non-flammability and high solvent capacity [1-3]. Thus, ILs have been extensively examined as an alternative to conventional organic solvents in reaction and separation processes [4,5]. Mainly based on their negligible vapour pressure, the ILs have been considered as potentially environmentally friendly. However, it has been stated that they exhibit a wide range of environmental toxicity and persistency [6]. The most deeply-studied ILs are those based on an alkylmethylimidazolium cation paired with a wide variety of inorganic and organic anions. A main advantage of ILs is that the selection of the cation and anion can be tailored to achieve desirable physical and chemical properties. As a relevant example of their tuneable properties, the solubility of imidazolium based ILs in water is drastically modified by the length of alkyl chain and the hydrophilic/hydrophobic nature of the anion, covering a range from almost immiscibility to complete miscibility with water. The number of commercial applications of ILs is rapidly growing and the rate of appearance of patents on IL technology has been rising exponentially for years. Examples of these ILs applications in industry have been recently reported, some of them involving water streams in the process [7]. On the other hand, the synthesis routes of ILs both at laboratory and larger scales frequently include aqueous media, especially for the complicated IL purification step [8]. Then, generation of wastewaters from IL industrial processing and use may represent an important problem demanding adequate solutions. For this reason, a downstream treatment step may be required to remove the ILs from the aqueous effluents. Generally, ILs are purified or recycled by decantation and distillation, being these techniques not affordable for removing ILs at low concentrations. Destructive treatments for imidazolium ILs have been recently investigated based on advanced oxidation processes [9-13].

Imidazolium cations of hydrophilic ILs are readily degraded by chemical oxidation, although the toxicity of the remaining anions and oxidation products has to be considered. The usefulness of advanced oxidation systems for the degradation of largely hydrophobic or hydrolytically stable IL residues in water has not still been examined. On the other hand, biological treatments are limited by the low biodegradability and even high toxicity to sludge microorganism of the long chain imidazolium cations [6]. In any case, the alternative of recovering ILs should be promoted in terms of viability and sustainability. It has been argued that the retention of the large ions used in ILs should not be problematic [6]; however, to our

knowledge, no separation processes to control water pollution by ILs have been reported. Therefore, the potential of ILs to become persistent pollutants requires the development of effective separation strategies for removing ILs from aqueous streams.

Adsorption is an important separation technology widely used to remove pollutants from gas and water streams, being activated carbon (AC) the most commonly used adsorbent by far [14]. Therefore, the application of AC to the removal of ILs from aqueous effluents is an interesting approach. Few data are available concerning adsorption of ILs on AC. An earlier work by Brennecke et al. [15] showed a low adsorption capacity of AC for 1-methyl-3-methylimidazolium hexafluorophosphate, which is partially miscible with water. However, recent studies have revealed that imidazolium cations can be strongly adsorbed onto natural soils and sediments, evidencing the influence of both the cation exchange capacity and the soil organic matter content on sorption [16-21]. In fact, these works showed that the hydrophobic chains of the cation contribute significantly to sorption capacity, indicating the role of Van der Waals interactions between the non-polar groups of the cation and the organic matter of soils and sediments. Nevertheless, the sorption behaviour of IL anions has not been studied in depth. On the other hand, supported ionic liquid phase (SILP) materials are nowadays being extensively investigated in catalysis applications [22,23]. Among other porous solid supports, ACs have been effectively used for the immobilization of ILs by physisorption phenomena [24-26].

The aim of this work is to investigate the adsorption with AC for the separation of imidazolium based ILs from aqueous solutions at low concentrations, as expected in the water effluents resulting from processes involving these ILs. Firstly, the adsorption phenomenon of 1-octyl-3-methylimidazolium hexafluorophosphate (OmimPF₆) on a commercial microporous AC was studied in detail as a case of reference. The equilibrium isotherms were obtained in aqueous medium at temperatures in the range of 25 – 45 °C and analyzed with the aid of the well-known Freundlich and Langmuir models. Thermodynamic parameters such as free energy, enthalpy and entropy of adsorption were estimated to illustrate solvent-adsorbate-adsorbent interactions. Both the virgin AC and the IL-supporting AC were characterized by means of N₂ adsorption-desorption and elemental analysis. Since the reversibility of adsorption is a determining factor for regenerating the adsorbent in industrial applications, desorption experiments with acetone were carried out. Secondly, the adsorption study was extended to a representative number of ILs, in order to analyze the effect of the cation and anion nature on the adsorption phenomena. Thus equilibrium data were obtained for 17

imidazolium based ILs, by including the ionic species 1-ethyl- (Emim⁺), 1-butyl- (Bmim⁺), 1-hexyl- (Hmim⁺), 1-benzyl- (Bzmim⁺) and 1-octyl-3-methylimidazolium (Omim⁺), 1-butyl-2,3-dimethylimidazolium (bmmim⁺) and the anions chloride (Cl⁻), methylsulfonate (MeSO₃⁻), trifluoroacetate (TFA⁻), tetrafluoroborate (BF₄⁻), trifluoromethanesulfonate (OTf⁻), hexafluorophosphate (PF₆⁻) and bis(trifluoromethanesulfonyl)imide (NTf₂⁻). Finally, the influence of the surface chemical composition of AC on its performance as adsorbent was analyzed by using differently oxidized ACs.

On the other hand, the application of predictive models to simulate the adsorption phenomena of ILs is of great interest for this investigation, mainly because there are more than 300 ILs commercialized and more than a million possible counterion combinations [7]. In this work, a computational approach based on the quantum chemical COSMO-RS method [27] was developed to estimate the molecular and thermodynamic properties of AC-IL-water ternary systems. Thus COSMO-RS calculations were related to experimental adsorption data, being also compared to common adsorption descriptors (octanol-water partition coefficient and Parachor value) for understanding and predicting the adsorption behaviour of ILs on AC.

2. Procedure

2.1. Materials

The ILs used in this study as adsorbates were the following: OmimPF₆, HmimCl and BmimPF₆ supplied by Green Solutions, OmimBF₄, OmimCl, BmimNTf₂, BmimTFA, BmimBF₄ and EmimNTf₂ supplied by Solchemar, HmimPF₆, BzmimCl, BzmimBF₄, BzmimPF₆, BmmimPF₆, BmimOTf, BmimCl and BmimMeSO₃ supplied by Sigma-Aldrich, in the highest purity available (purity > 97-98%). The ILs were used without previous purification.

The AC (AC-MkU) was supplied by Merck. This commercial AC was subjected to thermal (AC-Mk900) and two different oxidative (AC-MkN and AC-MkS) treatments in order to modify its surface chemical composition. Nitric acid treatment of AC-MkN was carried out by boiling 1 g of AC in 10 mL of a 6N solution for 20 min. Oxidation of AC-MkS was performed with ammonium persulfate by treating 1 g of AC in 10 ml of 1 M solution at room temperature. Afterwards the AC-MkN and AC-MkS samples were washed with distilled water

until neutrality and dried overnight at 100 °C. The thermal treatment of AC was accomplished in a horizontal tube furnace (2,5 cm i.d.) under a nitrogen flow of 60 N mL min⁻¹ at 900 °C for 3 h. The heating rate was of 100 °C min⁻¹. Previous analysis in our laboratory showed that both porous structure and oxygen surface functional groups of AC are modified through oxidation and/or thermal treatment, the results being summarized in Table 1 [28]. Nitric acid and ammonium persulfate used in the oxidative process of AC were supplied by Riedel de Hën and acetone used for desorption was supplied by Panreac.

Table 1. Nomenclature and characterization results of the untreated and treated ACs.

Sample	Treatment	A_{BET} (m ² ·g ⁻¹)	A_s (m ² ·g ⁻¹)	CO and CO ₂ released from AC upon TPD	
				CO ₂ ^a (μmol·g ⁻¹)	CO ^b (μmol·g ⁻¹)
AC-MkU	None	927	155	182.8	490.4
AC-Mk900	Thermal	906	136	111.7	322.2
AC-MkS	Oxidation (NH ₄) ₂ S ₂ O ₈	872	113	351.7	1052.5
AC-MkN	Oxidation (HNO ₃)	856	109	573.8	1878.8

^aAssigned to carboxylic acid, lactone and carboxylic anhydride groups
^bAssigned to carboxylic anhydride, phenol, carbonyl and lactone groups

2.2. Adsorption/desorption experiments.

The equilibrium adsorption tests were carried out in stoppered glass bottles (100 mL) placed in an orbital incubator (Julabo Shake Temp, model SW-22) at 200 rpm equivalent stirring rate and 35 °C. Adsorbate solutions were prepared with concentrations from 0 to 5 mmol L⁻¹ of IL in distilled water. Samples of 50 mL of IL solutions were put in contact with 12.5 mg of AC accurately weighted. The equilibrium time was five days for all the samples. The equilibrium data for the case of OmimPF₆ were obtained at different temperatures in the range of 25 - 45 °C. Adsorbate concentrations were determined by UV spectroscopy (Varian, model Cary 1E) at 211 nm, which is the approximate maximum of absorption measured for the imidazolium cations.

Two well-known isotherms equations were used to fit the equilibrium data: Langmuir (eq. I.1) and Freundlich (eq. I.2) models, which are written as:

$$q_e = \frac{q_{\max} BC_e}{1 + BC_e} \quad \text{eq. I.1}$$

$$q_e = K_F C_e^n \quad \text{eq. I.2}$$

Appendix 1 provides the parameters definitions. Apparent distribution coefficients K_d ($\text{L}\cdot\text{kg}^{-1}$) were calculated to evaluate the capacity (q_e) of AC for the adsorption of the different adsorbates at identical equilibrium concentration (C_e):

$$K_d = \frac{q_e}{C_e} \quad \text{eq. I.3}$$

The thermodynamic study performed from the equilibrium data was described elsewhere [29,30], assuming a dynamic process of adsorption-desorption ($A+S\leftrightarrow AS$), where ΔH , ΔG and ΔS values were estimated using, respectively, the Van't Hoff equation, the Freundlich equation and the Gibbs-Helmholtz equation.

Desorption experiments were carried out to remove OmimPF₆ from AC using acetone as regenerating agent. AC samples after IL adsorption were put in contact with acetone during one hour under magnetic stirring at 25 °C. Then, the regenerated AC sample was filtered, dried overnight at 50 °C and its porous structure was characterized by means of 77 K N₂ adsorption-desorption. Subsequently, the adsorption capacity of the regenerated AC was studied by exposure to OmimPF₆ solutions of 500 mg L⁻¹ (1.2 mmol·L⁻¹) at 35 °C. Four replicates of each regeneration cycle were conducted, being the average values reported here. Three successive regeneration cycles were carried out together with a blank experiment where AC was subjected to acetone washing at 25 °C and then drying at 50 °C in absence of IL.

2.3. Characterization of AC adsorbent

The porous structure of AC adsorbents (virgin and used) was characterized by means of adsorption-desorption of N₂ at 77 K using a Quantachrome apparatus (Autosorb-1 model). The samples were previously outgassed at 150 °C for 8 hours to a residual pressure of 10⁻⁵ Torr. The BET equation was used to obtain the apparent surface area (A_{BET}) and the Dubinin-Radushkevich equation for micropore volume ($d_{\text{pore}} < 2$ nm). The external or non-micropore

area (A_s) was obtained from the t-method. The difference between the N_2 adsorbed volume at 0.95 relative pressure and the micropore volume was taken as mesopore volume ($2 \text{ nm} > d_{pore} > 50 \text{ nm}$). Elemental analyses of original and used AC were carried out in a Perkin-Elmer analyzer (210 CHN model) to obtain C, H and N elemental percentages.

2.4. Computational details

The molecular geometry of all molecular models (AC, water and ILs) were optimized at B3LYP/6-31++G** computational level in the ideal gas-phase using quantum chemical Gaussian03 package [31]. Vibrational frequency calculations were performed for each case to confirm the presence of an energy minimum. Then, the standard procedure was applied for COSMO-RS calculations, which consists of two steps: First, Gaussian03 was used to compute the COSMO files. The ideal screening charges on the molecular surface for each species were calculated by the continuum solvation COSMO model using BVP86/TZVP/DGA1 level of theory [32,33]. Subsequently, COSMO files were used as an input in COSMOtherm [34] code to calculate the thermodynamic properties for the binary (water-IL, IL-AC) and ternary (water-IL-AC) systems involved in the adsorption phenomena. According to our chosen quantum method, the functional and the basis set, we used the corresponding parameterization (BP_TZVP_C21_0106) that is required for the calculation of physicochemical data and contains intrinsic parameters of COSMOtherm as well as element specific parameters.

3. Results and discussion

3.1. Experimental

A previous observation at our laboratory evidenced the high retention of OmimPF₆ by a commercial Merck's AC (AC-MkU) from water solution. As result of that, the first objective of this work was to perform an adsorption equilibrium study of OmimPF₆ onto AC-MkU. The adsorption isotherms of OmimPF₆ on AC-MkU at 25, 35 and 45 °C are depicted in Figure 1.

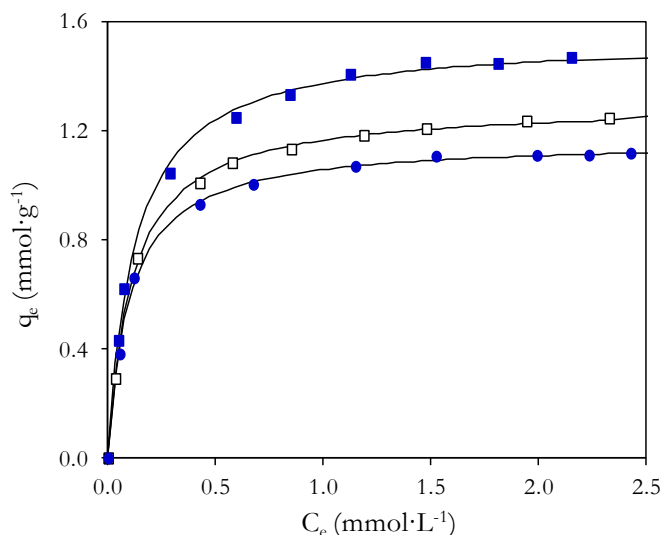


Figure 1. Experimental equilibrium data (dots) and Langmuir fits (curves) for the adsorption of OmimPF₆ on AC-MkU at different temperatures, 25 °C (■), 35 °C (□) and 45 °C (●).

These experiments revealed a high capacity of the AC, exhibiting a maximum uptake of about 45% (w/w) for OmimPF₆ at 25 °C. Comparing the amount of OmimPF₆ adsorbed ~ 450 mg·g⁻¹ (1.4 mmol·g⁻¹) with that measured for phenol ~ 225 mg g⁻¹ (2.4 mmol·g⁻¹) and that reported for toluene ~ 260 mg·g⁻¹ (2.8 mmol·g⁻¹) [35] at 25 °C, a substantially higher uptake can be noticed for the IL here studied. Regarding the available ILs sorption studies, AC-MkU showed, as expected, higher adsorption capacity to retain ILs than aquatic sediments (~ 0.12 mmol·g⁻¹ of OmimCl) [20] and natural soils (~ 0.03 mmol·g⁻¹ of BmimCl) [17,18]. These results suggest the potential of adsorption on AC as a separation method for removing ILs from aqueous solutions. The shape of the adsorption isotherms shown in Figure 1 suggests that there is no strong solvent-adsorbate competition to occupy the adsorption sites. These isotherms also prove the favourable retention of OmimPF₆ at low concentrations by AC-MkU. The experimental data were fitted to the usual Langmuir and Freundlich models for aqueous-phase adsorption, being the values of the fitting parameters shown in Table 1S of Supplementary material. Both equations reproduce well the experimental values, although the Langmuir equation provides a better approach, with square correlation coefficients (R^2) higher than 0.999. The experimental data obtained in the adsorption runs conducted between 25 and 45 °C clearly show that the adsorption capacity decreases as temperature increases.

Table 2. Thermodynamic results for the adsorption of OmimPF₆ on AC-MkU at different surface coverages.

q_e (mmol·g ⁻¹)	$K'_{o, 25-45^\circ\text{C}}$ (L·mmol ⁻¹)	$\Delta H_{25-45^\circ\text{C}}$ (KJ·mol ⁻¹)	$\Delta G_{25^\circ\text{C}}$ (KJ·mol ⁻¹)	$\Delta G_{35^\circ\text{C}}$ (KJ·mol ⁻¹)	$\Delta G_{45^\circ\text{C}}$ (KJ·mol ⁻¹)
			-12.08	-10.99	-10.33
			ΔS (J·K ⁻¹ ·mol ⁻¹)	ΔS (J·K ⁻¹ ·mol ⁻¹)	ΔS (J·K ⁻¹ ·mol ⁻¹)
0.8	1.8E-03	-20.72	-29.00	-31.61	-32.67
0.9	9.2E-05	-27.33	-51.18	-53.07	-53.45
1.0	3.2E-07	-40.83	-96.47	-96.89	-95.90

The thermodynamic study carried out from the equilibrium data provides information about the process tendency to occur spontaneously and the stability of the adsorbed phase. The thermodynamic parameters ΔH , ΔG and ΔS shown in Table 2 were calculated as described elsewhere [29,30]. The enthalpy of the process is negative (See Figure 1S in Supplementary material), implying an exothermic process.

In addition, the estimated values for free energy changes were negative, indicating the spontaneous character of the adsorption. Likewise, the negative values of adsorption entropy evidenced a lower degree of freedom of the OmimPF₆ species on the adsorbed phase. The estimated values of ΔH , ΔG and ΔS are close to those reported for AC adsorption of aromatic compounds [30] and for natural soil sorption of 1-alkyl-3-methylimidazolium chloride ILs [19]. The results obtained in this study are indicative of a physical adsorption phenomenon.

Table 3. Surface areas, pore volumes and elemental analysis of AC-MkU at different percentages (w/w) of OmimPF₆ adsorbed.

% IL	A_{BET} (m ² ·g ⁻¹)	A_s (m ² ·g ⁻¹)	$V_{\text{microp.}}$ (cm ³ ·g ⁻¹)	$V_{\text{mesop.}}$ (cm ³ ·g ⁻¹)	%C	%H	%N
0	927	155	0.358	0.143	87.7	0.68	0.64
2	810	151	0.337	0.143	86.5	0.74	0.76
5	700	150	0.304	0.145	85.8	0.93	0.93
10	585	127	0.239	0.121	84.5	1.08	1.22
20	348	116	0.125	0.113	81.0	1.50	1.85
30	88	88	0.000	0.092	77.6	1.85	2.27
40	55	55	0.000	0.073	73.8	2.21	2.90

Adsorption experiments provided an indirect measurement of the amount of OmimPF₆ incorporated onto AC. In this work, elemental analyses of virgin and used AC-MkU allowed quantifying the adsorption of OmimPF₆ onto AC (Table 3). An important rise of nitrogen content takes place as the amount of OmimPF₆ uptaken increases, which can be attributed to the incorporation of imidazolium cation. As it can be observed in Figure 2, there is a linear relation between the percentage of N on IL-supporting AC-MkU from elemental analysis and the amount of OmimPF₆ incorporated on AC-MkU from adsorption data, i.e., estimated by liquid phase analysis. These results suggest that elemental analysis could be alternatively used for estimating the amount of IL incorporated onto AC in adsorption or other applications such as supported ionic liquid materials.

To learn more on the adsorption phenomena, the effect of retained OmimPF₆ on the porous structure of AC was analysed from the 77 K N₂ adsorption-desorption isotherms. The BET surface area and pore volumes of IL-supporting AC-MkU with increasing amounts of OmimPF₆ are collected in Table 3. This analysis can be carried out thanks to the nearly negligible volatility of ILs. As it can be seen in Figure 2, the BET surface area drastically decreased as the mass percentage of OmimPF₆ on the solid increased. In fact, the AC-MkU supporting ~40% (w/w) of OmimPF₆ showed a BET surface area ~95% lower than that of the initial AC-MkU. The analysis of N₂ adsorption-desorption isotherms summarized in Table 3 indicates that at low capacity values (<10%) OmimPF₆ fills or blocks significantly micropores and that beyond an IL uptake of 30 % (w/w) the micropores are no longer available for N₂ adsorption. From this point, further adsorption of OmimPF₆ takes place on mesopores and, possibly, macropores. At OmimPF₆ uptakes higher than 30%, the available BET surface area corresponds to the estimated external or non-microporous surface area (Table 3).

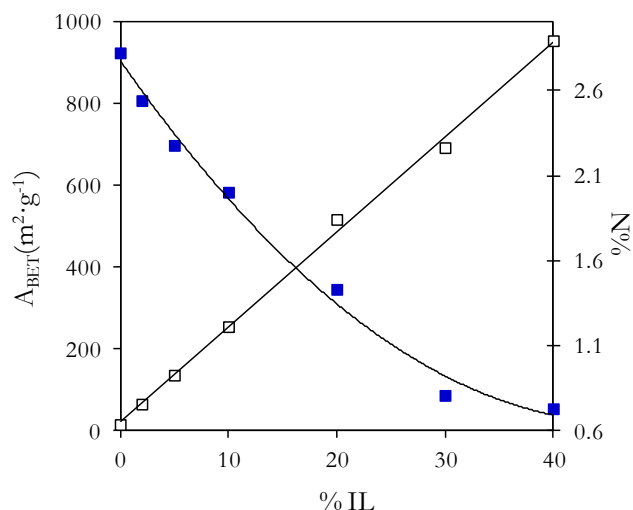


Figure 2. BET area (■) and percentage of N (□) of IL-supporting AC-MkU against the mass percentage of OmimPF₆ on AC-MkU estimated by liquid phase analysis.

In order to examine the regeneration of AC and the recovery of IL, a set of desorption experiments were carried out. Acetone was tested as regenerating agent since it effectively dissolves imidazolium based ILs. Thus, the exhausted IL-supporting AC-MkU was washed with acetone at room temperature and subsequently filtered and dried. Then, the performance of the regenerated AC-MkU was evaluated by later adsorption experiments of OmimPF₆, being characterized by means of the apparent distribution coefficients K_d ($\text{L} \cdot \text{kg}^{-1}$). In addition, the BET surface area of the acetone-washed AC-MkU was determined. The results in Table 4 indicate that the exhausted AC-MkU was successfully regenerated, maintaining adsorption capacities and surface areas above ~90% of their initial values. A blank was carried out to determine how textural properties and adsorption capacity of AC-MkU are modified by acetone extraction and further drying. Similar results were found for AC-MkU from blank and for AC-MkU subjected to successive IL adsorption-desorption cycles, concluding an efficient removal of OmimPF₆. Lately, OmimPF₆ was easily recovered from acetone solutions by atmospheric distillation.

Table 4. BET area and K_d coefficient (calculated for an initial concentration of $1.2 \cdot \text{mmol L}^{-1}$) of AC-MkU after OmimPF₆ adsorption and regeneration cycles.

	$A_{\text{BET}} (\text{m}^2 \cdot \text{g}^{-1})$	$k_d (\text{L} \cdot \text{kg}^{-1})$
AC Initial	927	1091
1 cycle	861	874
2 cycles	848	892
3 cycles	850	866
Blank	889	918

It is well stated that AC adsorption depends on the structure and the surface chemistry of the adsorbent but also on the size and chemical nature of adsorbates [29]. In addition, the IL sorption studies onto natural soils evidenced that the adsorption capacity is affected by organic matter content, cation exchange capacity and particle size distribution of the soils [16-19]. Furthermore, the sorption of imidazolium based ILs was shown significantly influenced by the alkyl chain size of the cation [16-18]. However, to our knowledge, the effect of IL anion on sorption has not been investigated.

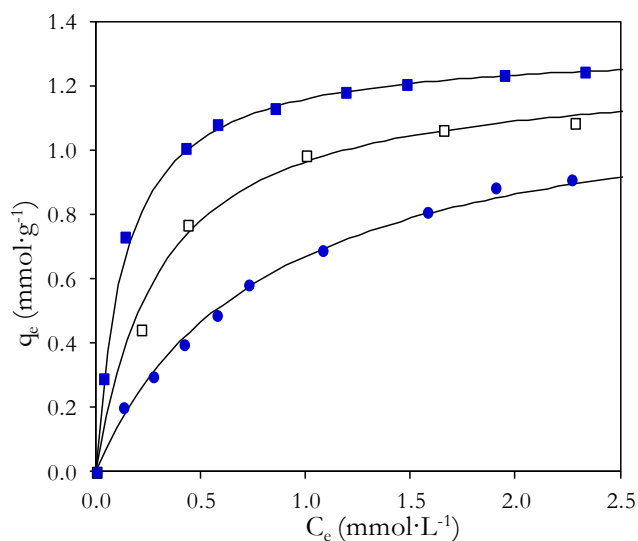


Figure 3. Experimental equilibrium data (dots) and Langmuir fits (curves) for the adsorption of OmimPF₆ (■), HxmimPF₆ (□) and BmimPF₆ (●) on AC-MkU at 35 °C.

The affinity of IL for AC should be the result of several simultaneous sorption mechanisms. For this reason, it was also our aim to analyze the effect of both cation and anion nature on the IL adsorption on AC, by extending the experimental adsorption study to a wide group of imidazolium based ILs. Figure 3 reports the adsorption isotherms in water at 35 °C of a cation series of 1-alkyl-3-methylimidazolium hexafluorophosphate with different lengths of alkyl chain onto AC-MkU adsorbent. A significant rise in adsorption capacity is observed as the length of the alkyl chains of IL increases. This behaviour was also observed in natural soils and assigned to the increasing hydrophobic nature of the ILs with a larger alkyl chain [18,19]. To provide additional insight into the role of IL structure, for the first time, this work analyses the role of anion on IL adsorption. The experimental adsorption equilibrium data for the anion series of 1-butyl-3-methylimidazolium ILs are depicted in Figure 4. The results prove the high influence of the anion on the adsorption process. A wide range of adsorption capacities was observed with values varying from 0.1 to 1 mmol·g⁻¹ and following the sequence of hydrophobicity of the IL anions (NTf₂⁻ > PF₆⁻ > OTf > BF₄⁻ > TFA⁻ > Cl⁻).

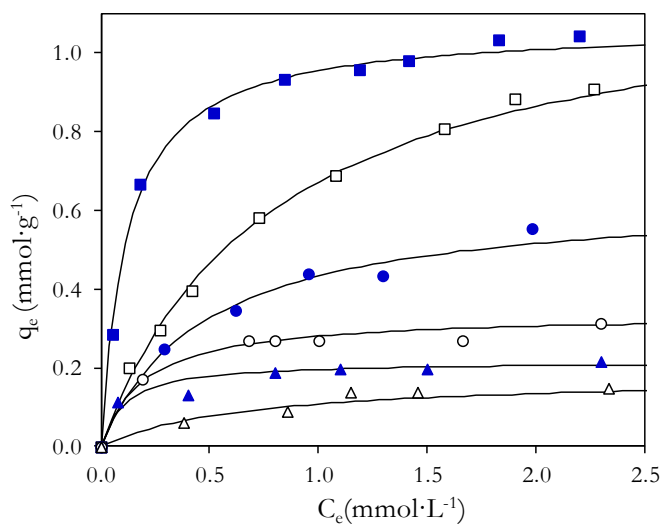


Figure 4. Experimental equilibrium data (dots) and Langmuir fits (curves) for the adsorption isotherms of BmimNTf₂ (■), BmimPF₆ (□), BmimOTf (●), BmimBF₄ (○), BmimTFA (▲) and BmimCl (Δ) on AC-MkU at 35 °C.

The study was completed by obtaining the adsorption isotherms of nine additional imidazolium based ILs, synthesised with different anions or cations. In order to summarize the information obtained, the equilibrium data were fitted to Langmuir and Freundlich models and the results collected in Table 5. The AC adsorbents used in industrial applications for

removal of organic pollutants typically present adsorption capacities higher than $200 \text{ mg}\cdot\text{g}^{-1}$. Therefore, we can conclude that imidazolium based ILs can be effectively separated by adsorption with AC-MkU provided that they are composed of hydrophobic anions (as NTf_2^- and PF_6^-) or hydrophobic cations (Omim^+ , Hmim^+ and Bzmim^+ , for instance).

Table 5. Parameters of Freundlich and Langmuir isotherms from experimental equilibrium data and K_d coefficient estimated at $C_e = 2 \text{ mmol}\cdot\text{L}^{-1}$ for 17 ILs onto AC-MkU at $35 \text{ }^\circ\text{C}$.

	Langmuir model			Freundlich model			$k_d \text{ (L}\cdot\text{kg}^{-1}\text{)}$
	$q_{\text{max}} \text{ (mmol}\cdot\text{g}^{-1}\text{)}$	$B \text{ (L}\cdot\text{mmol}^{-1}\text{)}$	R^2	$k_f \text{ (mmol}^{1-1/n}\cdot\text{L}^{1/n}\cdot\text{g}^{-1}\text{)}$	n	R^2	
Omim PF₆	1.32	7.30	0.989	1.09	0.23	0.951	621
Bzmim PF₆	1.42	2.32	0.994	0.93	0.40	0.947	583
Hmim PF₆	1.28	3.15	0.989	0.91	0.26	0.846	555
Bmim NTf₂	1.07	8.38	0.991	0.92	0.23	0.894	530
Omim BF₄	1.06	8.23	0.968	0.86	0.18	0.842	479
Emim NTf₂	1.18	1.44	0.965	0.65	0.43	0.884	435
Bmim PF₆	1.21	1.25	0.995	0.62	0.45	0.962	431
Bmmim PF₆	1.12	1.40	0.970	0.62	0.38	0.838	407
Bzmim BF₄	1.02	1.3	0.985	0.53	0.46	0.932	360
Omim Cl	0.65	3.42	0.963	0.47	0.22	0.702	284
Bmim OTf	0.64	2.12	0.981	0.41	0.29	0.878	258
Bzmim Cl	0.52	2.05	0.988	0.32	0.28	0.900	206
Hmim Cl	0.45	2.02	0.957	0.29	0.24	0.746	175
Bmim BF₄	0.26	9.41	0.996	0.22	0.11	0.839	123
Bmim TFA	0.24	3.69	0.991	0.18	0.17	0.790	103
Bmim Cl	0.17	1.57	0.993	0.10	0.28	0.892	61
Bmim MeSO₃	0.14	3.95	0.987	0.10	0.15	0.732	58

In order to analyze the influence of the surface chemistry of AC on IL adsorption, four ACs with different surface composition [commercial AC (AC-MkU); heat-treated AC (AC-Mk900); and oxidized ACs (AC-MkN and AC-MkS)] were examined by equilibrium adsorption experiments. Earlier analyses in our laboratory [28] reported porous structure and TPD results of AC-MkU, AC-Mk900, AC-MkN and AC-MkS (reproduced in Table 1). The adsorption isotherms at $35 \text{ }^\circ\text{C}$ for OmimPF_6 are shown in Figure 5.

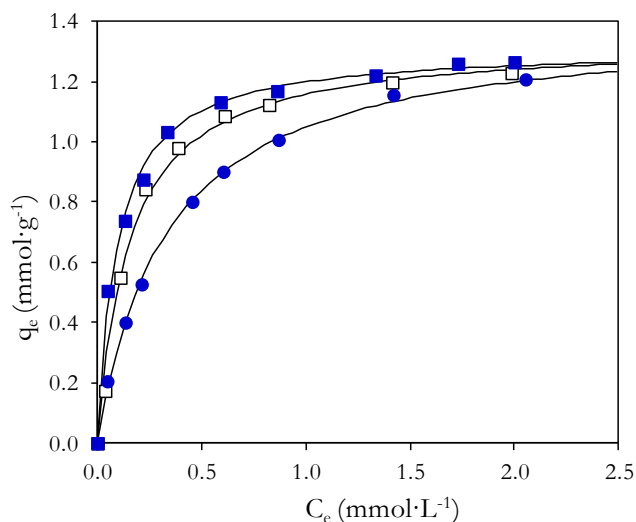


Figure 5. Experimental equilibrium data (dots) and Langmuir fits (curves) for the adsorption of OmimPF₆ on untreated and treated ACs [AC-MkU (■), AC-Mk900 (□), AC-MkN (●)].

It can be seen that the removal of oxygen surface groups by thermal treatment results in a slight increase in adsorption capacity. In contrast, the creation of oxygenated groups on the AC surface reduces the adsorption capacity from AC-MkU to AC-MkN to AC-MkS for the hydrophobic OmimPF₆ at low to medium concentration. Nevertheless, it is remarkable that in the higher concentration range ($C_e > 1.5 \text{ mmol}\cdot\text{L}^{-1}$) the adsorption capacities of all the treated ACs were quite similar to that of the virgin AC-MkU, even though the oxidized AC-MkS and AC-MkN show a substantially higher amount of oxygen surface groups (see Table 1) whereas AC-Mk900 presents a significant decrease. These results indicate that the influence of oxygen functional groups on AC adsorption capacity is not significant in the case of OmimPF₆.

Regarding the influence of the porous texture on OmimPF₆ adsorption it should be noticed that the different treatments affect it in a fairly different extent. Whereas thermal treatment (AC-Mk900) and oxidation with ammonium persulfate (AC-MkS) led to a slight reduction of A_{BET}, oxidation with HNO₃ (AC-MkN) scarcely increased the surface texture. However, the adsorption capacities of the 4 activated carbons with respect to OmimPF₆ remained very close in the high concentration range (C_e > 1.5 mmol·L⁻¹). Moreover, since AC-MkS and AC-MkN presented a slight reduction of micropore volume respect to AC-MkU without a significant effect on the adsorption capacity (AC-MkU micropore area 772 m²·g⁻¹; AC-MkS 759 m²·g⁻¹ and AC-MkN 747 m²·g⁻¹), it can be inferred that the uptake of OmimPF₆ takes place essentially at micropores area.

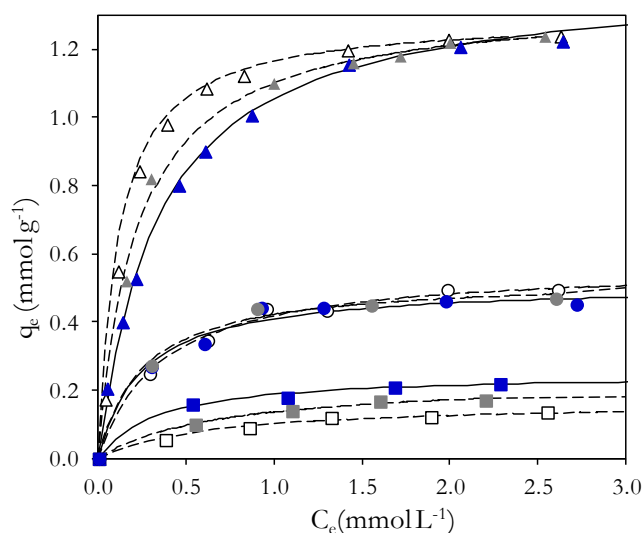


Figure 6. Experimental equilibrium data (dots) and Langmuir fits (curves) for the adsorption of BmimCl (squares), BmimOTf (circles) and OmimPF₆ (triangles) on AC-MkS (filled symbols), AC-MkN (gray coloured symbols) and AC-MkU (open symbols) at 35 °C.

One interesting feature to be investigated concerns the modification of AC surface chemistry for improving the retention of ILs initially refractory to adsorption, as those ILs including highly basic anions (Cl⁻, acetate, etc.). It is well stated that hydrophilicity of ILs with common cation is generally related to the anion basicity [2], increasing in this case in the order Cl⁻ > BF₄⁻ > OTf⁻ > PF₆⁻ > NTf₂⁻. Thus, it is expected that the presence of hydrogen-bond donor groups (hydroxyls, for instance) in AC surface would increase its adsorption capacity for hydrophilic ILs with low affinity for AC.

Table 6. Apparent distribution coefficient (K_d) estimated at $C_e = 2 \text{ mmol}\cdot\text{L}^{-1}$ for six ILs onto AC-MkS and AC-MkN and the percent modification of K_d parameter respect to that obtained with AC-MkU ($\% \Delta K_d$) at 35 °C.

	AC-MkN		AC-MkS	
	$k_d \text{ (L}\cdot\text{kg}^{-1})$	$\% \Delta K_d$	$k_d \text{ (L}\cdot\text{kg}^{-1})$	$\% \Delta K_d$
Omim PF₆	595	-5	618	-4
Bmim OTf	234	-3	235	-3
Bmim BF₄	125	2	148	2
Bmim TFA	116	9	175	14
Bmim Cl	107	41	133	51
Bmim MeSO₃	125	52	134	59

In excellent agreement with this hypothesis, [Figure 6](#) shows that the oxidation of AC-MkU significantly improves the uptake of the ILs containing highly basic anions (Cl⁻, MeSO₃⁻); on the contrary, it has an inverse and lower influence on the AC adsorption of those ILs containing more hydrophobic anions (PF₆⁻, OTf⁻). According to these results, [Table 6](#) reports K_d values for the adsorption of six ILs onto the oxidized AC-MkS and AC-MkN activated carbons together with the modification percent of that coefficient ($\% \Delta K_d$) respect to the original untreated AC-MkU (in addition, the estimated Langmuir and Freundlich parameters are reported in [Table 2S](#) of Supplementary material). The $\% \Delta K_d$ values significantly increase with the basic character of the anion, from -5 / -4 % (PF₆⁻) to 52 / 76 % (MeSO₃⁻) for AC-MkS / AC-MkN. As can be seen in [Table 6](#), the uptake of the highly adsorbed ILs (as OmimPF₆) is not significantly affected by the type of oxidation treatment. In contrast, the uptake of hydrophilic ILs (as BmimCl) is higher by AC-MkN than by AC-MkS, which indicates that the textural properties of the activated carbon may be a relevant factor for the adsorption of these ILs and future studies are needed to learn on this question. In sum, current preliminary results provide evidences on the fact that the separation of ILs from aqueous streams by AC adsorption can be effectively tuned by appropriately modifying the carbon surface.

3.2. Computational

Adsorption phenomena of organic solutes on AC have been shown to depend on the structural and physico-chemical properties of both adsorbate and adsorbent, being determined by polar, Van de Waals and hydrogen bonding interactions [29]. Furthermore, it has been suggested that the sorption of imidazolium based IL onto soils also occurs by means of electrostatic, π - π and hydrogen bonding interactions with the organic matter and the clay of soils [16-20].

In this work, the resulting macroscopic adsorption behaviour of ILs on AC will be analyzed from a molecular point of view using the quantum-chemical COSMO-RS method. For this purpose, a computational approach based on COSMO-RS was developed to describe structural properties and solvent-adsorbate-adsorbent intermolecular interactions, with the aim of better understanding their effect on the adsorption mechanism. COSMO-RS has shown general suitability to calculate thermodynamic properties of IL systems from electronic information of individual molecules [36]. Concretely, COSMO-RS provides a very good prediction of densities of imidazolium ILs [37], which are calculated using the molecular surface and molecular volume given by the continuum solvation COSMO model. Table 3S of Supplementary material reports a series of calculated properties by COSMO-RS for a set of 13 ILs included in this study, which were used here as complementary information.

According to quantum-chemical calculations, the molecular surface of the largest IL (OmimPF₆) has a value of 3.4 nm². The maximum uptake for OmimPF₆ at 25 °C was over 450 mg g⁻¹, which led to a reduction in the BET area of AC of 862 m² g⁻¹. If one assumes the simplification that only one half of the OmimPF₆ molecular surface is in contact with the AC surface, an uptake of 450 mg·g⁻¹ would correspond to a covered surface of 1280 m²·g⁻¹. Since adsorption experiments suggested that OmimPF₆ is not filling but blocking micropores, whose assessed surface area is 772 m²·g⁻¹, a multilayer adsorption can be postulated, in which OmimPF₆ is mainly adsorbed on the mesopore and macropore surface.

For prediction purposes, the sorption coefficients for organic solutes on adsorbents have been extensively estimated by quantitative structure–activity relationships. QSARs using a variety of physico-chemical descriptors, mainly related to

- i) adsorbate molecular size and
- ii) adsorbate solubility in water [38].

In this work, COSMO-RS was used to compare the experimental adsorption coefficients K_d (Table 5) and the calculated physical and chemical properties of ILs.

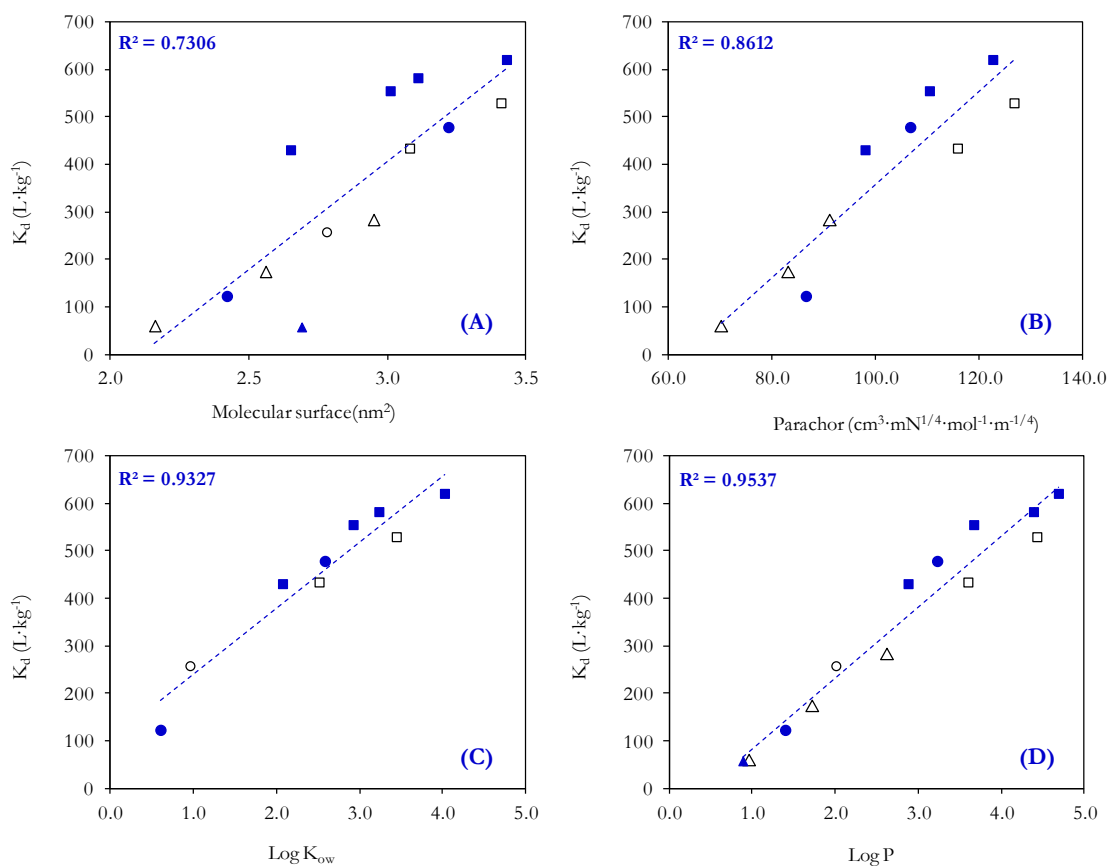


Figure 7. Plot of K_d coefficient against different COSMO-RS descriptors for 1-alkyl-3-methyl imidazolium-based ILs with different anions: PF_6 (■), NTf_2 (□), BF_4 (●), OTf (○), CH_3SO_3 (▲) and Cl (△).

Regarding to the influence of the adsorbate molecular size, the literature reports some relationships between the total molecular surface and the adsorption distribution coefficients [38]. In this sense, Figure 7A compares the COSMO-RS molecular surface values to the apparent adsorption coefficients (K_d) estimated at $C_e = 2 \text{ mmol}\cdot\text{L}^{-1}$ for 13 ILs on AC-MkU at 35 °C. A more commonly used descriptor is Parachor parameter, a structurally derived property related to the molar volume of the compound [39]. Table 3S (Supplementary material) reports the estimated Parachor values for ILs, calculated using COSMO-RS densities and experimental surface tension. As it can be seen in Figure 7B, Parachor correlates to K_d

better than molecular surface, since it introduces intermolecular interactions between IL molecules in some extent. In sum, it can be observed that larger ILs were, as a general trend, adsorbed in a larger extent on AC.

Regarding the solubility in water, our experimental results clearly indicate that ILs with high hydrophobicity present a high affinity toward the AC surface. The most widely used descriptor for predicting adsorption coefficients is the octanol-water partition coefficient (K_{ow}). Since experimental K_{ow} values are only available for a few ILs in the literature, they were calculated by COSMO-RS method (Table 3S in Supplementary material). Figure 7C shows a good linear relationship between the calculated values of K_{ow} and the experimental K_d , with the exception of those ILs with Cl⁻ and MeSO₃⁻ anions, which deviate from this behaviour. The trend shown by the data of Figure 7C implies that hydrophobic ILs (those with imidazolium cation with long alkyl chain or anion with low basicity) are better adsorbed by activated carbon from aqueous solution than ILs of hydrophilic character (as those with small imidazolium cation or with strongly basic anion such as Cl⁻ and MeSO₃⁻). The behaviour of this later type of ILs strongly deviates from that of the rest, in Figure 7C, because K_{ow} only includes the solvent-IL interactions, but excludes possible interactions between the IL and the functional groups on the AC surface. In fact, the affinity of the adsorbate towards the AC surface has to be considered since a diversity of intermolecular interactions (polar, π - π , Van der Waals and hydrogen bonding) are expect to contribute to adsorption [16-19].

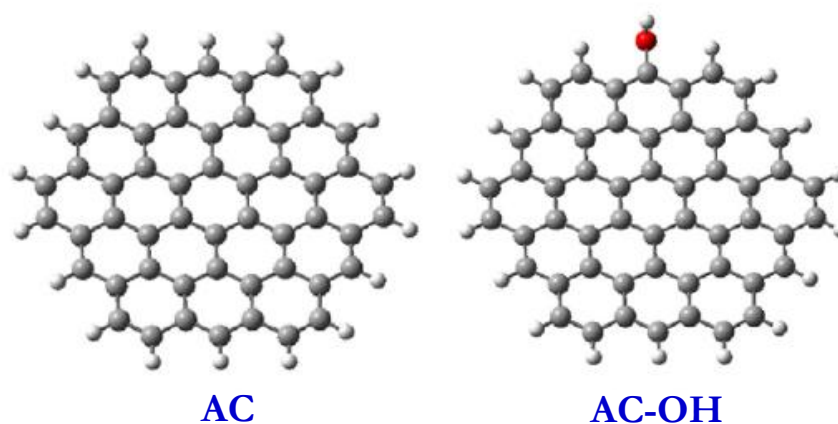


Figure 8. Molecular models for activated carbon.

Two earlier works by Peukert et al. [40,41] showed that COSMO-RS method can also be applied to predict adsorption equilibrium data from aqueous solutions. Based on those promising results, COSMO-RS will be here applied to provide insight into the adsorbate-adsorbent interactions. For this purpose we developed a computational approach in which IL adsorbate is described by an ion-pair structure, the aqueous media by individual water molecule and AC adsorbent is simulated by a molecular model using the two simple AC units of Figure 8. Then, the partition coefficient (P) of IL between AC and water phases at infinite dilution were calculated by COSMO-RS at 25 °C. AC phase is modelled by mixing AC structures in a molar proportion of AC (90): AC-OH (10). This molar proportion is an approach based on the proportion of the oxygen surface groups containing hydroxyl groups obtained by X-ray photoelectron spectroscopy (XPS) for AC-MkU [42]. XPS provides information about the nature of the external surface, which was shown before to play an important role in the adsorption of ILs. Figure 7D shows the Log(P) values, calculated by COSMO-RS for the AC molecular models, versus the apparent adsorption coefficients (K_d) for 13 imidazolium based ILs with a wide variety of cations and anions. It should be remarked the excellent linear relationship between both distribution coefficients, obtained experimentally and computationally. A relevant contribution of this computational approach is that it introduces the solute-solid physico-chemical interactions in the analysis, which determines the AC adsorption of ILs. An additional advantage of COSMO-RS method is that it provides enthalpy estimations for the different intermolecular interactions (polar, Van der Waals and hydrogen-bonding) between the IL adsorbate and both fluid and solid phases. The predicted COSMO-RS contributions of IL-AC and IL-water interactions for the hydrophobic OmimPF₆ and the hydrophilic BmimCl are compared in Figure 9.

It can be observed that the attractive Van der Waals interactions play the main role in the adsorption of hydrophobic OmimPF₆. On the contrary, hydrogen bonding is the main contribution in the case of the adsorption of the hydrophilic BmimCl, being the influence of Van der Waals interactions lower, probably due to the shorter length of the alkyl chain.

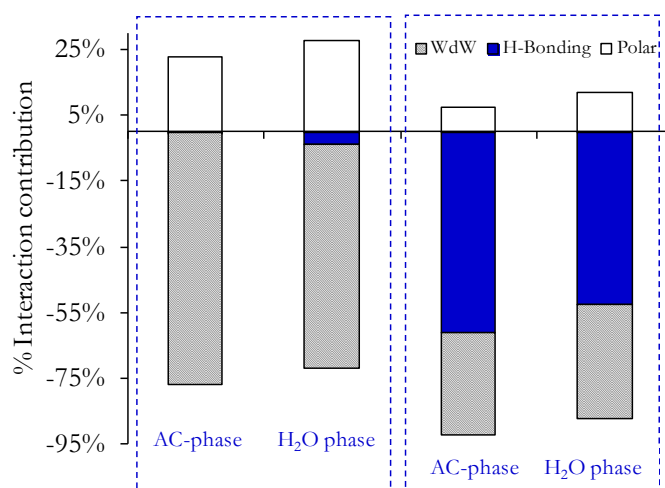


Figure 9. Predicted COSMO-RS contributions of IL-AC and IL-water interactions.

The developed COSMO-RS approach showed the relevant contribution of including the AC properties in the simulation of adsorption phenomena. In addition, COSMO-RS provides a description of the different interactions between the components of the system, which will be object of a detailed analysis in the future for better understanding AC adsorption of ILs from aqueous solution.

4. Conclusions

The possibility of removing imidazolium based ILs from aqueous streams by effective adsorption with AC was demonstrated by equilibrium study for IL adsorption on AC at different temperatures, being suggested acetone as an efficient solvent to regenerate the exhausted AC and recover the ILs.

Factors strongly influencing the adsorption capacities were the size and hydrophobic nature of both cation and anion of IL, but also the surface chemistry of AC. Experimental evidences were examined at molecular level using the quantum-chemical COSMO-RS method. The experimental and calculated data are consistent with a multilayer adsorption mechanism occurring spontaneously with exothermic effect, being modulated by attractive Van der Waals and hydrogen bonding adsorbate-adsorbent interactions.

The developed COSMO-RS computational approach was shown as a valuable tool to: *i*) rapid and reliable prediction of the behavior of new ILs in adsorption processes and *ii*) design tailor-made AC adsorbents with improved surface chemistry for selective IL adsorption.

References

- [1] Welton T. Room-temperature ionic liquids. Solvents for synthesis and catalysis. *Chemical reviews* 1999;99(8):2071-83.
- [2] Wasserscheid P, Welton T. *Ionic liquids in synthesis*. Weinheim: Wiley-VCH; 2008.
- [3] Robin D. Rogers, Kenneth R. Seddon. *Ionic Liquids as green solvents: progress and prospects*. Washington 669 (DC): American Chemical Society; 2003.
- [4] Rogers R, Seddon K. *Ionic liquids IIIB: Fundamentals, progress, challenges, and opportunities: Transformations and processes*. American Chemical Society (Acs Symposium Series) 2005;902.
- [5] Han X, Armstrong DW. Ionic liquids in separations. *Acc.Chem.Res.* 2007;40:1079-86.
- [6] Ranke J, Stolte S, Stormann R, Arning J, Jastorff B. Design of sustainable chemical products - The example of ionic liquids. *Chem.Rev.* 2007;107(6):2183-206.
- [7] Plechkova NV, Seddon KR. Applications of ionic liquids in the chemical industry. *Chem.Soc.Rev.* 2008;37(1):123-50.
- [8] Burrell AK, Del Sesto RE, Baker SN, McCleskey TM, Baker GA. The large scale synthesis of pure imidazolium and pyrrolidinium ionic liquids. *ACS symposium series* 2007;9:449-54.
- [9] Stepnowski P, Zaleska A. Comparison of different advanced oxidation processes for the degradation of room temperature ionic liquids. *Journal of Photochemistry and Photobiology A-Chemistry* 2005;170(1):45-50.
- [10] Morawski A, Janus M, Goc Maciejewska I, Syguda A, Pernak J. Decomposition of ionic liquids by photocatalysis. *Pol.J.Chem.* 2005;79(12):1929-35.
- [11] Pernak J, Sobaszekiewicz K, Foksowicz-Flaczyk J. Ionic liquids with symmetrical dialkoxymethyl-substituted imidazolium cations. *Chemistry: A European journal* 2004;10:3479-85.
- [12] Li X, Zhao J, Li Q, Wang L, Tsang SC. Ultrasonic chemical oxidative degradations of 1,3-dialkylimidazolium ionic liquids and their mechanistic elucidations. *Dalton transactions* 2007;1875-80.
- [13] Siedlecka EM, Mroziak W, Kaczynski Z, Stepnowski P. Degradation of 1-butyl-3-methylimidazolium chloride ionic liquid in a Fenton-like system. *J.Hazard.Mater.* 2008;154(1-3):893-900.

- [14] Radovic LR, Silva IF, Ume JI, Menéndez JA, Leon y Leon CA, Scaroni AW. An experimental and theoretical study of the adsorption of aromatics possessing electron-withdrawing and electron-donating functional groups by chemically modified activated carbons. *Carbon* 1997;35:1339-48.
- [15] Anthony JL, Maginn EJ, Brennecke JF. Solution thermodynamics of imidazolium-based ionic liquids and water. *J Phys Chem B* 2001;105(44):10942-9.
- [16] Gorman-Lewis DJ, Fein JB. Experimental study of the adsorption of an ionic liquid onto bacterial and mineral surfaces. *Environ.Sci.Technol.* 2004;38(8):2491-5.
- [17] Stepnowski P. Preliminary assessment of the sorption of some alkyl imidazolium cations as used in ionic liquids to soils and Sediments. *Aust.J.Chem.* 2005;58(3):170-3.
- [18] Stepnowski P, Mroziak W, Nischthäuser J. Adsorption of alkylimidazolium and alkyipyridinium ionic liquids onto natural soils. *Environ.Sci.Technol.* 2007;41(2):511-6.
- [19] Studzinska S, Sprynskyy M, Buszewski B. Study of sorption kinetics of some ionic liquids on different soil types. *Chemosphere* 2008;71(11):2121-8.
- [20] Beaulieu JJ, Tank JL, Kopacz M. Sorption of imidazolium-based ionic liquids to aquatic sediments. *Chemosphere* 2008;70:1320-8.
- [21] Matzke M, Stolte S, Arning U, Uebbers U, Filser J. Imidazolium based ionic liquids in soils: effects of the side chain length on wheat (*Triticum aestivum*) and cress (*Lepidium sativum*) as affected by different clays and organic matter. *Green Chem.* 2008;10(5):584-91.
- [22] Rüisager A, Fehrmann R, Flicker S, van Hal R, Haumann M, Wasserscheid P. Very stable and highly regioselective supported ionic-liquid-phase (SILP) catalysis: Continuous flow fixed-bed hydroformylation of propene. *Angewandte Chemie-International Edition* 2005;44(5):815-9.
- [23] Rüisager A, Fehrmann R, Haumann M, Wasserscheid P. Supported ionic liquids: versatile reaction and separation media. *Topics in Catalysis* 2006;40(1-4):91-102.
- [24] Mikkola JP, Warna J, Virtanen P, Salmi T. Effect of internal diffusion in supported ionic liquid catalysts: Interaction with kinetics. *Ind Eng Chem Res* 2007;46(12):3932-40.
- [25] Ruta M, Yuranov I, Dyson PJ, Laurency G, Kiwi-Minsker L. Structured fiber supports for ionic liquid-phase catalysis used in gas-phase continuous hydrogenation. *Journal of Catalysis* 2007;247(2):269-76.
- [26] Mikkola JT, Virtanen PP, Kordás K, Karhu H, Salmi TO. SILCA—Supported ionic liquid catalysts for fine chemicals. *Applied Catalysis A: General* 2007;328(1):68-76.
- [27] Klamt A. *COMSO-RS: from quantum chemistry to fluid phase thermodynamics and drug design.* Amsterdam: Elsevier, 1st ed. 2005.
- [28] Calvo L, Gilarranz MA, Casas JA, Mohedano AF, Rodríguez JJ. Hydrodechlorination of 4-chlorophenol in aqueous phase using Pd/AC catalysts prepared with modified active carbon supports. *Applied Catalysis B: Environmental* 2006;67(1-2):68-76.

- [29] Radovic LR. Carbon materials as adsorbents in aqueous solutions. In: Radovic LR, editor. New York: M. Dekker; 2001, p. 1-66.
- [30] Cotoruelo LM, Marques MD, Rodriguez-Mirasol J, Cordero T, Rodriguez JJ. Adsorption of aromatic compounds on activated carbons from lignin: Equilibrium and thermodynamic study. *Ind Eng Chem Res* 2007;46(14):4982-90.
- [31] Frisch MJ, Trucks GW, Schlegel HB, Scuseria GE, Robb MA, Cheeseman JR, et al. Gaussian03, revision B.05; 2004.
- [32] Perdew JP. Density-Functional Approximation for the Correlation-Energy of the Inhomogeneous Electron-Gas. *Physical Review B* 1986;33(12):8822-4.
- [33] Sosa C, Andzelm J, Elkin BC, Wimmer E, Dobbs KD, Dixon DA. A Local Density Functional-Study of the Structure and Vibrational Frequencies of Molecular Transition-Metal Compounds. *J.Phys.Chem.* 1992;96(16):6630-6.
- [34] COSMOtherm C2.1, release 01.06. Leverkusen, Germany: GmbH & Co. KG; 2003.
- [35] Chatzopoulos D, Varma A. Aqueous-Phase Adsorption and Desorption of Toluene in Activated Carbon Fixed-Beds - Experiments and Model. *Chemical Engineering Science* 1995;50(1):127-41.
- [36] Palomar J, Ferro VR, Torrecilla JS, Rodriguez F. Density and molar volume predictions using COSMO-RS for ionic liquids. An approach to solvent design. *Ind Eng Chem Res* 2007;46(18):6041-8.
- [37] Palomar J, Torrecilla S, Ferro VR, Rodriguez F. Development of an a Priori Ionic Liquid Design Tool. 1. Integration of a novel COSMO-RS Molecular Descriptor on Neural Networks. *Industrial engineering chemistry research* 2008;47:4523-32.
- [38] Doucette WJ. Quantitative structure-activity relationships for predicting soil-sediment sorption coefficients for organic chemicals. *Environmental Toxicology and Chemistry* 2003;22(8):1771-88.
- [39] McGowan JC. Analysis of polyimide dielectric coatings using attenuated total reflectance. *Anal Chem* 1969;41:2074-85.
- [40] Mehler C, Klamt A, Peukert W. Use of COSMO-RS for the prediction of adsorption equilibria. *AIChE journal* 2002;48(5):1093-9.
- [41] Mehler C, Peukert W. Adsorption from aqueous solutions: Comparison of different theoretical strategies to predict the Henry's law coefficients (Reprinted from *Chem. Ing. Tech.*, vol 72, pg 822-826, 2000). *Chemical engineering technology* 2001;24:789-94.
- [42] Calvo L, Gilarranz MA, Casas JA, Mohedano AF, Rodriguez JJ. Effects of support surface composition on the activity and selectivity of Pd. *Ind Eng Chem Res* 2005;44(17):6661-7.

Supplementary material

Table 1S. Fits of Langmuir and Freundlich isotherms for experimental OmimPF₆ adsorption data at different temperatures.

T(°C)	Langmuir			Freundlich			
	q_{max}	B	R^2	K_f	n	R^2	K_d
45	1.17	9.83	0.999	0.99	0.21	0.892	555
35	1.30	8.89	0.999	1.11	0.23	0.889	621
25	1.54	8.16	0.999	1.30	0.26	0.932	760

q_{max} (mmol g⁻¹); B (L mmol⁻¹); K_f (mmol^{1-1/n} L^{1/n} g⁻¹); K_d (L kg⁻¹)

Table 2S. Parameters of Freundlich and Langmuir isotherms from experimental equilibrium data for 6 ILs onto AC-MkS at 35 °C.

	Langmuir			Freundlich		
	q_{max}	B	R^2	K_f	N	R^2
OmimPF₆	1.41	2.94	0.999	0.99	0.38	0.957
BmimOTf	0.51	3.98	0.984	0.39	0.19	0.767
BmimBF₄	0.29	3.32	0.997	0.20	0.14	0.817
BmimTFA	0.25	4.96	0.996	0.21	0.18	0.900
BmimCl	0.25	3.01	0.994	0.18	0.16	0.903
BmimMeSO₃	0.27	7.26	0.992	0.23	0.10	0.901

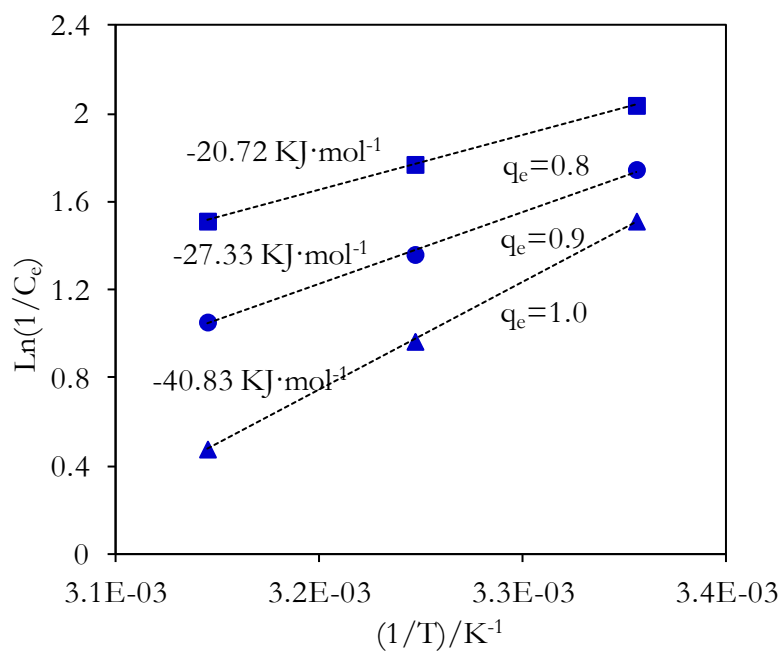
q_{max} (mmol g⁻¹); B (L mmol⁻¹); K_f (mmol^{1-1/n} L^{1/n} g⁻¹)

Table 3S. Molecular surface (S) molecular volume (V), molar density (δ) and other parameters estimated by COSMO-RS for 13 ILs.

	S	V	δ	Parachor	LogK _{ow}	LogP
OmimPF₆	3.43	0.39	1215	122.6	4.02	4.69
BzmimPF₆	3.11	0.35	1385		3.23	4.39
HmimPF₆	3.01	0.35	1265	110.4	2.92	3.67
BmimNTf₂	3.41	0.42	1452	126.7	3.44	4.43
OmimBF₄	3.22	0.36	1106	106.7	2.58	3.23
EmimNTf₂	3.08	0.37	1530	115.8	2.51	3.60
BmimPF₆	2.65	0.30	1320	98.0	2.07	2.88
OmimCl	2.95	0.32	1071	91.1	-0.91	2.62
BmimOTf	2.78	0.32	1318		0.96	2.01
HmimCl	2.56	0.27	1108	83.1	-1.90	1.72
BmimBF₄	2.42	0.27	1193	86.6	0.60	1.40
BmimCl	2.16	0.23	1166	70.2	-2.94	0.96
BmimMeSO₃	2.69	0.29	1231		-2.10	0.89

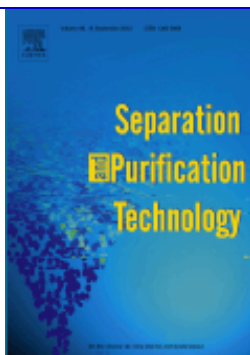
S (nm²); *V* (nm³); δ (kg m⁻³); *Parachor* (cm³mN^{1/4}·mol⁻¹m^{-1/4})

Figure S1. Plots for estimating the enthalpy of adsorption (KJ·mol⁻¹) of OmimPF₆ on AC-MkU at different surface coverages (q_e in mmol·g⁻¹; C_e in mmol·L⁻¹).



ESSAYS ON IONIC LIQUID/ACTIVATED CARBON SYSTEMS AND THEIR APPLICATION TO POLLUTANT REMOVAL

Doctoral dissertation, [Madrid 2012](#), Jesús Lemus Torres



Paper II

DEVELOPING CRITERIA FOR THE RECOVERY OF IONIC LIQUIDS FROM AQUEOUS PHASE BY ADSORPTION WITH ACTIVATED CARBON

107-130

J. Lemus, J. Palomar, F. Heras, M.A. Gilarranz, J.J. Rodríguez.

DEVELOPING CRITERIA FOR THE RECOVERY OF IONIC LIQUIDS FROM AQUEOUS PHASE BY ADSORPTION WITH ACTIVATED CARBON

Separation and Purification Technology. 2012 (97) 11-19

Resumen

Esta segunda publicación complementa el estudio termodinámico de la anterior y se centra en el análisis en profundidad de la adsorción de líquidos iónicos en carbones activos como una aplicación medioambiental abordable para eliminar y recuperar líquidos iónicos de corrientes acuosas. Se ha desarrollado un análisis exhaustivo de la separación de líquidos iónicos imidazolios de corrientes acuosas mediante experimentos de equilibrio a 35 °C. El estudio incluye 5 carbones activos comerciales y 4 modificados, con propiedades estructurales y químicas variadas, un negro de humo y 2 adsorbentes inorgánicos. Estos materiales han sido probados y caracterizados por una amplia variedad de técnicas para establecer las relaciones entre su naturaleza física y química con la capacidad de adsorción. Los carbones activos con contenido en microporo elevado y concentración baja en grupos polares en su superficie se comportan como materiales óptimos para la retención de líquidos iónicos hidrofóbicos, llegando a alcanzar retenciones de un gramo de líquido iónico por gramo de adsorbente. La influencia tanto del anión como del catión fue analizada mediante isothermas de adsorción de 27 líquidos iónicos diferentes. La dependencia de la capacidad de adsorción con la naturaleza química del líquido iónico es explicada mediante el método químico-cuántico COSMO-RS, que proporciona información de las interacciones moleculares entre el adsorbato (líquido iónico) y el adsorbente (carbón activo). El modelo computacional nos permite conocer qué modificaciones son necesarias para la mejora en la adsorción de líquidos iónicos específicos, obteniendo que la adsorción de líquidos iónicos hidrofílicos es más efectiva utilizando como adsorbentes carbones activos oxidados.

Por otra parte, se propone acetona como disolvente para la regeneración de dos carbones activos comerciales saturados de líquido iónico en sucesivos ciclos de adsorción-desorción. Por último, la acetona puede ser separada del líquido iónico por destilación atmosférica, recuperando el líquido iónico sin cambios en su estructura.

Abstract

Adsorption with activated carbons (ACs) has been recently reported as an affordable environmental application to remove and recover ionic liquids (ILs) from water streams. In this work, an extensive analysis of the separation of imidazolium-based ILs from aqueous solution, based on adsorption equilibrium experiments at 35 °C, has been performed. The study includes 5 commercial and 4 modified ACs, with a wide variety of structural and chemical properties, a carbon black and also 2 inorganic adsorbents. The materials tested were characterized by several techniques in order to establish the role of the porous structure and chemical surface on their adsorption capacities. We found that the microporous ACs with low concentration of polar groups in their surface are the best candidates for adsorption of hydrophobic ILs, reaching uptakes of up to one gram of IL per gram of adsorbent. The influence of both cation and anion on the adsorption process was analyzed from the adsorption isotherms of 27 different ILs. The dependence of the adsorption uptake with the chemical structure of the ILs was explained by means of the quantum-chemical COSMO-RS model, which provides information of the intermolecular interactions between the IL adsorbate and the AC adsorbent. As a result, some insight into the adsorbent modifications needed for improving of the adsorption of specific ILs were achieved and successfully applied to the adsorption of hydrophilic ILs by oxidized ACs.

In addition, a procedure for regenerating the exhausted adsorbent and recovering the IL by acetone extraction was validated upon successive adsorption-desorption cycles with two commercial ACs. Finally, the acetone was separated by atmospheric distillation, being the IL recovered without structural modification.

1. Introduction

Ionic liquids (ILs) have important advantages with respect to traditional organic solvents because of their outstanding physical properties, such as low vapor pressure [1], high solvent capacity [2], chemical stability [3] and tenability [4]. During the last years, ILs have gained considerable attention for a broad range of different applications, including synthesis and catalysis [5,6] and biocatalytic reactions [7], separation processes [8-15], electrochemical applications [16], solar cells [17], supercapacitors [18], nanomaterials [19], polymer science [20], biomass processing [21] or lubricants [22], with some processes operating at industrial scale [23,24]. The ILs have been considered as potentially environmentally friendly solvents for industry, because their extremely low volatility prevents their emission to the atmosphere. However, it has been stated that they exhibit a wide range of environmental toxicity [25], low biodegradability [26] and potential accumulation in soils [27-30]. In addition, they are partially miscible with water and their use at large scale may lead to transfer to the aqueous environment. Then, the generation of wastewaters from IL industrial processing may represent an important problem demanding adequate solutions [31,32]. For this reason, it is necessary to develop techniques to remove ILs avoiding the negative effects of a potential environmental persistency [33]. Generally, the techniques employed for regeneration and recovery of ILs (vacuum distillation, crystallization, liquid-liquid extraction, nanofiltration, etc.) are not affordable for removing ILs at low concentrations [33]. Different destructive methods, such as thermal degradation [34,35], chemical oxidation [36-38] or biological treatments [39-42], have been recently investigated for eliminating common ILs from wastewater. With independence of the different efficiency reported for such destructive treatments, these techniques do not permit the IL recovery. Due to the unusual high costs of ILs and the environmental and financial policy of the waste framework legislation, recovery and regeneration are crucial issues in process development, in order to extend IL lifetime by, respectively, re-use and recycling [33]. Therefore, the research of non-destructive treatments for removing ILs from wastewater present the additional interest of the opportunity of later recovery of IL compound [43].

In a previous work, we reported the possibility of removing imidazolium-based ILs from aqueous streams by effective adsorption by using a commercial activated carbon (AC) [44], thanks to the favourable IL-AC interactions [44-47]. In the current work, we extend the investigation on adsorption of imidazolium-based IL from aqueous stream using a variety of adsorbents, with the main aim of determining the characteristics that must include an

adsorbent for successful recovering a specific IL. For this purpose, the adsorption of 1-octyl-3-methylimidazolium hexafluorophosphate (OmimPF₆), used as reference of hydrophobic IL, was studied on twelve adsorbents with different chemical and physical properties. The adsorbent sample includes five commercial ACs with wide range of porosity (A_{BET} from 800 to 2000 m² g⁻¹), four chemically and physically modified ACs and three adsorbents of different chemical nature, carbon black, silica or alumina. Both porous structure and chemical surface of adsorbents may be essential to assess their capacity to retain different solutes in aqueous solution [48,49]. For this reason, the materials employed were characterized by several techniques, including measurements of 77K N₂ adsorption-desorption isotherms, mercury porosimetry, elemental analysis and pH_{slurry} . As the combination of anion and cation making the ILs are multiple [50], it was found a great diversity of available ILs, opening a wide range of characteristics. Previous studies demonstrated the high influence of the chemical structure of IL in the adsorption process [44,51]. In this study, the adsorption isotherms at 35 °C were carried out for 27 ILs, including ten different cations and seven different anions. The analysis of the chemical structure of the adsorbate was completed by using the quantum-chemical COSMO-RS method, which was successfully applied to predict thermodynamic data and interaction energies of IL-AC-H₂O ternary systems involved in adsorption phenomena [44]. As a result, some criteria on the selection of physical and chemical properties of efficient adsorbents for IL can be proposed. Based on this, commercial ACs were subjected to chemical treatments for increasing their polarity with the aim of improving the adsorption of hydrophilic ILs, whereas the retention of hydrophobic ILs was improved by thermal treatment of commercial ACs, which removes polar groups from their surface. Lately, a successful regeneration process for the exhausted adsorbent, based on acetone solvent, was validated for two commercial AC. Atmospheric distillation to remove acetone solvent from regenerating solution was carried out, obtaining the recovery of the IL compound, whose chemical structure was analyzed by ¹H-NMR spectroscopy.

2. Procedure

2.1 Experimental

Five commercial ACs were tested in this study as adsorbents were supplied by Norit (CAPSUPER, SXPLUS and GXS) and Merck (MkU). The carbon black ENA250G was supplied by Timcal. Alumina and silica were supplied by Sigma-Aldrich. Some of the commercial ACs were subjected to thermal and oxidative treatments in order to modify their surface chemical composition. The thermal treatment of the ACs was accomplished in a quartz horizontal tube furnace (2.5 cm i.d. and 15 cm length) under a nitrogen flow of 60 mL·min⁻¹ at 900 °C for 3 h. This temperature was reached at 100 °C·min⁻¹. On the other hand, oxidative treatment with nitric acid of the ACs was carried out by boiling 1 g of AC in 10 mL of a 6 N nitric acid solution for 20 minutes. Afterwards the oxidized AC samples were washed with distilled water until neutral pH and dried overnight at 100 °C [52]. The nitric acid used in the oxidative process of AC was supplied by Riedel de Haën. The acetone used for desorption was supplied by Panreac. The ionic liquids OmimPF₆ and BmimCl used in this study as adsorbates were supplied by Iolitec, in the highest purity available (purity > 99%). The rest of ILs were supplied by different companies such as Sigma-Aldrich, Solchemar and Iolitec, always with purity over 98%, (see supplementary material). The ILs were as purchased used without previous purification.

The porous structure of the adsorbents (fresh and used) was characterized by means of 77 K N₂ adsorption–desorption using a Micromeritics apparatus (Tristar II 3020 model) and by mercury porosimetry with a Quantachrome apparatus (PM-3310 model). Previous to N₂ adsorption isotherm of, the samples were outgassed at 150 °C for 8 h to a residual pressure of 10⁻⁵ Torr. The BET equation was used to obtain the apparent surface area (A_{BET}) and the Dubinin–Radushkevich equation for micropore volume. It was also obtained the pore volume up to 8 nm pore width from the N₂ adsorbate (expressed as liquid) up to 0.787 relative pressure. The difference between the N₂ adsorbed volume at 0.95 relative pressure and the micropore volume was taken as mesopore volume [53].

Elemental analyses of the fresh and used ACs were carried out in a Perkin–Elmer analyzer (210 CHN model) to obtain the C, H and N percentages. The pH_{slurry} was determined measuring, until constant value, the pH of an aqueous suspension of support in distilled water (1 g of solid per 10 mL of water) [54].

The equilibrium adsorption tests were carried at 35 °C following the procedure described in a previous work [44], being the experimental equilibrium data analyzed using the Langmuir equation [55]. Apparent distribution coefficients, K_d ($L \cdot kg^{-1}$), were calculated for the sake of comparison the adsorption of the different IL onto the AC tested. The coefficients were calculated as:

$$K_d = \frac{q_e}{c_e} \quad \text{eq. II.1}$$

being q_e the adsorption capacity at 1.2 and 2.0 $mmol \cdot L^{-1}$ equilibrium concentration (C_e).

Regeneration of the AC after OmimPF₆ adsorption was carried out with acetone, following the procedure described in a previous work [44]. The regenerated AC were filtered and dried overnight at 50 °C. The porous structure was characterized as it was described for the virgin materials. The adsorption capacity of the regenerated ACs was tested upon successive adsorption-regeneration cycles using OmimPF₆ solutions of 500 $mg \cdot L^{-1}$ (1.2 $mmol \cdot L^{-1}$). Three replicates of each regeneration cycle were carried out on the average values reported here. Finally, the IL was recovered from regenerating solution by evaporating acetone in a Buchi Rotavapor R-205 at atmospheric pressure and 60 °C over 2 h.

NMR experiments of fresh and recovered IL were recorded on a Varian Unity 500 spectrometer, using a solution of OmimPF₆ and acetone-d₆ over 10 mmol.

2.2 Computational

The molecular geometry of all molecular models (AC, water and ILs) were optimized at B3LYP/6-31++G** computational level in the ideal gas-phase using quantum chemical Gaussian03 package [56]. Vibrational frequency calculations were performed for each case to confirm the presence of an energy minimum. Then, the standard procedure was applied for COSMO-RS calculations, which consists of two steps: First, Gaussian03 was used to compute the COSMO files. The ideal screening charges on the molecular surface for each species were calculated by the continuum solvation COSMO model using BVP86/TZVP/DGA1 level of theory. Subsequently, COSMO files were used as an input in COSMOtherm [57] code to calculate the thermodynamic properties of the individual components and the ternary (water-IL-AC) system involved in the adsorption phenomena.

The computational approach was described elsewhere [44] and describes IL adsorptive by an ion-pair structure, the aqueous media by individual water molecule and AC adsorbent by a mixture of two AC structures (see Figure 1S in Supplementary material) in a 90/10 molar AC/AC-OH ratio, in order to introduce in the simulation the measured concentration of oxygenated groups of the MkU activated carbon [58]. The AC/water partition coefficient (P) of IL at infinite dilution was calculated by COSMO-RS at 25 °C. According to the chosen quantum method, the functional and the basis set, we used the corresponding parameterization (BP_TZVP_C21_0106) that is required for the calculation of physicochemical data and contains intrinsic parameters of COSMOtherm as well as element specific parameters.

3. Results and discussion

3.1. Adsorption of ILs from aqueous solution

In a previous work, we demonstrated the possibility of removing imidazolium-based ILs from aqueous streams by effective adsorption with a commercial AC (MkU in this work) [44]. The uptake of hydrophobic ILs, as OmimPF₆ (~450 mg·g⁻¹), was significantly higher than that achieved for common adsorbates as phenol (~225 mg·g⁻¹) or toluene (~260 mg·g⁻¹) at 25 °C [44]. Since it is well stated that adsorption depends on both the porous structure and the chemical surface of the adsorbent [59], in this work twelve materials, with a wide variety of physical and chemical properties, have been examined as potential adsorbents of ILs from aqueous solution.

Table 1. Nomenclature, suppliers, treatments, physical and chemical characterization of twelve adsorbents and K_d values obtained using OmimPF₆ as adsorbate with $C_e = 2.0$ mmol·L⁻¹ at 35 °C.

Sample	Supplier	Treatment	A_{BET} (m ² ·g ⁻¹)	$V_{microp.}$ (cm ³ ·g ⁻¹)	$V_{mesop.}$ (cm ³ ·g ⁻¹)	$V_{macrop.}$ (cm ³ ·g ⁻¹)	V_{Total}	%C	pH _{slurry}	K_d (L·kg ⁻¹)
CAPSUPER	NORIT	None	1915	0.66	0.63	1.02	2.32	81.0	3.3	1520
CAP-900	NORIT	Thermal (900°C)	1434	0.51	0.42	1.11	2.04	91.3	--	1200
CAP-N	NORIT	Oxidative (HNO ₃)	1686	0.54	0.51	1.00	2.05	73.6	--	1000
MKU	MERCK	None	927	0.36	0.22	0.22	0.80	88.9	5.4	635
MKU-900	MERCK	Thermal (900°C)	906	0.36	0.23	0.25	0.84	88.8	--	635
MEN	MERCK	Oxidative (HNO ₃)	856	0.33	0.24	0.26	0.83	81.9	--	620
SXPLUS	NORIT	None	1210	0.53	0.38	0.53	1.44	89.8	5.2	1300
ENA350G	TIMCAL	None	912	0.40	0.40	1.64	2.45	98.0	6.0	840
GXS	NORIT	None	802	0.27	0.33	0.86	1.46	87.5	5.0	600
ENA250G	TIMCAL	None	79	0.00	0.08	1.40	1.48	98.8	6.1	105
SiO ₂	SIGMA	None	212	0.00	0.26	3.07	3.33	--	6.7	95
Al ₂ O ₃	SIGMA	None	136	0.00	0.21	0.12	0.33	--	8.1	15

The sample includes five commercial ACs (CAPSUPER, MkU, SXPLUS, ENA350G and GXS), four chemically or thermally treated ACs (CAP-900, CAP-N, Mk-900 and MkN), one carbon black (ENA250G) and commercial silica and alumina (see Table 1). As a first step, equilibrium adsorption experiments were carried using OmimPF₆ as reference of common imidazolium-based IL. The adsorption isotherms of OmimPF₆ at 35 °C for eight commercial adsorbents, without previous treatment, are depicted in Figure 1. From the results of Figure 1A, most of commercial ACs tested can be postulated as good adsorbents of OmimPF₆, showing capacities above 1 mmol·g⁻¹ (> 340 mg IL per g AC) at the least and substantially higher in some cases. On the opposite, inorganic materials, as silica and alumina, show fairly lower IL adsorption (Figure 1B). The carbon black ENA250G also presents low adsorption capacity for OmimPF₆ (Figure 1B). Remarkably, a commercial AC from Norit (CAPSUPER in Figure 1A) exhibits a maximum uptake of 3.3 mmol·g⁻¹, *i.e.*, yielding the significant retention of ~1000 mg of IL per gram of adsorbent. These results strongly support the potential of adsorption with ACs for recovering ILs from water solutions [44].

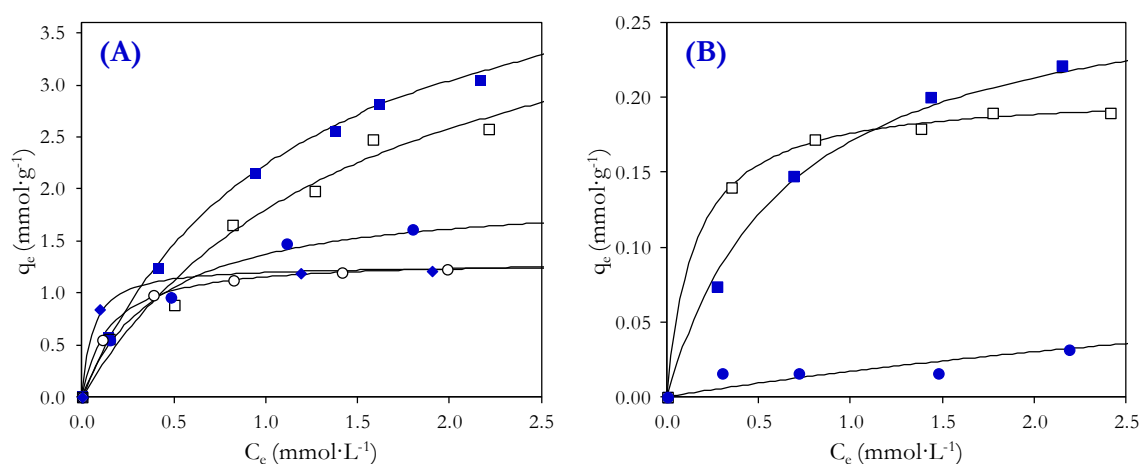


Figure 1. Experimental data (dots) and Langmuir fits (curves) for the adsorption equilibrium of OmimPF₆ onto different adsorbents: (A) CAPSUPER (■), SXPLUS (□), ENA350G (●), MkU (○) and GXS (◆); and (B) ENA250G (■), SiO₂ (□) and Al₂O₃ (●) at 35 °C.

The next aim was to analyze the influence of the adsorbent properties on IL adsorption. For this purpose, the characterization of the materials tested was carried out by several techniques, whose results are collected in Table 1. As can be seen from Figure 2A, adsorption capacity (in terms of K_d) consistently increases with the surface area (A_{BET}) of the adsorbent. In order to achieve a deeper understanding of the porous structure of those materials, the Hg porosimetry and 77 K N_2 adsorption-desorption measurements were combined to determine the size distribution of available pore volume following the IUPAC criteria: macropore, $50 \text{ nm} < \text{Pore diameter or width} (d_{pore}) < 1000 \text{ nm}$; mesopore, $2 \text{ nm} < d_{pore} < 50 \text{ nm}$; and micropore, $d_{pore} < 2 \text{ nm}$. This pore volume distribution is shown in Figure 2B.

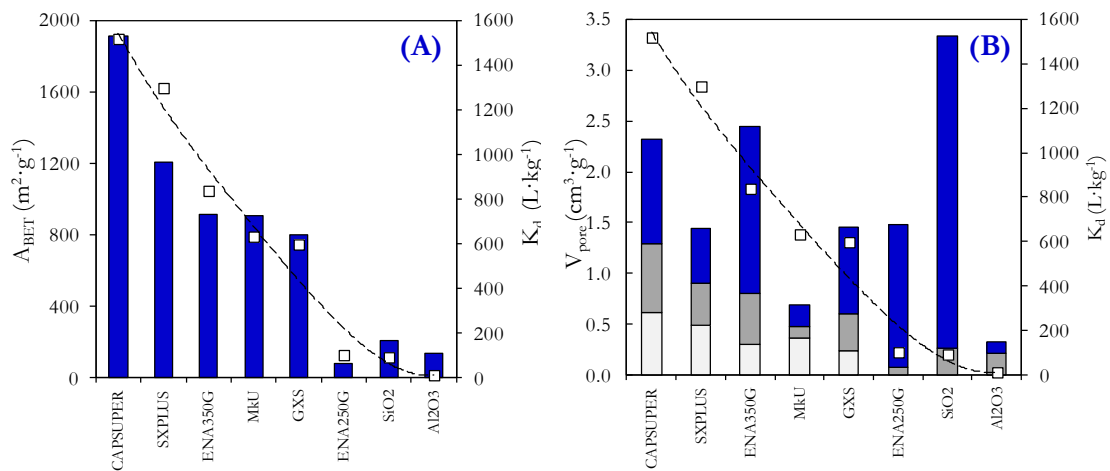


Figure 2. (A) Plot of apparent distribution coefficient (K_d (\square), obtained for the $C_e = 2.0 \text{ mmol} \cdot \text{L}^{-1}$ at $35 \text{ }^\circ\text{C}$) for OmimPF₆ adsorption against the BET surface of adsorbents (\blacksquare); and (B) and available pore volume distribution of adsorbents divided on micropore (white), mesopore (grey) and macropore (blue).

In principle, a clear relationship between the total available pore volume of each solid and its capacity for adsorbing OmimPF₆ from water cannot be inferred. However, a more detailed analysis within different pore size intervals allows obtaining a linear relationship between the uptake of OmimPF₆ (in terms of the apparent distribution coefficient, K_d) and the pore volume below 8 nm width (micropore + narrow mesopore) of the adsorbent, as can be seen in Figure 3A. Furthermore, Figure 3B shows that the maximum uptake of IL, expressed in volume (calculated using the molar density of OmimPF₆ at $35 \text{ }^\circ\text{C}$, $1.228 \text{ g} \cdot \text{cm}^{-3}$) [60] is in reasonably good agreement with the available pore volume up to 8 nm width. In a previous work, we concluded that the available micropore area was insufficient for the amount of OmimPF₆ adsorbed on MkU activated carbon, arguing the formation of multilayer on the

mesopore and macropore surface [44]. Current results indicate that the pores within the size range up to 8 nm are playing a main role in IL adsorption from aqueous solution, providing nearly the necessary volume for the IL uptake. This conclusion seems to be consistent with the recent evidence of preferential filling by IL of micropores and narrow mesopores in the preparation of supported ionic liquid phase (SILP) [45]. In sum, the analysis performed for a wide variety of adsorbent materials shows that the porous structure is a determining criteria for selecting adequate adsorbents for ILs.

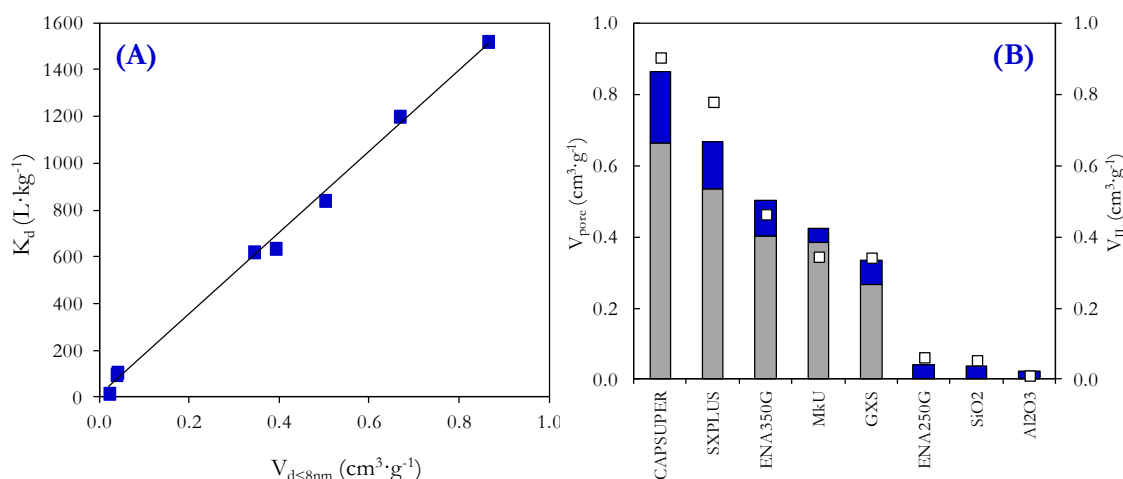


Figure 3. (A) Plot of apparent distribution coefficient (K_d , $\text{L} \cdot \text{kg}^{-1}$) against pore volume up to 8 nm width; (B) Maximum IL uptake (V_{IL} bar diagram) versus available pore volume ($d_{pore} < 2$ nm (■) and $2 < d_{pore} < 8$ nm (■)).

In addition to the role of porous structure, it was also demonstrated for a sample of thirteen ILs that a factor strongly affecting ILs adsorption is the nature of both cation and anion of the IL [44]. Thus, working with MkU adsorbent a significant increase of adsorption was observed as the hydrophobic character of IL increased due to longer the alkyl chains of the imidazolium cation or according to the sequence of hydrophobicity of the anions ($\text{NTf}_2^- > \text{PF}_6^- > \text{OTf}^- > \text{BF}_4^- > \text{TFA}^- > \text{Cl}^-$). These results were analyzed by means of quantum-chemical COSMO-RS method, which was successfully applied to predict equilibrium data for adsorption from aqueous solutions [44]. In addition, COSMO-RS provided insight into the adsorbate-adsorbent interactions, revealing that the attractive Van der Waals interactions determine the efficient adsorption of hydrophobic ILs [44]. In the present work, experimental evidences for 27 imidazolium-based ILs have been examined at molecular level using COSMO-RS method. In this IL sample, the hydrophobic character of four families with common anion (NTf_2^- , PF_6^- , BF_4^- and Cl^-) increases upon progressive addition of carbon

atoms to the cation alkyl chain. The partition coefficient (P) at infinite dilution, calculated by COSMO-RS, serves to quantify the affinity of the IL for the AC in aqueous phase. Figure 4A (data collected in Table 2) compares the values of $\text{Log}(P)$ with those of experimental apparent adsorption coefficient (K_d) for 22 imidazolium-based ILs using the AC-MkU as adsorbent. These results show a good relationship between both distribution coefficients, up to a value of $\text{Log}(P)$ around 5, from which K_d decreases.

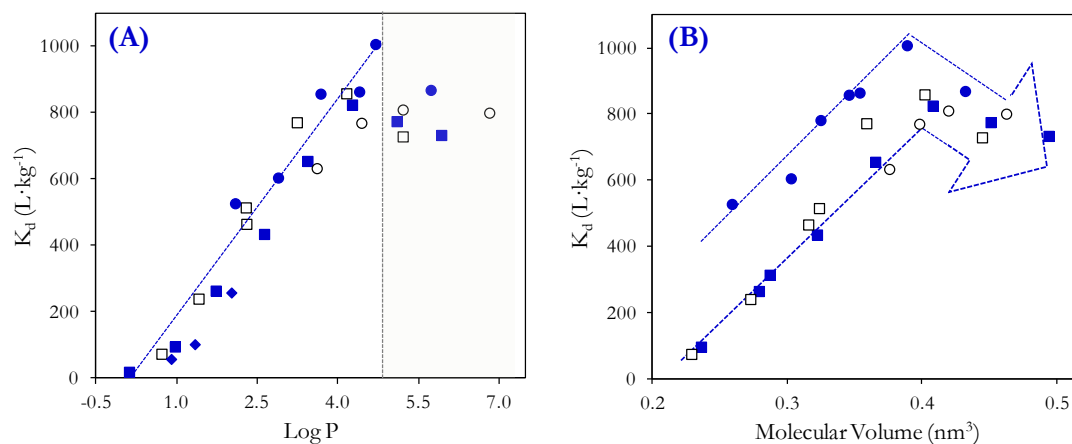


Figure 4. K_d versus $\text{Log } P$ (A) and IL molecular volume (B) predicted by COSMO-RS for 1-alkyl-3-methylimidazolium based ILs with different anions: PF_6^- (●), NTf_2^- (□), BF_4^- (■), Cl^- (○), and other anions (◆) using MkU as adsorbent.

Table 2. Molecular volume, LogP of IL solute and K_d , (obtained for the $C_e = 1.5$ mmol·L⁻¹ at 35 °C using AC-MkU as adsorbent) for 27 imidazolium based ILs.

Ionic liquid		Volume (Å ³)	LogP	K_d (L·kg ⁻¹)
Emim	Cl	192	0.11	20
Bmim	Cl	236	0.96	96
Hxmim	Cl	279	1.72	264
Omim	Cl	322	2.62	435
Dcmim	Cl	365	3.43	655
Ddmim	Cl	408	4.26	825
Tdmim	Cl	451	5.09	775
Hdmim	Cl	494	5.92	733
Emim	BF ₄	229	0.71	74
Bmim	BF ₄	273	1.40	240
Hxmim	BF ₄	316	2.29	465
Omim	BF ₄	359	3.23	772
Dcmim	BF ₄	402	4.15	859
Ddmim	BF ₄	445	5.20	729
Emim	PF ₆	259	2.08	528
Bmim	PF ₆	303	2.88	605
Hxmim	PF ₆	346	3.67	858
Bzmim	PF ₆	354	4.39	864
Omim	PF ₆	389	4.69	1008
Dcmim	PF ₆	432	5.72	869
Emim	NTf ₂	376	3.60	633
Prmim	NTf ₂	398	4.43	770
Bmim	NTf ₂	420	5.20	810
Hxmim	NTf ₂	463	6.81	801
Bmim	OTf	317	2.01	258
Bmim	TFA	310	1.33	103
Bmim	MeSO ₃	289	0.89	58

For most cases, the increasing hydrophobic character of IL imply a higher affinity for the non-polar AC environment respect to the polar water media, observing a broad uptake range with the IL nature, from $K_d = 20$ to $1000 \text{ L}\cdot\text{kg}^{-1}$. For the exception cases (TdmimCl, HdmimCl, DdmimBF₄, DdmimPF₆ and HxmimNTf₂), the expected higher hydrophobic character of IL, which is well-predicted by COSMO-RS, is not associated to a higher retention by the AC. In order to evaluate possible steric effects, Figure 4B presents the apparent adsorption coefficient (K_d) against the molecular volume of ILs calculated by COSMO-RS. In general, increasing the compound size through chain enlarging in a IL family with common anion implies a more efficient adsorption. However, it can be appreciated that for all the families studied, the ILs with molecular volume higher than 0.4 nm^3 do not follow that trend. Therefore, the accessibility of ILs with higher molecular volume than 0.4 nm^3 can be restricted to small pores of MkU adsorbent.

A remarkable advantage of ACs as adsorbents is that their structure and surface chemistry can be conveniently modified by chemical and thermal treatments, so that the interactions with solutes can be conveniently favoured [44]. Thus, it was confirmed that the adsorption of refractory hydrophilic ILs can be improved by increasing the amount of oxygen groups on the AC surface, which promote hydrogen-bonding interactions with the anions of hydrophilic ILs.

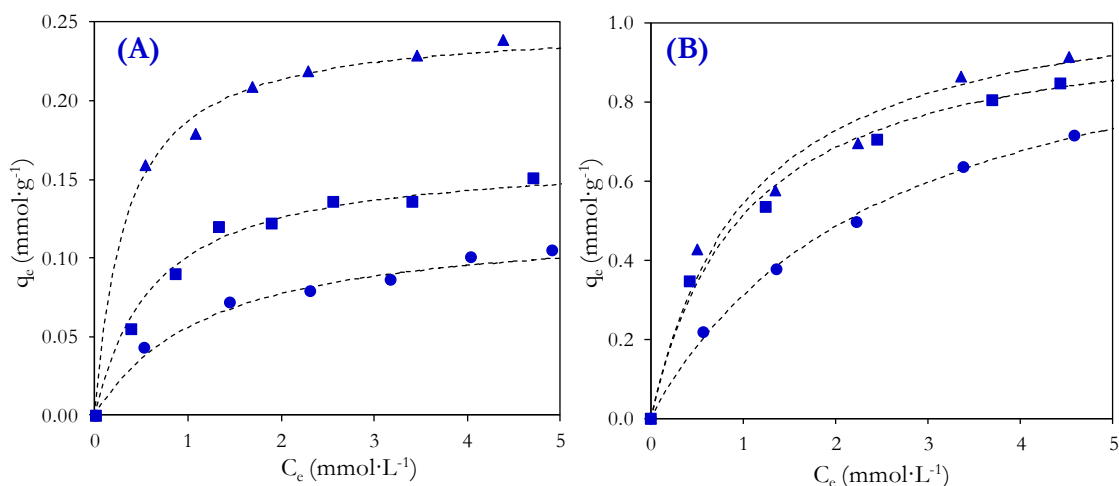


Figure 5. Experimental data (dots) and Langmuir fits (curves) for the adsorption equilibrium of BmimCl onto (A) MkU and (B) CAPSUPER subjected to different treatments: none treatment (■), oxidative treatment (▲) and thermal treatment (●).

In order to analyze the influence of the surface chemistry of AC on IL adsorption fresh, oxidized and heat treated ACs were compared in adsorption tests. [Figure 5A](#) shows the adsorption isotherms of a hydrophilic ionic liquid, BmimCl at 35 °C, using MkU, Mk-900 and MkN. It can be seen that the formation of oxygenated groups on the AC surface (MkN) significantly improves the uptake of BmimCl. On the contrary, the removal of oxygen surface groups by thermal treatment in N₂ atmosphere (Mk-900) results in a decreased adsorption capacity. It should be remarked that oxidative and thermal treatments only modified slightly the porous structure of the virgin MkU, as can be seen in [Table 1](#). On the other hand, [Figure 5B](#) depicts the adsorption isotherms of BmimCl at 35 °C using with the CAPSUPER, CAP-900 and CAP-N. The commercial CAPSUPER is an AC with much higher contribution of acidic surface groups than MkU, as can be inferred from their pH_{slurry} values of 3.3 and 5.4, respectively ([Table 1](#)). Therefore, the higher affinity of BmimCl for CAPSUPER determines a sixfold increase in capacity respect to MkU, whereas for the hydrophobic IL OmimPF₆ only a two fold increase takes places, which can be mostly ascertained to the difference in porous structure. The differences in surface composition also results in a different behaviour after modification. On one hand, due to the initial nature of carbon surface the change in polarity upon oxidation treatment of CAPSUPER is not as drastic as for MkU and a lower influence of such treatment in capacity can be expected. On the other hand, the oxidation of CAPSUPER leads to a larger reduction of micropore and mesopore volume. Such loss of porosity of AC surface may counteract the increase of polarity and as a result of it the overall in capacity is of low significance.

This interpretation of the combined influence of textural properties and surface composition is supported by the results obtained with the hydrophobic IL OmimPF₆ ([Figure 6](#)). In this case, Van der Waals interactions between alkyl chain attached to the imidazolium group of IL and the aromatic rings of the graphene layers of AC take place. Mk-900 ([Figure 6A](#)) shows a slightly improved adsorption capacity with respect to virgin MkU consistently with the lower concentration of surface oxygen groups of polar character and the similar porous structure, whereas oxidized MkN shows the lowest adsorption capacity in agreement with a more polar surface due to a higher surface oxygen groups content. Otherwise, CAP-900 show lower adsorption capacity for OmimPF₆ than the virgin CAPSUPER, because of the prevailing negative effects associated to the decrease of surface area due to thermal treatment. Of special importance is the loss of capacity for CAP-N because of both increase of the polarity of the surface and reduction of the pore volume. Summarizing, the results obtained indicate that the selective adsorption of ILs of different chemical nature can be efficiently

improved by tuning the chemical composition of the adsorbent surface but preserving its porous structure. In this sense, AC can be, in general, easily modified by simple treatments to become effective adsorbents [59].

Table 3. BET area, and K_d coefficient (calculated for an initial concentration of $1.2 \text{ mmol}\cdot\text{L}^{-1}$) of MkU and CAPSUPER after OmimPF₆ adsorption on regeneration cycles and blank experiments.

	MkU		CAPSUPER	
	$K_d \text{ (L}\cdot\text{kg}^{-1})$	$K_d \text{ (L}\cdot\text{kg}^{-1})$	$K_d \text{ (L}\cdot\text{kg}^{-1})$	$K_d \text{ (L}\cdot\text{kg}^{-1})$
First	927	1091	1915	1475
One cycle	861	874	1863	1400
Two cycles	848	892	1785	1300
Blank	889	918	1840	1420

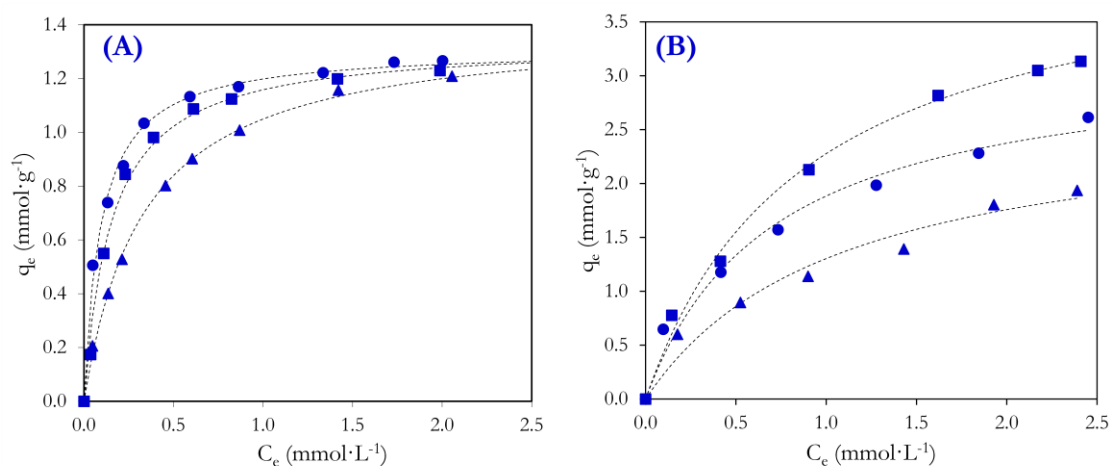


Figure 6. Experimental data (dots) and Langmuir fits (curves) for the adsorption equilibrium of OmimPF₆ onto (A) MkU and (B) CAPSUPER subjected to different treatments: none treatment (■), oxidative treatment (▲) and thermal treatment (●).

3.2. Adsorbent regeneration and IL recovery

Regeneration of an exhausted adsorbent for re-use is a determining factor regarding its potential application at industrial scale. If adsorption wants to be applied for ILs, the recovery of this type of compounds becomes a critical point due to their high valued and toxicity which would give the character of toxic waste to the exhausted adsorbent. Reuse (or preparing for reuse) is a prioritized strategy in the waste hierarchy established by the 2008/98 European directive [33].

In this section, both the regeneration of exhausted AC adsorbents and the later recovery of an IL of reference, OmimPF₆, have been checked using acetone as regenerating agent, following a procedure described in previous work [44]. Acetone presents the advantages of high volatility and high solvent capacity. Briefly, AC-supported IL samples were contacted with a small amount of acetone (10 mL solvent per gram of AC) for 1h under magnetic stirring at room temperature. In the current work, the AC sample, after extraction, was filtered and dried overnight at 60 °C. Subsequently, the regenerated AC was characterized by means of 77 K N₂ adsorption–desorption to evaluate the effect of the regeneration procedure on its porous structure. Finally, the adsorption capacity of the regenerated AC was checked by exposure to OmimPF₆ aqueous solutions of 1.2 mmol·L⁻¹ at 35 °C. Three adsorption-desorption cycles were conducted, with the average values being reported here (Table 3). A blank was carried out to learn on any possible modification of the textural properties and adsorption capacity of bare ACs after contacted with. The regeneration procedure was evaluated for CAPSUPER and MkU. The characterization of the porous structure revealed no significant differences between the fresh and regenerated ACs. The measured K_d (L·kg⁻¹) maintained the favourable values of both ACs through the successive cycles, indicating that the exhausted ACs are successfully regenerated, maintaining adsorption capacities and surface areas above ~90% of the initial values.

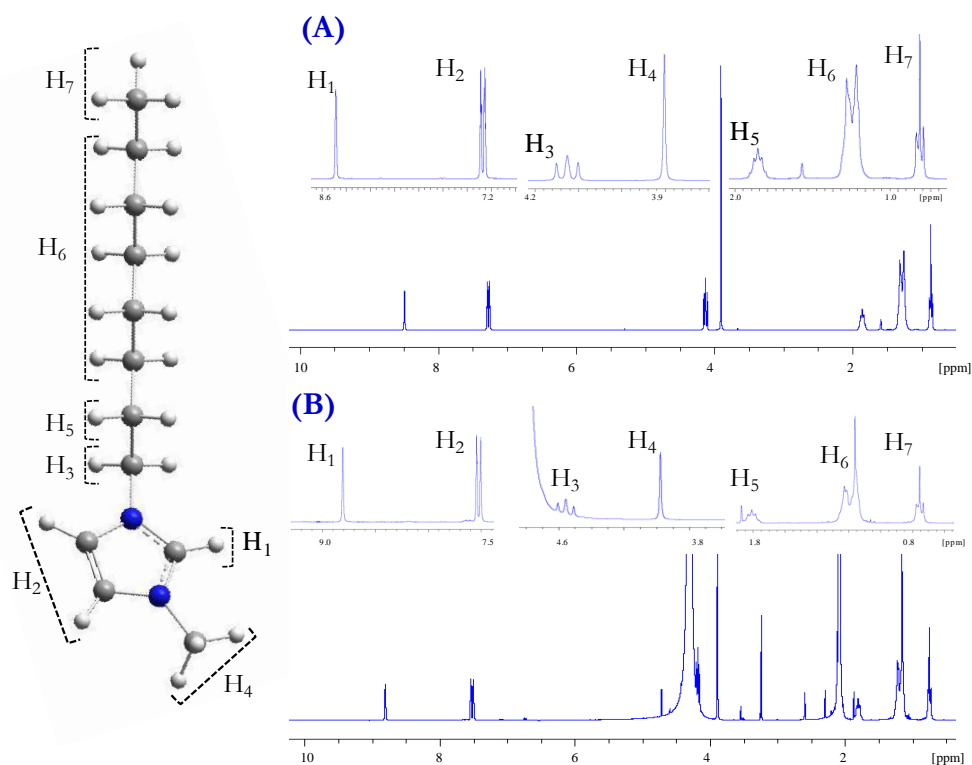


Figure 7. 500 MHz ^1H -NMR spectra of (A) fresh and (B) regenerated OmimPF₆ dissolved in deuterated acetone.

Finally, the recovery of IL from the regenerating acetone solution was evaluated by atmospheric distillation at 60 °C. Once evaporated the acetone solvent, the recovered IL, OmimPF₆, was analyzed by mean of ^1H -NMR spectroscopy using d₆-acetone as solvent in sample preparation. The ^1H -NMR spectra of fresh and recovered OmimPF₆ are shown in Figure 7. As can be seen, the recovered IL exhibits the same ^1H -NMR peaks than original, with absence of unassigned signals in the spectrum, thus allowing to conclude the successful regeneration of IL.

As indicated before, the amount of acetone used in the regeneration process was 10 mL per gram of adsorbent, which is a fairly reasonable proportion. The IL concentration in the regeneration solution operation would be within the mass range of 10 - 5% for maximum uptakes with CAPSUPER and MkU. Future research will be conducted for the purpose of checking other regenerating agents and optimizing the operating conditions.

4. Conclusions

Experimental equilibrium studies on the adsorption of several imidazolium-based ILs in water were carried out with a variety of commercial adsorbents and the results analyzed by quantum-chemical COSMO-RS method. Interesting conclusions about the selection of adsorbents for efficiently removing specific ILs from aqueous phase were achieved, depending on the physical and chemical properties of both solute and adsorbent. Thus, microporous/narrow mesoporous activated carbons (with high content of pore with diameter lower than 8 nm) present highest adsorption capacities, with maximum uptake of up to 1 gram of IL per gram of adsorbent. In addition, adsorption process can be favored by adequate modification of the adsorbent chemical surface. Thus, hydrophilic ILs were more efficiently removed from aqueous streams by using ACs with high content of polar groups in their surface, which promote hydrogen bonding adsorbate-adsorbent interactions. In addition, materials with low polarity, as thermally treated ACs, are preferred for the effective retention of hydrophobic ILs. Current results also evidenced some steric effects restricting the adsorption of ILs with large molecular volume.

In addition, a procedure for regenerating exhausted adsorbent by using acetone as solvent was validated for two commercial ACs. As additional contribution, the evaporation of volatile acetone by atmospheric distillation allowed the successfully recovery of the IL compound.

References

- [1] Wasserscheid P, Welton T. Ionic liquids in synthesis. Weinheim: Wiley-VCH; 2008.
- [2] Padua A, Gomes M, Lopes J. Molecular solutes in ionic liquids: A structural, perspective. *Acc.Chem.Res.* 2007;40(11):1087-96.
- [3] Sowmiah S, Srinivasadesikan V, Tseng MC, Chu YH. On the Chemical Stabilities of Ionic Liquids. *Molecules* 2009;14(9):3780-813.
- [4] Weingaertner H. Understanding ionic liquids at the molecular level: Facts, problems, and controversies. *Angewandte Chemie-International Edition* 2008;47(4):654-70.
- [5] Parvulescu V, Hardacre C. Catalysis in ionic liquids. *Chem.Rev.* 2007;107(6):2615-65.
- [6] Olivier-Bourbigou H, Magna L, Morvan D. Ionic liquids and catalysis: Recent progress from knowledge to applications. *Applied Catalysis A-General* 2010;373(1-2):1-56.

- [7] van Rantwijk F, Sheldon R. Biocatalysis in ionic liquids. *Chem.Rev.* 2007;107(6):2757-85.
- [8] Han X, Armstrong DW. Ionic liquids in separations. *Acc.Chem.Res.* 2007;40:1079-86.
- [9] Huang H, Ramaswamy S, Tschirner UW, Ramarao BV. A review of separation technologies in current and future biorefineries. *Separation and Purification Technology* 2008;62(1):1-21.
- [10] Pereiro AB, Rodriguez A. Azeotrope-breaking using BmimMeSO₄ ionic liquid in an extraction column. *Separation and Purification Technology* 2008;62(3):733-8.
- [11] Ortiz A, Ruiz A, Gorri D, Ortiz I. Room temperature ionic liquid with silver salt as efficient reaction media for propylene/propane separation: Absorption equilibrium. *Separation and Purification Technology* 2008;63(2):311-8.
- [12] Ortiz A, Galan LM, Gorri D, de Haan AB, Ortiz I. Kinetics of reactive absorption of propylene in RTIL-Ag⁺ media. *Separation and Purification Technology* 2010;73(2):106-13.
- [13] Martinez-Aragon M, Burghoff S, Goetheer ELV, de Haan AB. Guidelines for solvent selection for carrier mediated extraction of proteins. *Separation and Purification Technology* 2009;65(1):65-72.
- [14] Shiflett MB, Shiflett AD, Yokozeki A. Separation of tetrafluoroethylene and carbon dioxide using ionic liquids. *Separation and Purification Technology* 2011;79(3):357-64.
- [15] Claudio AFM, Freire MG, Freire CSR, Silvestre AJD, Coutinho JAP. Extraction of vanillin using ionic-liquid-based aqueous two-phase systems. *Separation and Purification Technology* 2010;75(1):39-47.
- [16] Armand M, Endres F, MacFarlane D, Ohno H, Scrosati B. Ionic-liquid materials for the electrochemical challenges of the future. *Nature Materials* 2009;8(8):621-9.
- [17] Kuang D, Uchida S, Humphry Baker R, Zakeeruddin S, Gratzel M. Organic dye-sensitized ionic liquid based solar cells: Remarkable enhancement in performance through molecular design of indoline sensitizers. *Angewandte Chemie* 2008;47(10):1923-7.
- [18] Xu B, Wu F, Chen R, Cao G, Chen S, Yang Y. Mesoporous activated carbon fiber as electrode material for high-performance electrochemical double layer capacitors with ionic liquid electrolyte. *J.Power Sources* 2010;195(7):2118-24.
- [19] Migowski P, Dupont J. Catalytic applications of metal nanoparticles in imidazolium ionic liquids. *Chemistry* 2007;13(1):32-9.
- [20] Lu J, Yan F, Texter J. Advanced applications of ionic liquids in polymer science. *Progress in polymer science* 2009;34(5):431-48.
- [21] Fort D, Remsing R, Swatloski R, Moyna P, Moyna G, Rogers R. Can ionic liquids dissolve wood? Processing and analysis of lignocellulosic materials with 1-n-butyl-3-methylimidazolium chloride. *Green Chem.* 2007;9(1):63-9.
- [22] Ding L, He T, Xiong Y, Wu J, Chen L, Chen G. Ionic Liquids as Novel Lubricants. *hua xue jin zhan* 2010;22(2-3):298-308.

- [23] Plechkova NV, Seddon KR. Applications of ionic liquids in the chemical industry. *Chem.Soc.Rev.* 2008;37(1):123-50.
- [24] Werner S, Haumann M, Wasserscheid P. Ionic Liquids in Chemical Engineering. *Annual review of chemical and biomolecular engineering* 2010;1:203-30.
- [25] Ranke J, Stolte S, Stormann R, Arning J, Jastorff B. Design of sustainable chemical products - The example of ionic liquids. *Chem.Rev.* 2007;107(6):2183-206.
- [26] Coleman D, Gathergood N. Biodegradation studies of ionic liquids. *Chem.Soc.Rev.* 2010;39(2):600-37.
- [27] Matzke M, Stolte S, Arning U, Uebers U, Filser J. Imidazolium based ionic liquids in soils: effects of the side chain length on wheat (*Triticum aestivum*) and cress (*Lepidium sativum*) as affected by different clays and organic matter. *Green Chem.* 2008;10(5):584-91.
- [28] Mroziak W, Jungnickel C, Ciborowski T, Pitner W, Kumirska J, Kaczynski Z. Predicting mobility of alkyimidazolium ionic liquids in soils. *Journal of soils and sediments* 2009;9(3):237-45.
- [29] Jungnickel C, Mroziak W, Markiewicz M, Luczak J. Fate of Ionic Liquids in Soils and Sediments. *Current Organic Chemistry* 2011;15(12):1928-45.
- [30] Studzinska S, Kowalkowski T, Buszewski B. Study of ionic liquid cations transport in soil. *J.Hazard.Mater.* 2009;168(2-3):1542-7.
- [31] Petkovic M, Seddon K, Rebelo L, Pereira C. Ionic liquids: a pathway to environmental acceptability. *Chem.Soc.Rev.* 2011;40(3):1383-403.
- [32] Thi P, Cho C, Yun Y. Environmental fate and toxicity of ionic liquids: A review. *Water Res.* 2010;44(2):352-72.
- [33] Fernandez JF, Neumann J, Thoeming J. Regeneration, Recovery and Removal of Ionic Liquids. *Current Organic Chemistry* 2011;15(12):1992-2014.
- [34] Awad W, Gilman J, Nyden M, Harris R, Sutto T, Callahan J. Thermal degradation studies of alkyl-imidazolium salts and their application in nanocomposites. *Thermochimica acta* 2004;409(1):3-11.
- [35] Hao Y, Peng J, Hu S, Li J, Zhai M. Thermal decomposition of allyl-imidazolium-based ionic liquid studied by TGA-MS analysis and DFT calculations. *Thermochimica Acta* 2010;501(1-2):78-83.
- [36] Czerwicka M, Stolte S, Muller A, Siedlecka E, Golebiowski M, Kumirska J. Identification of ionic liquid breakdown products in an advanced oxidation system. *J.Hazard.Mater.* 2009;171(1-3):478-83.
- [37] Siedlecka E, Golebiowski M, Kaczynski Z, Czupryniak J, Ossowski T, Stepnowski P. Degradation of ionic liquids by Fenton reaction the effect of anions as counter and background ions. *Applied catalysis.B, Environmental* 2009;91(1-2):573-9.

- [38] Siedlecka E, Stepnowski P. The effect of alkyl chain length on the degradation of alkylimidazolium- and pyridinium-type ionic liquids in a Fenton-like system. *Environ.Sci.Pollut.Res.Int.* 2009;16(4):453-8.
- [39] Markiewicz M, Jungnickel C, Markowska A, Szczepaniak U, Paszkiewicz M, Hupka J. 1-Methyl-3-octylimidazolium Chloride-Sorption and Primary Biodegradation Analysis in Activated Sewage Sludge. *Molecules* 2009;14(11):4396-405.
- [40] Neumann J, Grundmann O, Thoeming J, Schulte M, Stolte S. Anaerobic biodegradability of ionic liquid cations under denitrifying conditions. *Green Chem.* 2010;12(4):620-7.
- [41] Deive F, Rodriguez A, Varela A, Rodrigues C, Leitao M, Houbraken J. Impact of ionic liquids on extreme microbial biotypes from soil. *Green Chem.* 2011;13(3):687-96.
- [42] Abrusci C, Palomar J, Pablos J, Rodriguez F, Catalina F. Efficient biodegradation of common ionic liquids by *Sphingomonas paucimobilis* bacterium. *Green Chem.* 2011;13(3):709-17.
- [43] Clare B, Sirwardana A, MacFarlane D. Synthesis, Purification and Characterization of Ionic Liquids. *Top.Curr.Chem.* 2009;290:1-40.
- [44] Palomar J, Lemus J, Gilarranz MA, Rodriguez JJ. Adsorption of ionic liquids from aqueous effluents by activated carbon. *Carbon* 2009;47(7):1846-56.
- [45] Lemus J, Palomar J, Gilarranz MA, Rodriguez JJ. Characterization of Supported Ionic Liquid Phase (SILP) materials prepared from different supports. *Adsorption-Journal of the International Adsorption Society* 2011;17(3):561-71.
- [46] Vijayaraghavan K, Pham TPT, Cho CW, Won SW, Choi SB, Juan M, et al. An Assessment on the Interaction of a Hydrophilic Ionic Liquid with Different Sorbents. *Ind Eng Chem Res* 2009;48(15):7283-8.
- [47] Ghatee M, Moosavi F. Physisorption of Hydrophobic and Hydrophilic 1-Alkyl-3-methylimidazolium Ionic Liquids on the Graphenes. *The journal of physical chemistry.C* 2011;115(13):5626-36.
- [48] Yin CY, Aroua MK, Daud WMAW. Review of modifications of activated carbon for enhancing contaminant uptakes from aqueous solutions. *Separation and Purification Technology* 2007;52(3):403-15.
- [49] Lazo-Cannata JC, Nieto-Marquez A, Jacoby A, Paredes-Doig AL, Romero A, Sun-Kou MR, et al. Adsorption of phenol and nitrophenols by carbon nanospheres: Effect of pH and ionic strength. *Separation and Purification Technology* 2011;80(2):217-24.
- [50] Deetlefs M, Seddon KR. Ionic liquids: fact and fiction. *Chimica Oggi-Chemistry Today* 2006;24(2):16.
- [51] Ranke J, Othman A, Fan P, Muller A. Explaining Ionic Liquid Water Solubility in Terms of Cation and Anion Hydrophobicity. *International journal of molecular sciences* 2009;10(3):1271-89.

-
- [52] Calvo L, Gilarranz MA, Casas JA, Mohedano AF, Rodríguez JJ. Hydrodechlorination of 4-chlorophenol in aqueous phase using Pd/AC catalysts prepared with modified active carbon supports. *Applied Catalysis B: Environmental* 2006;67(1-2):68-76.
- [53] Sing K. Adsorption methods for the characterization of porous materials. *Advances in colloid and interface science* 1998;76:3-11.
- [54] Zazo JA, Fraile AF, Rey A, Bahamonde A, Casas JA, Rodríguez JJ. Optimizing calcination temperature of Fe/activated carbon catalysts for CWPO. *Catalysis Today* 2009;143(3-4):341-6.
- [55] Langmuir I. The adsorption of gases on plane surfaces of glass, mica and platinum. *J. Am. Chem. Soc.* 1918;40:1361-403.
- [56] Frisch MJ, Trucks GW, Schlegel HB, Scuseria GE, Robb MA, Cheeseman JR, et al. *Gaussian03*, revision B.05; 2004.
- [57] COSMOtherm C2.1, release 01.06. Leverkusen, Germany: GmbH & Co. KG; 2003.
- [58] Calvo L, Gilarranz MA, Casas JA, Mohedano AF, Rodríguez JJ. Effects of support surface composition on the activity and selectivity of Pd. *Ind Eng Chem Res* 2005;44(17):6661-7.
- [59] Radovic LR. Carbon materials as adsorbents in aqueous solutions. In: Radovic LR, editor. New York: M. Dekker; 2001, p. 1-66.
- [60] Pereiro AB, Legido JL, Rodríguez A. Physical properties of ionic liquids based on 1-alkyl-3-methylimidazolium cation and hexafluorophosphate as anion and temperature dependence. *Journal of Chemical Thermodynamics* 2007;39(8):1168-75.

Supplementary material

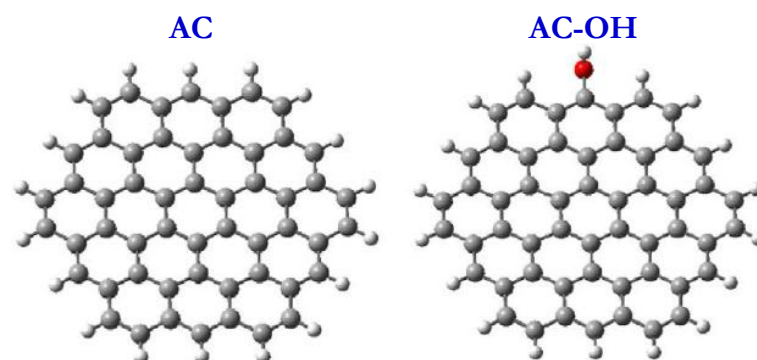


Figure 1S. Molecular model for AC used in COSMO-RS calculations.

ESSAYS ON IONIC LIQUID/ACTIVATED CARBON SYSTEMS AND THEIR APPLICATION TO POLLUTANT REMOVAL

Doctoral dissertation, [Madrid 2012](#), Jesús Lemus Torres



Paper III

ON THE KINETICS OF IONIC LIQUIDS ADSORPTION ONTO ACTIVATED CARBONS FROM AQUEOUS SOLUTION

131-155

J. Lemus, J. Palomar, M.A. Gilarranz, J.J. Rodríguez.

ON THE KINETICS OF IONIC LIQUIDS ADSORPTION ONTO
ACTIVATED CARBONS FROM AQUEOUS SOLUTION

Industrial and Engineering Chemistry Research. 2012 (Submitted)

Resumen

El tercer artículo que cierra el bloque de la adsorción de líquidos iónicos en fase acuosa se centra en el estudio de la cinética de adsorción de un líquido iónico hidrofóbico (1-metil-3-octilimidazolio hexafluorofosfato, OmimPF₆) en un carbón activo comercial (MkU). Los resultados obtenidos muestran que la cinética de adsorción del líquido iónico es destacadamente más lenta que la del fenol, usado como soluto de referencia. El efecto de diferentes condiciones de operación (agitación, tamaño de partícula, temperatura y concentración inicial del líquido iónico) se ha estudiado en la velocidad de adsorción. Se han empleado modelos cinéticos empíricos y fenomenológicos para describir los datos experimentales de adsorción con el fin de desarrollar criterios de mejora en la cinética de adsorción de líquidos iónicos sobre carbón activo. El análisis cinético indica que el mecanismo de adsorción del líquido iónico sobre el carbón está controlado por transferencia de masa en el interior de los poros. Por lo tanto, una selección adecuada del tamaño de partícula del adsorbente cobrará especial relevancia en el desarrollo de una futura aplicación en el tratamiento de adsorción de líquidos iónicos. Un incremento de la temperatura provoca un aumento significativo en la velocidad adsorción, comportamiento interesante para la eliminación/recuperación de líquidos iónicos de corrientes acuosas, a pesar de una ligera disminución en la capacidad de adsorción.

Abstract

Adsorption with activated carbons (ACs) has been recently proposed as a thermodynamically favored treatment to remove and/or recover ionic liquids (ILs) from aqueous streams. In this work, a kinetic analysis of the adsorption of a hydrophobic IL (1-methyl-3-octylimidazolium hexafluorophosphate, OmimPF₆) by commercial ACs was performed. The results indicated that adsorption kinetics is remarkably slower for the IL than for phenol, used as a reference solute. Then, the effect of main operating conditions (stirring, AC particle size, temperature and IL initial concentration) on the adsorption rate were investigated. For the purpose of developing criteria to improve the kinetics of IL adsorption with ACs, different empirical and phenomenological kinetic models were applied to describe the experimental adsorption data. The kinetic analysis indicated that the mechanism of IL adsorption onto ACs is mainly controlled by the mass transfer into the pores. Therefore, the selection of adequate particle size of the adsorbent plays a major role in the development of feasible IL adsorption. Increasing the temperature led to significantly faster adsorption, which it was found to be of interest for removing and/or recovering IL from aqueous solution in spite of the associated decrease of equilibrium capacity.

1. Introduction

During the last decade, ILs have become one of the most promising and rapidly developing areas of modern chemistry, technology and engineering, focusing on the ultimate aim of large scale industrial applications [1,2]. ILs are characterized by their exceptional properties such as negligible vapor pressure and non-flammability under ambient conditions, high thermal and chemical stability, a wide liquid window and high solvent capacity [3-5]. However, probably the most important attribute of ILs is the possibility of designing their properties by an adequate selection of the counterions. Thanks to the enormous number of cation and anion combinations, ILs can possess a wide spectrum of physical and chemical properties (solubility, polarity, viscosity, etc.) and they are already recognized by the chemical industry as new target-oriented reaction and separation media [6,7]. However, the application of ILs to industrial scale may involve an environmental risk as a result of their transport, storage, release in wastewaters, etc [8,9]. Therefore, the removal/recovery of ILs from aqueous streams has to be taken into account for a proper use of ILs in industrial processes, since it has been recently demonstrated that ILs present a wide range of toxicity and biodegradability [10-12].

Destructive and non destructive treatments for the removal of ILs from aqueous effluents have been recently investigated. The most studied destructive techniques include advanced oxidation [13,14] and biological treatments [15,16]. It is important to consider that ILs are consider still quite expensive, and their recycling after regeneration or recovery needs to be regarded [8]. Among available non destructive technologies, distillation [17], crystallization [18], nanofiltration [19], pervaporation [20,21] and adsorption onto solids [21-26] are being increasingly studied. Adsorption by activated carbons (ACs) has been recently demonstrated as an effective non-destructive technique for removing ILs from aqueous solutions and recovering them for the process [23,24]. ACs are interesting candidates among other adsorbents [27] due to their high surface area, surface chemistry tailoring, harmfulness to the environment and easy handling in operation [28]. Previous adsorption equilibrium analysis by our group [23,24] showed that the structural properties and chemical surface of the AC can be conveniently modified to adsorb efficiently ILs with different structures, indicating the viability of IL adsorption from a thermodynamic point of view. However, the kinetic aspects have been not discussed in our previous works and it is necessary to know them for design purposes. Several empirical and phenomenological kinetic models have been applied to describe the adsorption rate of organic solutes onto different adsorbents [29-31], as they can

provide insight in the adsorption mechanisms for further design of adsorption systems. A recent study by Duclaux *et al.* [25], focused on the adsorption of hydrophilic ILs by ACs, showed that not only thermodynamics but also kinetics of ILs adsorption were dependent on the properties of the AC adsorbent, suggesting the need of checking different kinetic models according to the ACs used [25].

In this work, a detailed kinetic analysis of the adsorption of a hydrophobic IL (1-octyl-3-methylimidazolium hexafluorophosphate, OmimPF₆) from water onto different commercial ACs has been performed from the adsorption kinetic curves obtained in batch stirred tank at different operating conditions. Firstly, the kinetics of IL (OmimPF₆) adsorption was compared to that of a reference organic solute (phenol). Secondly, a systematic screening of different kinetic models, developed for organic solutes, was performed to better describe the IL adsorption rate onto AC. Those models included pseudo-first order, second order, Lagergren and intra-particle diffusion [32-34]. The operating variables whose influence in the adsorption kinetics and thermodynamics of OmimPF₆ onto commercial AC was evaluated were stirring velocity (200 to 700 rpm), AC particle size (100 to 2000 μm), initial concentration of OmimPF₆ (0.1 to 3.2 mmol·L⁻¹) and temperature (35 to 75 °C). Summarizing, the kinetic analysis performed provides insights on the optimization of the operating conditions for the adsorption of ILs by ACs, useful for the design of viable systems for the removal and recovery of ILs from industrial aqueous streams.

2. Procedure

2.1. Materials and characterizations

Three commercial ACs were tested in this study, supplied by Merck (MkU), Norit (CAP) and Timcal (ENA). The ACs were sieved to different ranges of particle size (d_p : 2000-1000 μm; 1000-500 μm; 500-300 μm; 300-100 μm; and $d_p < 100$ μm). The commercial ACs were subjected to thermal treatment in order to remove surface oxygen groups thus reducing their differences in surface chemical composition. The thermal treatment of the ACs was accomplished in a quartz horizontal tube furnace (2.5 cm i.d. and 15 cm length) under a nitrogen flow of 60 mL·min⁻¹ at 900 °C. This temperature was reached at a 100 °C·min⁻¹ rate and maintained for 3 hours.

The porous structure of the adsorbents was characterized by means of 77 K N₂ adsorption–desorption using a Micromeritics apparatus (Tristar II 3020 model). Previous to N₂ adsorption the samples were outgassed at 150 °C for 8 h under a constant flow of N₂ at atmospheric pressure. The BET equation was used to obtain the surface area (A_{BET}) and the Dubinin–Radushkevich equation was applied for micropore volume calculation. The difference between the volume of N₂ adsorbed at 0.95 relative pressure and the micropore volume was taken as mesopore volume.

The amount of surface oxygen groups of the ACs was determined by temperature programmed desorption (TPD), heating 0.1 g of the AC sample up to 1100 °C in a vertical quartz tube under continuous N₂ flow of 1 NL·min⁻¹ at a heating rate of 10 °C·min⁻¹. The evolved amounts of CO and CO₂ were analyzed by means of a non-dispersive infrared absorption analyzer (Siemens, model Ultramat 22). The CO and CO₂ TPD profiles were deconvoluted using PeakFit 4.12 software, selecting a multiple Gaussian function to fit each deconvolution peak of the TPD profile [35]. The characterization of fresh and heat-treated ACs is depicted in Table 1.

OmimPF₆ and phenol were used as adsorptive solutes and were not purified prior to use (purity of 99%). They were supplied by Iolitec and Sigma-Aldrich, respectively. Distilled water was employed for preparing all the solutions.

Table 1. Characterization of the fresh and modified ACs.

	A (m ² ·g ⁻¹); V (cm ³ ·g ⁻¹)				Groups evolved as CO ₂ (μmol·g ⁻¹)					Groups evolved as CO (μmol·g ⁻¹)				
	A_{BET}	A_{s}	$V_{\text{microp.}}$	$V_{\text{mesop.}}$	Carboxylic acids	Anhydrides	Lactones	Pirones	Total	Anhydrides	Phenols	Carbonyl	Chromenes	Total
MkU	927	155	0.36	0.22	63	20	39	61	183	50	74	315	51	490
Mk-900	906	102	0.36	0.23	38	28	19	28	113	48	57	69	149	323
ENA3	912	350	0.40	0.40	14	16	38	40	108	6	17	68	25	116
ENA3-900	901	339	0.34	0.40	12	14	24	23	73	4	11	65	19	99
CAP	1915	667	0.66	0.63	103	109	816	176	1204	454	508	556	345	1863
CAP-900	1434	346	0.51	0.42	80	61	54	33	228	46	123	78	< 1	247

2.2. Batch mode adsorption studies

The effect of adsorbent particle size (300–1000 μm), initial OmimPF₆ concentration (0.1 to 3.2 $\text{mmol}\cdot\text{L}^{-1}$) and temperature (35–75 °C) on the adsorption kinetic and the equilibrium was studied with MkU in batch stirred tank runs. For the kinetic tests, 50 mL of OmimPF₆ aqueous solution of predetermined initial concentration was placed in stoppered flasks together with AC (1 $\text{g}\cdot\text{L}^{-1}$). The flasks were stirred at 200 rpm equivalent stirring rate in a thermostated rotary shaker (Julabo Shake Temp, model SW-22) for contact times between 0 and 400 min. The equilibrium adsorption tests were also carried at 200 rpm and 35 °C. Ionic liquid solutions were prepared with concentrations from 0 to 3.2 $\text{mmol}\cdot\text{L}^{-1}$ of IL in distilled water. Samples of 50 mL of IL solutions were placed in contact with 12.5 mg of AC. An equilibration time of 5 days was given to all the samples.

The study of the influence of stirring rate was carried out in a 1L jacketed glass reactor coupled with a laboratory stirrer. 500 mL of 3.2 $\text{mmol}\cdot\text{g}^{-1}$ OmimPF₆ solution was placed into the reactor together with the AC (1 $\text{g}\cdot\text{L}^{-1}$) at 35 °C. Samples were collected at regular contact times.

OmimPF₆ and phenol concentration in water was determined by UV spectroscopy (Varian, model Cary 1E) at 212 and 271 nm respectively, which were the maximum of absorption spectra measured for these compounds.

2.3. Adsorption kinetic models

Table 2 summarizes the five kinetic models checked in this work to describe the adsorbate concentration onto the adsorbent (q_t , $\text{mmol}\cdot\text{g}^{-1}$) as a function of the contact time (t , min). The experimental q_t values were obtained as indicated above using the MkU activated carbon as adsorbent. The hyperbolic model (eq. III.1) [36] is a simple mathematical equation widely used to fit kinetic experimental data in terms of the empirical coefficients q_e ($\text{mmol}\cdot\text{g}^{-1}$) and k_f (min). The parameter q_e is the asymptotic value of q_t and is commonly used as a reference of maximum uptake of solute onto the adsorbent. The pseudo first-order equation (eq. III.2) for the liquid-solid adsorption is an empirical kinetic model proposed in the Lagergren's original paper [37], which provides a pseudo-first order rate constant k_f (min^{-1}) by defining the driving force for the process as $(q_e - q_t)$. Pseudo-second-order (eq. III.3) and

Lagergren (eq. III.4) models [38,39] are modifications of the pseudo-first order equation by defining the driving adsorption forces as $(q_e - q_t)^2$ and $(q_e - q_t)^n$, respectively, providing the apparent rate constants k_2 and k_s ($\text{g}\cdot\text{mol}^{-1}\cdot\text{min}^{-1}$) for the adsorption process. In these last three simple models all the steps of adsorption such as external diffusion, internal diffusion, and adsorption are lumped together in the corresponding rate constants and it is assumed that the difference between the average and the equilibrium solid phase concentrations is the driving force for adsorption. On the other hand, the intraparticle diffusion model [40] is a phenomenological kinetic model assuming that adsorbate transport through the adsorbent particle is the prevailing rate-controlling step in the adsorption process, which is often the case, especially in a well stirred batch systems [30,41-43]. The parameter k_{id} ($\mu\text{mol}\cdot\text{g}^{-1}\cdot\text{min}^{-0.5}$) is defined as the pore diffusion rate constant, whereas the intercept I is a constant related with the thickness of boundary layer.

Table 2. Kinetic models checked.

Model	Equation		Adjustable parameters	Ref.
<i>Hyperbolic</i>	$q_t = \frac{q_e \cdot t}{k_f + t}$	eq. III.1	q_e ($\text{mmol}\cdot\text{g}^{-1}$), k_f (min)	[37]
<i>Pseudo first-order</i>	$\log(q_e - q_t) = \log q_e - \frac{k_1}{2.303} t$	eq. III.2	k_1 (min^{-1})	[38]
<i>Pseudo second-order</i>	$\frac{t}{q_t} = \frac{1}{k_2 q_e^2} + \frac{t}{q_e}$	eq. III.3	k_2 ($\text{g}\cdot\text{mol}^{-1}\cdot\text{min}^{-1}$)	[39]
<i>Lagergren</i>	$\frac{t}{q_t} = \frac{1}{k_s q_e^n} + \frac{t}{q_e}$	eq. III.4	k_s ($\text{g}\cdot\text{mol}^{-1}\cdot\text{min}^{-1}$), n	[40]
<i>Intraparticle diffusion</i>	$q_t = k_{id} t^{1/2} + I$	eq. III.5	k_{id} ($\text{mmol}\cdot\text{g}^{-1}\cdot\text{min}^{-1}$), I ($\text{mmol}\cdot\text{g}^{-1}$)	[41]

3. Results and discussion

3.1. Comparison of the adsorption kinetics of OmimPF₆ and phenol

Table 2 compares the physical properties of OmimPF₆ and phenol of interest for adsorption [44,45]. As can be seen, OmimPF₆ presents much higher viscosity and molecular volume than phenol. These characteristics anticipate lower rates of physical adsorption with ACs for OmimPF₆. Figure 1 shows the adsorption kinetic curves of phenol (1A) and OmimPF₆ (1B) with commercial activated carbon MkU. In spite of the fact that equilibrium experiments revealed similar adsorption equilibrium capacity (1.32 and 1.68 mmol·g⁻¹ for OmimPF₆ and phenol, respectively) of MkU for both solutes at equivalent aqueous phase concentration, important differences were found regarding the kinetic behavior of these solutes. Thus, while an uptake of 1 mmol·g⁻¹ of phenol was achieved at 10 minutes, to obtain equivalent adsorption of OmimPF₆ took around 300 minutes. Therefore, the adsorption rate of a common IL, as OmimPF₆, onto AC seems to be significantly lower than that of conventional low molecular weight organic solutes. Thus, the following will be focused on analyzing the effects of operating conditions on the rate of IL adsorption by ACs.

Table 3. Physical properties of OmimPF₆ and phenol of interest for adsorption.

	Density (g·cm ⁻³) ^a	Viscosity (mPa·s ⁻¹) ^a	M _{volume} (Å ³) ^a	M _{weight} (g·mol ⁻¹)	Surface tension (mN·m ⁻¹)	Parachor (cm ³ ·mN ^{1/4} ·mol ⁻¹ ·m ^{-1/4})
OmimPF₆	1.19	85.7	457	340.3	34.9 [45]	694.2
Phenol	1.07	10.0	121	94.1	39.3 ^b [46]	220.2

^a Density, viscosity and molecular volume obtained from COSMO-RS (Computational details available in Supporting Information); ^b T = 40 °C

Figure 1. Experimental curves for the adsorption kinetics of OmimPF₆ (A) and phenol (B) onto MkU (d_p : 1000 - 2000 μm , 1000 $\text{mg}\cdot\text{L}^{-1}$ initial IL concentration, 200 rpm, 35 °C).

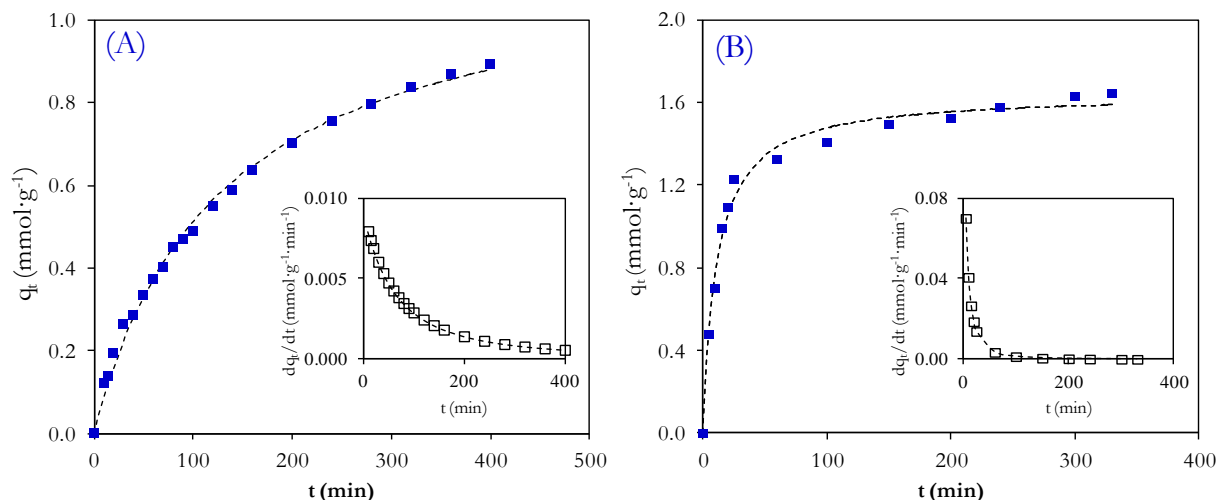


Figure 1 shows the kinetic curves obtained for the adsorption of OmimPF₆ and phenol, with the activated carbon MkU. Table 4 summarizes the values of the fitting parameters for the five kinetic models checked. Reasonably to frankly good correlation coefficients (R^2) were obtained for all the kinetic models evaluated. All of them serve to describe fairly well the experimental data (see Figure S1 in Supplementary material). The models fulfill the statistical criteria since the confidence interval for their parameters do not include the zero value. Statistical analysis shows that Lagergren model provides the best description of kinetic curves for OmimPF₆ solute, with R^2 value of 0.997 and by far the lowest value of mean standard deviation ($\text{RMSD} = 0.6\%$). Remarkably, the apparent kinetic constant (k_s) obtained by Lagergren model indicates six-fold lower adsorption rates for IL adsorption than for phenol. Although these four empirical simple kinetic models satisfactorily reproduced the experimental data of Figure 1, they do not provide mechanistic information on the adsorption process. Typically, various phenomena can control the adsorption rate, the most limiting being related with diffusion, including external, boundary layer and intraparticle diffusion. A phenomenological intraparticle diffusion model (Eq. 6 in Table 2) was also checked to analyze the measured kinetic behavior of IL adsorption onto AC. Figure 2 depicts the experimental and calculated values of q_t vs $t^{1/2}$ for IL and phenol adsorption (see the fitting values of k_{id} and I together with the statistical parameters in Table 4). As can be seen, the adsorption curve for phenol shows two regions, being the first linear part ($0 < t < 5$ min) attributed to intraparticle diffusion and the second plateau-like branch to the equilibrium-approaching stage. In contrast, OmimPF₆ presents a wider time range for the linear part ($0 < t$

< 225 min). These results, together with the negligible I value (0.01), the high correlation coefficient ($R^2 = 0.996$) and the low SD (0.02) and $RMSD$ (6.6 %) values, indicate that intraparticle diffusion may be the rate-controlling step during the first stage of adsorption of the hydrophobic IL OmimPF₆ onto MkU, which is a common situation in the adsorption of organic compounds by ACs [46,47].

Table 4. Thermodynamic and kinetic analysis for the adsorption of OmimPF₆ and phenol onto MkU (d_p : 1000 - 2000 μm , 1000 $\text{mg}\cdot\text{L}^{-1}$ initial IL concentration, 200 rpm, 35 °C).

	<i>Equilibrium capacity</i>		<i>Kinetic analysis Hyperbolic model</i>			
	q_s	q_e	k_f	R^2	SD	$RMSD$ (%)
OmimPF₆	1.32	1.26 ± 0.03	125.4 ± 6.2	0.995	0.02	9.1
Phenol	1.68	1.64 ± 0.03	11.1 ± 0.9	0.988	0.04	5.2

q_s ($\text{mmol}\cdot\text{g}^{-1}$); q_e ($\text{mmol}\cdot\text{g}^{-1}$); k_f (min)

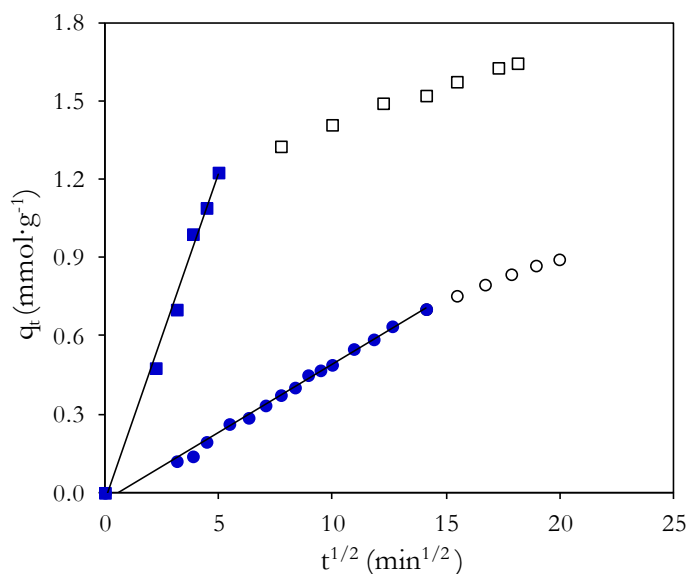
	<i>Kinetic analysis</i>							
	<i>1st order model</i>				<i>2nd order model</i>			
	k_1	R^2	SD	$RMSD$ (%)	k_2	R^2	SD	$RMSD$ (%)
OmimPF₆	3.68 ± 0.11	0.984	0.02	34.2	8.6 ± 0.2	0.988	8.5	6.0
Phenol	54.3 ± 2.3	0.992	0.20	21.2	42.7 ± 0.1	0.999	2.8	6.9

k_1 ($10^3\cdot\text{min}^{-1}$); k_2 ($\text{g}\cdot\text{mol}^{-1}\cdot\text{min}^{-1}$)

	<i>Kinetic analysis</i>									
	<i>Lagergren model</i>					<i>Intra-particle diffusion</i>				
	n	k_s	R^2	SD	$RMSD$ (%)	I	k_{id}	R^2	SD	$RMSD$ (%)
OmimPF₆	2.1	7.1 ± 0.2	0.997	0.02	0.6	-0.03 ± 0.01	52.4 ± 1.0	0.996	0.02	6.6
Phenol	2.1	54.0 ± 10.7	0.968	0.08	6.3	-0.03 ± 0.04	250.6 ± 12.2	0.991	0.05	6.3

k_s ($\text{g}\cdot\text{mol}^{-1}\cdot\text{min}^{-1}$); I ($\text{mmol}\cdot\text{g}^{-1}$); k_{id} ($\text{mmol}\cdot\text{g}^{-1}\cdot\text{min}^{-0.5}$)

Figure 2. Fitting of the intraparticle diffusion model for the adsorption of phenol (■, □) and OmimPF₆ (●, ○) onto MkU (d_p : 1000 - 2000 μm , 1000 $\text{mg}\cdot\text{L}^{-1}$, 200 rpm, 35 °C).



3.2. Effect of operating conditions on the kinetic of OmimPF₆ adsorption

In this work, the effect of main operating conditions (stirring velocity, AC particle size, temperature and IL initial concentration) on the adsorption rate of hydrophobic IL (OmimPF₆) onto commercial activated carbon MkU were investigated. It was found that the intraparticle diffusion model (Eq. III.6 in Table 2) enables a satisfactory reproduction of the experimental adsorption curves of OmimPF₆ onto MkU for the whole range of operating conditions tested (see the values of the statistical parameters R^2 , SD and $RMSD$ in Table 5 and the predicted kinetic data in Figure S2 in Supplementary material).

Table 5. Equilibrium capacity and kinetic analysis for the adsorption of OmimPF₆ onto commercial MkU at different operating conditions (200 rpm, d_p : 500-1000 μm , 3.2 $\text{mmol}\cdot\text{L}^{-1}$ initial concentration, 35 $^\circ\text{C}$).

	Operating conditions	Equilibrium analysis	Kinetic analysis				
			Intra-particle diffusion				
	Shaking (rpm)	q_s	I	k_{id}	R^2	SD	$RSMD$ (%)
1	700	1.29	0.07 ± 0.06	134.6 ± 13.2	0.954	0.08	8.8
2	500	1.33	0.05 ± 0.06	133.8 ± 14.8	0.953	0.06	8.8
3	300	1.31	0.05 ± 0.05	135.1 ± 14.4	0.955	0.07	8.0
Particle diameter (μm)							
4	$2000 < d_p < 1000$	1.30	-0.03 ± 0.01	52.4 ± 1.0	0.995	0.01	6.6
5	$1000 < d_p < 500$	1.32	-0.08 ± 0.03	87.6 ± 4.7	0.977	0.04	4.7
6	$500 < d_p < 300$	1.33	0.05 ± 0.16	134.9 ± 7.4	0.985	0.04	5.8
7	$300 < d_p < 100$	1.35	0.06 ± 0.01	280.6 ± 60.1	0.955	0.17	12.8
C_{initial} ($\text{mmol}\cdot\text{L}^{-1}$)							
8	0.10	0.68	0.00 ± 0.00	6.2 ± 0.2	0.994	0.002	3.8
9	0.57	1.00	-0.02 ± 0.01	23.9 ± 1.1	0.984	0.01	6.2
10	1.55	1.18	-0.04 ± 0.02	40.1 ± 2.4	0.976	0.03	12.1
11	2.18	1.25	-0.01 ± 0.01	65.7 ± 1.3	0.997	0.01	4.4
12	3.20	1.32	-0.08 ± 0.03	87.6 ± 4.7	0.977	0.04	4.7
Temperature ($^\circ\text{C}$)							
13	35	1.32	-0.08 ± 0.01	87.6 ± 0.01	0.977	0.04	4.7
14	55	1.25	-0.02 ± 0.01	90.7 ± 0.01	0.990	0.03	4.9
15	75	1.21	0.05 ± 0.01	120 ± 12.2	0.966	0.05	9.2

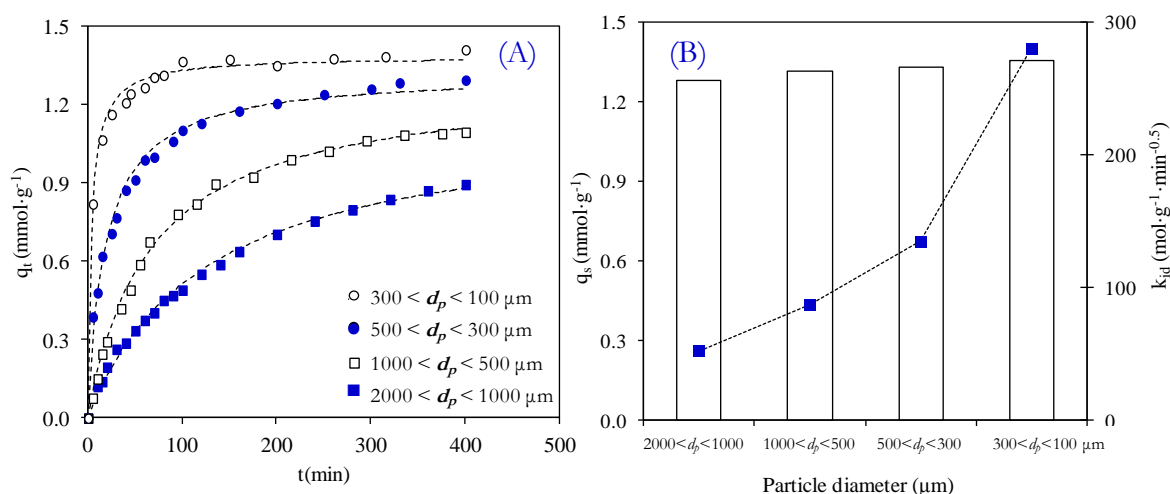
q_s ($\text{mmol}\cdot\text{g}^{-1}$); I ($\text{mmol}\cdot\text{g}^{-1}$); k_{id} ($\mu\text{mol}\cdot\text{g}^{-1}\cdot\text{min}^{-0.5}$)

The effect of stirring velocity was tested within the range of 300-700 rpm using the commercial MkU with 500-1000 μm particle size, at 3.2 $\text{mmol}\cdot\text{L}^{-1}$ (1000 $\text{mg}\cdot\text{L}^{-1}$) of IL initial concentration and 35 $^\circ\text{C}$. No significant differences were observed (see Table 5 and Figure S3 in Supplementary material), indicating that external mass transfer does not have a significant influence on the adsorption kinetics of OmimPF₆ under the operating conditions used. The adsorption capacity at equilibrium at these operating conditions was around 1.3 $\text{mmol}\cdot\text{g}^{-1}$.

Figure 3 shows the results obtained at different particle sizes of MkU. As can be seen, the rate adsorption of OmimPF₆ clearly increases when decreasing the AC particle size, whereas the equilibrium capacity remains almost constant. The intraparticle diffusion model provides an adequate description of these experimental results (see the low I , SD and $RSMD$ and the good R^2 values summarized in Table 5). The values obtained for the pore diffusion

rate constant (k_{id}) shifted from $52.4 \mu\text{mol}\cdot\text{g}^{-1}\cdot\text{min}^{-0.5}$ for d_p : 2000-1000 μm to $280.6 \mu\text{mol}\cdot\text{g}^{-1}\cdot\text{min}^{-0.5}$ for d_p : 300-100 μm particle size (Figure 3). These results strongly support the conclusion that intraparticle diffusion is the step controlling the rate of adsorption of OmimPF₆ onto AC as it occurs in general with organic solutes, most in particular those of high molecular size [48,49]. The effect of particle size on the adsorption kinetics was much lower in the case of phenol (see Figure S4 in Supplementary material).

Figure 3. Effect of the particle size on the kinetics of adsorption of OmimPF₆ onto MkU at different particle size (200 rpm; $3.2 \text{ mmol}\cdot\text{L}^{-1}$ initial IL concentration; 35 °C).



The influence of the initial IL concentration ($0.1\text{--}3.2 \text{ mmol}\cdot\text{L}^{-1}$) on the adsorption onto MkU is shown in Figure 4 and summarized in Table 5. As can be seen, the values of k_{id} increase substantially with the particle size. Increasing the initial concentration provokes a higher driving force giving rise to a faster adsorption in agreement with the commonly observed with conventional organic solutes [50,51]. Thanks to this higher driving force the plateau of the kinetic curves is reached at equivalent contact time regardless the initial IL concentration. The equilibrium capacity (q_s) increases by two-fold within the range of initial IL concentration tested.

Figure 4. Effect of the initial concentration of OmimPF₆ on the kinetics of adsorption onto MkU (200 rpm, d_p : 500 - 1000 μm , 35 °C).

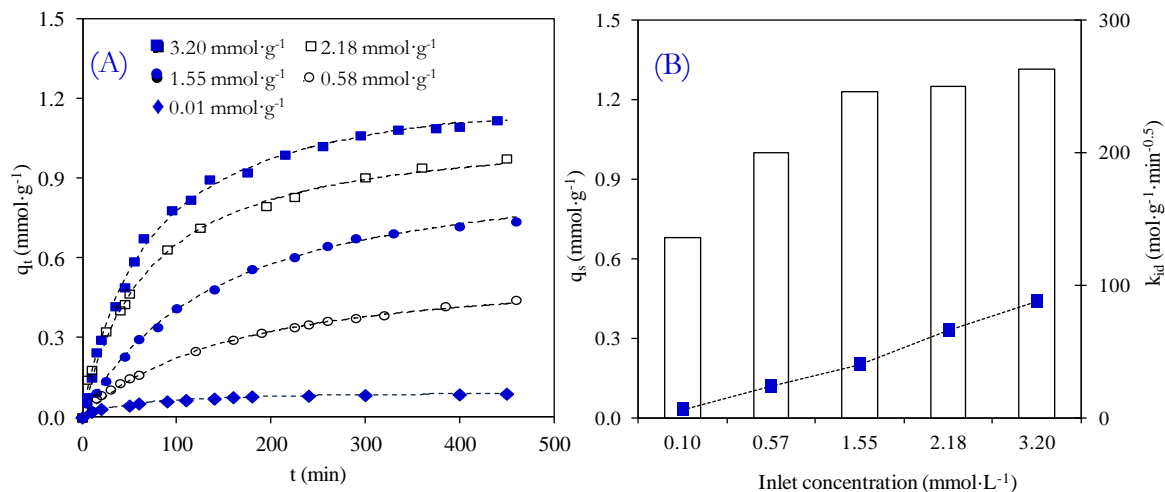
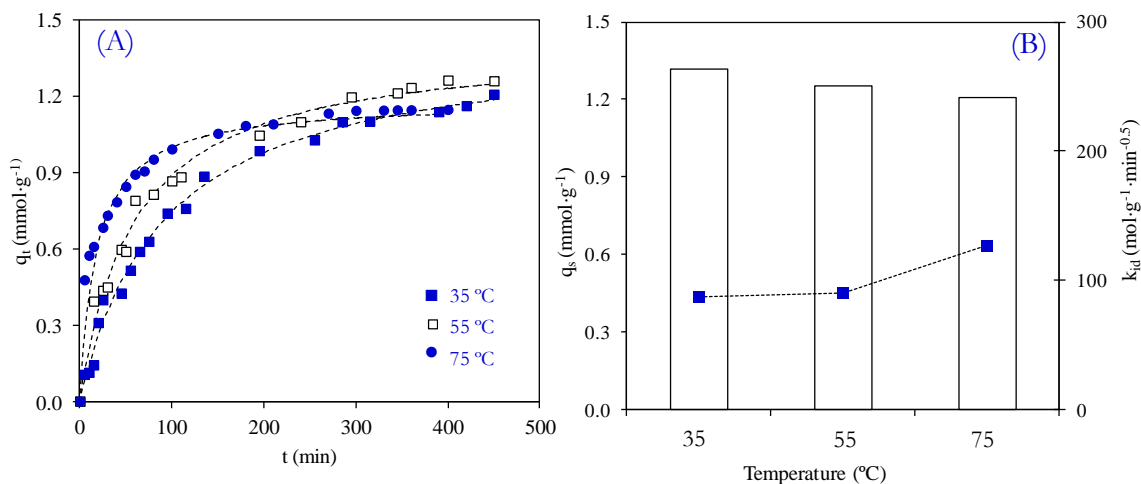


Figure 5 shows the effect of temperature on the adsorption of OmimPF₆ on MkU within the range of 35-75 °C. The values of adsorption rate constant, k_{id} , obtained from the intraparticle diffusion model increased with temperature from 88 $\mu\text{mol}\cdot\text{g}^{-1}\cdot\text{min}^{-0.5}$ (35 °C) to 120 $\mu\text{mol}\cdot\text{g}^{-1}\cdot\text{min}^{-0.5}$ (75 °C), (Table 5). On the other hand, the equilibrium capacity (q_s) is higher at lower temperature as expected in physical adsorption [52-54]. From a technical point of view, in spite of the lower equilibrium capacity working at higher temperature has the advantage of a faster adsorption. Thus q_t values c.a. 1 mmol·g⁻¹ are reached in around 150 min at 75 °C, whereas contact times higher than 300 min are needed to achieve such capacity at 35 °C. For long contact times a higher capacity is obtained at lower temperature, but this would not be justified by the high contact time that would be required. The apparent activation energy for the adsorption of OmimPF₆ onto MkU can be estimated assuming an Arrhenius type dependence of the intraparticle diffusion rate constant with temperature. A value of 8.8 kJ·mol⁻¹ was obtained consistent with a mechanism of physical adsorption controlled by intraparticle diffusion [47,54,55].

Figure 5. Effect of temperature on the adsorption of OmimPF₆ onto MkU (200 rpm; d_p : 500 - 1000 μm ; $3.2 \text{ mmol}\cdot\text{L}^{-1}$ initial concentration).



3.3. Adsorption of OmimPF₆ onto modified activated carbons

A recent study by our group [24] showed that the uptake of hydrophobic ILs from water by adsorption can be increased by selecting ACs with: i) high surface area; ii) high content of accessible pores narrower than 8 nm; and iii) low concentration of oxygen surface groups on the carbon surface. In the current work the effect of the adsorbent characteristics on the kinetics of adsorption of OmimPF₆ from aqueous phase has been analyzed. For this purpose, three commercial ACs (MkU, CAP and ENA) were subjected to thermal treatment in order to reduce their oxygenated surface groups content, giving rise to Mk-900, CAP-900 and ENA-900. The set of ACs prepared were compared at equivalent small particle size ($d_p < 100 \mu\text{m}$). The characterization of the fresh and heat-treated ACs is summarized in Table 1. The 77 K N₂ adsorption-desorption isotherms (included as Supplementary material, Figure S5) showed that the thermal treatment does not affect significantly to the porous structure of MkU and ENA, whereas has a much more marked effect in the case of CAP. As expected, the results from deconvolution of the TPD curves (Figure S6 of Supplementary material) showed a significant decrease in the amount of surface oxygen groups of the heat-treated carbons (see Table 1) [56].

Figure 6 shows the experimental kinetic curves for the adsorption of OmimPF₆ onto the fresh and modified ACs with small particle size ($d_{pore} < 100 \mu\text{m}$). These results were well described by the intraparticle diffusion model (see R^2 , SD and $RMSD$ in Table 6). High values of the pore diffusion rate constant ($k_{id} > 350 \mu\text{mol}\cdot\text{g}^{-1}\cdot\text{min}^{-0.5}$) were obtained in all cases. The fresh MkU and ENA gave quite similar k_{id} values and their thermal treatment had only a small effect on the adsorption rate of OmimPF₆. On the opposite, frankly important differences were observed in the case of CAP where the adsorption rate constant decreased by 35% upon thermal treatment. In addition to this, the high value of the I parameter may suggest that intraparticle diffusion is not the rate-controlling step for the fresh CAP, probably due to its high external area. CAP-900 shows a much lower external area and a lower value of the I parameter. On the other, the equilibrium capacity (q_s) for the adsorption of the hydrophobic IL OmimPF₆ onto ACs is mainly determined by the surface area and the volume of pore $< 8 \text{ nm}$ of the adsorbent [25]; as consequence q_s value decreases in all cases upon thermal treatment of the ACs, being that effect much more accused in the case of CAP according to the remarkably decrease of A_{BET} and $V_{\text{microp.}}$ for the treated CAP-900 sample.

Figure 6. Experimental curves for the adsorption kinetics of OmimPF₆ onto the fresh (solid symbols) and heat-treated (open symbols) activated carbons ($d_p < 100 \mu\text{m}$; $1.6 \text{ mmol}\cdot\text{L}^{-1}$ initial concentration; 200 rpm; 35 °C).

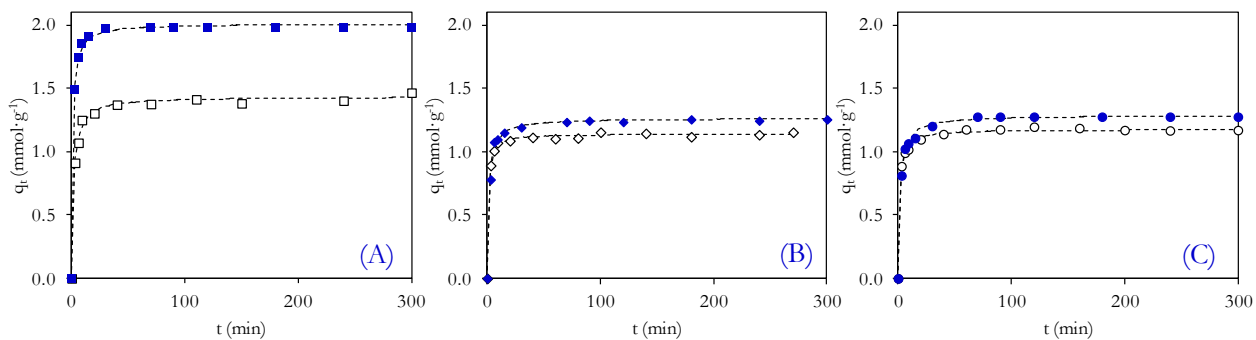


Table 6. Equilibrium capacity and kinetic analysis for the adsorption of OmimPF₆ onto fresh and heat-treated activated carbons (200 rpm, $d_p < 100\mu\text{m}$, $1.6\text{ mmol}\cdot\text{L}^{-1}$ initial concentration, 35 °C).

<i>AC</i>	<i>Equilibrium analysis</i>		<i>Kinetic analysis</i>			
	<i>q_s</i>	<i>I</i>	<i>Intra-particle diffusion</i>			
	<i>q_s</i>	<i>I</i>	<i>k_{id}</i>	<i>R²</i>	<i>SD</i>	<i>RSMD (%)</i>
MkU	1.34	0.06 ± 0.11	372 ± 54	0.959	0.1	10.3
Mk-900	1.30	0.08 ± 0.16	356 ± 77	0.914	0.2	14.4
ENA3	1.58	0.04 ± 0.05	387 ± 49	0.968	0.1	8.8
ENA3-900	1.41	0.08 ± 0.15	370 ± 70	0.933	0.2	12.9
CAP	3.04	0.12 ± 0.23	643 ± 107	0.947	0.2	11.7
CAP-900	1.65	0.05 ± 0.10	421 ± 49	0.974	0.1	8.8

q_s (mmol·g⁻¹); *I* (mmol·g⁻¹); *k_{id}* (μmol·g⁻¹·min^{-0.5})

4. Conclusions

A detailed kinetic study on the adsorption of the hydrophobic ionic liquid 1-methyl-3-octylimidazolium hexafluorophosphate (OmimPF₆) onto three commercial and modified activated carbons from water solution has been carried out, including the analysis of the influence of main operating conditions as stirring velocity, adsorbent particle size, temperature and solute initial concentration. The results showed relatively slow adsorption of OmimPF₆ respect to a benchmark organic solute as phenol. Different kinetic models have been tested to describe the measured curves of IL onto AC. Experimental and theoretical evidences indicated that intraparticle diffusion is the prevailing rate-controlling step in the adsorption mechanism of the OmimPF₆ onto AC. As a result, it is obtained for a variety of ACs with different porous structure and chemical surface that the adsorption rate of the IL can be efficiently enhanced by decreasing the adsorbent particle size. The new insights on the knowledge of IL adsorption by ACs indicated the viability of this treatment at larger scale for removal/recovery of IL from industrial wastewaters.

References

- [1] Plechkova NV, Seddon KR. Applications of ionic liquids in the chemical industry. *Chem.Soc.Rev.* 2008;37(1):123-50.
- [2] Wasserscheid P, Welton T. *Ionic liquids in synthesis*. Weinheim: Wiley-VCH; 2008.
- [3] Ranke J, Stolte S, Stormann R, Arning J, Jastorff B. Design of sustainable chemical products - The example of ionic liquids. *Chem.Rev.* 2007;107(6):2183-206.
- [4] Kokorin A. *Ionic Liquids: Theory, Properties, New Approaches*. Rijeka, Croatia: Alexander Kokorin; 2011.
- [5] Brennecke JF, Maginn EJ. Ionic liquids: Innovative fluids for chemical processing. *AICHE J.* 2001;47(11):2384-9.
- [6] Huang J, Riisager A, Berg RW, Fehrmann R. Tuning ionic liquids for high gas solubility and reversible gas sorption. *Journal of Molecular Catalysis A-Chemical* 2008;279(2):170-6.
- [7] Gardas RL, Coutinho JAP. A group contribution method for viscosity estimation of ionic liquids. *Fluid Phase Equilib.* 2008;266(1-2):195-201.
- [8] Fernandez JF, Neumann J, Thoeming J. Regeneration, Recovery and Removal of Ionic Liquids. *Current Organic Chemistry* 2011;15(12):1992-2014.
- [9] Petkovic M, Seddon K, Rebelo L, Pereira C. Ionic liquids: a pathway to environmental acceptability. *Chem.Soc.Rev.* 2011;40(3):1383-403.
- [10] Zhao DB, Liao YC, Zhang ZD. Toxicity of ionic liquids. *Clean-Soil Air Water* 2007;35(1):42-8.
- [11] Torrecilla JS, Palomar J, Lemus J, Rodriguez F. A quantum-chemical-based guide to analyze/quantify the cytotoxicity of ionic liquids. *Green Chem.* 2010;12(1):123-34.
- [12] Coleman D, Gathergood N. Biodegradation studies of ionic liquids. *Chem.Soc.Rev.* 2010;39(2):600-37.
- [13] Stepnowski P, Zaleska A. Comparison of different advanced oxidation processes for the degradation of room temperature ionic liquids. *Journal of Photochemistry and Photobiology A-Chemistry* 2005;170(1):45-50.
- [14] Czerwicka M, Stolte S, Muller A, Siedlecka E, Golebiowski M, Kumirska J. Identification of ionic liquid breakdown products in an advanced oxidation system. *J.Hazard.Mater.* 2009;171(1-3):478-83.
- [15] Stolte S, Arning J, Thoeming J. Biodegradability of Ionic Liquids - Test Procedures and Structural Design. *Chemie Ingenieur Technik* 2011;83(9):1454-67.

-
- [16] Abrusci C, Palomar J, Pablos J, Rodriguez F, Catalina F. Efficient biodegradation of common ionic liquids by *Sphingomonas paucimobilis* bacterium. *Green Chem.* 2011;13(3):709-17.
- [17] Meindersma GW, de Haan AB. Conceptual process design for aromatic/aliphatic separation with ionic liquids. *Chemical Engineering Research & Design* 2008;86(7A):745-52.
- [18] Nockemann P, Binnemans K, Driesen K. Purification of imidazolium ionic liquids for spectroscopic applications. *Chemical Physics Letters* 2005;415(1-3):131-6.
- [19] Krockel J, Kragl U. Nanofiltration for the separation of nonvolatile products from solutions containing ionic liquids. *Chem.Eng.Technol.* 2003;26(11):1166-8.
- [20] Schafer T, Rodrigues CM, Afonso CAM, Crespo JG. Selective recovery of solutes from ionic liquids by pervaporation - a novel approach for purification and green processing. *Chemical Communications* 200;1(17):1622-3.
- [21] Mahmoud M, Al Bishri H. Supported hydrophobic ionic liquid on nano-silica for adsorption of lead. *Chem.Eng.J.* 2011;166(1):157-67.
- [22] Anthony JL, Maginn EJ, Brennecke JF. Solution thermodynamics of imidazolium-based ionic liquids and water. *J Phys Chem B* 2001;105(44):10942-9.
- [23] Palomar J, Lemus J, Gilarranz MA, Rodriguez JJ. Adsorption of ionic liquids from aqueous effluents by activated carbon. *Carbon* 2009;47(7):1846-56.
- [24] Lemus J, Palomar J, Heras F, Gilarranz MA, Rodriguez JJ. Developing criteria for the recovery of ionic liquids from aqueous phase by adsorption with activated carbon. *Separation and Purification Technology* 2012;97:11-7.
- [25] Farooq A, Reinert L, Levêque J, Papaiconomou N, Irfan N, Duclaux L. Adsorption of ionic liquids onto activated carbons: Effect of pH and temperature. *Microporous and Mesoporous Materials* 2012;158(0):55-63.
- [26] Lemus J, Palomar J, Gilarranz MA, Rodriguez JJ. Characterization of Supported Ionic Liquid Phase (SILP) materials prepared from different supports. *Adsorption-Journal of the International Adsorption Society* 2011;17(3):561-71.
- [27] Bansal R, Goyal M. *Activated carbon adsorption*. Florida: Taylor and Francis; 2005.
- [28] Yin CY, Aroua MK, Daud WMAW. Review of modifications of activated carbon for enhancing contaminant uptakes from aqueous solutions. *Separation and Purification Technology* 2007;52(3):403-15.
- [29] Rouquerol J, Rouquerol F, Sing K. *Adsorption by Powders and Porous Solids. Principles, Methodology and Applications*. London: Academic Press; 1999.
- [30] Kannan N, Sundaram M. Kinetics and mechanism of removal of methylene blue by adsorption on various carbons - a comparative study. *Dyes and Pigments* 2001;51(1):25-40.

- [31] Cotoruelo LM, Marques MD, Diaz FJ, Rodriguez-Mirasol J, Rodriguez JJ, Cordero T. Equilibrium and Kinetic Study of Congo Red Adsorption onto Lignin-Based Activated Carbons. *Transp.Porous Media* 2010;83(3):573-90.
- [32] McKay G, Blair H, Gardner J. Adsorption of Dyes on Chitin .1. Equilibrium Studies. *J Appl Polym Sci* 1982;27(8):3043-57.
- [33] Tsukamoto M. Intraparticle diffusion of cesium and strontium cations into rock materials. *Chem.Geol.* 1991;90(1):31-44.
- [34] Crank J. *Mathematics of diffusion*. London, England. Oxford at the Clarendon Press. 1956.
- [35] Rey A, Faraldos M, Casas JA, Zazo JA, Bahamonde A, Rodriguez JJ. Catalytic wet peroxide oxidation of phenol over Fe/AC catalysts: Influence of iron precursor and activated carbon surface. *Applied Catalysis B-Environmental* 2009;86(1-2):69-77.
- [36] Cotoruelo LM, Marques MD, Rodriguez-Mirasol J, Rodriguez JJ, Cordero T. Cationic dyes removal by multilayer adsorption on activated carbons from lignin. *Journal of Porous Materials* 2011;18(6):693-702.
- [37] Ho Y. Citation review of Lagergren kinetic rate equation on adsorption reactions. *Scientometrics* 2004;59(1):171-7.
- [38] Ho YS, McKay G. Pseudo-second order model for sorption processes. *Process Biochemistry* 1999;34(5):451-65.
- [39] Cotoruelo LM, Marques MD, Rodriguez-Mirasol J, Rodriguez JJ, Cordero T. Lignin-based activated carbons for adsorption of sodium dodecylbenzene sulfonate: Equilibrium and kinetic studies. *J.Colloid Interface Sci.* 2009;332(1):39-45.
- [40] Srivastava S, Tyagi R, Pant N. Adsorption of Heavy-Metal Ions on Carbonaceous Material Developed from the Waste Slurry Generated in Local Fertilizer Plants. *Water Res.* 1989;23(9):1161-5.
- [41] Mezenner NY, Bensmaili A. Kinetics and thermodynamic study of phosphate adsorption on iron hydroxide-eggshell waste. *Chem.Eng.J.* 2009;147(2-3):87-96.
- [42] Qadeer R. Kinetic study of erbium ion adsorption on activated charcoal from aqueous solutions. *Adsorption-Journal of the International Adsorption Society* 2005;11(1):51-5.
- [43] Qiu H, Lv L, Pan B, Zhang Q, Zhang W, Zhang Q. Critical review in adsorption kinetic models. *Journal of Zhejiang University-Science a* 2009;10(5):716-24.
- [44] Gardas RL, Coutinho JAP. Applying a QSPR correlation to the prediction of surface tensions of ionic liquids. *Fluid Phase Equilib.* 2008;265(1-2):57-65.
- [45] Poling B, Prausnitz J, O'Connell J. *The properties of gases and liquids*. : McGraw-Hill; 1958 5th edition.
- [46] Moreno-Castilla C. Adsorption of organic molecules from aqueous solutions on carbon materials. *Carbon* 2004;42(1):83-94.

- [47] Sarkar M, Acharya PK, Bhattacharya B. Modeling the adsorption kinetics of some priority organic pollutants in water from diffusion and activation energy parameters. *J. Colloid Interface Sci.* 2003;266(1):28-32.
- [48] Vadivelan V, Kumar K. Equilibrium, kinetics, mechanism, and process design for the sorption of methylene blue onto rice husk. *J. Colloid Interface Sci.* 2005;286(1):90-100.
- [49] Porkodi K, Kumar KV. Equilibrium, kinetics and mechanism modeling and simulation of basic and acid dyes sorption onto jute fiber carbon: Eosin yellow, malachite green and crystal violet single component systems. *J. Hazard. Mater.* 2007;143(1-2):311-27.
- [50] Navarrete-Casas R, Navarrete-Guijosa A, Valenzuela-Calahorra C, Lopez-Gonzalez JD, Garcia-Rodriguez A. Study of lithium ion exchange by two synthetic zeolites: Kinetics and equilibrium. *J. Colloid Interface Sci.* 2007;306(2):345-53.
- [51] Li L, Liu S, Zhu T. Application of activated carbon derived from scrap tires for adsorption of Rhodamine B. *Journal of Environmental Sciences-China* 2010;22(8):1273-80.
- [52] Demirbas E, Nas MZ. Batch kinetic and equilibrium studies of adsorption of Reactive Blue 21 by fly ash and sepiolite. *Desalination* 2009;243(1-3):8-21.
- [53] Demirbas E, Dizge N, Sulak MT, Kobya M. Adsorption kinetics and equilibrium of Cu from aqueous solutions using hazelnut shell activated carbon. *Chem. Eng. J.* 2009;148(2-3):480-7.
- [54] Acemioglu B. Batch kinetic study of sorption of methylene blue by perlite. *Chem. Eng. J.* 2005;106(1):73-81.
- [55] Dogan M, Ozdemir Y, Alkan M. Adsorption kinetics and mechanism of cationic methyl violet and methylene blue dyes onto sepiolite. *Dyes and Pigments* 2007;75(3):701-13.
- [56] Figueiredo JL, Pereira MFR. The role of surface chemistry in catalysis with carbons, *Catalysis Today*. 2010;(150):2-7.

Supplementary material

Figure S1. Experimental versus predicted curves for the adsorption kinetics of OmimPF₆ (A) and phenol (B) onto MkU (35 °C; 200 rpm; d_p : 2000-1000 μm ; 3.2 $\text{mmol}\cdot\text{L}^{-1}$ initial concentration).

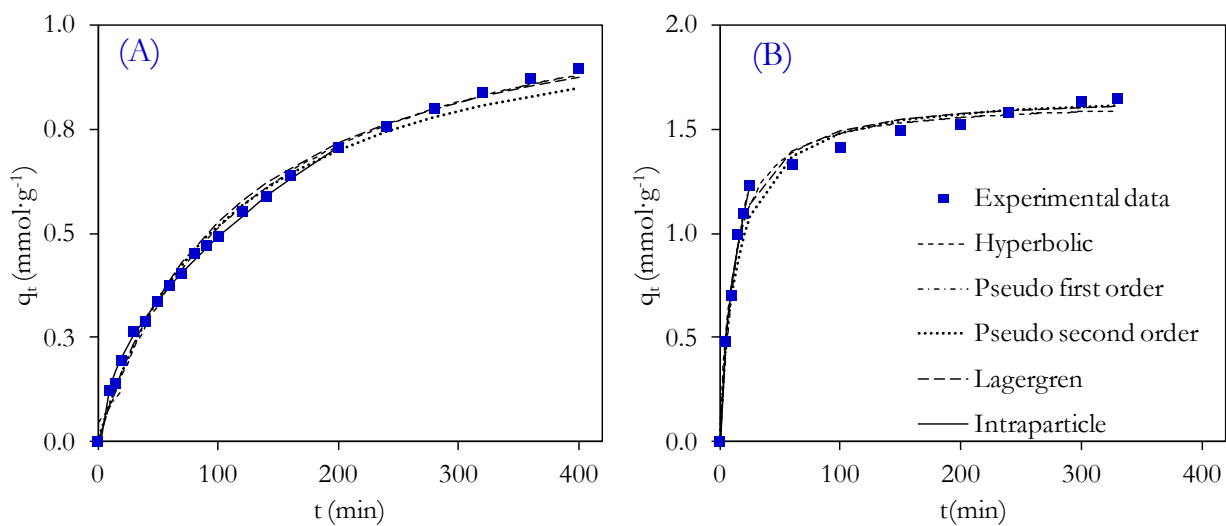


Figure S2. Fitting of the intraparticle diffusion model for adsorption of OmimPF₆ onto MkU at different operating conditions: Stirring velocity (A), particle size (B), initial concentration (C) and temperature (D).

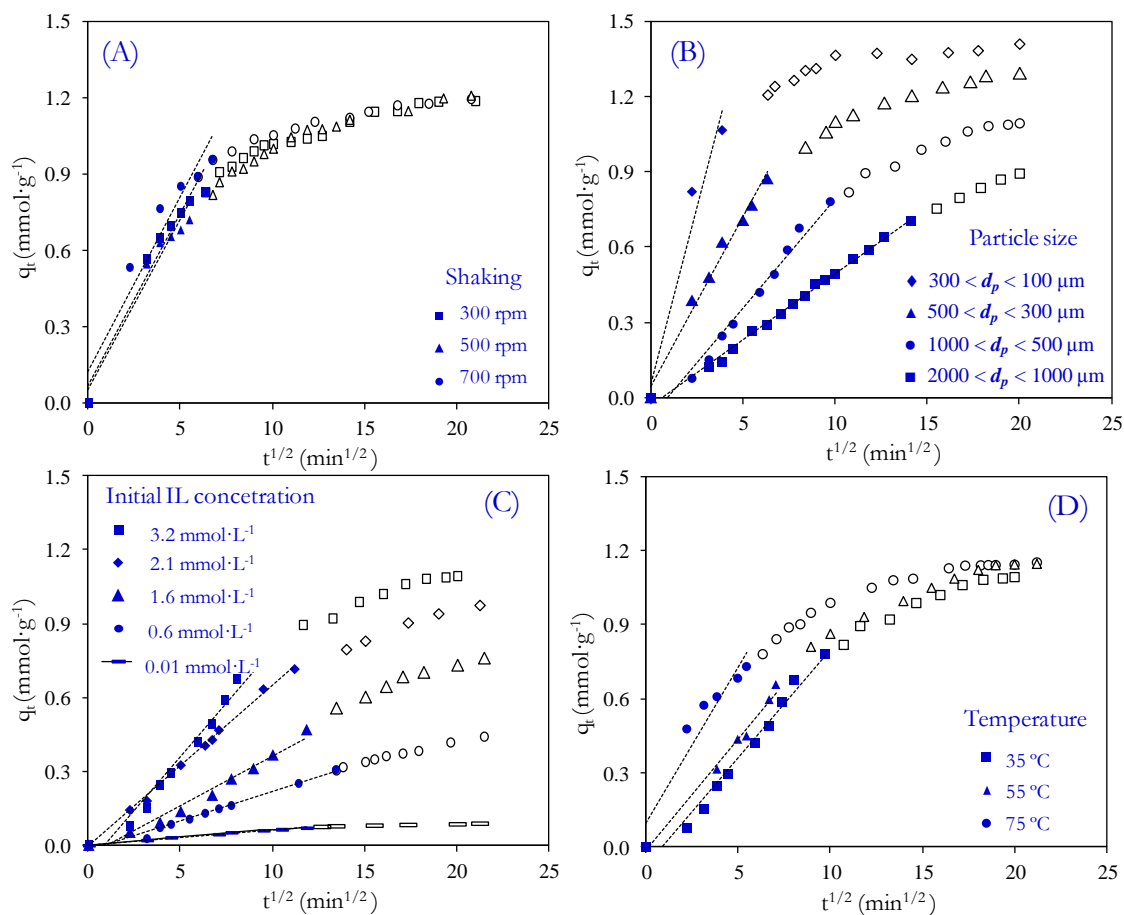


Figure S3. Effect of stirring velocity on the adsorption kinetics of OmimPF₆ onto MkU (d_p : 1000-500 μm , 3.2 $\text{mmol}\cdot\text{L}^{-1}$ initial IL concentration, 35 $^\circ\text{C}$).

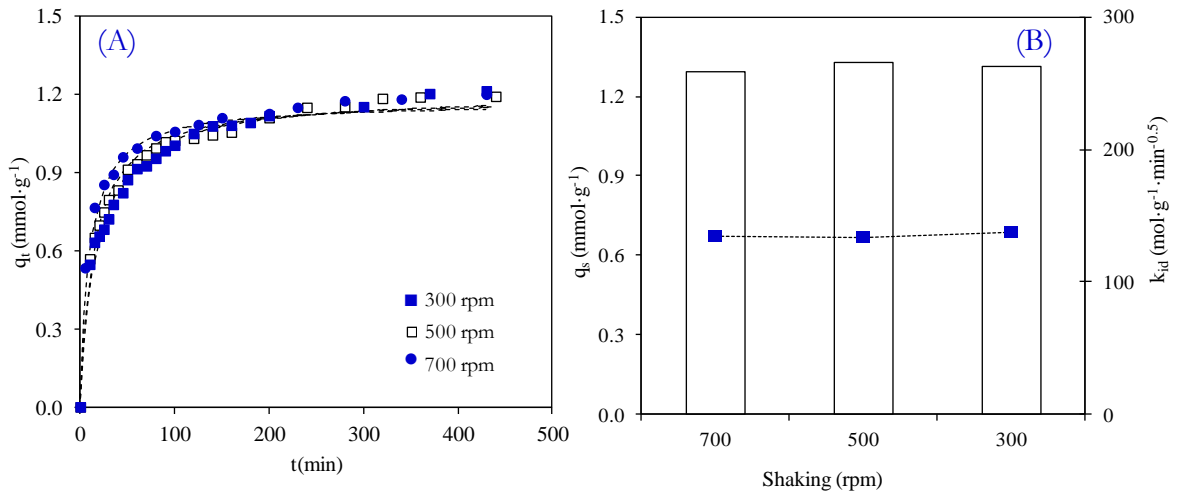


Figure S4. Experimental curves for the adsorption kinetics of phenol onto MkU at different particle sizes and 35 $^\circ\text{C}$.

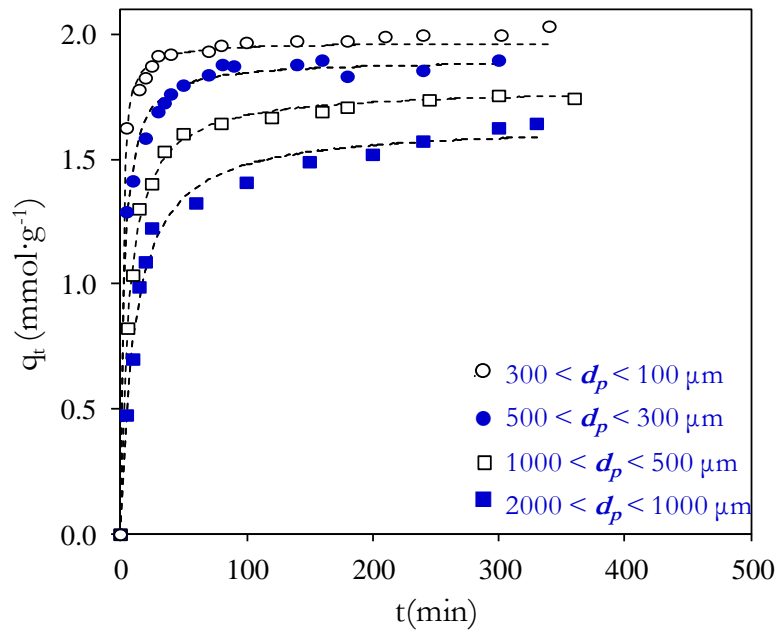


Figure S5. Nitrogen adsorption/desorption isotherms at 77 K of fresh (solid symbols) and heat-treated (open symbols) activated carbons.

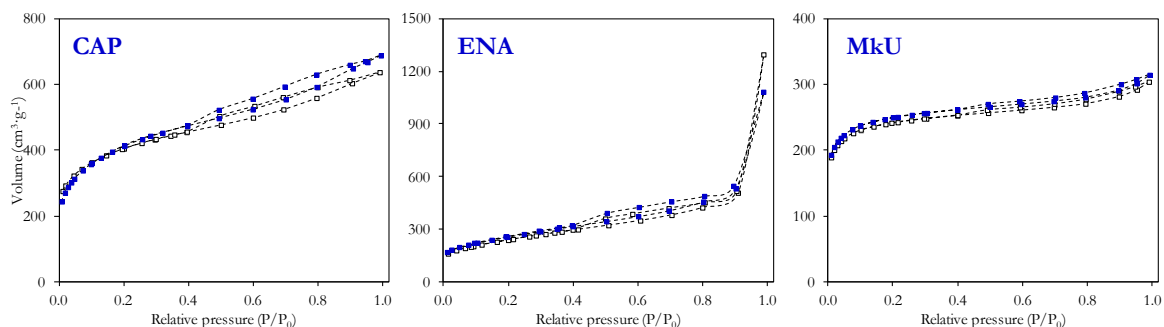
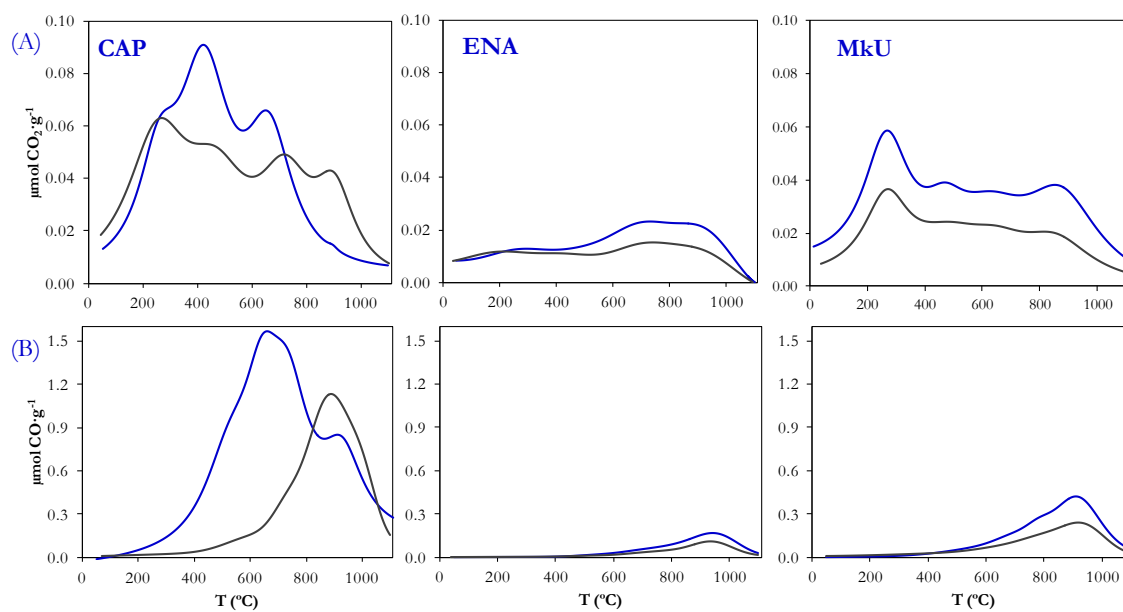


Figure S6. TPD spectra of fresh (black line) and heat-treated (grey line): (A) CO_2 evolution; (B) CO evolution.



ESSAYS ON IONIC LIQUID/ACTIVATED CARBON SYSTEMS AND THEIR APPLICATION TO POLLUTANT REMOVAL

Doctoral dissertation, [Madrid 2012](#), Jesús Lemus Torres



Paper IV

CHARACTERIZATION OF SUPPORTED IONIC LIQUID PHASE (SILP) MATERIALS PREPARED FROM DIFFERENT SUPPORTS

157-179

J. Lemus, J. Palomar, M.A. Gilarranz, J.J. Rodríguez.

CHARACTERIZATION OF SUPPORTED IONIC LIQUID PHASE (SILP)
MATERIALS PREPARED FROM DIFFERENT SUPPORTS

Adsorption. 2011, 17 (3) 561-571

Resumen

El cuarto artículo y primero del segundo bloque de resultados se centra en la obtención de materiales avanzados basados en líquido iónico. Los materiales SILP consisten en una fina película de líquido iónico soportado sobre una matriz sólida porosa, lo que permite aunar las ventajas del líquido iónico (volatilidad despreciable, capacidad disolvente alta, etc.) con la de los materiales sólidos. Estos materiales novedosos se obtienen usando una gama amplia de soportes que presentan porosidad y naturaleza química muy variada. Se ha utilizado como líquido iónico de referencia el 1-metil-3-octilimidazolio (OmimPF₆) que se ha incorporado en diferentes proporciones (5-60% en masa) a la superficie de los diferentes soportes estudiados (tres carbones activos comerciales, sílice, alúmina y óxido de titanio).

El trabajo muestra por primera vez una caracterización sistemática de los materiales SILP que proporciona una valiosa información para su posterior aplicación. Se han utilizado las siguientes técnicas de caracterización para evaluar el confinamiento del líquido iónico en la matriz sólida del material SILP; análisis elemental (EA), isotermas de adsorción-desorción de N₂ a 77 K, porosimetría de mercurio, análisis termogravimétrico (TGA), calorimetría diferencial de barrido (DSC), microscopía diferencial de barrido (SEM) y energía de dispersión de rayos-X (EDX). Los resultados obtenidos ponen de manifiesto que el análisis elemental es una herramienta útil para la cuantificación de la cantidad de líquido iónico imidazolio incorporado en el soporte, independientemente de la naturaleza del sólido. Se encontró una excelente correlación entre el porcentaje de nitrógeno elemental y el líquido iónico incorporado al soporte. La combinación de dos técnicas para el análisis de la estructura porosa de sólidos, como son las isotermas de adsorción de N₂ a 77 K y la porosimetría de mercurio nos

permite obtener información de cómo se dispone el líquido iónico en la superficie porosa del soporte. Dependiendo de los poros disponibles en el soporte, el líquido iónico parece disponer un mecanismo de incorporación jerárquico, rellenando en primer lugar los microporos, seguido de los mesoporos y por último los macroporos. Las propiedades térmicas de los materiales SILP se siguió mediante análisis termogravimétricos (TGA) y calorimétricos (DSC), obteniendo que la estabilidad de los materiales SILP y el mecanismo de descomposición del líquido iónico está fuertemente influenciado por la superficie química del soporte sólido. La microscopía de barrido (SEM) y los análisis de dispersión de rayos X (EDX) evidencian que la superficie externa y los macroporos están cubiertas por cantidades de líquido iónico grandes.

Abstract

Supported ionic liquid phase (SILP) materials are a recent concept where a film of ionic liquid (IL) is immobilized on a solid phase, combining the advantages of ILs (non volatility, high solvent capacity, etc.) with those of heterogeneous support materials. In this work, new SILP materials were prepared using a series of supports with different porosity and chemical nature. An imidazolium-based IL, 1-methyl-3-octylimidazolium hexafluorophosphate (OmimPF₆), was confined at variable contents (5–60% w/w) in three different activated carbons (ACs), silica (SiO₂), alumina (Al₂O₃) and titania (TiO₂).

For the first time, a systematic characterization of different SILP systems has been carried out applying a variety of analytical and spectroscopic techniques to provide information of interest on these materials. Elemental analysis (EA), adsorption–desorption isotherms of N₂ at 77 K, mercury porosimetry, thermogravimetric analysis (TGA), differential scanning calorimetry (DSC), scanning electronic microscopy (SEM) and energy dispersive X-ray (EDX) were conducted to explore confinement effects. The results demonstrate that EA is a useful tool for quantifying the amount of imidazolium-based IL incorporated on support, independently of the nature of the solid. An excellent correlation has been obtained between the percentage of elemental nitrogen and the IL loaded on the support. The combination of nitrogen adsorption–desorption isotherms at 77 K and mercury porosimetry measurements was used to characterize the pore structure of both supports and SILP materials. It was found that depending on the available pores in the solid support, the IL tends to fill micropores firstly, then mesopores and lately in macropores. Thermal properties of SILP materials were studied herein by using both TGA and DSC methods, evidencing that the stability of SILP materials and the decomposition mechanism are strongly dependent on the surface chemistry of the solid support. SEM and EDX provided evidences of external surface coverage by ILs and filling of macropores at high IL load.

1. Introduction

ILs possess an array of properties that make them attractive for academy and industry: extremely low vapor pressure, high thermal and chemical stabilities, non-flammability and high solvent capacity [1-3]. Moreover, the solvent properties of the IL are tunable by the choice of the cation/anion combination [4]. Because of their unique properties the applications of ILs have been expanding in various fields [5]. Thus, ILs have been extensively examined as an alternative to conventional organic solvents in reaction and separation processes [5,6]. There are a number of advantages of ILs in separation and reaction systems, but in many cases there is a need to immobilize them on porous materials [2]. The supported ILs can be spread on the inner surface of the porous structure, maintaining large specific surface area and mechanical properties of the support [7]. The resulting material is usually referred as supported ionic liquid phase (SILP). The SILP concept results in a very efficient use of the IL, because of relatively short diffusion distances for the reactants compared to those in conventional two-phase systems with an IL phase. In addition, the negligible vapor pressure, large liquid range, and thermal stability of ILs ensure that the solvent is retained on the support in its fluid state even at elevated temperatures; this makes SILP highly suitable for continuous processes. The latest developments in SILP systems can be divided in two great blocks as catalysis [4,8-14] and separation processes [15-22]. In catalytic processes, a variety of reactions have been studied where SILP proved to be more active and selective than common systems. The final role that can be played by an IL in a catalytic process is simply as the solvent for the reaction and in this role SILP have been most widely used. Most studies in this topic have been focused on the screening of type reactions and the development of new SILP materials for hydroformylations, hydrogenations, and C–C coupling reactions, among others, is being widely investigated. The combination of well-defined catalyst complexes, non-volatile ILs, and porous solid supports offers many advantages over traditional catalysis in aqueous phase or conventional organic solvents, which are clearly limited by the volatility of the solvent. The SILP concept is considered as a significant contribution to the development of highly selective heterogenized homogeneous catalysts [23]. The use of SILP in separation applications has also awakened interest as alternative to traditional separation and purification processes of SO₂ as hydrodesulfuration [15,20]. SO₂ can be absorbed in SILP materials with a high absorption capacity and selectivity [24] and numerous ILs with SO₂ sorption ability have been reported [25]. Likewise, CO₂ separation and purification processes have also been extensively reported [26,27], based on the high solubility values of CO₂ in some ILs. SILP materials were prepared from a broad range of imidazolium-based ILs at loads varying from 5 to 60% (w/w)

[15,20,26,27]. Because of the great advantages of SILP materials and the need of a deeper understanding of their properties as reaction and separation media, the aim of this work was to gather characterization methods for SILP materials, including elemental analysis, chemical composition, porous structure, thermal stability and morphology.

Immobilization of ILs as thin layers on porous materials can be achieved simply by physisorption or by chemical binding to the support of one of the ions that compose the IL [13]. In this work, six solids of different porosity and chemical nature have been studied as supports for SILP materials. They can be grouped into three classes based on their pore diameter: microporous, $d_{pore} < 2.0$ nm; mesoporous, $2.0 < d_{pore} < 50$ nm; and macroporous, $d_{pore} > 50$ nm [28]. A diversity of support materials were selected of different chemical nature among those commonly used in SILP preparation, like TiO_2 [29], SiO_2 [7,15,19,30] or AC [13,20] among others [8]. In an earlier work [31], it was showed the possibility of following the amount of imidazolium-based IL on AC supports by measuring the percentage of elemental nitrogen in SILP from EA and it has been herein extended to several supports and SILP systems in order to generalize the use of this technique for direct quantification of IL loaded on SILP materials. Structural properties of highly porous supports and SILP materials were analyzed, using adsorption–desorption isotherms of N_2 at 77 K and mercury porosimetry. Both techniques give information on the available volume of micro, meso and macropores available and have been used in previous works showing the difference between a fresh support and a SILP material [7,28,29,32]. Thus, a systematic study on the variation of the porous structure has been carried out with the aim of better understanding how the IL is distributed onto the supports. In addition, results on the thermal stability of SILP materials at high temperature by means of TGA and DSC analysis are collected herein together for the first time. To the best of our knowledge, only thermal studies of ILs have been so far reported [33-35], but without analyzing the relationship between IL and support, except two recent works where a thermal study of SILP materials has been reported [7,20]. Some of the works published in the literature [7,15,20,36,37] showed SILP applications at high temperatures based on different supports. In the present work, a representative collection of supports has been investigated. Finally, the morphology and chemical composition of the surface of SILP materials have been analyzed via SEM-EDX. To the best of our knowledge, a work gathering these techniques for characterization of SILP materials has not been so far reported.

2. Procedure

2.1 Materials and reagents

All chemicals used in the experiments were analytical grade and were used without further purifications. OmimPF₆ was supplied by Iolitec in the highest purity available (purity >99%). The adsorbents used in this study were the following: CAPSUPER supplied by Norit, Mku supplied by Merck, ENA250G supplied by Timcal, SiO₂, Al₂O₃ and TiO₂ supplied by Sigma-Aldrich. Acetone (purity >99.5%) used in SILP preparation was supplied by Panreac.

To immobilize an IL the selection of support type and immobilization method are important depending on its application [15]. Immobilization or supporting of ILs can be carried out in many different ways, such as simple impregnation, grafting, polymerization sol-gel method, encapsulation or pore trapping, among others [13]. In this work, a straightforward preparation method of SILP materials based on a direct impregnation of the support material with OmimPF₆, dissolved in acetone was applied. To prevent hydration, IL and acetone were kept in their original tightly closed bottles in a desiccator before use. When any chemicals were used, they were always manipulated inside a glovebox under a dry nitrogen atmosphere. Impregnation was carried out mixing 1 ml of OmimPF₆ dissolved in acetone for each 100 mg of support. OmimPF₆ concentration in acetone solution was adjusted to obtain different IL loadings on the support. To ensure a homogeneous penetration of the IL solution into the pores, stirring in an orbital shaker for 1.5 h was applied followed by vacuum evacuation of acetone at 10 mbar and 60 °C over 2 h. Then, SILP materials were stored at 60 °C during 24 h prior to their characterization. After vacuum evaporation of acetone, the SILP contains from 5 to 60% (w/w) of IL phase. To check the amount of IL immobilized on the supporting material, all the supports and SILP materials were weighed before and after impregnation. The mass percentages given in this work for IL load are SILP basis. All the SILP materials prepared had the resemblance and behavior of a powdered material. As a first approach, different commercially available supports with a variety of porosities and chemical natures were used to incorporate IL in their pore structure. Three activated carbons (CAPSUPER, Mku and ENA250G), SiO₂, Al₂O₃ and TiO₂ were used to evaluate the influence of the chemical surface. [Table 1](#) summarizes the supporting characteristics of the supports.

Table 1. Characterization of the supports.

<i>Nomenclature</i>	<i>Source</i>	A_{BET}	A_S	$V_{microp.}$	$V_{mesop.}$	$V_{macrop.}$	V_{Total}	%C	%H	%N	% Volatile	% Ash	pH_{slurry}
CAPSUPER	NORIT	1915	667	0.66	0.63	1.02	2.32	81.0	2.30	0.43	14.0	1.80	3.3
MkU	MERCK	927	155	0.36	0.14	0.22	0.72	88.9	0.66	0.57	3.49	5.30	5.4
ENA250G	TIMCAL	79	68	0.00	0.08	1.40	1.48	98.8	0.17	0.03	2.40	0.00	6.1
TiO₂	SIGMA	50	45	0.00	0.06	0.96	1.02	0.23	0.16	0.05	1.05	98.9	5.6
SiO₂	SIGMA	212	212	0.00	0.26	3.07	3.32	0.23	1.95	0.03	0.10	98.7	6.7
Al₂O₃	SIGMA	136	136	0.00	0.21	0.12	0.33	0.10	0.74	0.02	5.88	98.4	8.1
A ($m^2 g^{-1}$); V_{pore} ($cm^3 g^{-1}$)													

2.2. Characterization and instruments

The chemical nature of the supports and SILP materials was determined by means of EA in a Perkin–Elmer analyzer (LECO CHNS-932 model) to obtain C, H and N percentages. Volatile matter was calculated by difference between the weight of fresh support and after ten minutes in a ceramic vessel at 900 °C under nitrogen atmosphere. Ash matter was calculated by difference between the weight of fresh support and after eight hours in a ceramic vessel at 650 °C under oxidizing atmosphere. The $\text{pH}_{\text{slurry}}$ was determined measuring, until constant value, the pH of an aqueous suspension of support in distilled water ($1 \text{ g} \cdot 10 \text{ ml}^{-1}$). The porous structure of supports and SILP materials was characterized by means of nitrogen adsorption–desorption isotherms at 77 K using aMicromeritics apparatus (Tristar II 3020 model) and mercury porosimetry using Quantachrome apparatus (PM-3310 model). Before adsorption–desorption experiments, samples were outgassed at 150 °C under a residual pressure lower than 10^{-3} Pa. The BET equation was applied to determine the BET surface area (A_{BET}) and Dubinin–Radushkevich equation for micropore volume. The external area (A_{s}) was obtained from the t-method. The difference between N_2 adsorbed volume at 0.95 of relative pressure and the micropore volume was taken as mesopore volume. In the mercury porosimetry measurements the estimation of pore diameter from the applied pressure was based on the Washburn equation. The surface tension of mercury was taken as $4.8 \cdot 10^{-3}$ N/cm and the mercury contact angle as 141°. Thermogravimetric analysis (TGA) of OmimPF₆, supports and SILP materials was conducted on a Mettler Toledo Instrument (TGA/SDTA851e model) under nitrogen with a heating rate of $10 \text{ }^\circ\text{C} \cdot \text{min}^{-1}$. The accuracy of temperature and mass measurements was 0.1 °C and 10^{-3} mg, respectively. A dynamic method was used with a temperature range from 50 to 600 °C at a heating rate of $10 \text{ }^\circ\text{C} \cdot \text{min}^{-1}$ while purging with $50 \text{ ml} \cdot \text{min}^{-1}$ of dry nitrogen. The mass of the sample placed in TGA analyses were between 4 and 12 mg. In all TGA runs, aluminum pans with a capacity of 70 ml were used.

Differential scanning calorimetry (DSC) analyses of OmimPF₆, solid supports and SILP materials were carried out on a Mettler Toledo instrument (DSC/821e model). The temperature measurements were carried out with accuracy better than 0.1 °C. DSC curves of samples were determined at a $10 \text{ }^\circ\text{C} \cdot \text{min}^{-1}$ heating rate between 50 and 600 °C. In all experiments, stainless steel pans with a volume of 120 μl and a purge flow of $50 \text{ ml} \cdot \text{min}^{-1}$ of dry nitrogen were used. The sample mass range used in DSC experiments was between 10 and 20 mg. The morphology of the IL layer on the carbonaceous support was characterized by scanning electron microscopy (SEM) (Hitachi S-3000N model) before and after IL phase

deposition. The samples were placed in the microscope chamber after gold metallization treatment; SEM micrographs at 25000× were taken with an accelerating voltage of 20 kV. SEM was equipped with an energy dispersive X-ray (EDX) analyzer (INCAx-sight model). EDX was used to study the distribution of the different chemical elements of interest in the supported IL.

3. Results and discussion

3.1. Quantification of the IL amount on SILP materials

The development of quantitative procedures for determining the amount of IL incorporated to the supports is of interest not only to check SILP materials preparation, but also to evaluate the stability in applications where IL losses can occur. In a previous work [31], a method based on EA was proposed as a procedure to determine the load of OmimPF₆ on AC, thus a linear regression was found between the percentage of elemental nitrogen obtained by EA and the weight percentage of IL incorporated on the support. In this work, the analytical process is extended to six different supports, as depicted in [Figure 1A](#), where the same linear dependence was found for all the SILP material supports.

As can be seen, the y-intercept of the lineal correlations of [Figure 1A](#) depends on the initial amount of nitrogen in the starting support (see [Table 1](#)). Normalized nitrogen contents were calculated excluding the nitrogen content of the starting support from SILP material. A very good correlation was obtained, as shown in [Figure 1B](#). Therefore, EA can be considered as a quantitative tool for determining the amount of IL supported on SILP materials and it has been used to calculate with accuracy the contribution of IL to SILP materials in this work.

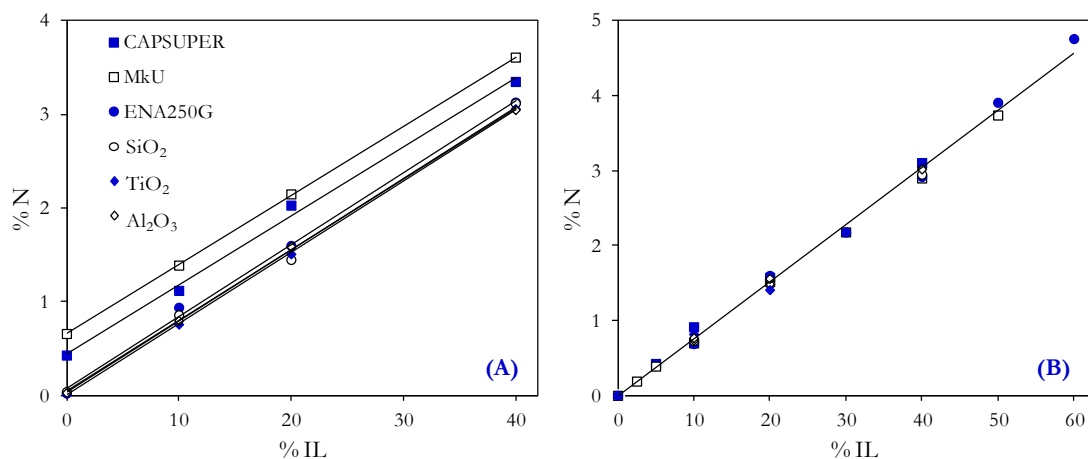


Figure 1. Mass percentage of elemental nitrogen of SILP materials against the OmimPF₆ load (A) total nitrogen and (B) normalized nitrogen excluding nitrogen from the support.

3.2. Textural properties of SILP materials

ILs in SILP materials may be distributed on both the external and internal surface of the supports. Adsorption–desorption isotherms of N₂ at 77 K have been previously used to obtain information about the effect of ILs on the available micro and mesopores of the supports [15,28].

Figure 2 shows the adsorption–desorption isotherms obtained for two ACs of fairly different porous structure (CAPSUPER and ENA250G) at increasing loads of IL from 0 to 60% (w/w). The incorporation of IL to CAPSUPER structure leads to preferential loss of micropore volume, probably by filling or blocking of that pore range by IL. The hysteresis and the slope of the adsorption–desorption isotherms show that the loss of mesopore volume becomes significant for IL contents above 20%, suggesting a hierarchical mechanism of pore filling during impregnation with IL. For an IL load of 50% the SILP material does not show a significant microporosity but maintains some mesoporosity, which disappears when the IL load is increased to 60%. In the case of the SILP materials prepared from ENA250G, a maximum IL load of 40% was achieved in order to maintain powdered texture and avoid agglomeration. The series of SILP materials from ENA250G showed a progressive loss of porosity in the whole range of pore size during impregnation, as can be inferred from the isotherms. Although CAPSUPER and ENA250G differ substantially in porosity, the maximum load of IL incorporated is comparable. This result shows the important role that

macroporosity can play in the retention of ILs. In order to generalize the observation commented for Figure 2, the BET surface area of four SILP materials with increasing loads of OmimPF₆ were plotted in Figure 3, where it can be appreciated that supports of different porosity present BET surface affected on various ways. Thus, microporous supports (CAPSUPER and MkU) lose surface area in a larger extent with the incorporation of IL, while mesoporous and macroporous materials undergo a lower loss of surface area although they are capable of retaining similar IL loads.

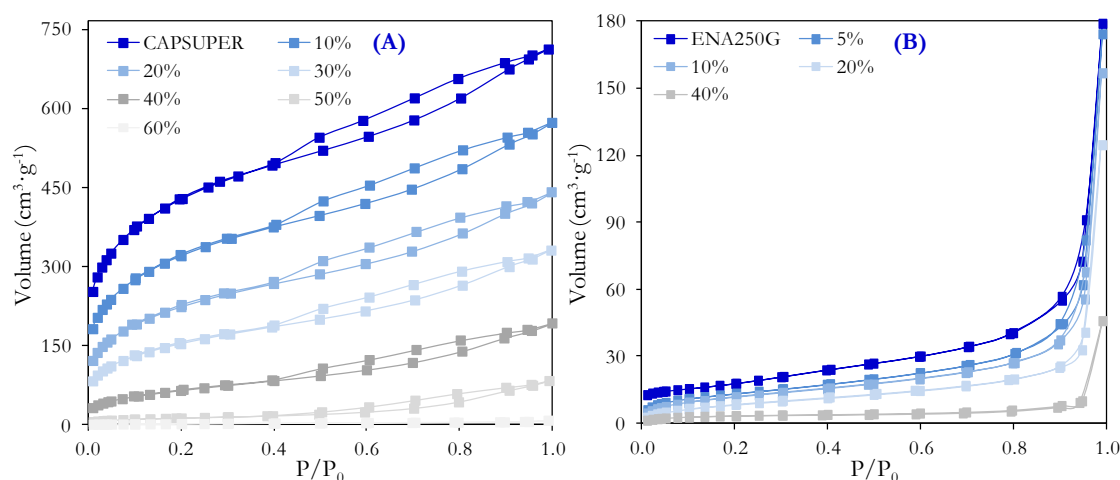


Figure 2. Nitrogen adsorption–desorption isotherms at 77 K of SILP with increasing amounts of OmimPF₆ (0–60% w/w) on CAPSUPER (A) and ENA250G (B).

In order to evaluate the distribution of IL onto the mesoporous and macroporous structure, mercury porosimetry of supports and SILP materials was carried out. Figure 4 shows the pore size distribution against pore diameter of SILP materials prepared with two kinds of supports for different IL loads. CAPSUPER support has a high contribution of mesopore volume that is lost progressively with increasing IL load. According to the nitrogen adsorption–desorption isotherms, some mesoporosity remains up to loads of 40–50%, and almost complete loss of mesoporosity takes place at 60% IL load. On the other hand, ENA250G shows a significant contribution of pores with diameter centered around 100 nm that are gradually filled as the amount of IL is increased, together with a loss of porosity in the whole range of macropores. It must be remarked the difficulty of analyzing mercury porosimetry results for SILP materials, which contain both IL and a solid support, instead of simply a porous solid. However, for SILP characterization, both techniques nitrogen

adsorption–desorption and mercury porosimetry were found highly complementary and can be grouped to obtain useful information about the distribution of ILs in SILP material, for comparison purposes between systems implying different IL loading and solid supports.

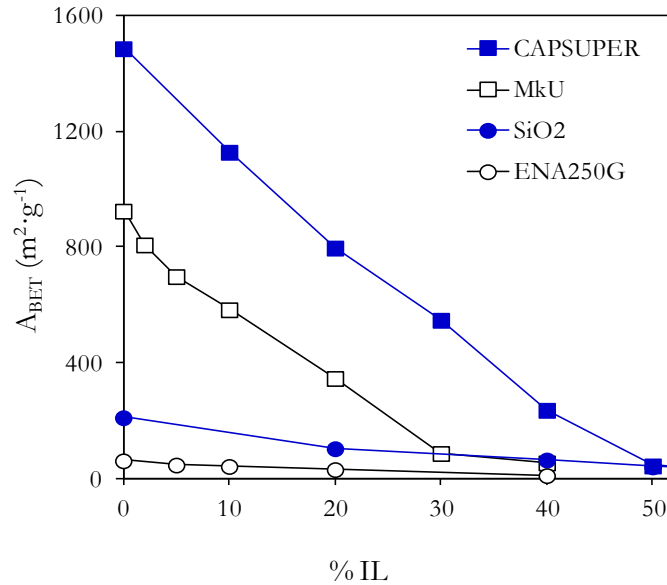


Figure 3. Variation of BET surface area of CAPSUPER, MkU, SiO₂ and ENA250G at increasing OmimPF₆ loads (0–50% w/w).

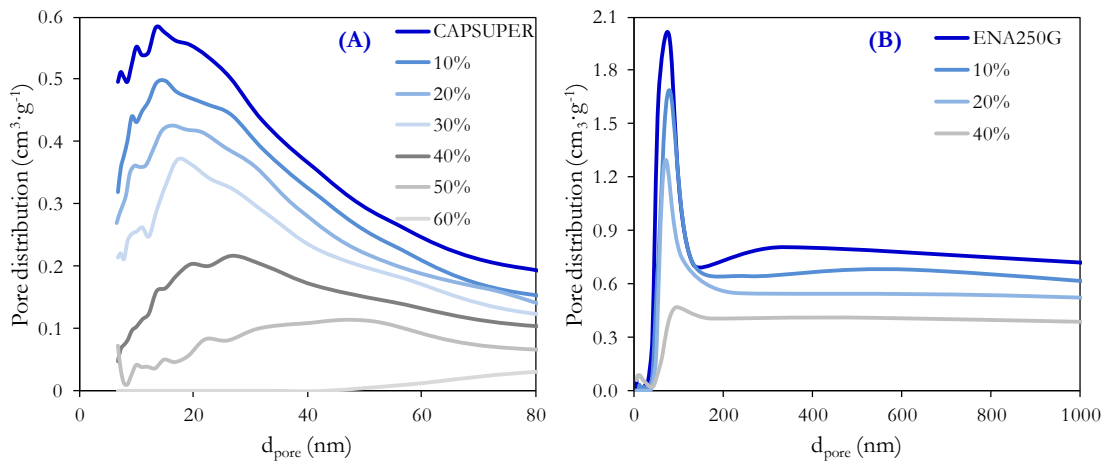


Figure 4. Pore size distribution (6 to 1000 nm) at increasing amounts of OmimPF₆ (from 0 to 60% (w/w)) on (A) CAPSUPER and (B) ENA250G as obtained from mercury porosimetry.

The combination of both techniques provides the impregnation pattern shown for CAPSUPER and ENA250G in Figure 5. In the case of CAPSUPER, IL seems to fill firstly the micropores followed then by mesopores and lately by macropores. On the contrary, in a support without micropore contribution such as ENA250G the filling takes place first in mesopores and afterward in macropores. As can be also seen in Figure 5, there is a reasonable agreement between the amount of IL volume incorporated to the SILP material, calculated from the experimental molar density, and the gradual loss of the pore volume available in the support, which may suggest access of IL to a substantial proportion of the micropore volume.

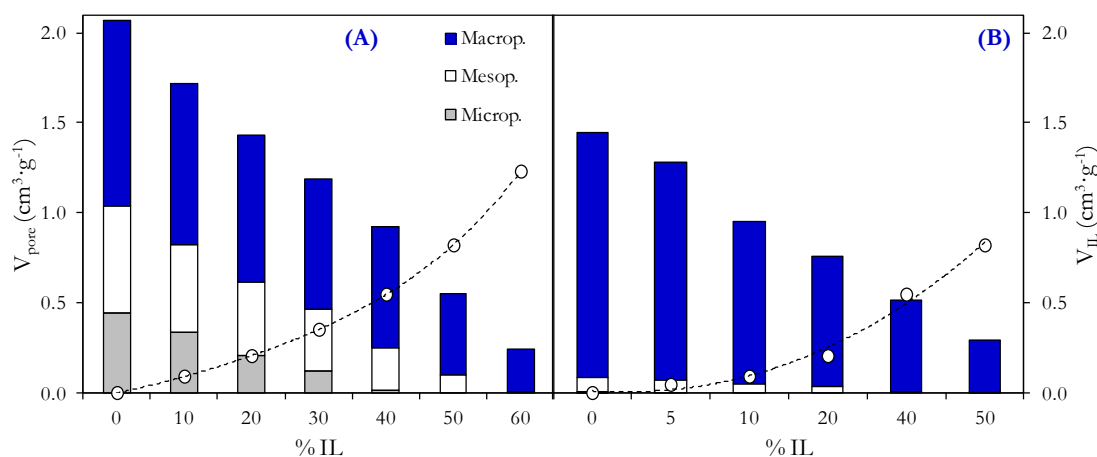


Figure 5. Pore size distribution at increasing amounts of OmimPF₆ (from 0 to 50–60%) on (A) CAPSUPER and (B) ENA250G as obtained from the combination of adsorption–desorption isotherms of N₂ at 77 K and mercury porosimetry and estimated volume occupied by the loaded IL (○).

The maximum IL load achieved in SILP materials against the total pore volume ($d_{\text{pore}} < 1000$ nm) quantified by combination of adsorption–desorption isotherms of N₂ at 77 K and mercury porosimetry is shown in Figure 6. The excellent correlation makes possible to assume that supports with high pore volume are preferred if a large IL loading is intended. Particularly interesting are the cases of CAPSUPER and SiO₂, which showed retention capacities of 63 and 77% (w/w), respectively, i.e. 1.7 and 3.3 grams of IL per gram of support. However, in certain cases lower IL loads may be desirable if maintaining some surface area of the SILP material is required for the specific application.

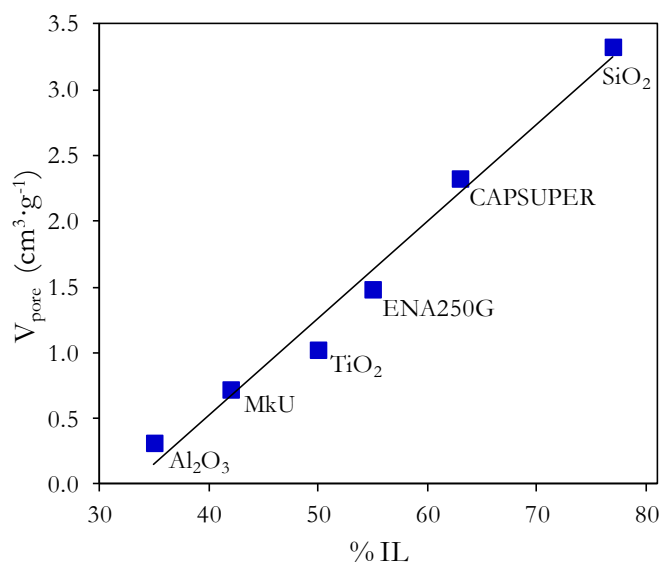


Figure 6. Total pore volume (up to 1000 nm) as obtained from the combination of adsorption–desorption isotherms of N_2 at 77 K and mercury porosimetry against maximum retention capacity of different supports at incipient wetness.

3.3. Thermal stability of SILP materials. TGA and DSC study

The thermal stability of SILP materials is of special interest for gas phase applications [20,24,25], where high temperatures may be required. Even though the decomposition temperature of pure IL is above the process temperature, the interaction with the support may lead to reduced stability. As a first approach, the thermal stability of pure IL was examined by TGA and DSC within range of 50–600 °C. Previous works showed that common imidazolium-based ILs, such as OmimPF₆, have very high thermal decomposition temperature and that the anion decomposes before the cation [33]. The TGA curve in Figure 7 shows that OmimPF₆ started to decompose at 350 °C and it decomposed almost completely at 500 °C, without any char formation. Figure 7 reports DSC results for OmimPF₆ showing two exothermic peaks, which were assigned to PF₆ anion at 370 °C and subsequently imidazolium cation at 400 °C, consistently with previous TGA observations and the difference in molar mass of the counterions [33].

Figure 7. TGA (blue line) and DSC (gray line) curves of OmimPF₆ under nitrogen atmosphere with a heating rate of 10 °C·min⁻¹.

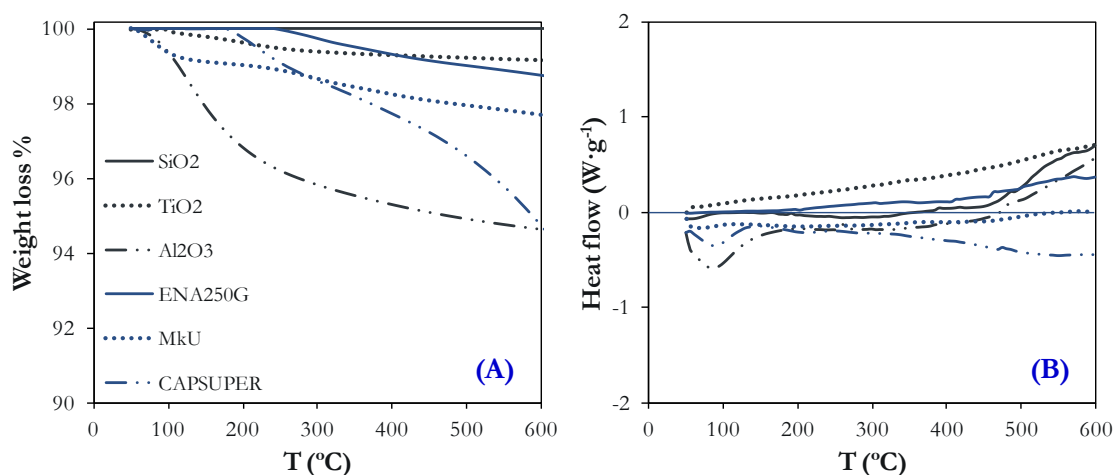
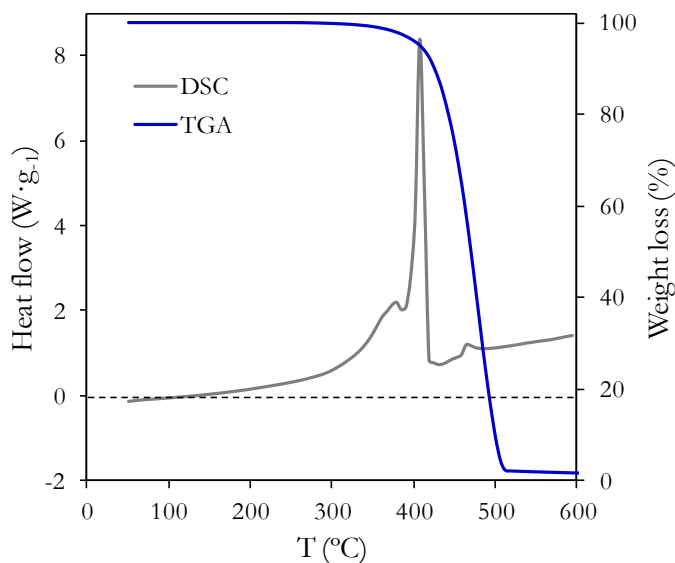


Figure 8. TGA (A) and DSC (B) curves of the supports under nitrogen atmosphere at a heating rate of 10 °C·min⁻¹.

Figure 8A shows the TGA curves of the supports after being subjected to oven drying at 105 °C for 2 hours. The mass losses of all the supports studied were below 6% at 600°C. Figure 8B shows the DSC curves for six supports, where the lack of neat peaks confirms their high stability. After separate evaluation of the thermal stability of IL and supports, the thermal stability of SILP materials was studied at IL loads of ca. 40% (w/w). Figure 9A depicts TGA and DTG for AC-based SILP materials. The stability is significantly influenced by the nature

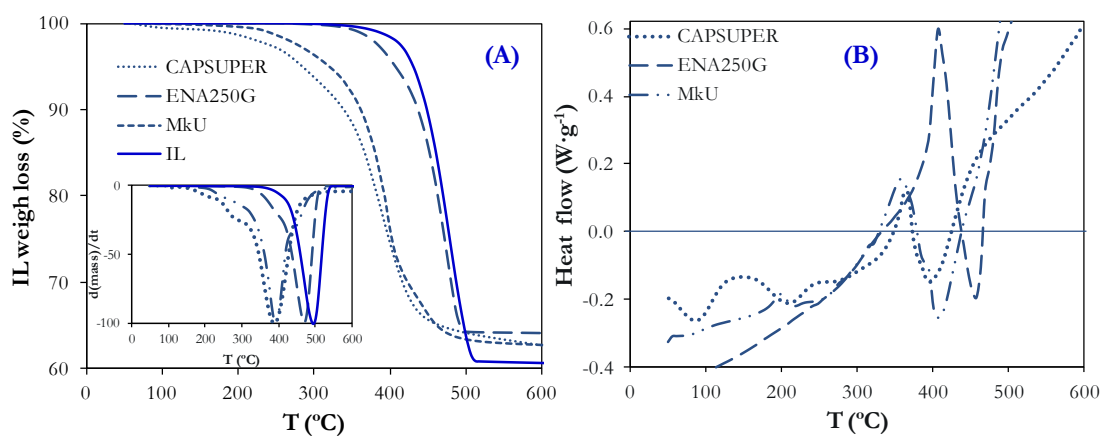
of the AC, being always lower than of pure IL. SILP material prepared using CAPSUPER support started to decompose at 200 °C, whereas those prepared with MkU started at 260 °C, however, the DTG peak, assigned to cation, is centered for both supports around 390 °C. The SILP based on ENA250G, showed higher thermal stability, starting to decompose at 360 °C and presenting the DTG peak of cation at 450 °C. DSC plots also show the changes in the thermal stability of IL due to the influence of the support (Figure 9B). In fact, DSC peaks coincide with the peak minima from TGA derivation, showing the agreement between both techniques. Moreover, whereas both decomposition peaks of DSC (anion and cation) are exothermic for pure IL, SILP materials present an exothermic peak assigned to anion and, subsequently, an endothermic peak allocated to cation that is endothermic. Attending to Table 1, the chemical nature of supports surface plays a main role in the thermal stability of SILP material. Measurements of $\text{pH}_{\text{slurry}}$ of carbonaceous supports indicate that the acidity of the support increases in the order ENA250 < MKU < CAPSUPER, i.e., the same order observed for decreasing anion decomposition temperature by TGA and DSC. The higher acidity of CAPSUPER and MkU, together with their higher surface area, seems to promote cracking of anion thus lowering the thermal decomposition temperature. The role of acid sites in promoting thermal decomposition reactions is a well known fact for cracking catalysts [38]. As indicated above, the thermal decomposition of cation was described by an endothermic process, which suggests a different decomposition mechanism.

Table 2. Temperatures (°C) of DTG and DSC peaks curves assigned to cation and anion of OmimPF₆ in the solid supports.

	$T_{\text{Cation-DTG}}$	$T_{\text{Cation-DSC}}$	$T_{\text{Anion-DTG}}$	$T_{\text{Anion-DSC}}$
CAPSUPER	390	396	280	362
MkU	393	401	290	350
ENA250G	450	452	383	407
Al₂O₃	463	458	220	198
TiO₂	450	447	315	303
SiO₂	360	350	220	209

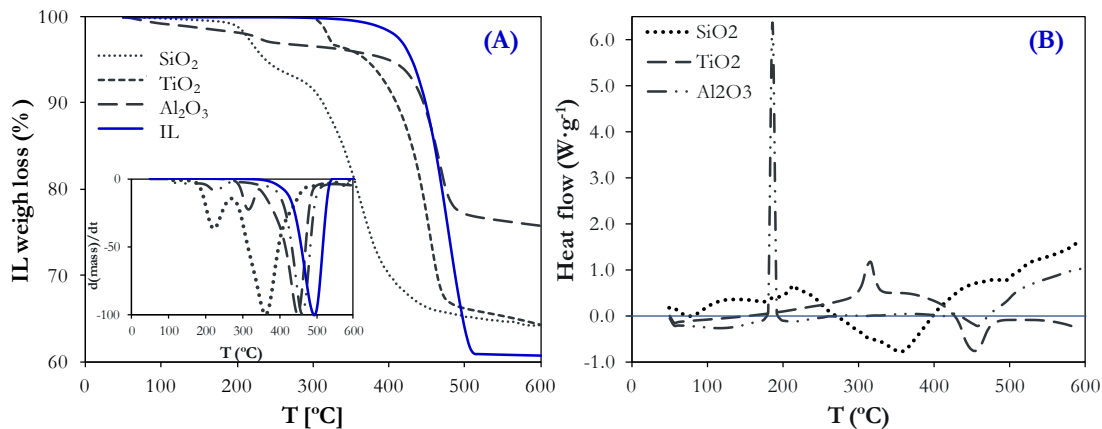
This hypothesis is supported by the formation of pyrolytic carbon from the decomposition of the organic part of IL (imidazolium cation), which was not observed for pure IL (see Figure 9A). In the cases of SILP materials not supported on AC, a remarkable effect of the nature of the support on SILP thermal stability can also be observed. The mass loss allocated to anion and cation appears at different temperatures depending on the supporting material (see Figure 10A). Silica is the most polar support and decomposition occurs before than for the rest (195 °C). Al₂O₃-based SILP decomposed at 215 °C, although overlapped with the weight loss of the own Al₂O₃ support. Lately, TiO₂ decomposed clearly at 310 °C. Figure 10B shows DSC curves for SILP materials supported on SiO₂, Al₂O₃ and TiO₂, presenting an exothermic peak assigned to anion and subsequently an endothermic peak assigned to cation. Table 2 summarizes the temperatures for DTG and DSC peaks for the six SILP materials prepared.

Figure 9. TGA curves and DGT peaks obtained under nitrogen at a heating rate of 10 °C·min⁻¹ for OmimPF₆ and SILP materials based on ACs loaded at ca. 40 wt % (A) and the corresponding DSC curves for SILP materials (B).



The DSC peaks are in agreement with the DTG ones, showing the consistency of both techniques for the evaluation of thermal stability. Further studies of thermal stability of SILP supported on organic and inorganic materials must be developed in the future to provide insight into the role of the surface chemistry of the supports, being TGA and DSC useful tools.

Figure 10. TGA curves and DGT peaks obtained under nitrogen at a heating rate of $10\text{ }^{\circ}\text{C}\cdot\text{min}^{-1}$ for OmimPF₆ and SILP materials not supported on AC loaded at ca. 40 wt % (A) and the corresponding DSC curves for SILP materials(B).



3.4. SEM and EDX studies

Scanning electron microscopy (SEM) combined with energy dispersive X-rays (EDX) analysis were used to examine the CAPSUPER AC surface and obtain information about its chemical composition before and after impregnation with IL. Figure 11 shows a progressive smoothing of the SILP surface with increasing IL load, particularly for a load of 60%, which indicates filling of macropores and some excess of IL on the surface. Table 3 provides results on the average chemical composition of the support and SILP materials surface, indicating a similar composition for the SILP materials with 40 and 60% IL load. The fluorine signal corresponding to the PF₆ cation indicates uniform distribution of IL on the external surface of the support for a 40% load, even though SEM does not indicate excess of IL filling macropores.

Table 3. Percentages of C, O, F and P from EDX of CAPSUPER and SILP loaded at 40 and 60% (w/w)

	CAPSUPER	SILP 40%	SILP 60%
%C	85.9	77.5	77.8
%O	13.8	12.8	11.2
%F	0	7.7	8.68
%P	0.31	2.07	2.35



Figure 11. SEM images ($\times 25000$) of CAPSUPER support (A) and SILP with an IL load of 40% (B) and 60% (w/w) (C).

4. Conclusions

The concept of SILP has been examined for the sake of learning on future potential applications in the fields of catalytic and separation processes. Using supports of different porous structures and ILs of different properties (polar nature) SILP systems can be designed and prepared for specific applications. In this work, we evaluated and proposed different techniques to characterize SILP materials, which may be applied in the future to relate their properties and behavior as reaction or separation media. Thus, EA has been demonstrated as a useful analytical tool to accurately quantify the amount of imidazolium-based IL loaded onto the support, through the percentage of elemental nitrogen. On the other hand, adsorption–desorption isotherm of N_2 at 77 K and mercury porosimetry have been successfully used to describe the distribution of IL onto the support surface for a variety of SILP materials. Attending to support porosity it was found that IL fills selectively small pores, but, when they do not exit, IL is charged on the available pores, as it happens with macroporous SiO_2 . The amount of IL can be modulated depending on the application of SILP, but when a SILP

material with a high IL load is required a highly porous support is needed. These SILP materials have a high IL content but they lose their pore structure. Finally, TGA and DSC measurements were consistently applied to evaluate the thermal stability of the SILPs. It was found that the nature of the support can remarkably affect to the thermal stability of the SILP systems, resulting the most stable those SILP materials prepared from supports of non polar acidic character.

References

- [1] Welton T. Room-temperature ionic liquids. Solvents for synthesis and catalysis. *Chemical reviews* 1999;99:2071.
- [2] Wasserscheid P, Welton T. *Ionic liquids in synthesis*. Weinheim: Wiley-VCH; 2008.
- [3] Robin D. Rogers, Kenneth R. Seddon. *Ionic Liquids as green solvents: progress and prospects*. Washington 669 (DC): American Chemical Society; 2003.
- [4] Riisager A, Wasserscheid P, van Hal R, Fehrmann R. Continuous fixed-bed gas-phase hydroformylation using supported ionic liquid-phase (SILP) Rh catalysts. *Journal of Catalysis* 2003;219(2):452-5.
- [5] Robin D. Rogers, Kenneth R. Seddon. *Ionic Liquids IIIA: fundamentals, progress, challenges and opportunities - transformations and processes*. Washington (DC): American 674 Chemical Society; 2005.
- [6] Han X, Armstrong DW. *Ionic liquids in separations*. *Acc.Chem.Res.* 2007;40:1079-86.
- [7] Vangeli OC, Romanos GE, Beltsios KG, Fokas D, Kouvelos EP, Stefanopoulos KL, et al. Grafting of Imidazolium Based Ionic Liquid on the Pore Surface of Nanoporous Materials- Study of Physicochemical and Thermodynamic Properties. *J Phys Chem B* 2010;114(19):6480-91.
- [8] Riisager A, Fehrmann R, Haumann M, Gorle BSK, Wasserscheid P. Stability and kinetic studies of supported ionic liquid phase catalysts for hydroformylation of propene. *Ind Eng Chem Res* 2005;44(26):9853-9.
- [9] Riisager A, Fehrmann R, Haumann M, Wasserscheid P. Supported ionic liquids: versatile reaction and separation media. *Topics in Catalysis* 2006;40(1-4):91-102.
- [10] Riisager A, Fehrmann R, Haumann M, Wasserscheid P. Supported Ionic Liquid Phase (SILP) catalysis: An innovative concept for homogeneous catalysis in continuous fixed-bed reactors. *European Journal of Inorganic Chemistry* 2006;4:695-706.

- [11] Virtanen P, Karhu H, Kordas K, Mikkola J. The effect of ionic liquid in supported ionic liquid catalysts (SILCA) in the hydrogenation of α,β -unsaturated aldehydes. *Chemical Engineering Science* 2007;62(14):3660-71.
- [12] Virtanen P, Karhu H, Toth G, Kordas K, Mikkola JP. Towards one-pot synthesis of menthols from citral: Modifying Supported Ionic Liquid Catalysts (SILCAs) with Lewis and Bronsted acids. *Journal of Catalysis* 2009;263(2):209-19.
- [13] Virtanen P, Mikkola JP, Toukoniiitty E, Karhu H, Kordas K, Eranen K, et al. Supported ionic liquid catalysts-From batch to continuous operation in preparation of fine chemicals. *Catalysis Today* 2009;147:S144-8.
- [14] Ruta M, Laurenczy G, Dyson PJ, Kiwi-Minsker L. Pd Nanoparticles in a Supported Ionic Liquid Phase: Highly Stable Catalysts for Selective Acetylene Hydrogenation under Continuous-Flow Conditions. *Journal of Physical Chemistry C* 2008;112(46):17814-9.
- [15] Zhang ZM, Wu LB, Dong J, Li BG, Zhu SP. Preparation and SO₂ Sorption/Desorption Behavior of an Ionic Liquid Supported on Porous Silica Particles. *Ind Eng Chem Res* 2009;48(4):2142-8.
- [16] Vioux A, Viau L, Volland S, Le Bideau J. Use of ionic liquids in sol-gel; ionogels and applications. *Comptes Rendus Chimie* 2010 2;13(1-2):242-55.
- [17] Sun AJ, Zhang JL, Li CX, Meng H. Gas Phase Conversion of Carbon Tetrachloride to Alkyl Chlorides Catalyzed by Supported Ionic Liquids. *Chinese Journal of Chemistry* 2009;27(9):1741-8.
- [18] Fontanals N, Ronka S, Borrull F, Trochimczuk AW, Marcé RM. Supported imidazolium ionic liquid phases: A new material for solid-phase extraction. *Talanta* 2009;80(1):250-6.
- [19] Fang G, Chen J, Wang J, He J, Wang S. N-Methylimidazolium ionic liquid-functionalized silica as a sorbent for selective solid-phase extraction of 12 sulfonylurea herbicides in environmental water and soil samples. *Journal of Chromatography A* 2010;1217(10):1567-74.
- [20] Kohler F, Roth D, Kuhlmann E, Wasserscheid P, Haumann M. Continuous gas-phase desulfurisation using supported ionic liquid phase (SILP) materials. *Green Chem.* 2010;12(6):979-84.
- [21] Werner S, Szesni N, Bittermann A, Schneider MJ, Harter P, Haumann M, et al. Screening of Supported Ionic Liquid Phase (SILP) catalysts for the very low temperature water-gas-shift reaction. *Applied Catalysis A-General* 2010;377(1-2):70-5.
- [22] Joni J, Haumann M, Wasserscheid P. Continuous gas-phase isopropylation of toluene and cumene using highly acidic Supported Ionic Liquid Phase (SILP) catalysts. *Applied Catalysis A: General* 2010;372(1):8-15.
- [23] Rüsager A, Fehrmann R, Flicker S, van Hal R, Haumann M, Wasserscheid P. Very stable and highly regioselective supported ionic-liquid-phase (SILP) catalysis: Continuous flow fixed-bed hydroformylation of propene. *Angewandte Chemie-International Edition* 2005;44(5):815-9.

- [24] Wu WZ, Han BX, Gao HX, Liu ZM, Jiang T, Huang J. Desulfurization of flue gas: SO₂ absorption by an ionic liquid. *Angewandte Chemie-International Edition* 2004;43(18):2415-7.
- [25] Huang J, Riisager A, Wasserscheid P, Fehrmann R. Reversible physical absorption of SO₂ by ionic liquids. *Chemical Communications* 2006(38):4027-9.
- [26] Ilconich J, Myers C, Pennline H, Luebke D. Experimental investigation of the permeability and selectivity of supported ionic liquid membranes for CO₂/He separation at temperatures up to 125 degrees C. *J.Membr.Sci.* 2007;298(1-2):41-7.
- [27] Bara J, Carlisle T, Gabriel C, Camper D, Finotello A, Gin D. Guide to CO₂ Separations in Imidazolium-Based Room-Temperature Ionic Liquids. *Industrial engineering chemistry research* 2009;48(6):2739-51.
- [28] Zhang J, Ma Y, Shi F, Liu L, Deng Y. Room temperature ionic liquids as templates in the synthesis of mesoporous silica via a sol-gel method. *Microporous and Mesoporous Materials* 2009;119(1-3):97-103.
- [29] Chen SY, Han CC, Tsai CH, Huang J, Chen-Yang YW. Effect of morphological properties of ionic liquid-templated mesoporous anatase TiO₂ on performance of PEMFC with Nafion/TiO₂ composite membrane at elevated temperature and low relative humidity. *J.Power Sources* 2007;171(2):363-72.
- [30] Mehnert CP. Supported ionic liquid phases. *Chemistry-a European Journal* 2005;11(1):50-6.
- [31] Palomar J, Lemus J, Gilarranz MA, Rodriguez JJ. Adsorption of ionic liquids from aqueous effluents by activated carbon. *Carbon* 2009;47(7):1846-56.
- [32] Shi F, Deng Y. Abnormal FT-IR and FT-Raman spectra of ionic liquids confined in nanoporous silica gel. *Spectrochimica Acta Part A: Molecular and Biomolecular Spectroscopy* 2005;62(1-3):239-44.
- [33] Fernandez A, Torrecilla JS, Garcia J, Rodriguez F. Thermophysical properties of 1-ethyl-3-methylimidazolium ethylsulfate and 1-butyl-3-methylimidazolium methylsulfate ionic liquids. *J.Chem.Eng.Data* 2007;52:1979-83.
- [34] Holbrey JD, Reichert WM, Swatloski RP, Broker GA, Pitner WR, Seddon KR, et al. Efficient, halide free synthesis of new, low cost ionic liquids: 1,3-dialkylimidazolium salts containing methyl- and ethyl-sulfate anions. *Green Chem.* 2002;4(5):407-13.
- [35] Karna M, Lahtinen M, Valkonen J. Preparation and characterization of new low melting ammonium-based ionic liquids with ether functionality. *J.Mol.Struct.* 2009;922(1-3):64-76.
- [36] Muldoon MJ. Modern multiphase catalysis: new developments in the separation of homogeneous catalysts. *Dalton Transactions* 2010;39(2):337-48.
- [37] Kim KM, Park NG, Ryu KS, Chang SH. Characterization of poly(vinylidene fluoride-co-hexafluoropropylene)-based polymer electrolyte filled with TiO₂ nanoparticles. *Polymer* 2002;43(14):3951-7.

- [38] van Grieken R, Serrano DP, Aguado J, Garcia R, Rojo C. Thermal and catalytic cracking of polyethylene under mild conditions. *J.Anal.Appl.Pyrolysis* 2001;58:127-42.

ESSAYS ON IONIC LIQUID/ACTIVATED CARBON SYSTEMS AND THEIR APPLICATION TO POLLUTANT REMOVAL

Doctoral dissertation, [Madrid 2012](#), Jesús Lemus Torres



Paper V

REMOVAL OF CHLORINATED ORGANIC VOLATILE COMPOUNDS BY GAS PHASE ADSORPTION WITH ACTIVATED CARBON

181-204

J. Lemus, M. Martín-Martínez, J. Palomar, L. Gómez-Sainero,

M. A. Gilarranz, J. J. Rodríguez

REMOVAL OF CHLORINATED ORGANIC VOLATILE COMPOUNDS
BY GAS PHASE ADSORPTION WITH ACTIVATED CARBON

Chemical Engineering Journal. 2012

(<http://dx.doi.org/10.1016/j.cej.2012.09.021>)

Resumen

Este capítulo analiza eliminación de compuestos orgánicos volátiles (COVs) de corrientes gaseosas mediante su adsorción en columnas de lecho fijo, utilizando como material adsorbente un carbón activo comercial y diferentes condiciones de operación (concentración inicial, temperatura, presión, caudal de entrada del gas y altura del lecho). Las curvas de adsorción de los Cl-COVs sobre carbón activo se ajustaron al modelo de Yoon and Nelson, que utiliza dos parámetros de ajuste para predecir la curva de ruptura entera. Posteriormente, el carbón activo saturado se regenera bajo condiciones de operación suaves, (temperatura ambiente y presión atmosférica). La metodología COSMO-RS se utiliza para justificar y validar el proceso de adsorción de los Cl-COVs sobre el carbón activo, relacionando la estructura superficial del carbón activo con los diferentes solutos clorados (monoclorometano, diclorometano y cloroformo). Esta información puede ser de utilidad para el diseño de carbones activos con funcionalizaciones efectivas para mejorar sus capacidades de adsorción. Para comprobar estas evidencias preliminares, un carbón activo comercial se modificó mediante un tratamiento térmico y tratamientos oxidativos (con ácido nítrico y con persulfato amónico), con una posterior caracterización de los materiales mediante diferentes técnicas. Los carbones activos modificados se han utilizado en experimentos de adsorción en reactor de lecho fijo con diferentes compuestos orgánicos volátiles clorados (Cl-COVs). Una de las conclusiones más relevantes para el tratamiento de estos compuestos es el aumento de la retención con el carácter básico de la superficie del carbón activo.

Abstract

This chapter discusses the removal of chlorinated volatile organic compounds (Cl-VOCs) from gas streams by means of fixed-bed adsorption with a commercial activated carbon (AC). Column experiments were performed at different conditions (inlet concentration, temperature, pressure, gas flow rate and bed length). A two-parameter model introduced by Yoon and Nelson was applied to predict the entire breakthrough curves for chloromethane adsorption. Complete regeneration of the exhausted AC was performed at mild conditions (atmospheric pressure and room temperature). In order to gain a better knowledge on the effect of the surface chemistry of AC on the adsorption of Cl-VOCs, the quantum-chemical COSMO-RS method was used to simulate the interactions between AC surface groups and different Cl-VOCs as monochloromethane, dichloromethane and chloroform. This information can be useful for tailoring the ACs with the objective of improving their adsorption capacities by further functionalization. To confirm this, the commercial AC tested was modified by means of different thermal and oxidative treatments (nitric acid and ammonium persulfate), being the surface chemistry and textural properties of the resulting materials characterized by different techniques. The modified ACs were then tested in column adsorption experiment with different Cl-VOCs. The uptake of these compounds increased with the basic character of the AC surface.

1. Introduction

Chlorinated volatile organic compounds (Cl-VOCs) play an important role in the chemical and pharmaceutical industries, where they are used as solvents and reagents. They are also employed in aerosols, adhesives, dry cleaning, etc. [1] Cl-VOCs are mainly regarded as xenobiotics, resistant to biodegradation and, hence, persistent in the environment. Most of them are toxic or carcinogenic and present potential hazard under exposure [2]. Therefore, Cl-VOCs are classified nowadays as hazardous gas pollutants and were included in the list of the seventeen highly harmful chemicals targeted in the emissions reduction effort of the U.S. Environmental Protection Agency [3,4]. Emissions of these compounds to the atmosphere contribute to the destruction of the ozone layer, to the formation of photochemical smog and to global warming. Hence, they are restricted by strong legal regulations. This enforces the need of developing effective technologies for the treatment of residual streams contaminated with Cl-VOCs. This paper will focus in three of the most common chlorinated compounds in off gases: monochloromethane (MCM), dichloromethane (DCM) and chloroform (TCM), which are associated to a number of industrial processes.

Nowadays, the main technique for the removal of these pollutants is incineration, but it may lead to more hazardous byproducts than the original contaminants, such as phosgene, dioxins and furans [5,6]. On the other hand, at low Cl-VOCs concentration the use of catalysts is required for reducing the thermal needs [7,8]. Thus, some other solutions are being investigated [9-11]. Hydrodechlorination using different active catalyst, like Pt or Pd, is one of the most promising [12-14]. High conversions have been reported for the most reactive chloromethanes (TCM>DCM>MCM), but catalyst deactivation is so far a main drawback [15-17]. Biological treatments using biofilters and biotrickling filters have been also studied [18-20].

Adsorption, absorption and condensation are the three most common non-destructive techniques for the removal/recovery of Cl-VOCs from gas streams [21-24]. Adsorption with activated carbon (AC) has been widely used for the removal of gaseous organic pollutants [25,26]. The application of different complex sorbent materials for Cl-VOCs adsorption has been reported in the literature [27,28]. Long *et al.* [27] achieved high adsorption capacities for TCM by means of a hypercrosslinked polymer as adsorbent. ACs present unique chemical and physical properties that make them well-known useful adsorbents [29,30]. Although AC adsorption has been used for decades in industry [31], the

question of the interactions between the adsorptive molecules and the AC surface is still open for a better understanding. The case of Cl-VOCs entails a particular interest due to their significance as hazardous pollutants [31].

In the present work, column adsorption experiments of three Cl-VOCs (monochlorometane, dichloromethane and chloroform) at low concentration using a commercial AC supplied by Merck have been carried out. Firstly, the influence of several variables (inlet concentration, temperature, pressure, gas flow rate and bed length) has been analyzed in order to optimize the operating condition for an effective adsorption of DCM. The breakthrough curves are described by a two-parameter theoretical model introduced by Yoon and Nelson [28,32] which was demonstrated that successfully predicts experimental adsorption data for a wide variety of gas solutes (including chlorinated compounds) onto AC at different operating concentrations and flow rates, allowing a better understanding of the specific factors influencing contaminant breakthrough [28,33]. The length of the mass transfer zone (H_{MTZ}), which characterizes the wave front of the fixed-bed column, has been also estimated since it is useful information for design considerations. Subsequently, the quantum-chemical COSMO-RS (Conductor-like Screening Model for Real Solvents) model, developed by Klamt and co-workers [34], is used to analyze the Cl-VOC-AC interactions. Previous works have showed that COSMO-RS method can successfully be applied to predict thermodynamic adsorption [35,36] and absorption [37-40] data. In this work, COSMO-RS predictions of Henry's law constants, as thermodynamic parameter of reference for solute-adsorbent interactions of MCM, DCM and TCM in differently functionalized AC models (Figure 1) have been performed, with the aim of designing tailor-made AC adsorbents with improved surface chemistry for selective adsorption of Cl-VOCs. Finally, the influence of the surface chemical composition of AC on the adsorbent performance has been experimentally evaluated by testing thermally and chemically treated ACs showing different surface polarity. These ACs have been tested as adsorbents in fixed-bed experiments for MCM, DCM and TCM. The characterization of the modified ACs by 77K N₂ adsorption-desorption and temperature programmed desorption (TPD) allows correlating the porous structure and surface chemistry of the adsorbents with their capacity for retaining Cl-VOC from gas streams.

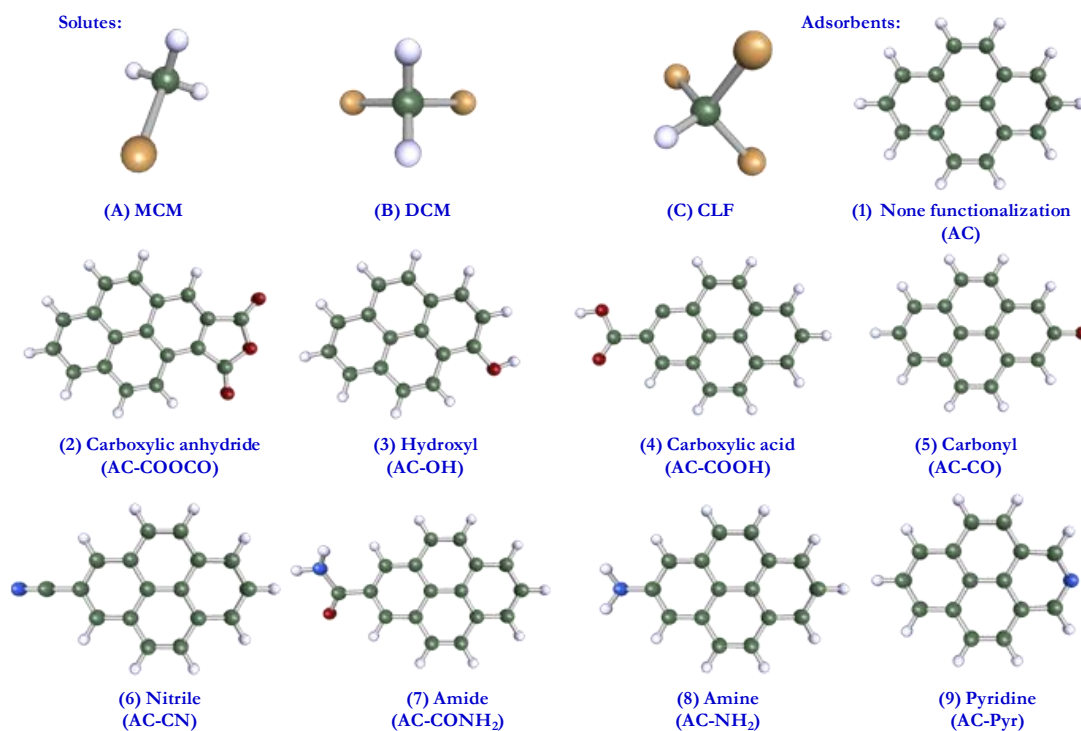


Figure 1. Molecular models of Cl-VOCs and the nine different functionalized ACs tested.

2. Experimental

2.1. Materials

A commercial AC supplied by Merck (AC-MkU) was used as adsorbent both virgin and after modification by oxidative treatments with nitric acid and ammonium persulfate. These two reagents were supplied, respectively, by Riedel de Haën and Sigma-Aldrich (both with purity >98%). Nitric acid treatment was carried out by boiling 1 g of AC in 10 mL of 6 N nitric acid solution for 20 minutes as described elsewhere [41], giving rise to AC-MkN. Oxidation with ammonium persulfate was performed by treating 1 g of AC in 10 mL of 1 M solution at room temperature [42], leading to AC-MkS. After these treatments the samples were washed with distilled water until neutrality and dried overnight at 100 °C. Finally, the ACs were grinded and the fraction between 0.1-0.5 mm particle size was separated by sieving and used in the experiments.

Commercial mixtures of N₂ with MCM, DCM and TCM (at 4000 ppmv in all cases) and bare N₂ (purity ~99.999%) were supplied by Praxair.

2.2. Adsorption experiments

The adsorption of Cl-VOCs was evaluated in a continuous flow system (depicted in Figure 2, Microactivity-Reference unit, PID End&Tech), consisting basically of a quartz fixed-bed column (1/4 inch diameter), coupled to a gas chromatograph with a flame ionization detector (Varian 450-GC). Experiments were conducted under different conditions of temperature, pressure, total gas flow, inlet chloromethane concentration and bed length. Desorption experiments were performed after exhaustion of the adsorbents using the same experimental set-up, passing a N₂ flow of 100 mL·min⁻¹ through the column.

The inlet gas, with a chloromethane concentration from 200 to 4000 ppmv, was prepared by mixing adequate proportions of the starting chloromethane/N₂ commercial mixture and N₂. The values of initial concentration (C_0) reported are those registered by gas chromatograph.

The porous structure of the starting and modified AC was characterized from -196 °C N₂ adsorption–desorption using a Micromeritics apparatus (Tristar II 3020 model). The samples were previously outgassed at 150 °C for 8 h to a residual pressure of 10⁻⁵ Torr. The BET equation was used to obtain the apparent surface area (A_{BET}) at relative pressure between 0.01 and 0.25 [43] and the Dubinin–Radushkevich equation for micropore volume estimation. The difference between the volume of N₂ adsorbed (as liquid) at 0.95 relative pressure and the micropore volume was taken as mesopore volume and DFT method was used to obtain the pore size distribution of the ACs [44].

The amount of surface oxygen groups (SOGs) of the ACs was determined by temperature programmed desorption (TPD). The evolved amounts of CO and CO₂ were analyzed by means of a non-dispersive infrared absorption analyzer (Siemens, model Ultramat 22). The CO and CO₂ TPD profiles were deconvoluted using PeakFit 4.12, selecting a multiple Gaussian function to fit each deconvolution peak [45]. TPD experiments were carried out by heating 0.1 g of the AC sample up to 1100 °C in an electrically heated vertical quartz tube under continuous N₂ flow of 1 NL·min⁻¹ at a heating rate of 10 °C·min⁻¹.

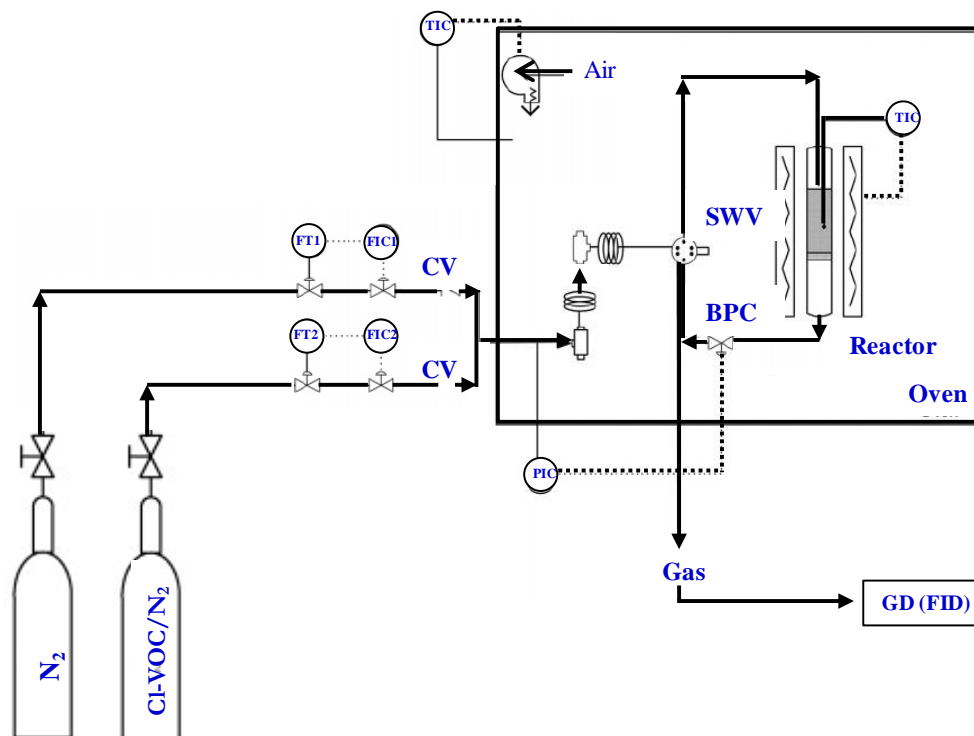


Figure 2. Schematic diagram of the gas adsorption system.

2.3. Computational details

The molecular geometry of all compounds (MCM, DCM, TCM and AC models) was optimized at the B3LYP/6-31++G** computational level in the ideal gas phase using the quantum chemical Gaussian03 package [46]. Vibrational frequency calculations were performed in each case to confirm the presence of an energy minimum. Once the molecular models were optimized, Gaussian03 was used to compute the COSMO files. The ideal screening charges on the molecular surface for each species were calculated by the continuum solvation COSMO model using BVP86/TZVP/DGA1 level of theory. Subsequently, COSMO files were used as an input in COSMOthermX [47] code to calculate the thermodynamic properties (Henry's law constants of Cl-VOCs for different AC models). According to our chosen quantum method, the functional and the basis set, we used the corresponding parameterization (BP_TZVP_C21_0108) for COSMO-RS calculations in COSMOtherm code.

3. Results

3.1. Analysis of operating conditions

Figures 3 to 7 depict the breakthrough curves obtained for the adsorption of DCM onto the commercial AC-MkU at the different operating conditions. For the sake of comparison, we have obtained the values of DCM adsorption capacity at saturation (q_s) of AC-MkU from the breakthrough curves for each experiment, calculated by:

$$q_s = \frac{Q}{m} \int_0^{t_s} C_0 - C dt \quad \text{eq. V.1}$$

where Q is the gas flow rate ($\text{N}\cdot\text{L}\cdot\text{min}^{-1}$); m is the mass of adsorbent in the column (mg); t is the time flow at which $C=C_0$ and C_0 and C the inlet and outlet DCM concentrations ($\text{mg}\cdot\text{L}^{-1}$). Also, the theoretical model developed by Yoon and Nelson [32,48-50] was applied to describe the breakthrough curves, which were fitted to the expression:

$$t = t_{0.5} + \frac{1}{k} \ln \frac{C}{C_0 - C} \quad \text{eq. V.2}$$

where t is the operation time (min) and $t_{0.5}$ is the time at which the outlet concentration is one half of the inlet and k is a proportionality constant (h^{-1}). The parameter k of Yoon and Nelson model is named an effective kinetic constant depending on a dimensionless adjustable constant, the inlet concentration of contaminant, the gas flow rate and the mass of adsorbent. This model has been successfully applied to describe the breakthrough curves of the fixed-bed adsorption for different contaminant gases onto solid sorbents [32,48-50], including a recent treatment for Cl-VOCs [27], gathering in simple parameter information about the removal efficiency.

In addition, the length of mass transfer zone (H_{MTZ}) has been estimated from the breakthrough curves using the expression:

$$H_{MTZ} = H \cdot \frac{(t_{0.95} - t_{0.05})}{t_{0.95}} \quad \text{eq. V.3}$$

where H is the length of the entire AC bed in the column, $t_{0.95}$ and $t_{0.05}$ are the times at which the outlet DCM concentrations are 95 and 5% of the inlet one, respectively.

Table 1 summarizes the results of the adsorption experiments carried out with DCM and the original activated carbon AC-MkU at the different operating conditions tested, including the q_s and H_{MTZ} values of k from Yoon and Nelson model as well as the correlation coefficients. As can be seen, the experimental breakthrough curves are fairly well described by the Yoon and Nelson model.

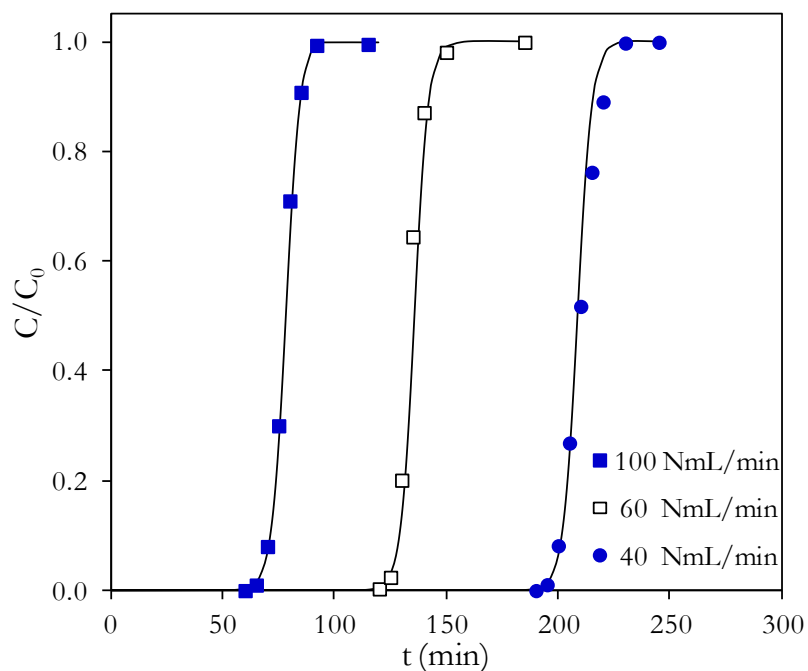


Figure 3. Experimental (dots) and predicted (lines) breakthrough curves of DCM adsorption with AC-MkU at different gas flow rates. Experiments carried out with 250 mg of AC-MkU, ~1000 ppmv of inlet DCM/N₂ concentration, 35 °C and 1.5 atm.

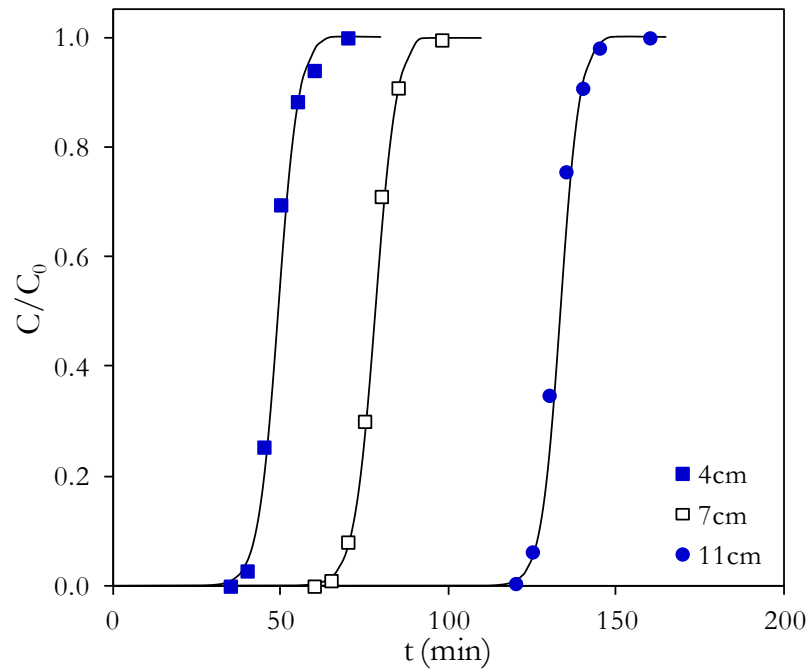


Figure 4. Experimental (dots) and predicted (lines) breakthrough curves of DCM adsorption with AC-MkU using different bed lengths. Experiments carried out at 1000 ppmv of inlet DCM/N₂ concentration, 35 °C, 1.5 atm and 100 N mL·min⁻¹ of gas flow rate.

As expected, the saturation capacity (q_s) is neither affected by the gas flow-rate (Q , Figure 3) nor by the amount of AC (m , Figure 4) provided the inlet DCM concentration is maintained practically constant. Varying the amount of adsorbent (AC-MkU) in the column gives rise to different bed lengths and, consequently, contact times. No significant effects on the kinetics of adsorption process were observed, as can be seen from the values of k and H_{MTZ} of Table 1. On the other hand, looking at the length of the mass-transfer zone (H_{MTZ}) it consistently increases with the gas flow-rate.

Table 1. Operating conditions and results of the adsorption experiments of DCM with commercial AC-MkU.

Operating conditions								
Q (N mL·min ⁻¹)	m (g)	C ₀ (ppmv)	T (°C)	P (atm)	q _s (mg·g ⁻¹)	H _{MTZ} (cm)	k (h ⁻¹)	R ²
100	0.25	1015	35	1.5	111.1	1.4	21.8	0.995
60	0.25	1003	35	1.5	115.7	0.9	19.6	0.950
40	0.25	983	35	1.5	115.9	0.6	18.7	0.977
100	0.42	1000	35	1.5	111.7	1.3	20.9	0.957
100	0.25	1015	35	1.5	111.1	1.4	21.8	0.995
100	0.16	1000	35	1.5	111.0	1.2	19.8	0.952
100	0.25	3998	35	1.5	200.8	1.3	48.4	0.937
100	0.25	2711	35	1.5	165.8	1.0	47.1	0.982
100	0.25	2001	35	1.5	187.1	1.1	30.4	0.982
100	0.25	1431	35	1.5	150.5	1.3	24.1	0.997
100	0.25	1015	35	1.5	111.1	1.4	21.8	0.995
100	0.25	808	35	1.5	108.0	1.2	19.1	0.979
100	0.25	500	35	1.5	107.5	0.8	17.0	0.952
100	0.25	207	35	1.5	61.7	1.0	10.3	0.992
100	0.25	996	100	1.5	29.4	2.7	33.9	0.950
100	0.25	1047	75	1.5	44.8	2.0	32.8	0.989
100	0.25	1024	50	1.5	81.7	1.3	29.9	0.958
100	0.25	1015	35	1.5	111.1	1.4	21.8	0.995
100	0.25	1066	35	4	156.1	0.8	27.5	0.979
100	0.25	1012	35	3	143.4	0.9	27.2	0.954
100	0.25	1001	35	2	121.7	1.1	24.5	0.999
100	0.25	1015	35	1.5	111.1	1.4	21.8	0.995

Figure 5A shows the breakthrough curves for DCM adsorption with AC-MkU at 35 °C and different DCM inlet concentrations. The values of adsorption capacity at saturation (q_s) and the rate constant (k) are collected in Table 1. The breakthrough curve is steeper at higher inlet concentration, since the concentration gradient (driving force) increases giving rise to higher values of the kinetic constant k . Obviously, saturation of the adsorbent bed occurs in less time due to the higher DCM mass flow. From these breakthrough curves, the adsorption isotherm of DCM can be obtained, being depicted in Figure 5B. The experimental data were fitted to the well-known Langmuir equation:

$$q_e = \frac{q_m B P_e}{1 + B P_e} \quad \text{eq. V.4}$$

where q_m refers to the monolayer adsorption capacity, P_e is the partial pressure of DCM at equilibrium and B is the Langmuir constant. The equilibrium data of Figure 5B reveal a fairly high adsorption capacity of AC-MkU for DCM (Langmuir isotherm parameters: $q_m = 249 \text{ mg}\cdot\text{g}^{-1}$ and $B = 0.0012 \text{ KPa}^{-1}$). The adsorption capacity value compares very well with the reported by Long *et al.* [27] using a complex hydrophobic hypercrosslinked polymer, recently proposed as an effective adsorbent for removal of Cl-VOCs.

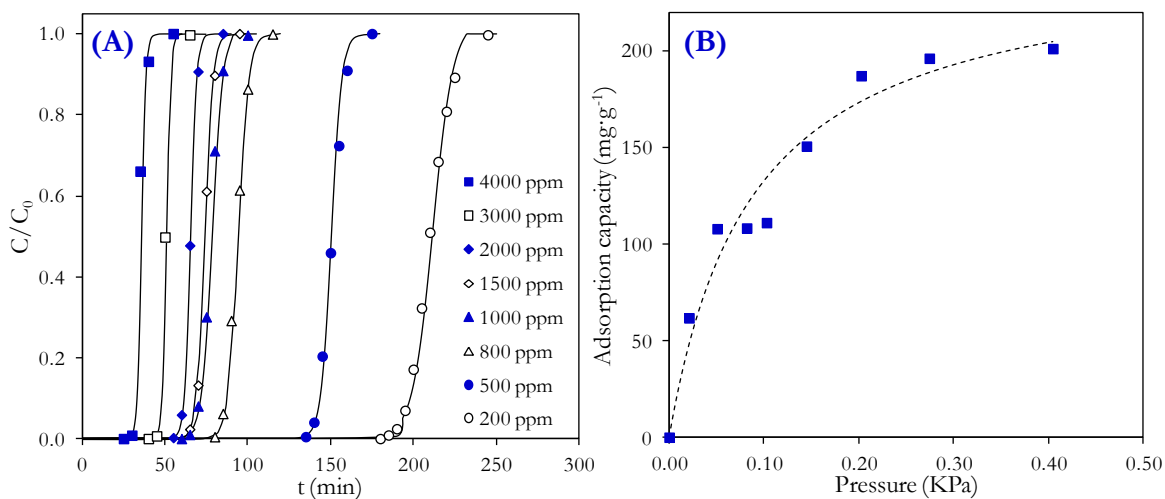


Figure 5. (A) Experimental (dots) and predicted (lines) breakthrough curves at different DCM/ N_2 inlet concentrations; and (B) adsorption isotherm obtained from the breakthrough curves. Experiments carried out with 250 mg of AC-MkU, 35 °C, 1.5 atm and 100 $\text{N mL}\cdot\text{min}^{-1}$ gas flow rate.

Another important operating condition is temperature. Figure 6 shows the breakthrough curves obtained at 35, 50, 75 and 100 °C for DCM adsorption with AC-MkU at 1000 ppmv inlet concentration. The adsorption capacity is significantly higher at lower temperature, indicative of physical adsorption. The favorable effect of temperature on the adsorption rate is confirmed by the k values (Table 1). Increasing the temperature leads to a higher volumetric gas flow giving rise to higher H_{MTZ} values in spite of higher adsorption rate.

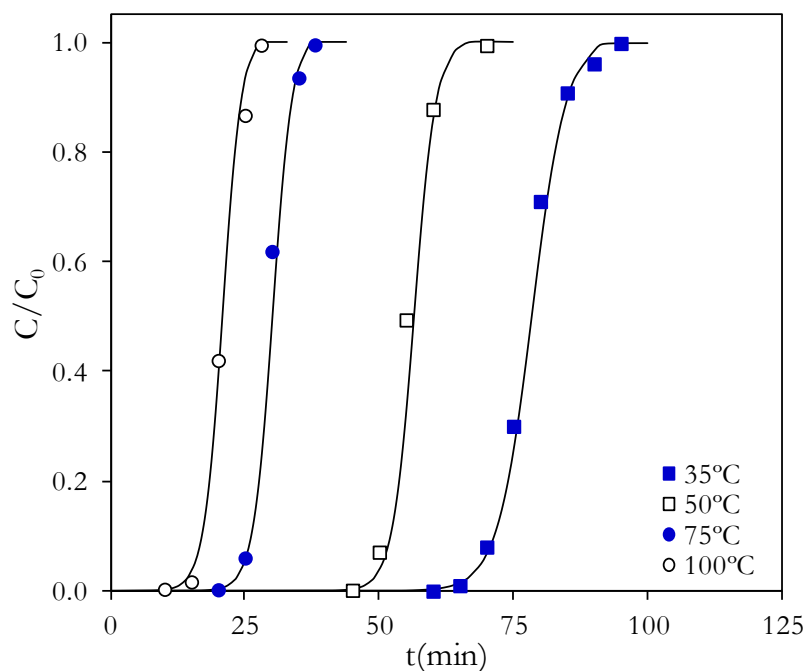


Figure 6. Experimental (dots) and predicted (lines) breakthrough curves of DCM adsorption at different temperatures. Experiments carried out with 250 mg of AC-MkU, 1000 ppmv of initial DCM/N₂ concentration, at 1.5 atm and 100 N mL·min⁻¹ gas flow rate.

Saturation capacity (q_s) increases with the operating pressure due to the higher relative pressure of DCM (Figure 7). Increasing the pressure at the same normal flow-rate (four last experiments of Table 1) also decreases H_{MTZ} due to the lower values of superficial velocity. Simultaneously the higher driving force improves the adsorption rate as can be seen from the corresponding k values of Table 1.

Regeneration of the adsorbent is an important issue regarding the potential application of adsorption. Figure 8 shows examples of DCM adsorption/desorption curves obtained with AC-MkU. Desorption was performed under continuous N₂ flow (100 NmL·min⁻¹) at the same temperature and pressure than adsorption (35 °C and 1 atm in this case). Complete desorption of DCM was achieved and the adsorption capacity after four successive regeneration cycles remained virtually constant.

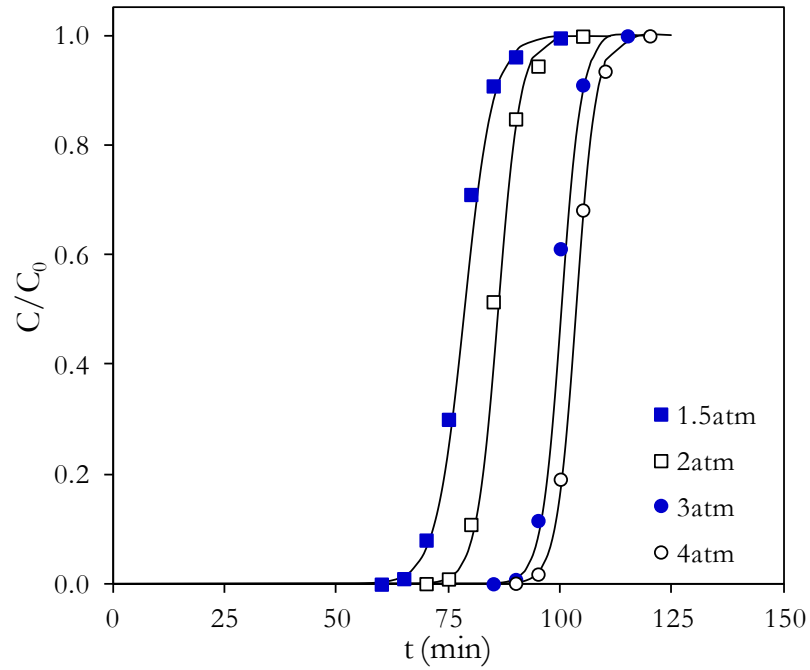


Figure 7. Experimental (dots) and predicted (lines) breakthrough curves of DCM adsorption with AC-MkU at different total pressures. Experiments carried out with 250 mg of AC-MkU, 1000 ppmv of inlet DCM/N₂ concentration, 35 °C and 100 N mL·min⁻¹ gas flow rate.

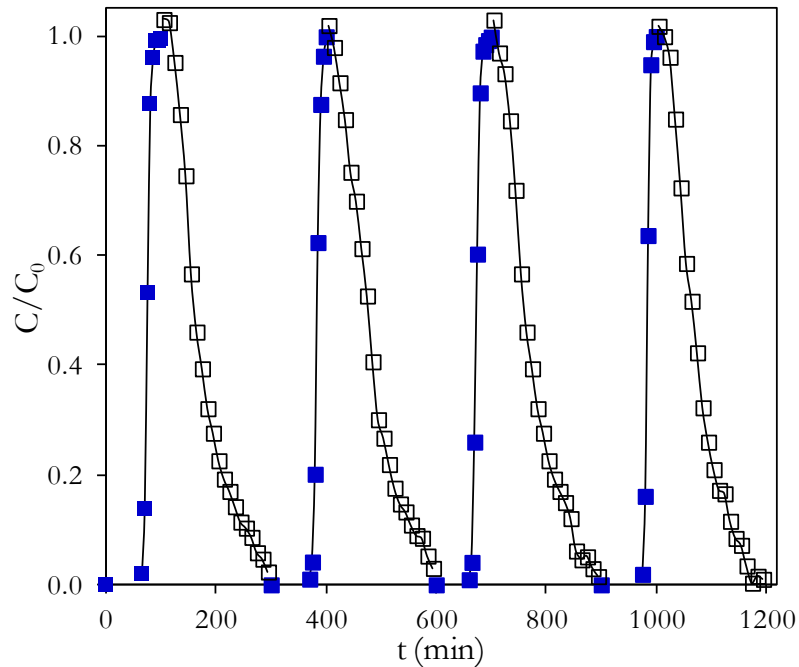


Figure 8. Experimental adsorption (■) desorption (□) curves of DCM. Experiments carried out with 250 mg of AC-MkU, at 35 °C and 1.5 atm, 1000 ppmv DCM/N₂ and 100 N mL·min⁻¹ of total gas flow.

3.2. Adsorption with chemically modified ACs.

It is well-known that both the porous structure and the surface chemistry of activated carbons are important issues determining the adsorption of different solutes [51]. Increasing the surface area of sorbent materials will generally lead to improved adsorption, but the effect of surface chemical functional groups of ACs on the solute adsorption is closely related to the chemical nature of the adsorptive. Therefore, we have analyzed the possible interactions between different functional groups in the surface of AC and Cl-VOCs. For this purpose, molecular models of AC with a wide variety of functional groups (Figure 1) were optimized by quantum-chemical calculations and used in COSMO-RS to calculate the Henry constants (partition coefficient between gas phase and AC) for the three Cl-VOCs (MCM, DCM and TCM). Those Henry constants were used for predicting the adsorption capacities. The results are collected in Table 2. The numerical value of Henry constant is reversely proportional to the predicted concentration of Cl-VOC retained in the AC phase, following the expression:

$$K_H = \frac{P_{eq}^{Cl-VOC}}{x_{AC}^{Cl-VOC}} \quad \text{eq. V.5}$$

where K_H is the Henry constant, x_{AC}^{Cl-VOC} is the mole fraction of the Cl-VOC solute in the AC phase and P_{eq}^{Cl-VOC} is the partial pressure of Cl-VOC compound in the gas phase. Therefore, a lower value of K_H means higher affinity of the adsorbent material for Cl-VOC compound. According with the values of Table 2 the adsorption capacities follow the order TCM > DCM > MCM for all the AC models studied. Therefore, the predicted uptake of Cl-VOCs by ACs increases with the number of chlorine atoms of the molecule, consistently with the lower volatility of the solute. In addition, the results of Table 2 indicate that the adsorption capacity is affected by the nature of the functional groups on the AC surface. The presence of hydrogen-bond (HB) acceptor groups, as carbonyl or carboxylic anhydride, enhances solute-AC interactions diminishing K_H values in some extent, being this effect more significant as the acidic character of Cl-VOCs increases in the order TCM>DCM>MCM. On the other hand, the functionalization of AC by surface oxygen groups (SOGs) with dominant HB donor character, as carboxylic acid or hydroxyl, results in similar or higher K_H values. In order to obtain further insights on the interactions between the components involved in adsorption phenomena, COSMO-RS analysis has been completed by calculating the excess enthalpies (H_E) of the mixture formed by AC and TCM, used as reference of Cl-VOC compound (Table S1 in Supplementary material), together with the contribution of the polar, hydrogen-bonding

and Van der Waals interactions to the H_E values. COSMO-RS calculations revealed an exothermic mixing of TCM with AC functionalized by HB-acceptor SOGs (AC-COOCO and AC-CO). The attractive hydrogen-bonding and polar interactions are the main responsible of this behavior and explain the lower K_H values obtained for AC-COOCO and AC-CO respect to AC specie. On the contrary, HB donor groups (AC-COOH and AC-OH) on AC surface promote repulsive hydrogen-bond interactions with the acidic TCM compound, giving a less favored mixture, in correspondence with the higher values of K_H reported in Table 2.

Table 2. Henry constants (bar) of MCM, DCM and TCM in the AC models showed in Figure 1 predicted by COSMO-RS at 35 °C.

AC model Figure 1	Functionalization	MCM	DCM	TCM
(1) AC	None	5.35	0.69	0.33
(2) AC-COOCO	carboxylic anhydride	4.78	0.46	0.24
(3) AC-OH	hydroxyl	4.85	0.68	0.38
(4) AC-COOH	carboxylic acid	5.98	0.69	0.33
(5) AC-CO	carbonyl	4.78	0.41	0.18
(6) AC-CN	nitrile	5.22	0.53	0.26
(7) AC-CONH ₂	amide	6.54	0.65	0.33
(8) AC-NH ₂	amine	4.95	0.64	0.38
(9) AC-Pyr	pyridine	5.20	0.37	0.12

In order to check experimentally the influence of the surface chemistry of AC on Cl-VOCs adsorption, the starting commercial AC (AC-MkU) was subjected to thermal treatment in N₂ atmosphere at 900 °C (AC-Mk900) and to oxidative treatment with nitric acid (AC-MkN) and ammonium persulfate (AC-MkS). Figure 9 shows the TPD profiles of these activated carbons. Both oxidized carbons, AC-MkN and AC-MkS, present a substantially increased amount of SOGs with respect to the starting activated carbon, evidenced by the significantly higher amounts of CO and CO₂ evolved upon TPD, whereas the thermal treatment in inert atmosphere provokes a loose of SOGs. Particularly significant was the oxidation with nitric acid, where the amount of oxygen surface groups increased by threefold (Table 3). It is also remarkable that the oxygen groups with hydrogen bond acceptor character (carbonyls, anhydrides) are majority in the adsorbent surface of all ACs. Table 3 shows that all used ACs presents high microporosity and an average pore with of 2.1-2.5 nm. Characterization analysis also showed that pore structure of the AC remains almost unchanged after the different treatments. Only small although monotonical decrease of the BET surface area can be observed as the amount of SOG increases. Untreated AC-MkU

presents the lowest mesopore volume and that a slight increase in mesoporosity takes place as a result of oxidation. This observation is in agreement with the increase in average pore size (Table 3) and with porosity generation upon oxidative treatments previously reported [52]. In addition to this, an increase in average pore size was observed for the activated carbon subjected to thermal treatment (AC-Mk900), which can be ascribed to burn-off generated by the desorption of SOGs [53].

Table 3. Textural characteristics and assessment of oxygen surface groups from deconvolution of TPD profiles for the starting and modified ACs.

	A_{BET} ($\text{m}^2 \cdot \text{g}^{-1}$)	Pore width (nm)	$V_{\text{microp.}}$ V ($\text{cm}^3 \cdot \text{g}^{-1}$)	$V_{\text{mesop.}}$	Groups evolved as CO_2 ($\mu\text{mol} \cdot \text{g}^{-1}$)				Groups evolved as CO ($\mu\text{mol} \cdot \text{g}^{-1}$)					
					Carboxylic acids	Anhydrides	Lactones	Pirones	Total	Anhydrides	Phenols	Carbonyl	Chromenes	Total
AC-MkU	927	2.13	0.36	0.22	63.1	19.9	39.1	60.7	182.8	50.4	73.9	315.1	51.0	490.4
AC-Mk900	906	2.35	0.36	0.23	37.9	27.5	18.6	27.7	111.7	47.5	57.0	69.2	148.5	322.2
AC-MkS	872	2.47	0.34	0.26	198.5	16.3	53.5	83.4	351.7	196.2	158.6	532.0	165.7	1052.5
AC-MkN	856	2.38	0.33	0.24	209.3	182.8	53.5	128.1	573.8	437.5	351.8	874.9	214.6	1878.8

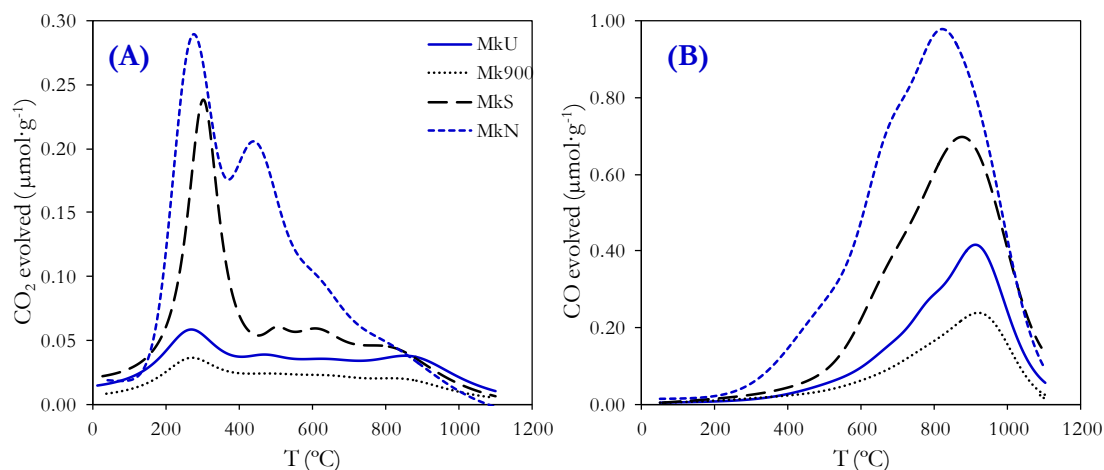


Figure 9. CO_2 (A) and CO (B) TPD profiles for the starting and modified AC.

Figure 10 compares the results of column tests of TCM, DCM and MCM adsorption with the starting and modified ACs. Table 4 summarizes the operating conditions and the values obtained for q , k and H_{MTZ} . As can be seen, the adsorption capacities significantly increased with the number of chlorine atoms of the Cl-VOC molecule, in agreement with COSMO-RS predictions. With regard to the effect of the surface chemistry of the ACs, it can be seen that the adsorption capacity increases in the order AC-Mk900 < AC-MkU < AC-MkS < AC-MkN, i.e. with the amount of SOGs of the AC, despite the small decrease of surface area. Oxidation is not selective at both HB acceptor and donor SOGs are generated (Table 3), however the attractive interactions with the dominating HB-acceptor SOGs prevails and the uptake increase upon oxidation, confirming COSMO-RS predictions respect to the positive effect of hydrogen-bond acceptor groups on the adsorption of chloromethanes.

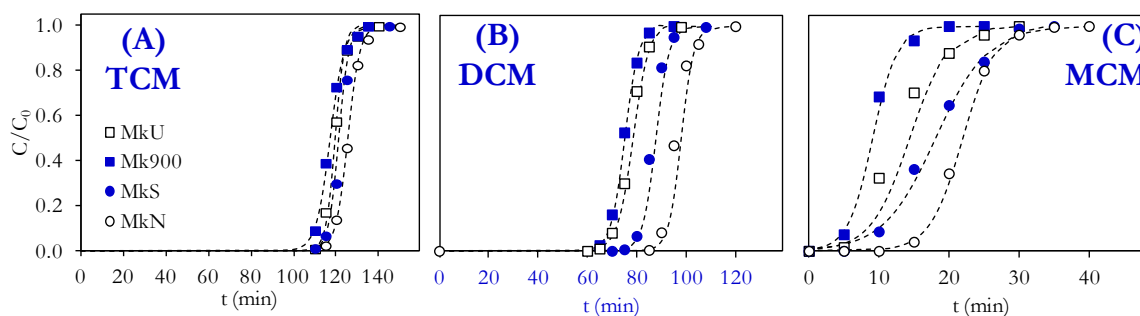


Figure 10. Experimental (dots) and predicted (lines) breakthrough curves of Cl-VOCs adsorption with the starting and modified ACs (250 mg AC-MkU, 35 °C, 100 N mL·min⁻¹ total gas flow and 1000 ppmv of inlet Cl-VOC/N₂ concentration).

Table 4. Results of the column tests of Cl-VOCs adsorption with the starting and modified ACs.

		Operating conditions								
Solute	Adsorbent	Q (N mL·min ⁻¹)	m (g)	C ₀ (ppmv)	T (°C)	P (atm)	q _s (mg·g ⁻¹)	H _{MTZ} (cm)	k (h ⁻¹)	R ²
TCM	AC-Mk900	100	0.25	846	35	1.5	197.3	1.1	18.0	0.989
TCM	AC-MkU	100	0.25	854	35	1.5	203.1	0.7	27.5	0.979
TCM	AC-MkS	100	0.25	849	35	1.5	205.0	0.8	25.0	0.993
TCM	AC-MkN	100	0.25	856	35	1.5	213.4	0.9	21.0	0.999
DCM	AC-Mk900	100	0.25	971	35	1.5	103.0	1.4	21.2	0.998
DCM	AC-MkU	100	0.25	1015	35	1.5	111.1	1.4	21.8	0.995
DCM	AC-MkS	100	0.25	971	35	1.5	116.4	1.1	23.2	0.956
DCM	AC-MkN	100	0.25	995	35	1.5	123.9	1.0	22.6	0.987
MCM	AC-Mk900	100	0.25	1068	35	1.5	8.4	5.1	34.0	0.986
MCM	AC-MkU	100	0.25	1135	35	1.5	14.1	5.1	21.9	0.935
MCM	AC-MkS	100	0.25	1046	35	1.5	16.2	5.3	16.2	0.983
MCM	AC-MkN	100	0.25	1192	35	1.5	22.2	3.3	25.6	0.995

4. Conclusions

Efficient and fast adsorption of dichloromethane from gas stream onto commercial activated carbon was proved by fixed-bed experiments at a wide range of operating conditions (total gas flow, bed length, inlet concentration, temperature and pressure). The effects of these operating conditions on the equilibrium capacity and the rate of adsorption have been analyzed. Desorption experiments showed that complete regeneration of the exhausted adsorbent can be successfully achieved under mild conditions (atmospheric pressure and room temperature). The quantum-chemical COSMO-RS method allowed predicting the relative order of adsorption of chloromethanes (TCM > DCM > MCM) and the favorable effect of introducing surface oxygen groups on the activated carbon. Those theoretical findings were experimentally confirmed indicating that the COSMO-RS method provides an interesting tool as a guide for activated carbon tuning addressed to improved adsorption of specific compounds from gas streams.

References

- [1] de Pedro ZM, Gomez-Sainero LM, Gonzalez-Serrano E, Rodriguez JJ. Gas-phase hydrodechlorination of dichloromethane at low concentrations with palladium/carbon catalysts. *Ind. Eng. Chem. Res.* 2006;45(23):7760-6.
- [2] Iranpour R, Coxa H, Deshusses M, Schroeder E. Literature review of air pollution control biofilters and biotrickling filters for odor and volatile organic compound removal. *Environ. Prog.* 2005;24(3):254-67.
- [3] Dobrzynska E, Posniak M, Szewczynska M, Buszewski B. Chlorinated Volatile Organic Compounds-Old, However, Actual Analytical and Toxicological Problem. *Crit. Rev. Anal. Chem.* 2010;40(1):41-57.
- [4] W.J. Hayes ERL. *Handbook of Pesticide Toxicology*. San Diego: Academic Press; 1991.
- [5] Verhulst D, Buekens A, Spencer P, Eriksson G. Thermodynamic behavior of metal chlorides and sulfates under the conditions of incineration furnaces. *Environ. Sci. Technol.* 1996;30(1):50-6.
- [6] Buekens A, Huang H. Comparative evaluation of techniques for controlling the formation and emission of chlorinated dioxins/furans in municipal waste incineration. *J. Hazard. Mater.* 1998;62(1):1-33.
- [7] Ballikaya M, Atalay S, Alpay H, Atalay F. Catalytic combustion of methylenechloride. *Combustion Sci. Technol.* 1996;120(1-6):169-84.
- [8] Atalay S, Alpay H, Atalay F. Catalyst preparation and testing for catalytic combustion of chloromethanes. *Principles and methods for accelerated catalyst design and testing.* 2002;(69):355-364.
- [9] Li C, Lee W, Chen C, Wang Y. CH₂Cl₂ decomposition by using a radio-frequency plasma system. *Journal of Chemical Technology and Biotechnology* 1996;66(4):382-8.
- [10] Everaert K, Baeyens J. Catalytic combustion of volatile organic compounds. *J. Hazard. Mater.* 2004;109(1-3):113-39.
- [11] Wang J, Chen J. Removal of dichloromethane from waste gases with a bio-contact oxidation reactor. *Chem. Eng. J.* 2006;123(3):103-7.
- [12] Gomez-Sainero L, Seoane X, Arcoya A. Hydrodechlorination of carbon tetrachloride in the liquid phase on a Pd/carbon catalyst: kinetic and mechanistic studies. *Applied Catalysis B-Environmental* 2004;53(2):101-10.
- [13] Gomez-Sainero L, Seoane X, Fierro J, Arcoya A. Liquid-phase hydrodechlorination of CCl₄ to CHCl₃ on Pd/carbon catalysts: Nature and role of Pd active species. *Journal of Catalysis* 2002;209(2):279-88.

- [14] Gomez-Sainero L, Seoane X, Tijero E, Arcoya A. Hydrodechlorination of carbon tetrachloride to chloroform in the liquid phase with a Pd/carbon catalyst. Study of the mass transfer steps. *Chemical Engineering Science* 2002;57(17):3565-74.
- [15] Alvarez-Montero MA, Gomez-Sainero LM, Juan-Juan J, Linares-Solano A, Rodriguez JJ. Gas-phase hydrodechlorination of dichloromethane with activated carbon-supported metallic catalysts. *Chem. Eng. J.* 2010;162(2):599-608.
- [16] Alvarez-Montero MA, Gomez-Sainero LM, Martin-Martinez M, Heras F, Rodriguez JJ. Hydrodechlorination of chloromethanes with Pd on activated carbon catalysts for the treatment of residual gas streams. *Applied Catalysis B-Environmental* 2010;96(1-2):148-56.
- [17] Alvarez-Montero MA, Gomez-Sainero LM, Mayoral A, Diaz I, Baker RT, Rodriguez JJ. Hydrodechlorination of chloromethanes with a highly stable Pt on activated carbon catalyst. *Journal of Catalysis* 2011;279(2):389-96.
- [18] Zuber L, Dunn I, Deshusses M. Comparative scale-up and cost estimation of a biological trickling filter and a three-phase airlift bioreactor for the removal of methylene chloride from polluted air. *J. Air Waste Manage. Assoc.* 1997;47(9):969-75.
- [19] Cox H, Deshusses M, Converse B, Schroeder E, Iranpour R. Odor and volatile organic compound treatment by biotrickling filters: Pilot-scale studies at hyperion treatment plant. *Water Environ. Res.* 2002;74(6):557-63.
- [20] Yu Jian-ming, Chen Jian-meng, Wang Jia-de. Removal of dichloromethane from waste gases by a biotrickling filter. *Journal of Environmental Sciences-China* 2006;18(6):1073-6.
- [21] Anfruns A, Martin MJ, Montes-Moran MA. Removal of odourous VOCs using sludge-based adsorbents. *Chem. Eng. J.* 2011;166(3):1022-31.
- [22] Gallego E, Roca FJ, Perales JF, Guardino X. Comparative study of the adsorption performance of a multi-sorbent bed (Carbotrap, Carbopack X, Carboxen 569) and a Tenax TA adsorbent tube for the analysis of volatile organic compounds (VOCs). *Talanta* 2010;81(3):916-24.
- [23] Ren X, Chen C, Nagatsu M, Wang X. Carbon nanotubes as adsorbents in environmental pollution management: A review. *Chem. Eng. J.* 2011;170(2-3):395-410.
- [24] Ghoshal A, Manjare S. Selection of appropriate adsorption technique for recovery of VOCs: an analysis. *J. Loss. Prev. Process. Ind.* 2002;15(6):413-21.
- [25] Navarri P, Marchal D, Ginestet A. Activated carbon fibre materials for VOC removal. *Filtration Sep.* 2001;38(1):34-40.
- [26] Zhang X, Zhao X, Hu J, Wei C, Bi HT. Adsorption dynamics of trichlorofluoromethane in activated carbon fiber beds. *J. Hazard. Mater.* 2011;186(2-3):1816-22.
- [27] Long C, Liu P, Li Y, Li A, Zhang Q. Characterization of Hydrophobic Hypercrosslinked Polymer as an Adsorbent for Removal of Chlorinated Volatile Organic Compounds. *Environ. Sci. Technol.* 2011;45(10):4506-12.

- [28] Tsai W, Chang C, Ho C, Chen L. Adsorption properties and breakthrough model of 1,1-dichloro-1-fluoroethane on granular activated carbon and activated carbon fiber. *Sep. Sci. Technol.* 2000;35(10):1635-50.
- [29] Xiang Z, Lu Y, Gong X, Luo G. Adsorption and desorption of gaseous toluene by an adsorbent microcapsules column. *J. Hazard. Mater.* 2010;173(1-3):243-8.
- [30] Ahmaruzzaman M. Adsorption of phenolic compounds on low-cost adsorbents: A review. *Adv. Colloid Interface Sci.* 2008;143(1-2):48-67.
- [31] Khan F, Ghoshal A. Removal of Volatile Organic Compounds from polluted air. *J Loss Prev Process Ind.* 2000;13(6):527-45.
- [32] Yoon YH, Nelson JH. Application of Gas-Adsorption Kinetics .1. a Theoretical-Model for Respirator Cartridge Service Life. *Am. Ind. Hyg. Assoc. J.* 1984;45(8):509-16.
- [33] Aksu Z, Gonen F. Biosorption of phenol by immobilized activated sludge in a continuous packed bed: prediction of breakthrough curves. *Process Biochemistry* 2004;39(5):599-613.
- [34] Klamt A, Eckert F. COSMO-RS: a novel and efficient method for the a priori prediction of thermophysical data of liquids. *Fluid Phase Equilib.* 2003;205(2):357-.
- [35] Palomar J, Lemus J, Gilarranz MA, Rodriguez JJ. Adsorption of ionic liquids from aqueous effluents by activated carbon. *Carbon* 2009 6;47(7):1846-56.
- [36] Mehler C, Klamt A, Peukert W. Use of COSMO-RS for the prediction of adsorption equilibria. *AIChE journal* 2002;48(5):1093-99.
- [37] Palomar J, Gonzalez-Miquel M, Bedia J, Rodriguez F, Rodriguez JJ. Task-specific ionic liquids for efficient ammonia absorption. *Separation and Purification Technology* 2011;82(0):43-52.
- [38] Bedia J, Palomar J, Gonzalez-Miquel M, Bedia J, Rodriguez F, Rodriguez JJ. Screening ionic liquids as suitable ammonia adsorbents on the basis of thermodynamic and kinetic analysis. *Separation and Purification Technology* 2012;(95):188–195.
- [39] Palomar J, Gonzalez Miquel M, Polo A, Rodriguez F. Understanding the Physical Absorption of CO₂ in Ionic Liquids Using the COSMO-RS Method. *Industrial engineering chemistry research* 2011;50(6):3452-63.
- [40] Gonzalez-Miquel M, Palomar J, Omar S, Rodriguez F. CO₂/N₂ Selectivity Prediction in Supported Ionic Liquid Membranes (SILMs) by COSMO-RS. *Ind. Eng. Chem. Res.* 2011;50(9):5739-48.
- [41] Prado-Burguete C, Linares-Solano A, Rodriguez-Reinoso F, Delecea C. The Effect of Oxygen-Surface Groups of the Support on Platinum Dispersion in Pt/carbon Catalysts. *Journal of Catalysis* 1989;115(1):98-106.
- [42] Moreno-Castilla C, Carrasco-Marin F, Mueden A. The creation of acid carbon surfaces by treatment with (NH₄)₂S₂O₈. *Carbon.* 1997;35(10-11):1619-26.

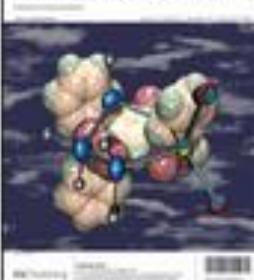
- [43] Kruk M, Jaroniec M, Gadkaree KP. Nitrogen adsorption studies of novel synthetic active carbons. *J. Colloid Interface Sci.* 1997;192(1):250-6.
- [44] Sing K. Adsorption methods for the characterization of porous materials. *Advances in colloid and interface science* 1998;76:3-11.
- [45] Rey A, Faraldos M, Casas JA, Zazo JA, Bahamonde A, Rodriguez JJ. Catalytic wet peroxide oxidation of phenol over Fe/AC catalysts: Influence of iron precursor and activated carbon surface. *Applied Catalysis B-Environmental* 2009;86(1-2):69-77.
- [46] Frisch MJ, Trucks GW, Schlegel HB, Scuseria GE, Robb MA, Cheeseman JR, et al. Gaussian03, revision B.05; 2004.
- [47] COSMOtherm C2.1, release 01.06. Leverkusen, Germany: GmbH & Co. KG; 2003.
- [48] Yoon YH, Nelson JH. Application of Gas-Adsorption Kinetics .2. a Theoretical-Model for Respirator Cartridge Service Life and its Practical Applications. *Am. Ind. Hyg. Assoc. J.* 1984;45(8):517-24.
- [49] Lodewyckx P, Wood G, Ryu S. The Wheeler-Jonas equation: a versatile tool for the prediction of carbon bed breakthrough times. *Carbon* 2004;42(7):1351-5.
- [50] Burkert CAV, Barbosa GNO, Mazutti MA, Maugeri F. Mathematical modeling and experimental breakthrough curves of cephalosporin C adsorption in a fixed-bed column. *Process Biochemistry* 2011;46(6):1270-7.
- [51] Marsh H, Rodriguez-Reinoso F. Activated carbon. Great Britain: Elsevier; 2006.
- [52] Mysyk R, Gao Q, Raymundo-Piñero E, Béguin F. Microporous carbons finely-tuned by cyclic high-pressure low-temperature oxidation and their use in electrochemical capacitors. *Carbon*. 2012;50(9):3367-74.
- [53] Heras F, Alonso N, Gilarranz MA, Rodriguez JJ. Activation of Waste Tire Char upon Cyclic Oxygen Chemisorption-Desorption. *Ind. Eng. Chem. Res.* 2009;48(10):4664-70.

Supplementary Material

Table S1. Excess enthalpies of the binary mixtures AC-TCM and the contribution of the different intermolecular interactions to these values predicted by COSMO-RS at 35 °C.

AC model	Figure 1	Functionalization	$H_E = H_{\text{Polar}} + H_{\text{HB}} + H_{\text{vdW}}$ (Cal/mol)			
			H_E	H_{Polar}	H_{HB}	H_{vdW}
(1)	AC	none	68	-29	0	97
(2)	AC-COOCO	carboxylic anhydride	-127	-130	-83	86
(3)	AC-OH	hydroxyl	144	26	33	85
(4)	AC-COOH	carboxylic acid	53	-62	33	83
(5)	AC-CO	carbonyl	-410	-232	-273	96
(6)	AC-CN	nitrile	-156	-164	-122	130
(7)	AC-CONH ₂	amide	-122	-96	-153	127
(8)	AC-NH ₂	amine	94	23	-29	100
(9)	AC-Pyr	pyridine	-728	-308	-537	118

ChemComm



Paper VI

*ENCAPSULATED IONIC LIQUIDS (ENILs): FROM CONTINUE TO
DISCRETE LIQUID PHASE*

205-222

J. Palomar, J. Lemus, N. Alonso-Morales, J. Bedia,

M. A. Gilarranz, J. J. Rodriguez

ENCAPSULATED IONIC LIQUIDS (ENILs): FROM CONTINUE TO
DISCRETE LIQUID PHASE.

Chemical Communications. 2012 (48) 10046-10048

Resumen

Este último capítulo muestra la preparación de un nuevo material denominado líquido iónico encapsulado (ENIL), que consiste en microcápsulas porosas de carbón con una gran cantidad de líquido iónico en su hueco interior. Este novedoso material puede contener hasta el 85% en masa de líquido iónico, pero con la ventaja de estar discretizado en microgotas de menos de 500 nm de diámetro, lo que hace que aumente el área de contacto respecto al líquido iónico aislado. Los materiales ENIL se han caracterizado por varias técnicas y se han empleado para la captura de amoníaco en medidas termogravimétricas y reactores de lecho fijo. Este material mixto (líquido iónico y carbón activo) mantiene las propiedades termodinámicas del líquido iónico, pero sus propiedades cinéticas han sido mejoradas. Por tanto, se presenta un material avanzado que permite pasar de un líquido iónico en su fase fluida a un material sólido, lo que abre la puerta a varios campos de aplicación, como pueden ser procesos catalíticos o de separación.

Abstract

This last chapter presents a new material called encapsulated ionic liquid (ENIL), consisting on ionic liquid introduced into hollow porous carbon submicrocapsules. The prepared ENIL systems contain $< 85\%$ in mass of IL but discretized in submicroscopic encapsulated drops with diameter < 500 nm, which drastically increases the surface contact area respect to the neat fluid. The prepared ENIL materials have been characterized by several techniques and tested for ammonia as capture in gravimetric and fixed-bed experiments. It was found that ENILs maintain the solvent capacity of the IL but significantly enhance the rate of mass transfer. Therefore, we present a new type of IL-advanced material, based on the idea of moving from continue to discrete fluid phase, with potential application in several fields, such as analysis, separation processes and catalysis.

1. Main text

Ionic liquids (ILs)[1,2] are being investigated in a wide diversity of fields involving chemistry [3,4], biochemistry [5], physics [6], engineering [7], material science [8,9], electrochemistry [10,11], polymer science [12,13], pharmacology [14] and many other areas. The increasing interest in academia and industry [15] (>15,000 publications and >3,000 patents) has resulted in a broad range of innovative IL applications, including catalysis [16,17], separation process [18,19], biomass conversion [20], analytics [21], nanoparticle synthesis [22], lubricants [23], thermal fluids [24] and electrochemical applications [25]. ILs present truly unique properties (low volatility, high solvent capacity, high chemical and thermal stability, etc.) [26-30] that can be tailored by the selection of adequate cation and anion to obtain a solvent with specific properties [27,31]. In most cases, the design of the IL to be used as separation or reaction media is based on thermodynamics (phase equilibrium data, activity coefficients, etc) or solvent effects (polarity, acidity and basicity). However, one main constraint for IL practical applications is the unfavorable transport properties of these solvents, which generally present higher viscosity and surface tension than conventional organic solvents. Undesired kinetic effects have been observed in phenomena controlled by mass transfer (gas absorption, liquid-liquid extraction or IL regeneration by distillation) [32-37]. Supported ILs on solids have been proposed as alternative materials that combine the advantages of ILs as solvents with those of solid-based technologies, as adsorption or heterogeneous catalysis [38,39]. The relatively short diffusion distances in a thin IL layer on the porous surface of supported ionic liquid phase (SILPs) [40,41] or supported catalyst ionic liquid layer (SCILL) [42] has been proposed to circumvent the problem of mass transport; however the low amount of IL in these materials may limit its benefit as solvent in reactions or separation processes.

In this work, we established the objective of discretizing the IL in small drops to increase the surface contact area and to improve mass transfer rate, shifting from continue to discrete fluid. For this purpose, we developed a new material named encapsulated ionic liquid (ENIL), consisting on IL confined into hollow submicrocapsules. The starting point for ENIL design was the high affinity found between ILs and activated carbon (AC), demonstrated by adsorption experiments with a wide number of IL compounds [43]. Higher retention efficiency was observed with carbonaceous adsorbents rich in small pores ($d_{pore} < 8$ nm) [44].

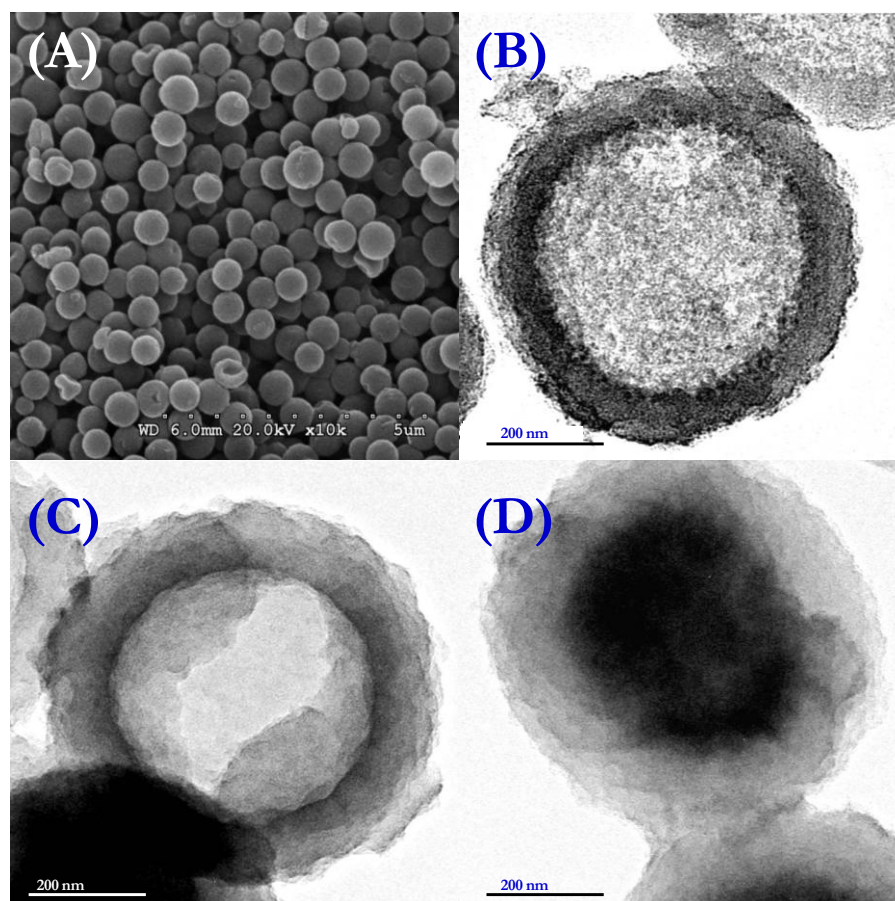


Figure 1. (A) SEM and (B) TEM images of C_{Cap} ; (C) and (D) TEM images, respectively, of ENIL- R_2 and ENIL- R_4 prepared with BmimFeCl $_4$ ionic liquid.

Taking into account these findings, the carbon submicrocapsules (C_{Cap}) with micro/mesoporous shell structure and hollow core, like those developed by Yoon *et al.* [45], were selected to prepare the ENIL materials. The spherical submicrocapsules were obtained in our lab [46], containing high carbon content (>94% w/w), homogeneous morphology (~500 nm of diameter and ~150 nm of shell thickness), high pore volume ($3.7 \text{ cm}^3 \cdot \text{g}^{-1}$) and BET surface area ($1558 \text{ m}^2 \cdot \text{g}^{-1}$) with a high contribution of pores with $d_{\text{pore}} < 8 \text{ nm}$ ($0.84 \text{ cm}^3 \cdot \text{g}^{-1}$). Scanning electron microscopy (SEM) and transmission electron microscopy (TEM) images of synthesized C_{Cap} are depicted in Figures 1A and 1B. The results of characterization of the carbon submicrocapsules by means of elemental analysis (EA), 77 K N_2 adsorption-desorption isotherm and mercury porosimetry are summarized in Table 1. The technique of direct impregnation that we employed in a previous work to prepare SILP systems [47], was used to introduce increasing amounts of the common ionic liquid 1-methyl-3-octyl-

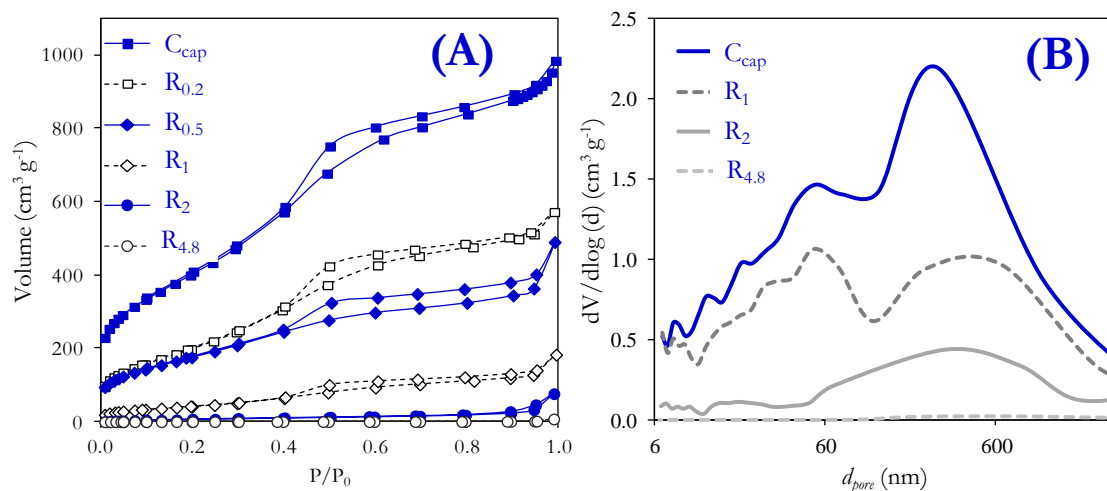
imidazolium hexafluorophosphate (OmimPF_6) into the C_{Cap} submicrocapsules, with a maximum IL mass load of 80% of IL [48]. The different ENIL materials were defined in terms of IL / carbon mass ratio, R_n (Table 1). Elemental analysis allowed quantifying the incorporation of IL to ENILs, by measuring the percentage of N in the material, which can be related to the uptake of imidazolium cation [47].

The EA results of Table 1 confirm the adequate incorporation of IL to ENIL- R_n material. Figures 1C and 1D present TEM images of the materials ENIL- R_2 and ENIL- R_4 (67 and 80% of IL, respectively), prepared in this case with the ionic liquid 1-methyl-3-octyl-imidazolium tetrachloroferrate (BmimFeCl_4) which allows improving the image contrast due to the iron atom. The IL partially fills the hollow in the case of ENIL- R_2 but it is completely filled in ENIL- R_4 , being also detectable onto the porous carbonaceous shell and in the particle interstices in the later case. For further evaluation of the progressive incorporation of IL, ENIL materials were characterized by 77 K N_2 adsorption-desorption isotherms, being the results depicted in Figure 2A. The available porosity in the shell of carbon submicrocapsules decreases when the amount of IL loaded on ENIL- R_n increases. In fact, at 20% IL incorporation (ENIL- $R_{0.2}$) a 50% reduction of carbon shell BET surface area takes place (Table 1), whereas ENIL- R_1 (50% of IL) shows available to the N_2 only 10% of the initial BET surface area of C_{Cap} shell, which utterly disappears in ENIL- R_n materials with $n > 2$. These results indicate that the IL is selectively located at the carbon shell in ENIL materials with low IL content, in concordance with the high IL-activated carbon affinity [43,44]. Figure 2B shows the pore size distribution (6 to 100 nm) curves of C_{Cap} and ENIL- R_n with increasing amounts of OmimPF_6 as obtained by means of mercury porosimetry. In good agreement with TEM images of Figure 1, the mesoporosity of the material progressively disappears from C_{Cap} to ENIL- R_n as n increases up to ENIL- R_4 , where the micro and mesopores of the carbon shell were occupied or blocked by IL (Table 1). In sum, a novel encapsulated ionic liquid-based material (ENIL- R_n) has been prepared. It posses solid appearance, but consists mainly of IL (83% w/w), and is integrated by spherical particles of ~500 nm diameter and no porous solid surface available.

Table 1. Characterization of the carbon submicrocapsules (C_{Cap}) and the encapsulated ionic liquids (ENIL- R_n) prepared with OmimPF₆ ionic liquid [46].

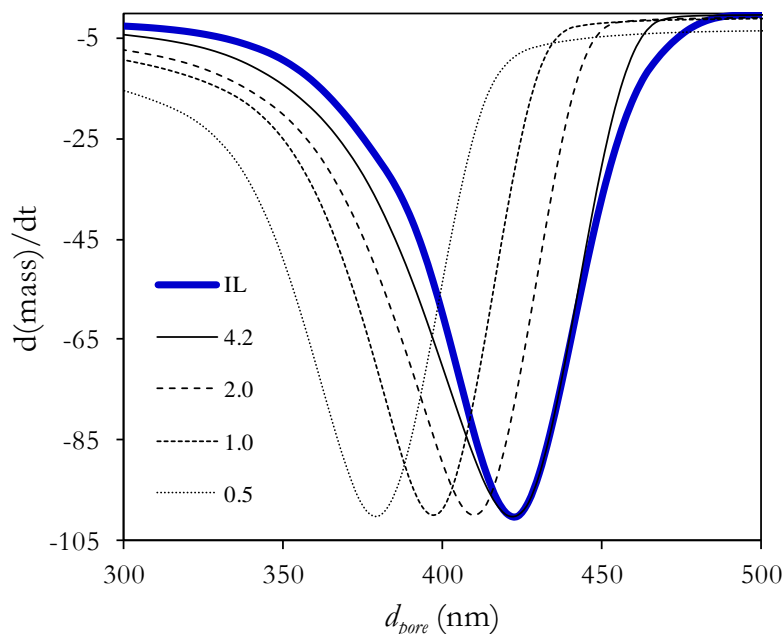
Characterization technique	Property	ENIL- R_n						
		C_{Cap}	$R_{0.2}$	$R_{0.5}$	R_1	R_2	R_4	$R_{4.8}$
Elemental analysis	% IL (w)	0	20	34	49	67	80	83
	% C (w)	93.3	83.8	76.1	67.4	54.7	52.2	51.1
	% N (w)	0.12	1.7	2.8	4	5.4	6.5	6.7
N_2 Adsorption isotherm	A_{BET} ($\text{m}^2 \cdot \text{g}^{-1}$)	1558	761	656	159	11	< 5	ng
	A_{External} ($\text{m}^2 \cdot \text{g}^{-1}$)	700	322	268	80	8	< 5	ng
	$V_{\text{Micropore}}$ ($\text{cm}^3 \cdot \text{g}^{-1}$)	0.55	0.4	0.27	0.09	1×10^{-3}	ng	ng
Hg porosimetry	V_{Mesopore} ($\text{cm}^3 \cdot \text{g}^{-1}$)	0.68	0.33	0.26	0.07	0.01	ng	ng
	$V_{\text{Macropore}}$ ($\text{cm}^3 \cdot \text{g}^{-1}$)	0.61	0.44	0.38	0.3	0.16	ng	ng

Figure 2. (A) Nitrogen adsorption-desorption isotherms at 77K and (B) Pore size distribution (6 to 100nm) from Hg porosimetry of carbon submicrocapsules (C_{cap}) and encapsulated ionic liquid (ENIL- R_n) materials with increasing amounts of OmimPF₆ (0-80% w/w).



The next step was to evaluate the ability of ENIL- R_n materials in practical applications based on IL systems. Recently, our group showed that ammonia-containing gas streams can be efficiently treated by absorption with task-specific ILs containing hydrogen-bond donor functional groups, as 1-2-(hydroxyethyl)-3-methylimidazolium tetrafluoroborate (EtOHmimBF₄) [48,49]. In this work, ENIL- R_2 and ENIL- $R_{4.8}$ materials were prepared with EtOHmimBF₄ and tested for NH₃ retention [46]. The thermal stability of these encapsulated ionic liquids (ENIL- R_n) was previously evaluated and compared with that of the neat IL (Figure 3).

Figure 3. Normalized derivative thermogravimetric curves (DTG) obtained under nitrogen atmosphere at a heating rate of $10\text{ }^{\circ}\text{C}\cdot\text{min}^{-1}$, for EtOHmimBF₄ and ENIL-R_n materials prepared with different amount of this IL.



It was found that ENIL-R_{4,8}, which consists of C_{cap} capsules completely filled by IL, present a thermal stability close to neat IL, whereas the ENIL material decompose at decreasing temperature as the IL load decreases. **Figure 4A** depicts the absorption and desorption of ammonia by EtOHmimBF₄ and this IL encapsulated as ENIL-R₄ measured in gravimetric experiments at 20 °C and 1 atm. These tests were carried out under continuous NH₃/N₂ gas flow ($100\text{ N cm}^3\cdot\text{min}^{-1}$) at an ammonia partial pressure of 0.08 MPa passing over a 25 mg sample of neat IL or IL incorporated into ENIL [46]. Since the amount of NH₃ absorbed is expressed per unit mass of IL, it can be seen that the absorption capacity of IL remains unchanged in the ENIL-R_{4,8} material. In addition, NH₃ is completely desorbed and the IL successfully regenerated by N₂ stripping in both IL and ENIL systems. However, absorption and desorption proceed remarkably faster in the discretized (ENIL) than in the conventional continuous IL phase.

Table 2. Results of NH_3 capture with the ionic liquid (IL) EtOHmimBF₄ and ENIL-R_n materials prepared with this IL obtained in thermogravimetric tests at 20 °C, 1 atm and 0.08 MPa NH_3 partial pressure, where the ammonia absorption capacity of IL-based system is expressed per unit mass of IL.

Thermogravimetric tests

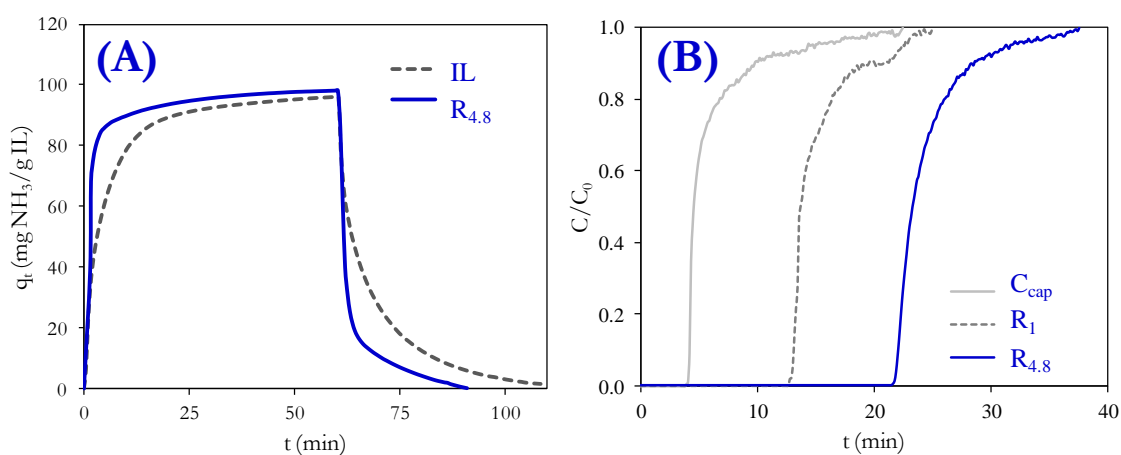
Pseudo-second order model

$$\frac{t}{q_t} = \frac{1}{k_2 q_s^2} + \frac{t}{q_s} \quad (\text{eq. VI.1})$$

	q_s	k_2	R^2
IL	101	3.5×10^{-3}	0.999
ENIL R₂	106	7.1×10^{-3}	0.998
ENIL R_{4.8}	104	12.8×10^{-3}	0.999

q_s (mg·g⁻¹); k_2 (mg·g⁻¹·min⁻¹)

Figure 4. (A) Ammonia absorption and desorption curves in IL and ENIL-R_{4.8} at 20 °C, 1 atm and 0.08 MPa NH_3 partial pressure, obtained in gravimetric experiments; and (B) breakthrough curves of NH_3 capture obtained with C_{cap} and ENIL-R_n in a 8 cm fixed-bed column (1/4 inch diameter) of at 20 °C, 0.1MPa, 20 N cm³·min⁻¹ gas flow rate and 2000 ppmv of inlet NH_3 concentration.

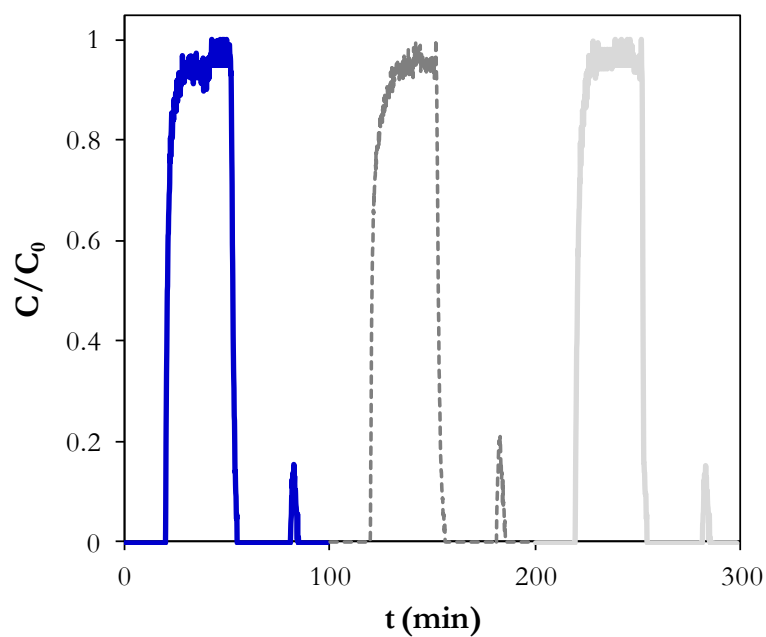


The experimental data of [Figure 4A](#) were successfully adjusted to an empirical second-order kinetic model, ([Table 2](#)), obtaining the kinetic constant k . Comparing IL, ENIL-R₂ and ENIL-R_{4,8} materials as NH₃ absorbents, the three systems present nearly identical sorption capacities with $q_s \approx 100$ mg NH₃/g IL at the testing conditions, *i.e.* the capacity of IL as absorbent is not affected by encapsulation. Nevertheless, the rate of NH₃ absorption, quantified in terms of k_2 values, with the encapsulated IL ENIL-R_{4,8} is almost four-fold that of the neat IL, as the result of the improved surface contact area after IL discretization in encapsulated submicrodrops. A similar effect was found for NH₃ desorption rate, indicating a facilitated regeneration of the saturated ENIL. Considering that the common contact equipments present a surface/volume ratio much higher than that used in current thermogravimetric measurements, ENILs are expected to improve even more the mass transfer rate in larger scale applications. The evaluation of ENIL systems for ammonia capture was completed by experiments carried out in fixed-bed column. This is a well-established technology in industrial gas treatment and, therefore, this type of experiment serves well to test ENIL application. [Figure 4B](#) presents the breakthrough curve obtained for NH₃ sorption with the starting carbon submicrocapsules (C_{Cap}) and the ENIL materials, using a 8 cm bed length, at 20 °C, 0.1 MPa, 20 N cm³·min⁻¹ gas flow rate and inlet NH₃ concentration of 2000 ppmv, representative of industrial gas effluents contaminated with ammonia. Again, it is found that the sorption capacity of the IL in ENIL materials remains nearly unchanged in fixed-bed systems, obtaining values of 1.9 mg NH₃ /g IL fairly close to that obtained from the gravimetric tests at identical operating conditions [49]. However, the amount of ammonia retained per unit of bed volume significantly increases from C_{Cap} (0.04 mg/m) to ENIL-R_{4,8} (0.21 mg·cm⁻³). Finally, the regeneration of exhausted ENIL-R_{4,8} in the fixed-bed column was carried out by stripping under continuous N₂ flow (20 N cm³·min⁻¹) increasing the temperature from 20 to 50 °C at 1 atm [46]. The regeneration of IL solvent in ENIL material was again successfully achieved, being reasonably preserved the NH₃ absorption capacity of IL upon successive cycles (See [Figure 5](#) and [Table 3](#)).

Table 3. Results of NH_3 adsorption-desorption with ENIL- R_4 material obtained in fixed bed reactor tests at 20 °C, 2000 ppmv of inlet ammonia concentration, $20 \text{ N cm}^3 \cdot \text{min}^{-1}$ of gas flow, atmospheric pressure in bed column of 8 cm of height and 1/4 inch diameter.

Cycle	$t_{0,5}$ (min)	q_s ($\text{mg} \cdot \text{g}^{-1}$)	q_s ($\text{mg} \cdot \text{cm}^{-3}$)	q_s ($\text{mg} \cdot \text{m}^{-1}$)
1	20.4	1.85	0.214	6.79
2	19.8	1.80	0.208	6.59
3	20.2	1.83	0.212	6.73

Figure 5. Sorption-desorption breakthrough curves of NH_3 capture obtained with ENIL- $\text{R}_{4,8}$ in fixed-bed column tests.



We have developed novel IL-based systems named encapsulated ionic liquids (ENILs), which present high content (>85 % w/w) of IL introduced into hollow porous carbon submicrocapsules, based on the idea of moving from continue to discrete fluid phase. ENILs present the remarkable properties of preserving the solvent capacity of ILs but enhancing the rate of mass transfer-controlled applications by increasing the surface contact area upon the discretization of the IL fluid encapsulated in submicrodrops (particle diameter < 500 nm). ENIL advanced materials can be applicable to well-established technologies based on solid systems (as NH₃ gas capture successfully tested in this work) , but also can contribute to several IL research fields, including separation processes, analysis, electrochemistry and catalysis, among other.

2. Procedure section

2.1. Submicrocapsule C_{cap} synthesis:

The carbon submicrocapsules were synthesized by template method [45]. A solid core and mesoporous shell aluminosilicate (SCMS) were used as template. The solid core were achieved following the Störb synthesis [50], a volume of 15 mL of tetraethoxysilane (TEOS) was added to a reaction medium formed by 12.6 mL of ammonia aqueous solution (20%, v), 185 mL of ethanol and 20.3 mL of deionized water. The mixture was maintained at 30 °C with vigorous stirring during 1 hour to achieve a colloidal solution of silica spheres. A mixture containing 12.5 mL of TEOS and 5 mL of octadecyltrimethoxysilane (C18TMS), was added to the colloidal solution to form the mesoporous shell around them [51]. After 1 hour of reaction, the spheres formed were isolated by filtration and calcined at 550 °C for 6 h under an air atmosphere. The silica spheres were impregnated by a solution consisting on 0.27 g of Al₃·6H₂O in 0.3 mL of deionized water. This step was repeated one more time. The powder resulting was dried in air at 80 °C and calcined at 550 °C for 5 h in air to form SCMS aluminosilicate. A phenol-formaldehyde resin has been used as carbon precursor to obtain carbon submicrocapsules. A mixture of 0.374 g of phenol per gram of template was heated at 100 °C for 14 h under 150 mm of Hg static vacuum (rotavapor equipment). Then, 0.238 g of paraformaldehyde per g of SCMS was added and maintain during 24 h under static vacuum at 130 °C to obtain a phenol-formaldehyde resin into the SCMS template. This material was heated to 160 °C at rate of 1 °C·min⁻¹ and held at that temperature for 5 h under a nitrogen flow of 100 NmL·min⁻¹ in a vertical furnace (i.d. 26 mm, length 12 cm). Then, the

temperature was raised up to 850 °C with a heat rate of 5 °C·min⁻¹ and held at that temperature for 7 h. The resulting carbon aluminosilicate was washed with HF (48%, v) to generate the carbon submicrocapsules.

2.2. ENIL preparation:

The submicrocapsules (C_{cap}) were filled of IL by means of a direct impregnation, dissolving the IL in acetone. To prevent hydration, IL and acetone were kept in their original tightly closed bottles in a desiccator before use. Impregnation was carried out mixing 1 ml of IL dissolved in acetone for each 100 mg of submicrocapsules. IL concentration in acetone solution was adjusted to obtain different IL loadings on the support. To ensure a homogeneous penetration of the IL solution into the pores, the IL solution was added drop by drop over the surface of the C_{cap} . Then, synthesized ENIL materials were stored at 60 °C during 24 h prior to their use. After evaporation of acetone, the ENIL contains from 20 to 83% (w/w) of IL phase.

2.3. Characterization:

The porous structure of supports and ENIL materials was characterized by means of nitrogen adsorption–desorption isotherms at 77 K using a Micromeritics apparatus (Tristar II 3020 model) and mercury porosimetry using Quantachrome apparatus (PM-3310 model). Before adsorption–desorption experiments, samples were outgassed at 150 °C under a residual pressure lower than 10⁻³ Pa. The BET equation was applied to determine the BET surface area (A_{BET}) and Dubinin–Radushkevich equation for micropore volume (0-2 nm). The external or non-micropore area (A_s) was obtained from the t -method. The difference between the volume of N₂ (as liquid) at 0.95 relative pressure and the micropore volume was taken as mesopore volume (2-50 nm). In the mercury porosimetry measurements the estimation of pore diameter from the applied pressure was based on the Washburn equation. The surface tension of mercury was taken as 4.8×10⁻³ N·cm⁻¹ and the mercury contact angle as 141°. The macropore volume was estimated in the 50-100 nm range. Elemental analyses (EA) of C_{cap} and ENILs were carried out in a Perkin–Elmer analyzer (210 CHN model) to obtain C, and N elemental percentages. Thermogravimetric analyses (TGA) of IL and ENIL materials were conducted in a Mettler Toledo Instruments (TGA/SDTA851e model) under nitrogen with a heating rate of 10°C/min. The accuracy of temperature and mass measurements was 0.1 °C

and 10^{-3} mg, respectively. A dynamic method was used with a temperature range from 50 to 600 °C at a heating rate of $10\text{ °C}\cdot\text{min}^{-1}$ while purging with $50\text{ ml}\cdot\text{min}^{-1}$ of dry nitrogen. The mass of the sample placed in TGA analyses were between 4 and 12 mg. In all TGA runs, aluminum pans with a capacity of 70 ml were used.

2.4. NH_3 capture tests in TGA:

Ammonia absorption experiments were carried out in the TGA analyzer at atmospheric pressure and temperatures of 20 and 40 °C using 20 mg of IL sample amount. The balance has a weight range of 0–1000 mg with a resolution of 0.1 mg. The temperature of the sample was maintained constant with a regulated external thermostat bath (Huber minisat 125). Gas–liquid–solid equilibrium and kinetic data of ammonia in ENIL materials and neat IL were obtained at 20 °C and 0.1 MPa, in a NH_3/N_2 gas flow of $100\text{ N cm}^3\cdot\text{min}^{-1}$, 80% (volume) of NH_3 and monitoring the increment on weight of the sample. Desorption experiments were carried out at the absorption temperature and pressure under dry nitrogen flow ($100\text{ N cm}^3\cdot\text{min}^{-1}$).

2.5. NH_3 capture tests in fixed-bed column:

The sorption of ammonia was also evaluated in a continuous flow system, which consists of a quartz fixed-bed column (1/4 inch diameter), coupled to a quadrupole mass analyzer (OmniStar/ThermoStar). Experiments were conducted under following operating condition: 20 °C of temperature, 2000 ppmv of inlet ammonia concentration, $20\text{ N cm}^3\cdot\text{min}^{-1}$ of gas flow, atmospheric pressure and 8 cm of height of adsorbent/absorbent material (C_{cap} , ENIL- R_2 and ENIL- R_4). Ammonia detection was carried out utilizing a single quadrupole mass analyzer. The signal selected in order to quantify the amount of NH_3 in the gas outlet of the reactor was an ion current of 14.98 A. Desorption experiments were performed after 50 minutes of NH_3 sorption on ENIL materials. A N_2 flow of $20\text{ N cm}^3\cdot\text{min}^{-1}$ was passing through the column with the exhausted ENIL materials at 20 °C, during 30 minutes and then the temperature was raised at 70 °C during 20 minutes and 0.1MPa for the completed regeneration. The regenerative cycles were conducted three times.

References

- [1] Dupont J, de Souza RF, Suarez PAZ. Ionic liquid (molten salt) phase organometallic catalysis. *Chem. Rev.* 2002;102(10):3667-91.
- [2] Huddleston JG, Willauer HD, Swatloski RP, Visser AE, Rogers RD. Room temperature ionic liquids as novel media for 'clean' liquid-liquid extraction. *Chemical Communications* 1998;(16):1765-6.
- [3] Wasserscheid P, Welton T. *Ionic liquids in synthesis*. Weinheim: Wiley-VCH; 2008.
- [4] Hallett JP, Welton T. Room-Temperature Ionic Liquids: Solvents for Synthesis and Catalysis. 2. *Chem. Rev.* 2011;111(5):3508-76.
- [5] Jain N, Kumar A, Chauhan S, Chauhan SMS. Chemical and biochemical transformations in ionic liquids. *Tetrahedron* 2005;61(5):1015-60.
- [6] Brennecke JF, Maginn EJ. Ionic liquids: Innovative fluids for chemical processing. *AIChE J.* 2001;47(11):2384-9.
- [7] Werner S, Haumann M, Wasserscheid P. Ionic Liquids in Chemical Engineering. *Annual review of chemical and biomolecular engineering* 2010;1:203-30.
- [8] Itoh H, Naka K, Chujo Y. Synthesis of gold nanoparticles modified with ionic liquid based on the imidazolium cation. *J. Am. Chem. Soc.* 2004;126(10):3026-7.
- [9] Nakashima T, Kimizuka N. Interfacial synthesis of hollow TiO₂ microspheres in ionic liquids. *J. Am. Chem. Soc.* 2003;125(21):6386-7.
- [10] Hapiot P, Lagrost C. Electrochemical reactivity in room-temperature ionic liquids. *Chem. Rev.* 2008;108(7):2238-64.
- [11] Armand M, Endres F, MacFarlane D, Ohno H, Scrosati B. Ionic-liquid materials for the electrochemical challenges of the future. *Nature Materials* 2009;8(8):621-9.
- [12] Kubisa P. Application of ionic liquids as solvents for polymerization processes. *Progress in Polymer Science* 2004;29(1):3-12.
- [13] Strehmel V. Ionic Liquids in Polymer Synthesis. *Chemie Ingenieur Technik* 2011;83(9):1443-53.
- [14] Hough W, Smiglak M, Rodriguez H, Swatloski R, Spear S, Daly D. The third evolution of ionic liquids: active pharmaceutical ingredients. *New journal of chemistry* 2007;31(8):1429-36.
- [15] Plechkova NV, Seddon KR. Applications of ionic liquids in the chemical industry. *Chem.Soc.Rev.* 2008;37(1):123-50.
- [16] Olivier-Bourbigou H, Magna L, Morvan D. Ionic liquids and catalysis: Recent progress from knowledge to applications. *Applied Catalysis A-General* 2010;373(1-2):1-56.

- [17] Cole AC, Jensen JL, Ntai I, Tran KLT, Weaver KJ, Forbes DC, et al. Novel bronsted acidic ionic liquids and their use as dual solvent-catalysts. *J. Am. Chem. Soc.* 2002;124(21):5962-3.
- [18] Han X, Armstrong DW. Ionic liquids in separations. *Acc.Chem.Res.* 2007;40:1079-86.
- [19] Bates ED, Mayton RD, Ntai I, Davis JH. CO₂ capture by a task-specific ionic liquid. *J. Am. Chem. Soc.* 2002;124(6):926-7.
- [20] Wang H, Gurau G, Rogers RD. Ionic liquid processing of cellulose. *Chem. Soc. Rev.* 2012;41(4):1519-37.
- [21] Anderson JL, Armstrong DW, Wei GT. Ionic liquids in analytical chemistry. *Anal. Chem.* 2006;78(9):2892-902.
- [22] Antonietti M, Kuang DB, Smarsly B, Yong Z. Ionic liquids for the convenient synthesis of functional nanoparticles and other inorganic nanostructures. *Angewandte Chemie-International Edition* 2004;43(38):4988-92.
- [23] Ye CF, Liu WM, Chen YX, Yu LG. Room-temperature ionic liquids: a novel versatile lubricant. *Chemical Communications* 2001;(21):2244-5.
- [24] Van Valkenburg ME, Vaughn RL, Williams M, Wilkes JS. Thermochemistry of ionic liquid heat-transfer fluids. *Thermochimica Acta* 2005;425(1-2):181-8.
- [25] Kuang DB, Wang P, Ito S, Zakeeruddin SM, Gratzel M. Stable mesoscopic dye-sensitized solar cells based on tetracyanoborate ionic liquid electrolyte. *J. Am. Chem. Soc.* 2006;128(24):7732-3.
- [26] Earle MJ, Esperanca JMSS, Gilea MA, Lopes JNC, Rebelo LPN, Magee JW, et al. The distillation and volatility of ionic liquids. *Nature* 2006;439(7078):831-4.
- [27] Huddleston JG, Visser AE, Reichert WM, Willauer HD, Broker GA, Rogers RD. Characterization and comparison of hydrophilic and hydrophobic room temperature ionic liquids incorporating the imidazolium cation. *Green Chem.* 2001;3(4):156-64.
- [28] Anderson JL, Ding J, Welton T, Armstrong DW. Characterizing ionic liquids on the basis of multiple solvation interactions. *J. Am. Chem.Soc.* 2002;124(47):14247-54.
- [29] Fredlake CP, Crosthwaite JM, Hert DG, Aki SNVK, Brennecke JF. Thermophysical properties of imidazolium-based ionic liquids. *J. Chem. Eng. Data* 2004;49(4):954-64.
- [30] Chowdhury S, Mohan R, Scott J. Reactivity of ionic liquids. *Tetrahedron* 2007;63(11):2363-89.
- [31] Weingaertner H. Understanding ionic liquids at the molecular level: Facts, problems, and controversies. *Angewandte Chemie-International Edition* 2008;47(4):654-70.
- [32] Gardas RL, Coutinho JAP. A group contribution method for viscosity estimation of ionic liquids. *Fluid Phase Equilib.* 2008;266(1-2):195-201.

- [33] Sangoro JR, Serghei A, Naumov S, Galvosas P, Kaerger J, Wespe C, et al. Charge transport and mass transport in imidazolium-based ionic liquids. *Physical Review E* 2008;77(5):051202.
- [34] Condemarin R, Scovazzo P. Gas permeabilities, solubilities, diffusivities, and diffusivity correlations for ammonium-based room temperature ionic liquids with comparison to imidazolium and phosphonium RTIL data. *Chem. Eng. J.* 2009;147(1):51-7.
- [35] Sidhuria KB, Daniel-da-Silva AL, Trindade T, Coutinho JAP. Supported ionic liquid silica nanoparticles (SILnPs) as an efficient and recyclable heterogeneous catalyst for the dehydration of fructose to 5-hydroxymethylfurfural. *Green Chem.* 2011;13(2):340-9.
- [36] Fernandez JF, Neumann J, Thoeming J. Regeneration, Recovery and Removal of Ionic Liquids. *Current Organic Chemistry* 2011;15(12):1992-2014.
- [37] Blahusiak M, Schlosser S, Cvengros J, Martak J. New approach to regeneration of an ionic liquid containing solvent by molecular distillation. *Chemical Papers* 2011;65(5):603-7.
- [38] Mehnert CP, Cook RA, Dispenziere NC, Afeworki M. Supported ionic liquid catalysis - A new concept for homogeneous hydroformylation catalysis. *J.Am.Chem.Soc.* 2002;124(44):12932-3.
- [39] Vidal L, Riekkola M, Canals A. Ionic liquid-modified materials for solid-phase extraction and separation: A review. *Anal. Chim. Acta* 2012;715:19-41.
- [40] Rüsager A, Fehrmann R, Flicker S, van Hal R, Haumann M, Wasserscheid P. Very stable and highly regioselective supported ionic-liquid-phase (SILP) catalysis: Continuous flow fixed-bed hydroformylation of propene. *Angewandte Chemie-International Edition* 2005;44(5):815-9.
- [41] Steinrueck H-, Libuda J, Wasserscheid P, Cremer T, Kolbeck C, Laurin M, et al. Surface Science and Model Catalysis with Ionic Liquid-Modified Materials. *Adv. Mater.* 2011;23(22-23):2571-87.
- [42] Kernchen U, Etzold B, Korth W, Jess A. Solid catalyst with ionic liquid layer (SCILL). A new concept to improve selectivity illustrated by hydrogenation of cyclooctadiene. *Chem. Eng. Technol.* 2007;30(8):985-94.
- [43] Palomar J, Lemus J, Gilarranz MA, Rodriguez JJ. Adsorption of ionic liquids from aqueous effluents by activated carbon. *Carbon.* 2009;47(7):1846-56.
- [44] Lemus J, Palomar J, Heras F, Gilarranz MA, Rodriguez JJ. Developing criteria for the recovery of ionic liquids from aqueous phase by adsorption with activated carbon. *Separation and Purification Technology* 2012;(97):11-19.
- [45] Yoon SB, Sohn K, Kim JY, Shin C-, Yu J-, Hyeon T. Fabrication of Carbon Capsules with Hollow Macroporous Core/Mesoporous Shell Structures. *Adv. Mater.* 2002;14(1):19-21.
- [46] Procedure details for the experiments reported in this communication are reported as procedure section.

- [47] Lemus J, Palomar J, Gilarranz MA, Rodriguez JJ. Characterization of Supported Ionic Liquid Phase (SILP) materials prepared from different supports. *Adsorption-Journal of the International Adsorption Society* 2011;17(3):561-571.
- [48] Palomar J, Gonzalez-Miquel M, Bedia J, Rodriguez F, Rodriguez JJ. Task-specific ionic liquids for efficient ammonia absorption. *Separation and Purification Technology* 2011;82(0):43-52.
- [49] Bedia J, Palomar J, Gonzalez-Miquel M, Bedia J, Rodriguez F, Rodriguez JJ. Screening ionic liquids as suitable ammonia absorbents on the basis of thermodynamic and kinetic analysis. *Separation and Purification Technology* 2012;(95):188–195.
- [50] Stober W, Fink A, Bohn E. Controlled Growth of Monodisperse Silica Spheres in Micron Size Range. *J. Colloid Interface Sci.* 1968;26(1):62-71.
- [51] Buchel G, Unger KK, Matsumoto A, Tsutsumi K. A novel pathway for synthesis of submicrometer-size solid core/mesoporous shell silica spheres. *Adv Mater* 1998;10(13):1036-1043.



Conclusiones / Conclusions

CONCLUSIONES

Los resultados presentados en este trabajo muestran las siguientes conclusiones:

1. El estudio termodinámico de la adsorción de un conjunto amplio de **LI**s de distinta naturaleza en medio acuoso sobre **CA**s permite seleccionar de forma eficaz las propiedades físicas y químicas del adsorbente para la retención de **LI**s. Los **CA**s con una microporosidad y mesoporosidad estrecha altamente desarrollada presentan las mayores capacidades de adsorción, llegando a alcanzar retenciones de 1 g de **LI**/g de **CA**, en el caso de **LI**s hidrofóbicos, mientras que los de naturaleza hidrofílica se muestran más refractarios a la adsorción. Además, los **LI**s con un volumen molecular grande (superiores a 0.4 nm^3 en el caso de la adsorción sobre un **CA** comercial de Merck, **MkU**) pueden presentar limitaciones estéricas que tienen que ser consideradas a la hora de diseñar la operación de adsorción.
2. La adsorción de **LI**s sobre **CA**s puede mejorarse modificando convenientemente la composición química de su superficie. Los **LI**s hidrofílicos pueden retirarse de corrientes acuosas de manera efectiva usando **CA**s con alto contenido en grupos oxigenados superficiales (**SOGs**), los cuales favorecerán las interacciones de puente de hidrógeno entre el adsorbato y el adsorbente. Por otra parte, los **LI**s hidrofóbicos presentan mayor afinidad por adsorbentes con baja polaridad, que en el caso de los **CA**s puede conseguirse por tratamientos térmicos que permiten eliminar los grupos oxigenados superficiales.
3. El **CA** saturado después de la adsorción de **LI** se puede regenerar empleando acetona como disolvente. Tras el proceso de regeneración, se ha comprobado que el **CA** mantiene sus propiedades adsorbentes con ciclos sucesivos de adsorción-desorción. Además, la separación de la acetona por destilación atmosférica permite recuperar el **LI**, cuya estabilidad se ha verificado mediante los correspondientes espectros de ^1H -RMN.
4. El método químico-cuántico **COSMO-RS** permite examinar a nivel molecular las interacciones adsorbato-adsorbente en la adsorción de **LI** en **CA** en fase acuosa. Los datos experimentales y simulados permiten establecer la adsorción como un proceso espontáneo con efectos exotérmicos que están regulados principalmente por interacciones del tipo van der Waals (**LI**s hidrofóbicos) y de enlace de hidrogeno (**LI**s hidrofílicos) adsorbente/adsorbato. Además, **COSMO-RS** se presenta como una herramienta capaz de predecir de forma rápida y útil el coeficiente de reparto del **LI** entre las fases agua y **CA**, lo que permite establecer las directrices adecuadas para funcionalizaciones eficientes en la adsorción de **LI**s, dependiendo de su naturaleza química.

5. El estudio cinético detallado de la adsorción de un **LI** de referencia (**OmimPF₆**) en **CAs** comerciales en medio acuoso permite establecer que la adsorción del **LI** es un fenómeno relativamente lento (comparado con la de otros solutos como el fenol) y que tiene lugar a través de un mecanismo de adsorción física controlado por la difusión interna. Este estudio se ha llevado a cabo en un amplio intervalo de condiciones de operación, así como utilizando diferentes tipos y tamaños de **CAs**. La velocidad de adsorción puede ser convenientemente mejorada reduciendo el tamaño de partícula del adsorbente, así como operando a temperaturas moderadamente superiores a la ambiente.

6. Los experimentos de adsorción llevados a cabo en columnas (lecho fijo) para el tratamiento de clorometanos (**Cl-VOCs**) en fase gaseosa, en un amplio intervalo de condiciones experimentales (presión, temperatura, concentración inicial, altura de lecho y caudal de entrada) con **CAs** comerciales, han proporcionado información útil para el diseño de materiales eficaces para la retención de este tipo de contaminantes de alta peligrosidad. Los **CAs** con polaridad desarrollada se presentan como candidatos eficientes y económicos para tratamientos de adsorción de **Cl-VOCs** en fase gas. Los experimentos de desorción mostraron una completa regeneración del **CA** saturado bajo condiciones suaves de presión y temperatura. La funcionalización del **CA** con grupos oxigenados superficiales mediante tratamientos oxidativos mejora su capacidad de adsorción de **Cl-VOCs**. Por otro lado, la experimentación llevada a cabo con líquidos iónicos soportados (**SILP**) muestra que la funcionalización de **CAs** mediante la incorporación de **LI** disminuye su capacidad para retener estos compuestos clorados en términos termodinámicos. Este resultado indica, por un lado, que los compuestos organoclorados (**MCM**, **DCM** y **CLF**) no son buenos solutos de referencia para el desarrollo de sistemas de tratamiento de gases basado en **LIs** y, por otro lado, que son necesarios sistemas alternativos a los materiales **SILP** para la retención de solutos gaseosos.

7. Se ha diseñado y preparado un nuevo tipo de materiales avanzados denominados líquidos iónicos encapsulados (**ENIL**), con objeto de evolucionar desde un fluido continuo a un fluido discretizado. Los sistemas **ENIL** presentan hasta un 85% en peso de **LI**, confinado en una submicroesfera sólida hueca de diámetro inferior a 500 nm. La caracterización de estos materiales indica que, aunque macroscópicamente sean sólidos, no presentan superficie de **CA** disponible y, por tanto, actúan vía absorción y no adsorción en procesos de separación de gases. Se ha demostrado asimismo que los sistemas **ENIL** con alto contenido en **LI** presentan una estabilidad térmica comparable a la del disolvente puro. En resumen, los nuevos materiales **ENIL** desarrollados mantienen las ventajas del **LI** como disolvente pero con un área de contacto sensiblemente mayor, que se traduce en velocidades de transferencia de materia claramente mejoradas respecto al **LI** solo.

8. Los materiales ENIL han demostrado su eficacia para retener amoníaco (NH_3) de corrientes gaseosas. Por una parte, se ha diseñado un sistema ENIL funcionalizado con el LI específico 1-(2-hidroxietil)-3-metilimidazolio tetrafluoroborato (EtOHmimBF_4), que presenta una alta capacidad de absorción de NH_3 ($\sim 100 \text{ mg/g}$), observándose que dicha capacidad del LI como disolvente se mantiene en el material ENIL. Por otra parte, se ha demostrado, mediante experimentación llevada a cabo en microbalanza y en columna de lecho fijo, que tanto la velocidad de retención como la de desorción de amoníaco en los sistemas ENIL mejora al menos por un factor de 3 respecto al LI o a las cápsulas de CA. La gran versatilidad de los nuevos materiales ENIL, así como su buen comportamiento, tanto en términos termodinámicos como cinéticos sugieren una amplia variedad de aplicaciones posibles en operaciones de separación, catálisis, análisis y electroquímica.

9. Se ha demostrado que el análisis elemental (EA) proporciona una herramienta capaz de cuantificar de forma precisa la cantidad de LI imidazolio presente en sistemas SILP y ENIL, mediante la simple determinación del contenido de nitrógeno elemental. Las isotermas de adsorción/desorción de nitrógeno a 77 K y la porosimetría de mercurio permiten evaluar satisfactoriamente la distribución del LI presente en la superficie del soporte para una gran variedad de materiales mixtos. Teniendo en cuenta la superficie porosa disponible en el soporte, el LI parece rellenar primero los poros de menor tamaño, pero cuando sólo hay poros grandes el LI se aloja en los huecos disponibles, independientemente del tamaño. Medidas basadas en termogravimetría (TGA) y calorimetría (DSC) permiten evaluar la estabilidad térmica de los materiales SILP y ENIL. La naturaleza química del soporte sólido afecta considerablemente la estabilidad del material mixto, resultando más estables los preparados a partir de soportes de naturaleza no polar, como CA.

10. COSMO-RS se presenta como una herramienta eficaz en la investigación sobre LIs, habiéndose aplicado con éxito tanto para el diseño de sistemas de separación basados en LIs como para la interpretación del comportamiento de mezclas conteniendo LIs. Así, COSMO-RS ha permitido: i) Predecir satisfactoriamente coeficientes de reparto de LI entre las fases agua y CA, permitiendo seleccionar los grupos funcionales de la superficie del CA para retener LIs de distinta naturaleza (hidrofilicos e hidrofóbicos) de la fase acuosa. ii) Seleccionar un LI con propiedades adecuadas para retener compuestos gaseosos (NH_3 o Cl-VOCs), en base a la selección del par iónico anión/catión con propiedades óptimas entre un amplio conjunto de candidatos, mediante el cálculo de constantes de Henry; iii) Su uso como guía para funcionalizar CAs de forma efectiva para el tratamiento de compuestos gaseosos específicos, (clorometanos en este estudio).

CONCLUSIONS

The results presented in this work support the following conclusions:

1. The thermodynamic study of the adsorption of a wide number of **ILs** with different nature in aqueous phase onto **ACs** keeps effectively selecting the physical and chemical properties of the adsorbent for their removal. **ACs** with microporosity and narrow mesoporosity highly developed have the largest adsorption capacities, achieving uptake about 1 g of **IL** /g of **AC** in the case of hydrophobic **ILs**, while the hydrophilic nature are shown as more refractory to adsorption. Furthermore, **ILs** with a large molecular volume (greater than 0.4 nm^3 in the case of adsorption on a commercial **AC** Merck **MKU**) may present steric limitations which must be considered in the designing of the adsorption operation.
2. Adsorption of **ILs** on **ACs** can be improved by suitably modifications on the chemical composition of its surface. The hydrophilic **ILs** can be effectively removed from aqueous phase using **ACs** with high content in surface oxygen groups (**SOGs**), which will back the hydrogen bond interactions between the adsorbate and adsorbent. Moreover, the hydrophobic **ILs** have greater affinity by hydrophobic adsorbents with low polarity, as in the case of **ACs** can be achieved by thermal treatments that eliminate the surface oxygenated groups.
3. The saturated **AC** obtained after adsorption of **IL** may be regenerated by using acetone as solvent. Following the regeneration process, the **AC** maintains its adsorbent properties by means of testing with successive adsorption-desorption cycles. Furthermore, the acetone separation by atmospheric distillation, allow us to retrieve the **IL** was achieved, verifying their stability by the corresponding $^1\text{H-NMR}$ spectrums.
4. The quantum-chemical method **COSMO-RS** allows us to examine the adsorbate-adsorbent interactions of the **IL** adsorption on **AC** in aqueous phase at molecular level. The simulated and experimental data allow to establish that the adsorption is a spontaneous process with exothermic effects which are mainly regulated by van der Waals interactions (hydrophobic **ILs**) and hydrogen bonding (hydrophilic **ILs**) between adsorbent/adsorbate. Furthermore, **COSMO-RS** is presented as a predictive tool to obtain fast and valuable **IL** partition coefficients between water and **AC** phases, establishing appropriate guidelines for efficient functionalizations on the **ILs** adsorption according to their chemical nature.

5. A detailed kinetic study of the adsorption of a reference IL (OmimPF_6) on commercial ACs present in aqueous phase allows to establish that the adsorption of IL is a relatively slow process (compared with other solutes, such as phenol) and takes place under a mechanism of physical adsorption control by intraparticle diffusion. This study was carried out under a wide variety of operating conditions (stirring, AC particle size, temperature and IL initial concentration) and the variation in the type and size of ACs. Thus, the adsorption rate could be improved with a decrease in particle size of the adsorbent, as well as operating at temperatures moderately above room temperature.

6. Adsorption experiments for the treatment of chloromethanes (Cl-VOCs) in gas phase onto commercial ACs carried out in fixed bed columns under a wide variety of operating conditions (inlet concentration, temperature, pressure, gas flow rate and bed length) have provided useful information for the design of effective materials for the retention of these dangerous pollutants. ACs with developed polarity are efficient and economical candidates in the treatment of gaseous Cl-VOCs. Desorption experiments showed a complete regeneration of saturated AC under mild conditions of pressure and temperature. Effective functionalizations on AC with surface oxygenated groups by oxidative treatments improve the adsorption capacity of Cl-VOCs. Moreover, the experimentation carried out with supported ionic liquid (SILP) shows that the functionalization of ACs by incorporating IL decreases its ability to retain these chlorinated compounds in thermodynamic terms. This result indicates that organochloride compounds (MCM, DCM and CLF) are not good reference solutes for the development of gas treatment based on ILs and, on the other hand, alternative systems to materials SILP are required for gaseous solute retention.

7. It is designed and developed a new kind of advanced materials called encapsulated ionic liquids (ENIL), based on the idea of moving from continue to discrete fluid phase. The prepared ENIL systems contain up 85% in mass of IL but discretized in a solid and hollow submicrosphere with diameter lower than 500 nm. The characterization of these materials indicates that, although while are macroscopically solids, they do not present available AC surface and, therefore, ENIL materials do not act via adsorption unless absorption in gas separation processes. It has also shown that ENIL systems with high content IL exhibit thermal stability comparable to that of the pure solvent. In summary, these novel ENIL materials maintaining the advantages of IL as solvent but with an appreciably greater contact area which represents transfer properties clearly improved respect the neat IL.

8. **ENIL** materials have been proved as effective systems for retaining ammonia from gaseous streams (NH_3), both thermodynamic and kinetically. Firstly, it is designed a functionalized **ENIL** system with the task specific 1-(2-hydroxyethyl)-3-methylimidazolium tetrafluoroborate (EtOHmimBF_4) **IL**, having a high absorbent capacity by NH_3 ($\sim 100 \text{ mg}\cdot\text{g}^{-1}$), showing that the capacity of this **IL** as solvent is remaining in **ENIL** material. Moreover, it has been demonstrated that both the retention and desorption rate of ammonia on **ENIL** systems improves at least by a factor of 3 compared to the neat **IL** or **AC** capsules by means of experimentation conducted in microbalance and fixed bed column. The high versatility of these novel materials and their favorable thermodynamic and kinetic properties suggest a wide variety of potential applications in operations separation, catalysis, analysis and electrochemistry.

9. Elemental analysis (**EA**) has been shown as a tool able to quantify precisely the amount of imidazolium-based **IL** presents on **SILP** and **ENIL** materials, by means of determining of elemental nitrogen. The adsorption/desorption isotherms of nitrogen at 77 K and mercury porosimetry to assess satisfactorily the distribution of **IL** on the surface of the support for a variety of mixed materials. Considering the available porous surface on the support, firstly **IL** seems to fill the smaller pores, but when there are only large pores, the **IL** is placed on the hole available independently of its size. Measures based on thermogravimetry (**TGA**) and calorimetry (**DSC**) to assess the thermal stability of **ENIL** and **SILP** materials. The chemical nature of the solid support affects significantly the stability of the composite, resulting more stable mixed materials prepared from nature non polar media, such as **AC**.

10. **COSMO-RS** is presented as an effective tool in the research on **ILs**, having been successfully applied to both the design separation systems based on **ILs** and interpretation of the mixtures behavior containing **ILs**. Thus, **COSMO-RS** keeps: i) Predict acceptably **IL** partition coefficients between water and **AC** phases, allowing the selection of **AC** surface oxygen groups for retaining **ILs** of various types (hydrophilic and hydrophobic) from aqueous phase. ii) Select an **IL** with suitable properties to uptake gaseous compounds (NH_3 or **Cl-VOCs**), based on the selection of the anion/cation pair with optimal properties from a wide range of candidates by means of Henry constant iii) its use as a guide to functionalize effectively **ACs** for the treatment of specific gaseous solutes, (**Cl-VOCs** in this study).



Appendix

APPENDIX 1. Nomenclature

A_{BET}	apparent surface area of AC ($\text{m}^2 \cdot \text{g}^{-1}$)
AC	activated carbon
A_s	external or non-micropore area of AC ($\text{m}^2 \cdot \text{g}^{-1}$)
B, q_{max}	empirical coefficients in Langmuir equation, q_{max} ($\text{mmol} \cdot \text{g}^{-1}$)
C_e	equilibrium concentration of adsorbate in fluid phase (mmol L^{-1})
Cl-VOC	chlorinated volatile organic compound
DCM	dichloromethane
ΔG	molar adsorption free energy change ($\text{KJ} \cdot \text{mol}^{-1}$)
ΔH	molar adsorption enthalpy change ($\text{KJ} \cdot \text{mol}^{-1}$)
ΔS	molar adsorption entropy change ($\text{J} \cdot \text{mol}^{-1} \cdot \text{K}^{-1}$)
DSC	differential scanning calorimetry
EA	elemental analysis
EDX	energy dispersive X-ray
ENIL	encapsulated ionic liquid
HB	hydrogen bond
H_E	excess enthalpy
IL	ionic liquid
k	adsorption equilibrium constant
K_d	apparent distribution coefficients ($\text{L} \cdot \text{kg}^{-1}$)
k_f, n	empirical coefficients in Freundlich equation ($\text{L} \cdot \text{g}^{-1}$)
K_H	Henry constant
$k_{\text{hyperbolic}}$	empirical coefficient of hyperbolic model (min^{-1})
k_{id}, I	diffusion rate constant ($\mu\text{mol} \cdot \text{g}^{-1} \cdot \text{min}^{-0.5}$) and intercept of intraparticle model ($\text{mmol} \cdot \text{g}^{-1}$)
K_{OW}	octanol–water partition coefficient

k_s, n	Lagergren rate constant ($\text{mmol}\cdot\text{g}^{-1}\cdot\text{min}^{-1}$) and apparent order of the model
$k_{Y-N}, t_{0.5}$	proportionality constant (time^{-1}) and time when outlet concentration is one half of the inlet (time)
k_2	pseudo second order model constant ($\text{mg}\cdot\text{g}^{-1}\cdot\text{min}^{-1}$)
Log(P)	logarithm of partition coefficient of IL solute between AC and aqueous phase
m	mass of adsorbent (g)
MCM	monochloromethane
NMR	nuclear magnetic resonance
q_e	equilibrium concentration of adsorbate in solid phase ($\text{mmol}\cdot\text{g}^{-1}$)
q_{max}	maximum concentration of adsorbate in solid phase ($\text{mmol}\cdot\text{g}^{-1}$)
R	ideal gas constant ($8.315 \text{ J}\cdot\text{mol}^{-1}\cdot\text{K}^{-1}$)
SEM	scanning electronic microscopy
SILP	supported ionic liquid phase
SOG	surface oxygen group
T	temperature
TCM	chloroform
TEM	transmission electron microscopy
TGA	thermogravimetric analysis
TPD	temperature programmed desorption
UV	Ultraviolet
VdW	van der Waals
$V_{\text{microp.}}$	micropore volume ($\text{cm}^3\cdot\text{g}^{-1}$)
$V_{\text{mesop.}}$	mesopore volume ($\text{cm}^3\cdot\text{g}^{-1}$)
V_{macrop}	macropore volume ($\text{cm}^3\cdot\text{g}^{-1}$)
VOC	volatile organic compound
V_{total}	total pore volume ($\text{cm}^3\cdot\text{g}^{-1}$)

 Ionic liquids

EmimCl	1-Ethyl-3-methylimidazolium chloride
BmimCl	1-Butyl-3-methylimidazolium chloride
BzmimCl	1-Benzyl-3-methylimidazolium chloride
HxmimCl	1-Hexyl-3-methylimidazolium chloride
OmimCl	1-Methyl-3-octylimidazolium chloride
DcmimCl	1-Decyl-3-methylimidazolium chloride
DdmimCl	1-Dodecyl-3-methylimidazolium chloride
TdmimCl	1-Methyl-3-tetradecilimidazolium chloride
HdmimCl	1-Hexadexyl-3-methylimidazolium chloride
EmimBF ₄	1-Ethyl-3-methylimidazolium tetrafluoroborate
BmimBF ₄	1-Butyl-3-methylimidazolium tetrafluoroborate
BzmimBF ₄	1-Benzyl-3-methylimidazolium tetrafluoroborate
HxmimBF ₄	1-Hexyl-3-methylimidazolium tetrafluoroborate
OmimBF ₄	1-Methyl-3-octylimidazolium tetrafluoroborate
DcmimBF ₄	1-Decyl-3-methylimidazolium tetrafluoroborate
DdmimBF ₄	1-Dodecyl-3-methylimidazolium tetrafluoroborate
EmimPF ₆	1-Ethyl-3-methylimidazolium hexafluorophosphate
BmimPF ₆	1-Butyl-3-methylimidazolium hexafluorophosphate
BmmimPF ₆	1-2- dibutyl-3-methylimidazolium hexafluorophosphate
HxmimPF ₆	1-Hexyl-3-methylimidazolium hexafluorophosphate
BzmimPF ₆	1-Benzyl-3-methylimidazolium hexafluorophosphate
OmimPF ₆	1-Methyl-3-octylimidazolium hexafluorophosphate
DcmimPF ₆	1-Decyl-3-methylimidazolium hexafluorophosphate
EmimNTf ₂	1-Ethyl-3-methylimidazolium bis(trifluoromethanesulfonimide)
PrmimNTf ₂	1-Methyl-3-propylimidazolium bis(trifluoromethanesulfonimide)

BmimNTf ₂	1-Butyl-3-methylimidazolium bis(trifluoromethanesulfonimide)
HxmimNTf ₂	1-Hexyl-3-methylimidazolium bis(trifluoromethanesulfonimide)
BmimOTf	1-Butyl-3-methylimidazolium trifluoromethanesulfonate
Bmim TFA	1-Butyl-3-methylimidazolium trifluoroacetate
BmimMeSO ₃	1-Butyl-3-methylimidazolium methylsulfonate
EtOHmimBF ₄	1-Ethyl-2-hidroxyethyl-3-methylimidazolium tetrafluoroborate

APPENDIX 2. Diffusion of results

Herein, the publications in international journals and the presentation on national and international congresses are listed. This diffusion has kept us to expand the knowledge related to the ionic liquid field.

Scientific publications of the dissertation:

1. J. Palomar, J. Lemus, M.A. Gilarranz, J.J. Rodríguez
Ionic liquids removal from aqueous effluents by adsorption onto activated carbon
Carbon. 2009 (47) 1846-1856.
2. J. Lemus, J. Palomar, M.A. Gilarranz, J.J. Rodríguez.
Characterization of Supported Ionic Liquid Phase (SILP) materials prepared from different supports.
Adsorption. 2011 (17) 561-571.
3. J. Lemus, J. Palomar, F. Heras, M.A. Gilarranz, J.J. Rodríguez.
Developing criteria for the recovery of ionic liquids from aqueous phase by adsorption with activated carbon.
Separation and Purification Technology. 2012 (97), 11-19.
4. J. Lemus, M. Martín, J. Palomar, L. Gómez, M.A. Gilarranz, J.J. Rodríguez.
Effective adsorption of chlorinated organic volatile compounds on commercial activated carbon
Chemical Engineering Journal. 2012 (<http://dx.doi.org/10.1016/j.cej.2012.09.021>).
5. J. Palomar, J. Lemus, N. Alonso, J. Bedia, M.A. Gilarranz, J.J. Rodríguez.
Encapsulated Ionic Liquids (ENILs): From continue to discrete liquid phase
Chemical communications. 2012, (48), 10046-10048
6. J. Lemus, J. Palomar, M.A. Gilarranz, J.J. Rodríguez.
On the kinetics of ionic liquids adsorption onto activated carbons from aqueous solution
Industrial and Engineering Chemistry Research. 2012 (submitted).

Other scientific publications:

7. J. Palomar, J.S. Torrecilla, J. Lemus, V. R. Ferro, F. Rodríguez.
Prediction of Non-Ideal Behaviour of Polarity/Polarizability Scales of Solvent Mixtures by Integration of a novel COSMO-RS Molecular Descriptor and Neural Networks.
Physical Chemistry Chemical Physics. 2008 (10) 5967-5975.
8. J.S. Torrecilla, J. Palomar, J. Lemus, F. Rodríguez
A quantum-chemical-based guide to analyze/quantify the cytotoxicity of ionic liquids.
Green Chemistry. 2010 (12) 123-134.

9. J. Palomar, J.S. Torrecilla, J. Lemus, V.R. Ferro, F. Rodríguez
A COSMO-RS based guide to analyze/quantify the polarity of ionic liquids and their mixtures with organic cosolvents.
Physical Chemistry Chemical Physics. 2010 (12) 1991-2000

10. M. Al Bahri, L. Calvo, J. Lemus, M.A. Gilarranz, J. Palomar, J.J. Rodríguez.
Mechanistic understanding of the behavior of diuron in the adsorption from water onto activated carbon.
Chemical Engineering Journal. 2012 (198-199) 346-354.

11. E.Vega, J. Lemus, A. Anfruns, R. Gonzalez-Olmos, J. Palomar, M.J. Martin.
Adsorption of odour-causing sulphur compounds onto modified activated carbons: effect of oxygen functional groups.
Hazardous materials. 2012 (submitted).

National and international congresses:

1. C. M. S. S. Neves, J. Lemus, M. G. Freire, J. Palomar, J. A. P. Coutinho
Treatment of aqueous solutions contaminated with ionic liquids by adsorption
ANQUE International Congress of Chemical Engineering, Sevilla (Spain) June 2012
(Poster presentation- collaboration)

2. E. Vega, J. Lemus, R. Gonzalez-Olmos, J. Palomar, M. Sánchez-Polo, M.J. Martin
Adsorption of odour-causing sulphur compounds at low concentrations on activated carbons: effects of oxygen functional groups.
(Oral presentation-collaboration)
and

J. Lemus, J. Palomar, N. Alonso, J. Bedia, M.A. Gilarranz, J.J. Rodríguez.
Encapsulated ionic liquids (ENIL): from continue to discrete fluid for enhancing transport phenomena kinetics in separation and reaction applications
The annual world conference on Carbon. Krakow (Poland) June 2012
(Oral presentation)

3. J. Lemus, J. Palomar, N. Alonso, J. Bedia, M.A. Gilarranz, J.J. Rodríguez.
Encapsulated ionic liquids (ENIL): from continue to discrete fluid for enhancing transport phenomena kinetics in separation and reaction applications
Workshop on Ionic Liquids - Seeds for New Engineering Applications. Lisbon (Portugal) February 2012.
(Poster presentation- Best poster award)

4. J. Lemus, J. Palomar, N. Alonso, J. Bedia, M.A. Gilarranz, J.J. Rodríguez.
Advanced materials. Encapsulated Ionic Liquids (ENILs)
Workshop on Ionic Liquids. Madrid (Spain). January 2012.
(Oral presentation)

-
5. E. Vega, *J. Lemus*, J. Palomar, M.J. Martín
Eliminación de Compuestos de Azufre causantes de Olor mediante Adsorción en Carbones activados
and
J. Lemus, J. Palomar, M.A. Gilarranz, J.J. Rodríguez.
Síntesis, caracterización y aplicación de líquidos iónicos encapsulados
11th Reunión del Grupo Español del Carbón (GEC). Badajoz (Spain). October 2011.
(Oral presentation)
 6. *J. Lemus*, J. Palomar, M.A. Gilarranz, J.J. Rodríguez.
Adsorption with activated carbon for removing ionic liquid from aqueous effluents.
Thermodynamic and kinetic study
1st International Conference on Ionic Liquids in Separation and Purification Technology (ILSEP). Sitges (Spain). June 2011.
(Oral presentation)
 7. *J. Lemus*, J. Palomar, M.A. Gilarranz, J.J. Rodríguez.
Guide to efficiently recover ionic liquid from water by adsorption with activated carbon
Scientific Fellows Congress. Minilubes.net. Vigo (Spain) May 2011.
(Oral presentation)
 8. J. Palomar, *J. Lemus*, M.A. Gilarranz, J.J. Rodríguez.
Highly adsorbent Activated Carbon for removing Ionic Liquids from aqueous effluents 4th
Congress on Ionic Liquids (COIL). Washington (USA) June 2011.
(Poster presentation)
 9. J. Palomar, *J. Lemus*, J. S Torrecilla, F. Rodríguez.
A COSMO-RS based guide to analyze/quantify the polarity of ionic liquid media
media
Green Solvents for Synthesis. Berchtesgaden (Germany). October 2010.
(Poster presentation)
 10. *J. Lemus*, J. Palomar, M.A. Gilarranz y J.J. Rodríguez
Líquidos Iónicos soportados. Elección del soporte
10th Reunión del Grupo Español del Carbón 2010. Girona (Spain). May 2010.
(Poster presentation)
 11. *J. Lemus*, J. Palomar, M.A. Gilarranz y J.J. Rodríguez
Influence of physical and chemical surface of Activated Carbon on the adsorption of Ionic
Liquids 3rd International Conference for Energy Storage/Conversion and Environment
Protection (CESEP). Torremolinos (Spain). October 2009.
(Poster presentation)
 12. *J. Lemus*, J. Palomar, M.A. Gilarranz y J.J. Rodríguez
Adsorption with Activated Carbon for removing Ionic Liquid from aqueous effluents
and
J. Palomar, *J. Lemus*, M.A. Gilarranz y J.J. Rodríguez
Simulation of Activated Carbon using COSMO-RS as predictive tool in adsorption of Ionic
Liquids
The annual world conference on Carbon. Biarritz (France). June 2009.
(Poster presentation)
-

13. J. Palomar, *J. Lemus*, M.A. Gilarranz y J.J. Rodríguez
Simulation of Supported Ionic Liquid Phase (SILP) by COSMO-RS to select appropriate adsorbents
and

J. Palomar, S. Torrecilla, V. Ferro, *J. Lemus*, F. Rodríguez
Structure-Property Maps based on Sigma-Profiles by COSMO-RS
COSMO-RS-Symposium. Leverkusen (Germany). March 2009.
(Poster presentation)

14. *J. Lemus*, J. Palomar, M.A. Gilarranz y J.J. Rodríguez
Ionic liquid removal from aqueous effluents by adsorption with activated carbon
11th Mediterranean Congress on Chemical Engineering. Barcelona (Spain). October 2008
(Oral presentation)

APPENDIX 3. Physical and chemical properties of gaseous solutes

Chloroform (TCM)

Chloroform (CHCl_3) is a colorless, sweet-smelling and dense liquid at room temperature. Several million tons are produced annually. The use of TCM as reactive in organic synthesis is one of the most important industrial applications, because of the polarity of C-Cl bonds. Moreover, because of its stability and immiscibility with a wide variety of organic compounds, it is used as solvent in biology molecular process (DNA extraction). In the past, TCM was used as analgesic in medicine, but nowadays it has been forsaken as result of it harmful and toxic character. Most of the TCM is found in the environment coming from the industry. It can be easily given out to the environment from a wide variety of sources such as synthesis, wastewater treatment or chlorinated pools because of its easy evaporation. The degradation of TCM in the atmosphere by means of photolysis is a slow process that could undergo more toxic subproducts than TCM, such as phosgene.

Dichloromethane (DCM)

Dichloromethane (CH_2Cl_2) is a colorless, volatile liquid with a moderately sweet aroma and it is widely used as a solvent. Although it is not miscible with water, it is miscible with many organic solvents. Most of DCM is produced by chlorination of methanol, forming also monochloromethane as subproduct. It could be also obtained by direct hydrodechlorination of methane. DCM is widely used in the industry, taking importance in chemical engineering, pharmaceuticals, synthesis of aerosols or adhesives, dry cleaning, as extractor of aromas or oils, polymerization process and refrigerant.

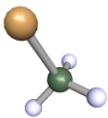
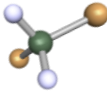
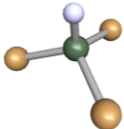
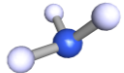
Monochloromethane (MCM)

Monochloromethane (CH_3Cl) is a colorless, non-corrosive, liquefiable gas which condenses to a colorless liquid. MCM is produced both industrial and natural sources. The industrial production of this compound is produced by chlorination of methanol with hydrogen chloride and less it is produced by the reaction of methane and chloride, obtaining hydrogen chloride as subproduct. In the past, MCM was used as refrigerant, but nowadays it has been forsaken as result of it harmful and toxic character. Almost of the commercial production of MCM is applied for the synthesis of silicones, agriculture products, methyl cellulose, quaternary amines and butyl rubber. The MCM presents in soils and water is rapidly evaporated to the atmosphere, where it shows a slow degradation rate, so its persistency is lasted by months or even years, thus its proper treatment is required.

Ammonia (NH_3)

Ammonia (NH_3) is a colorless gas with a characteristic strong and spicy smell. Ammonia emissions are an important contributor to air pollution formation, acidification of soils, eutrophication of ecosystems and alteration of the global greenhouse balance. Consequently, increased attention is being paid to accurate quantification and characterization of ammonia emissions. As compared to dominant ammonia source sectors such as livestock operations, the anthropogenic sources covered in this control are estimated to contribute small amounts to national and regional annual registers. Other sources that take on importance include composting, industrial sources, and domestic sources (i.e., losses due to the volatilization of ammonia refrigeration system or intensive livestock animal production) for contributing to atmospheric reactive nitrogen.

Table A3.1. Physical and chemical properties of MCM, DMC, CLF and NH₃.

	Monochloromethane	Dichloromethane	Chloroform	Ammonia
Molecular formula	CH ₃ Cl	CH ₂ Cl ₂	CHCl ₃	NH ₃
CAS number	74-87-3	75-09-2	67-66-3	7664-41-7
Appearance	Colorless gas	Colorless liquid	Colorless liquid	Colorless gas
Molecular weight (g·mol⁻¹)	50.49	84.93	119.38	17.03
Density (g·L⁻¹) at 25°C	0.9	1.3	1.5	1.0
Molecular volume (Å³)	93.87	110.40	133.99	28.26
LogP	1.52	1.72	2.34	-1.82
Melting point (°C)	-91.0	-96.7	-63.5	-77.7
Boiling point (°C)	~-26.0	39.6	61.2	-33.3
Structure				

APPENDIX 4. Treatment of Cl-VOCs

This appendix shows the experimental evidences of the sorption of Cl-VOCs (DCM or CLF depending on the experimental devices) on different sorbent material, to know AC, IL and SILP material. The procedure for general gaseous pollutant treatment using IL-based material consists on:

- i. Firstly, the proper selection of the IL, taking into accounts both the solubility of IL in the gaseous solute and the physical properties of the IL for further application.
- ii. Follow the experimental evaluation of the IL.
- iii. The next step is the preparation of the SILP material,
- iv. Concluding with SILP application.

So, the first step was to do a screening of ILs. A contour plot of 112 ion combinations based on the Henry constant which was obtained from COSMO-RS, as can be seen in [Figure A1](#). As it was explained before, lower Henry constant means higher solubility (affinity between the consider compounds, DCM and IL). Attending to the map, reddish colour is attributed to lower Henry constant (higher affinity) and bluish-white colour means less affinity. So, it can be found that solutes as DCM, which presents apolar character may be highly affected by the right selection of the anion, while the cation has less importance. Attending to the chemistry of the anion the efficiency increased in the hydrophilic order $\text{Cl}^- > \text{Acetate}^- \gg \text{BF}_4^- \gg \gg \text{NTf}_2^-$. Considering the cation, improvements are barely observed, but imidazolim cation with long alkyl chain is reported as the best option, Omim^+ .

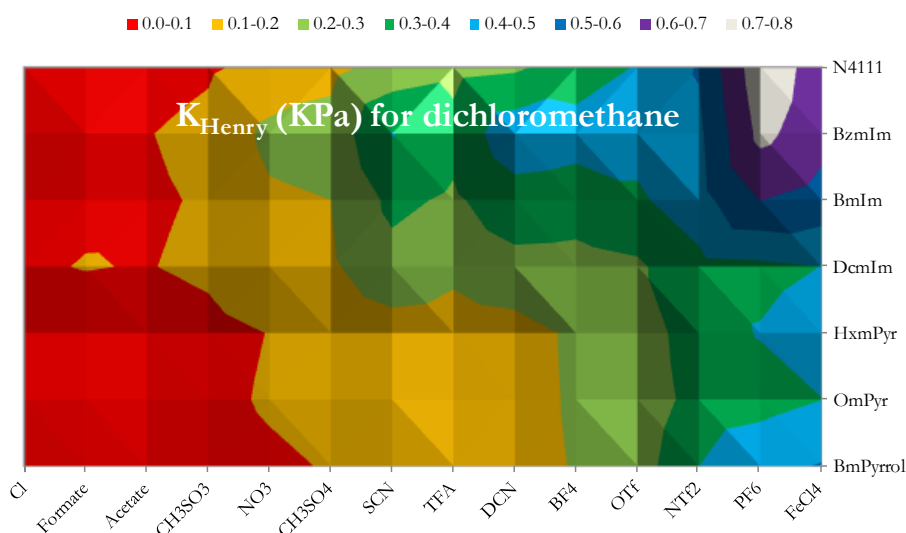


[Figure A1](#). Henry constants of dichloromethane in 144 different ILs predicted by COSMO-RS method at 25 °C.

As it was previously suggested, the application of SILP materials (a thin film of IL immobilized on a solid phase) as sorbents in separation processes it was justified because has recently been established to combine the advantages of ILs with those of heterogeneous supporting materials. This appendix shows the contribution of unpublished results where it is demonstrated the efficient of SILP materials in the adsorption of chloromethane (DCM for fix-bed reactor and CLF for thermogravimetric measurements).

Figure A2 depicts the absorption of CLF by OmimCl and the adsorption of CLF by commercial AC (MkU) measured in gravimetric experiment at 25 °C and 1 atm. These tests were carried out under continues CLF/N₂ gas flow (100 N cm³·min⁻¹) at a CLF partial pressure of 0.08 MPa passing over a 25 mg sample of sorbent material. It can be seen that the absorption capacity of IL is 8 fold less than the adsorption with commercial AC, see Table A2. This first result informs about the potential use of AC for adsorption and the limitation at the time to use ILs for this kind of solutes. However, the kinetic rate of the adsorption process is susceptible to be improved, by means of mixed materials.

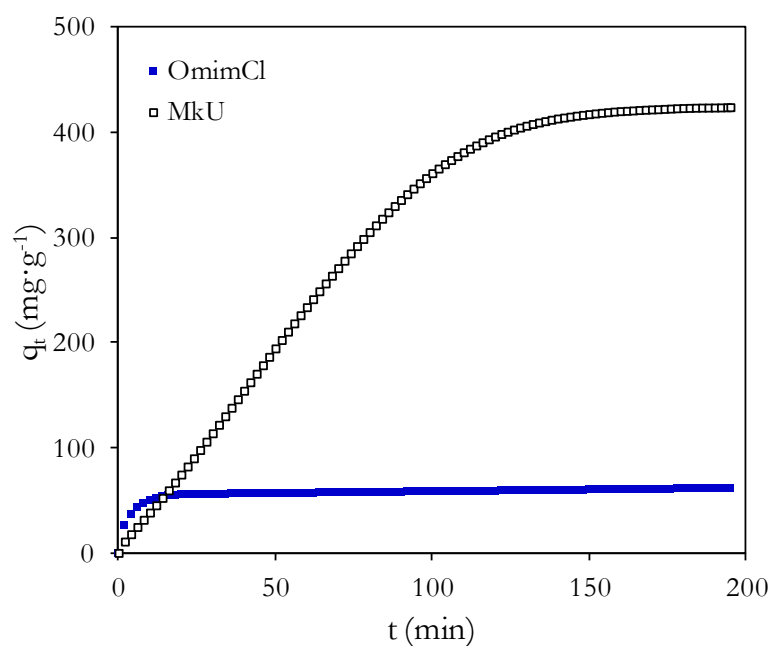


Figure A2. CLF sorption curves of IL (OmimPF₆) and SILP-10% at 25 °C, 1 atm and 1000 ppmv of inlet chloroform concentration, obtained in gravimetric experiments.

Table A2. Results of chloroform capture with the IL (OmimPF₆) and SILP-10% material prepared with this IL obtained in thermogravimetric tests at 20 °C, 1 atm and 1000 ppmv of inlet chloroform concentration.

	Pseudo-second order model		
	q_s (mg·g ⁻¹)	k (mg·g ⁻¹ ·min ⁻¹)	R^2
OmimPF₆	61.7	3.72×10^{-3}	0.9994
MkU	500.0	0.04×10^{-3}	0.9934

Figure A3 present the breakthrough curves obtained for DCM sorption with the starting AC-MkU and the SILP material, prepared by using 10% in weight of OmimCl. The experimental condition were 250 mg of bed length, at 25 °C, 0.1 MPa, 20 N cm³·min⁻¹ gas-flow rate and inlet DCM concentration of 1000 ppmv, representative of industrial gas effluents. Again, it is found that the adsorption capacity of AC-MkU is higher than the SILP material, practically two times as it shown in $t_{0.5}$ value of Table A3, which is a proportional value to adsorption capacity. So, Cl-VOCs are not suitable solutes for its application with IL based material, while adsorption on AC is an evident treatment to this end.

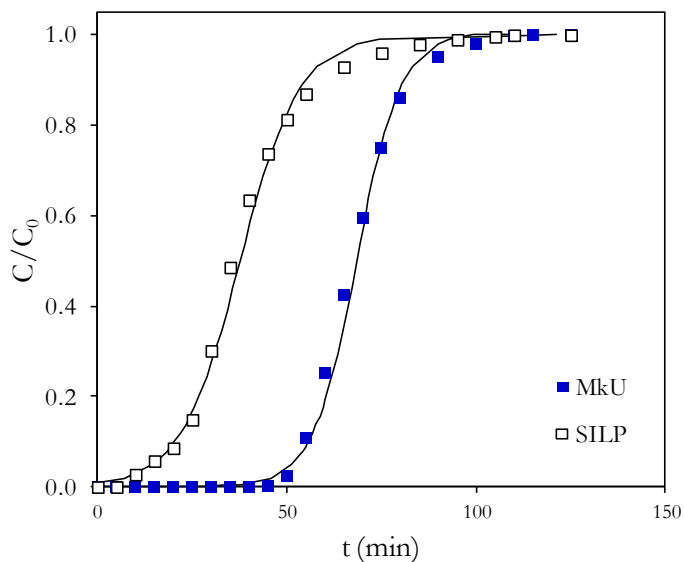


Figure A3. Breakthrough curves of DCM capture obtained with MkU and SILP-10% in 250 mg of sorbent material in a fixed-bed column (1/4 inch diameter) at 25°C, 100 N cm³·min⁻¹ gas-flow rate and 1000 ppmv of inlet DCM concentration.

Table A3. Results of the column tests of DCM adsorption with commercial AC-MkU and SILP material (10% (w/w) of OmimCl) at 25°C, 100 N cm³·min⁻¹ gas-flow rate and 1000 ppmv of inlet DCM concentration.

	Yoon and Nelsol parameters		
	$t_{0.5}$ (min)	k (h ⁻¹)	R^2
MkU	68.5	10.3	0.978
SILP	37.7	7.7	0.965

A new reconsideration in the sorbent material may have to take into account for further applications. Measurements of elemental nitrogen in the samples keep establishing a direct relationship between percentage of elemental nitrogen and the amount of IL incorporated. **Figure A4** shows the maximum retention of IL in different supports studied, showing the microcapsules as the best support to incorporate a largest amount of IL than the rest of supports previously studied. So, it is evidence the use of this material for next sorption treatments.

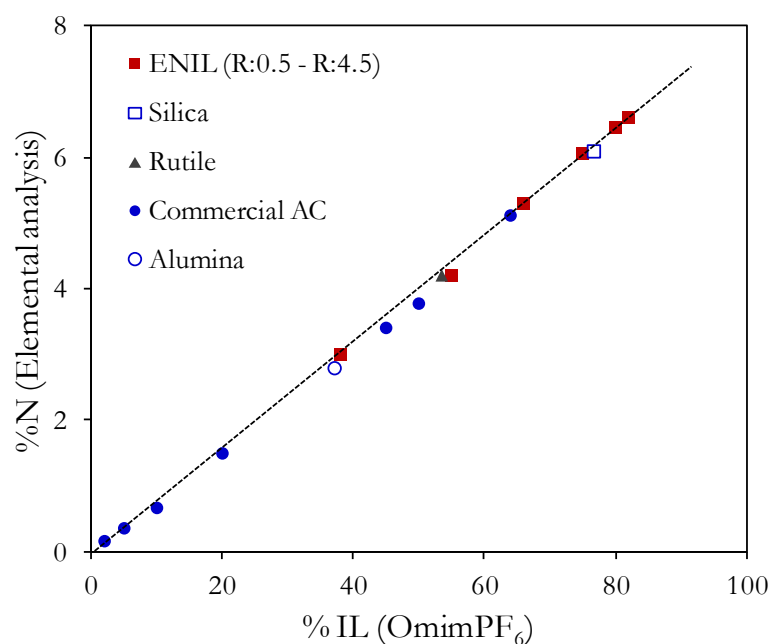
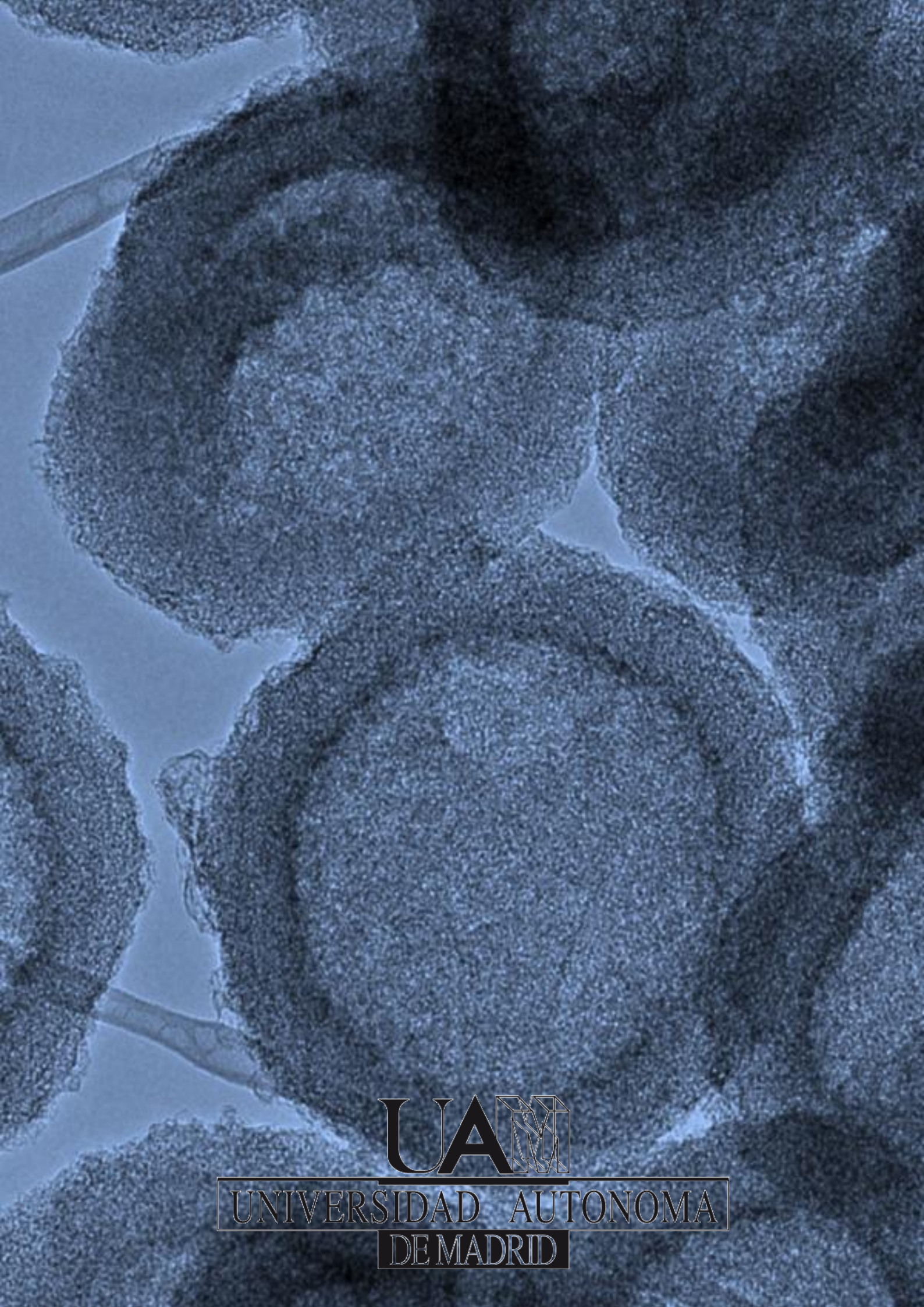


Figure A4. Normalized mass percentage of elemental nitrogen of mixed materials against the OmimPF₆ load.



UAM

UNIVERSIDAD AUTONOMA
DE MADRID